2019

Testing the Gliocentric Hypothesis of Brain Pathology

Ellwood, Sarah Hannah

http://hdl.handle.net/10026.1/14722

TESTING THE GLIOCENTRIC HYPOTHESIS OF BRAIN PATHOLOGY

by

SARAH HANNAH ELLWOOD

A thesis submitted to University of Plymouth
in partial fulfilment for the degree of

DOCTOR OF PHILOSOPHY

Faculty of Medicine and Dentistry

June 2019

ACKNOWLEDGEMENTS

First I would like to thank my supervisor Professor Bob Fern for his help, guidance and encouragement throughout my PhD and writing up. I would also like to thank the other and former members of the Fern lab, Daniel Hansen, Angelo da Rosa, who have taught me and advised me when I needed. Also to Sean Doyle and Chris Bulman, fellow PhD students who were good colleagues and friends.

I would not have got through my time in Plymouth had it not been for the friends I have made and who welcomed me into the JBB family. Special thanks to Jemma Dunn, Jon Davies, Robert Button and many others who added to my experience both in and out of the lab.

Finally I would like to thank my family, especially my parents Karen and Russell. Their unconditional love and unwavering support have allowed me to follow this path and I could not have done it without them.

Author's Declaration

At no time during the registration for the degree of Doctor of Philosophy has the author been registered for any other University award without prior agreement of the Doctoral College Quality Sub-Committee.

Work submitted for this research degree at the University of Plymouth has not formed part of any other degree either at the University of Plymouth or at another establishment.

This study was financed with the aid of a studentship from PUPSMD.

Presentations at conferences:

Poster presentation at PUPSMD annual research event, St Mellion, April 2016, oral and poster presentation at PUPSMD annual research event, St Mellion, March 2017

Word count of main body of thesis: 45,422

Signed

Date

ABSTRACT

Name: Sarah Hannah Ellwood

Title: Testing the gliocentric hypothesis of brain pathology.

Ischaemic stroke is a leading cause of death and disability worldwide, causing cell death and tissue damage. All cell types are affected by ischaemia, however until recently, the impact of acute ischaemia has been studied from a neuronal point of view. Currently, there is a greater interest in glial cells such as astrocytes and oligodendrocytes as they are essential for the correct working of the central nervous system (CNS). This thesis aimed to investigate the regional sensitivity of the glial cells and the mechanisms behind any regional differences. Three mechanistic areas were chosen to be examined; the role of glycogen stores, cytotoxic ion influx through glutamate receptors and the involvement of sodium and cell swelling.

Investigation into glial sensitivity was carried out via live imaging of brain slice and optic nerve preparations from transgenic mice which specifically expressed GFP in either astrocytes or oligodendrocytes. Ischaemia was modelled using oxygen glucose deprivation (OGD). It was determined that astrocytes display regional differences in sensitivity to ischaemic insult. The most sensitive region was the dentate gyrus (DG), and corpus callosum (CC) was the least sensitive. Mature oligodendrocyte somas were found to be tolerant to acute ischaemia.

Mechanistic investigation revealed that the presence and access to glycogen prevented and attenuated OGD induced cell death in CC. It was found that astrocyte injury may be mediated by AMPA receptors. OGD induced astrocyte cell death was found to be sodium dependent in DG but not in CC. The findings strongly indicate that astrocyte regional sensitivity to ischaemia exists and that there are different OGD induced cell death mechanisms depending upon the physical location of the astrocyte population. This provides further information about the effect of ischaemia on glial cells and provides targets to be further investigated to assist with the recovery of tissue after ischaemic insult.

Contents

LIST OF FIGURES AND TABLES

ABBREVIATIONS

2DOG – 2-deoxy-glucose

aCSF – artificial cerebrospinal fluid

ALDH1L1 – aldehyde dehydrogenase

AMPA – α-amino-3-hydroxy-5-methyl-4-isoxazolepropionic acid

ANLS – astrocyte-neuron lactate shuttle

ATP – adenosine triphosphate

AU – arbitrary units

BBB – blood brain barrier

BSK – brain slice keeper

CA1 – CA1 region of hippocampus

CAP – compound action potential

CC – copus callosum

CCC – cation chloride co-transporter

CNS – central nervous system

CTX - cortex

DG – dentate gyrus region of hippocampus

DIOA – 2-[[(2S-2-butyl-6,7-dichloro-2-cyclopentyl-1-oxo-3H-inden-5-yl]oxy]acetic acid

DMSO – dimethyl sulfoxide

DNA – deoxyribonucleic acid

E – embryonic day

EAAT – excitatory amino acid transporter

EDTA – ethylenediaminetetraacetic acid

(E)GFP – (enhanced) green fluorescent protein

GABA – γ-aminobutyric acid

GAPDH – glyceraldehyde-3-phosphate dehydrogenase

GATs – GABA transporters

GLAST – glutamate aspartate transporter

GFAP – glial fibrillary acidic protein

(i)GluR(s) – (ionotropic) glutamate receptor(s)

GLUT1 – glucose transporter 1

GM – grey matter

HEPES – 2-[4-(2-hydroxyethyl)piperazin-1-yl]ethanesulfonic acid

IA – sodium iodoacetate

IF – immunofluorescence

KCC – K-Cl co-transporter

MCAO – middle cerebral artery occlusion

MCT(s) – monocarboxylate transporter (s)

MK801 – ($5S$,$10R$)-(+)-5-methyl-10,11-dihydro-$5H$-dibenzo[a,d]cyclohepten-5,10-imine maleate

NBC – sodium-bicarbonate co-transporter

NBQX – 2,3-dioxo-6-nitro-1,2,3,4-tetrahydrobenzo[/]quinoxaline-7-sulfonamide

NCX – sodium-calcium exchanger

NHE – sodium-hydrogen exchanger

NKA – sodium/potassium ATPase

NKCC – sodium-potassium-chloride (Na-K-Cl) co-transporter

NMDA – N-methyl-D-aspartate

NSC – neural stem cell

N$_X$ – voltage-insensitive sodium channel

OGD – oxygen glucose deprivation

ON – optic nerve

OPC – oligodendrocyte precursor cell

P – postnatal day

PAS – Periodic acid Schiff

PBGST – phospate buffered saline containing 10% goat serum and 0.5% Triton-X-100

PBS – phosphate buffered saline

PCR – polymerase chain reaction

PFA – paraformaldehyde

PLP – proteolipid protein

RNA – ribonucleic acid

ROI – region of interest

ROS – reactive oxygen species

SEM – standard error of the mean

SCWM – sub-cortical white matter

STR – striatum

SVZ – subventricular zone

TBE – tris-borate-EDTA buffer

TCA – tricarboxylic acid

TG – transgenic

tPA – tissue plasminogen activator

UTR – untranslated region

VZ – ventricular zone

WM – white matter

CHAPTER 1

1 INTRODUCTION

1.1 GLIA

Historically, brain anatomy and neurological disease have been studied from the neuronal point of view. Neurons have had more appeal since they are the active output cell of the central nervous system (CNS). However, over the last 25 years the important role of glial cells has been recognised and research into this area has increased. The CNS contains different glial cell types which can be broadly divided into macroglia and microglia. Of the macroglial cells, the following work is concerned with astrocytes and oligodendrocytes. When first described, these cells were thought to exist only to give shape to the CNS and structural support to neuronal cells. This myth has since been dispelled and we now know that these cells are essential partners for neurons and are intimately involved in all the cellular functions of the CNS.

1.1.1 Astrocytes overview

Discovered in 1858 by Rudolf Virchow, astrocytes are known to be the most abundant cell type in the CNS. It was not until the 20th century that these glial cells became of greater interest and became a more prominent focus of research. Astrocytes are a heterogeneous cell population which are classically divided into two groups; fibrous and protoplasmic (figure 2.1). Fibrous astrocytes are found in white matter (WM), they have a smaller soma and have long, branched processes. Protoplasmic astrocytes reside in the grey matter (GM) and have shorter processes which are arranged around a larger cell body. The protoplasmic astrocyte processes are highly branched with ramified morphology. These cells occupy their own non-overlapping micro-domains which they monitor and modulate (Halassa *et al*., 2007; Ogata & Kosaka, 2002).

3

Protoplasmic astrocytes have the capability of partially wrapping synapses with their processes, giving rise to the tripartite synapse (Araque *et al.*, 1999). This allows protoplasmic astrocytes to interact and respond to synapses. Fibrous astrocytes directly contact and interact with neurons at axonal nodes of Ranvier (Butt, Duncan & Berry, 1994; Serwanski, Jukkola & Nishiyama, 2017). It has been suggested that this may allow astrocytes to monitor axonal function (Butt *et al.*, 1999). Nodes of Ranvier and perinodal processes contain a high concentration of sodium channels (Butt, Duncan & Berry, 1994), the clustering of which are thought to be encouraged by astrocytes (Black *et al.*, 1989).

1.1.2 Astrocyte development

The exact process of astrogenesis and development is unclear, although it has been suggested that in rodents astrocytes arise from neural stem cells (NSC) in the subventricular zone (SVZ) (Levison & Goldman, 1993). First these cells undergo asymmetric division to increase the pool of NSCs within the ventricular zone (VZ) (Molofsky & Deneen, 2015). These stem cells gain the ability to generate into glial cell precursors during the late gestation and perinatal period. At this time there is a molecular switch which causes the NSCs to become astrogenic, this occurs around embryonic day 16-18 in the cortex (Ge *et al.*, 2012; Hirabayashi & Gotoh, 2005). The regulation and stimulation of astrogenesis has been found to involve Sox9. Sox9 can modulate Nuclear Factor I-A, which has also been found to be involved in astrogenesis (Deneen *et al.*, 2006; Kang *et al.*, 2012).

The astrogenic NSCs leave the SVZ and migrate throughout the developing brain. The migration of astrocytes from their origin can occur along the processes of specialized radial glia, which act as a physical guide (Jacobsen & Miller, 2003; Zerlin, Levison & Goldman, 1995). Radial glia retain

the potential to differentiate into astrocytes, once neurogenesis is complete (Levison, de Vellis & Goldman, 2005). Astrocyte precursors can be identified through their expression of GLAST (glutamate aspartate transporter) (Shibata *et al.*, 1997). It has been shown that astrocytes display subtype patterning and are spatially connected to their origin (Tsai *et al.*, 2012). When situated in their final position, astrocyte proliferation occurs to populate CNS regions. The majority of the increase in cells occurs in the second and third postnatal weeks (Bandeira, Lent & Herculano-Houzel, 2009). A proportion of the astrocyte population is due to migratory cells, however the majority of cells are generated locally (Ge *et al.*, 2012). Intermediate astrocytes can then develop into mature fibrous and protoplasmic astrocytes dependent upon their final location. In mice structures such as the cortex, are only fully developed at the third or fourth week after birth (Rusnakova *et al.*, 2013).

1.1.3 Role of astrocytes in the CNS

Astrocytes occupy a complex niche within the brain, they are essential for the correct working of the CNS and are involved in almost every functional aspect of the CNS. They have structural, homeostatic, biochemical, signalling, maintenance and protective roles and are involved in CNS development. These multiple responsibilities illustrate the importance of astrocytes, how they support neurons and how they maintain the cellular environment. The various roles of astrocytes are discussed below.

1.1.3.1 Structural role of astrocytes

The compact ramified morphology of protoplasmic astrocytes and the non-overlapping nature of these cells (Bushong *et al.*, 2002; Ogata & Kosaka, 2002) creates micro-domains which are controlled by the individual astrocytes. This produces the effect of tiling the GM, which gives structure and organisation

to the brain (Halassa *et al.*, 2007). Perivascular astrocytes are a population of astrocytes which have close associations with blood vessels. These cells are involved in forming the structure of the blood brain barrier (BBB). The process endfeet contact and wrap around the blood vessels, covering their surface (Kacem *et al.*, 1998; Simard *et al.*, 2003). Tight junctions between perivascular astrocytes and endothelial cells (Janzer & Raff, 1987), as well as astrocyte interactions with pericytes help to form this physical barrier. The presence of astrocytes at the BBB and around blood vessels allows them to modulate blood flow and the permeability of the BBB through the secretion of vasodilators (Gordon, Mulligan & MacVicar, 2007).

1.1.3.2 Astrocyte control of homoeostasis

One of the major and perhaps most important functions of astrocytes is their role as homeostatic regulators of the extracellular space (ECS). The extracellular homeostasis of water, neurotransmitters, ion concentrations (figure 1.1) and pH is the responsibility of astrocytes. The micro-domains created by the arrangement of protoplasmic astrocytes allow the environment surrounding an astrocyte to be tightly controlled and monitored (Bushong *et al.*, 2002).

Astrocytes express aquaporin channels through which the homeostasis of water is achieved. Aquaporin 4 is highly expressed on the astrocyte endfeet that contact blood vessels (Engelhardt, Patkar & Ogunshola, 2014; Nielsen *et al.*, 1997). Through the regulation of water entry and exit from the blood flow, astrocytes maintain the volume of the ECS (Yao *et al.*, 2008) and are able to regulate synaptic interstitial fluid (Iliff *et al.*, 2012).

Neurotransmitter homeostasis, clearance and recycling is largely carried out by astrocytes, for example glutamate. This occurs via the uptake of

neurotransmitter from synapses by high affinity sodium dependent transporters and glutamate transporters such as EAAT1 and EAAT2 (Rothstein *et al.*, 1996). Glutamate is taken into astrocytes where it is converted into glutamine (glutamate precursor) (Deitmer, Bröer & Bröer, 2003), which is released for uptake by neurons where it is transformed into active neurotransmitter. Astrocytes also have the ability to synthesize glutamine, *de novo*, which neurons are unable to do (Schousboe *et al.*, 2014), thereby supplying neurons with neurotransmitter precursor when required. Astrocytes also express glutamate receptors, such as NMDA and AMPA glutamate receptors (Bowman & Kimelberg, 1984; Burnashev *et al.*, 1992; Seifert & Steinhauser, 2001). The binding of glutamate to the receptor causes the receptor pore to open and allow ion influx to occur (Clark & Barbour, 1997; Matsui, Jahr & Rubio, 2005). However, it is well known that in the case of NMDA receptors the receptor pore contains a magnesium ion block which prevents the opening of the pore. The magnesium block is voltage sensitive and so is removed when the cell depolarizes (Papadia & Hardingham, 2007; Schipke *et al.*, 2001). Neurons depolarize more frequently than astrocytes and so it may be that a different subunit arrangement is present in astrocyte expressed NMDA receptors (Burnashev, 1996; Seifert *et al.*, 1997) which makes the magnesium block more easily removed. There is evidence that astrocyte expressed NMDA receptors may be magnesium insensitive and lack a magnesium block (Lalo *et al.*, 2006).

The regulation of extracellular pH and maintenance of ion concentrations largely falls to astrocytes (Deitmer & Rose, 1996). This is achieved through a variety of exchangers and transporters (figure 1.1), some are active (Deitmer & Rose, 1996) whilst others are driven by ionic gradients, such as sodium as there is a maintained sodium gradient entering astrocytes. The main transporters

involved in this process include; the sodium-hydrogen exchanger (NHE) which allows the entry of sodium in exchange for hydrogen (Deitmer & Rose, 1996; Kintner *et al.*, 2004). The sodium/calcium exchanger (NCX) can move sodium out and calcium into the cell (Kirischuk, Kettenmann & Verkhratsky, 1997; Minelli *et al.*, 2007). This is a reversible transporter which will change direction depending on ion concentration and membrane potential. The voltage-insensitive sodium channels (N_X) (Rose & Verkhratsky, 2016) allow for sodium entry into astrocytes. The sodium-bicarbonate co-transporter (NBC) facilitates the entry of sodium and bicarbonate into the cell (Soleimani & Burnham, 2001). The sodium-potassium-chloride co-transporter (NKCC1) simultaneously transports a sodium ion, a potassium ion and two chloride ions into cells (Plotkin *et al.*, 1997). Sodium independent and sodium dependent bicarbonate/chloride exchanger (BCX) (Mellergard, Ouyang & Siesjo, 1994), which allow chloride entry and bicarbonate efflux. The sodium/potassium ATPase (NKA) is predominantly responsible for sodium extrusion (Rose & Verkhratsky, 2016; Watts *et al.*, 1991). Ion concentrations are also maintained through the action of cation chloride co-transporters such as NKCC1 and the potassium-chloride co-transporter. The pH is also maintained through proton buffering and sequestration (Deitmer & Rose, 1996).

Astrocytes are important for ECS potassium clearance (Djukic *et al.*, 2007), via a process known as spatial buffering (Orkand, Nicholls & Kuffler, 1966). It was determined in salamander retinal Müller cells that extracellular potassium increases cause potassium to enter Müller cells (Newman, Frambach & Odette, 1984). Newman *et al.* (1984) discovered the excess potassium almost immediately leaves cells via endfoot processes, creating a syphoning effect. They suggested that this may be carried out by astrocytes due to the interaction

of their process endfeet with blood vessels, thereby syphoning excess potassium into cerebrospinal fluid and the blood stream.
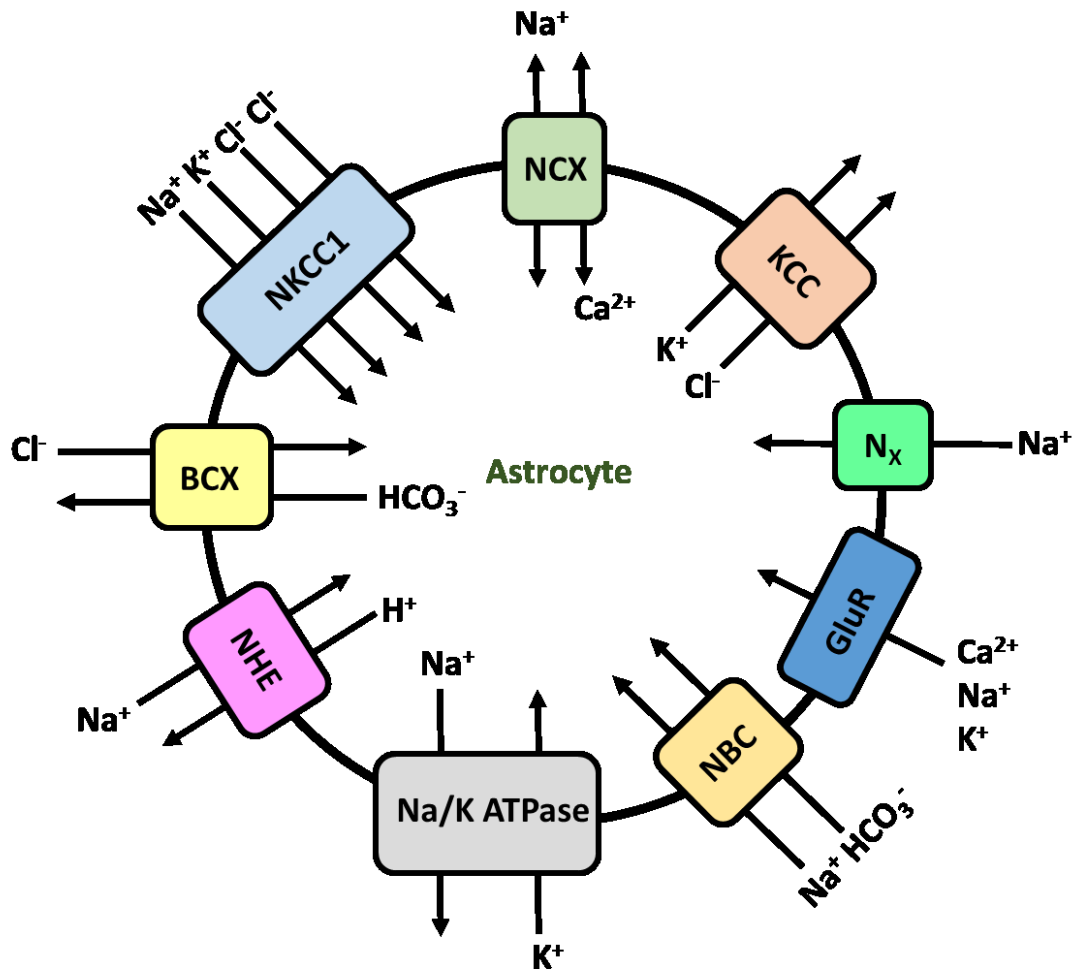
Figure 1.1: Key routes of astrocyte ion movement. Summary of key astrocyte ion transporters and channels, the ions transported and direction of transport. NCX - Sodium/Calcium exchanger, KCC - Potassium-chloride co-transporter, N_x - sodium channel, GluR - glutamate receptor, NBC - sodium/bicarbonate co-transporter, Na/K ATPase - sodium/potassium ATPase, NHE- sodium/proton exchanger, BCX - bicarbonate/chloride co-transporter, NKCC1 - sodium-potassium-chloride co-transporter.

1.1.3.3 Astrocyte involvement in axon growth and synaptogenesis

Astrocytes, their precursors and radial glia are involved in the stimulation and direction of neurite outgrowth (Liesi & Silver, 1988; Rakic, 1971). This guidance of growing axons occurs through the secretion of factors which either promote or inhibit neurite extension (Powell & Geller, 1999) or via cell-cell

interactions. Axonal growth can also be directed and inhibited through the formation of boundaries by immature astrocytes and radial glia (Laywell & Steindler, 1991).

The major role of astrocytes in synaptogenesis was illustrated by Pfrieger *et al.* (1997), who found that when cultured, neurons had sevenfold fewer synapses when grown in the absence of glia (Pfrieger & Barres, 1997). Synapse formation occurs through the involvement of astrocytes and the secretion of thrombospondins (Christopherson *et al.*, 2005). These were discovered in the media of cultured astrocytes and are known to have a role in cell adhesion. Hevin, an extracellular matrix protein, is another astrocyte derived factor which encourages the formation of excitatory synapses (Kucukdereli *et al.*, 2011). Both of these factors promote the structural formation of the synapse. Synapses only become mature and active with the release of glypicans from astrocytes (Allen *et al.*, 2012). The formation of synapses can also be activated by physical contact between astrocytes and neurons and is directed through integrin receptors (Hama *et al.*, 2004), which leads to synapse maturation.

Synaptic morphology is not static and is constantly changing depending on need and use. Synapses can be created, altered and eliminated via the actions of astrocytes (Slezak, Pfrieger & Soltys, 2006). The plasticity of synapses is achieved through the secretion of proteins by astrocytes. For example the function of glutamate receptors (GluRs) is affected by SPARC (secreted protein acidic and rich in cysteine), which alters the stability of GluRs (Jones *et al.*, 2011).

Synaptic function is also monitored and modulated by astrocytes. Within their individual territory it is possible for one astrocyte to contact several synapses, in the hippocampus this can be up to 140,000 synapses (Bushong *et*

al., 2002). The interaction of astrocytes with the pre- and post-synaptic terminals has been termed the tripartite synapse (Araque et al., 1999). This position allows astrocytes to directly respond to synaptic activity and enables the clearance of excess neurotransmitter. Synaptic efficacy is modulated by astrocytes releasing gliotransmitters, such as ATP (James & Butt, 2002) which is secreted via calcium dependent exocytosis (Pangrsic *et al.*, 2007). In the adult CNS a proportion of hippocampal astrocytes retain their ability to trigger neurogenesis in the developed brain and are responsible for the regulation of neurogenesis in the adult CNS (Song, Stevens & Gage, 2002).

1.1.3.4 Astrocyte involvement in metabolism

Due to their ensheathment of blood vessels and involvement in the BBB, metabolites such as glucose have to pass through astrocytes to get from the blood stream to neurons. Glucose can be retained by astrocytes, where it is converted into glycogen and can be stored. Astrocytes are known to be the major glycogen store in the brain (Wender *et al.*, 2000) and so have an important role to play in CNS metabolism.

It has been proposed that in times of hypoglycaemia or elevated neuronal activity these glycogen stores are utilized to preserve the function of neurons (Brown, Tekkok & Ransom, 2003). It has been suggested that the metabolites produced from glycogenolysis can be transported to neurons via the astrocyte-neuron lactate shuttle hypothesis (ANLS) (Pellerin *et al.*, 1998). This hypothesis suggests the export of lactate from astrocytes followed by its movement into axons where it is converted into pyruvate and can enter the Krebs cycle (Brown & Ransom, 2007; Pellerin *et al.*, 1998). First astrocytic glycogen is converted to lactate and exits the cell via monocarboxylate transporters (MCTs), both MCT1 and MCT4 are expressed by astrocytes (Bergersen *et al.*, 2001; Pierre *et al.*,

2000). The lactate is taken up by neuronal MCT2 (monocarboxylate transporter 2) into axons where it is converted to pyruvate by lactate dehydrogenase (Brown, Tekkok & Ransom, 2003). The existence of a lactate gradient between astrocytes and neurons further supports the ANLS hypothesis and suggests an important role for lactate in the CNS (Machler *et al.*, 2016). The lactate produced by astrocytes is not exclusively used by neurons, it has been discovered that lactate can be utilized as a metabolite by cultured oligodendrocytes, as well as for lipid synthesis (Sanchez-Abarca, Tabernero & Medina, 2001). The astrocytic MCTs may not only play a role in releasing lactate for neuronal use, but also to release lactate as a signalling molecule (Lauritzen *et al.*, 2014).

1.1.3.5 Astrocyte signalling

Astrocyte communication with neurons and other astrocytes occurs through the use of molecules such as nucleotides and amino acids, collectively termed gliotransmitters (Innocenti, Parpura & Haydon, 2000; Wang, Haydon & Yeung, 2000). Adenosine triphosphate (ATP) is a major substrate for glial communication (Butt, 2011) and causes increases in intracellular levels of calcium. Gliotransmitters are used by astrocytes to communicate with other astrocytes and cell types. When a signal is detected, astrocytes are able to tailor their response, thereby responding in a non-linear manner to stimuli (Perea, Sur & Araque, 2014).

Throughout the CNS astrocytes are coupled creating networks known as syncytia. Astrocytes couple via gap junctions which are formed at contact points between the fine processes of neighbouring cells, which express hemi-channels (Dermietzel *et al.*, 1991). Gap junctions are formed from connexins which create pores in the cell membrane; the predominant connexin expressed by astrocytes

is connexin 43 (Dermietzel *et al.*, 1991). The coupling of hemi-channels from different cells forms the gap junction, allowing the transport of ions and molecules to occur between cells. These pores allow the movement of signalling molecules between astrocytes (Ye *et al.*, 2003), allowing astrocyte communication across regions of the CNS through interconnected cells.

Instead of electrical excitability astrocytes are excited by changes in intracellular calcium concentration (Charles *et al.*, 1991). Calcium signalling occurs via waves (Cornell-Bell *et al.*, 1990; Dani, Chernjavsky & Smith, 1992; Innocenti, Parpura & Haydon, 2000) which utilize the astrocyte syncytium for transmission to neighbouring cells. Gap junctions are not just formed between astrocytes but are also formed between astrocytes and oligodendrocytes (Tress *et al.*, 2012). This allows communication to occur for axon maintenance and the transfer of metabolites.

Recently it has been discovered that astrocytes can use lactate as a signalling molecule as well as a metabolite. Lactate can be released in response to synaptic activity and glucose utilization due to energy consumption of the synapse (Pellerin & Magistretti, 1994). It is known that the release of lactate can cause cerebral vasodilation, thereby increasing blood flow. Excitatory synapses have been found to express the G-protein coupled receptor 81(GPR81), which binds lactate, suggesting that lactate can also act as an intercellular signalling molecule (Lauritzen et al., 2014). The binding of lactate to GPR81 has been found to cause a decrease in cyclic adenosine monophosphate (cAMP) which reduces glycolysis (Lauritzen et al., 2014).

1.1.4 Astrocyte Response to disease

When the CNS is injured or diseased, astrocytes respond by undergoing a process known as reactive gliosis (Sofroniew, 2009). This is a complex process which has not been clearly defined. However, four key features of reactive astrocytes have been suggested, 1) reactive gliosis is a spectrum of functional and expression changes, 2) these changes vary with the amount of damage from the insult, 3) any changes that occur relate to context, 4) during reactive gliosis astrocytes can undergo gain and loss of function which can be beneficial and damaging to the CNS (Sofroniew, 2009).

During reactive gliosis there is an up-regulation of GFAP expression (Eddleston & Mucke, 1993) which accompanies cell body and process hypertrophy (Wilhelmsson *et al.*, 2006). Whilst reactive, astrocytes retain their homeostatic functions to protect CNS tissue from further damage. They can take up any excess a glutamate (Rothstein *et al.*, 1996), thereby reducing excitotoxicity. They produce glutathione which prevents oxidative stress that can be caused by free radicals, reactive oxygen species (ROS) and nitric oxide (Chen *et al.*, 2001; Shih *et al.*, 2003). Astrocytes can protect neurons from ammonia induced cell death, which has been demonstrated in a co-culture model (Rao *et al.*, 2005). BBB damage can be repaired though the involvement of astrocytes as they form part of its structure, ablation of reactive astrocytes in this location resulted in failure of BBB repair (Bush *et al.*, 1999). Reactive astrocytes can regain ion balance and reduce oedema due to AQP4 expression (Manley *et al.*, 2000). Reactive astrocytes also regulate CNS inflammation during insults via the release of pro or anti-inflammatory cytokines (Eddleston & Mucke, 1993).

1.1.5 Oligodendrocytes overview

Oligodendrocytes are another type of macroglia and they are predominantly responsible for the myelination of axons in the CNS. These specialized cells are also responsible for the maintenance and survival of axons (Morrison, Lee & Rothstein, 2013). This role as a support cell is still being determined, but investigation has found that oligodendrocytes may have a significant part to play in metabolite transport and supply for axons (Saab, Tzvetanova & Nave, 2013). If oligodendrocytes are damaged or injured this can negatively affect axons and lead to neuronal injury (Morrison, Lee & Rothstein, 2013). Oligodendrocytes form networks by coupling to other oligodendrocytes and can form gap junction connections with astrocytes. This produces a network of glial cells in the WM, similar to the astrocyte syncytia found in the GM (see above) (Tress *et al.*, 2012).

1.1.6 Oligodendrocyte development

After neurogenesis, neural precursor cells are affected by a molecular switch which triggers the next phase of development, the gliogenic phase. Oligodendrocytes arise from oligodendrocyte precursor cells (OPC), this occurs in three waves. In mice, the first wave begins at around embryonic day 12.5 (E 12.5) and completely populates the cortex by E18 (Kessaris *et al.*, 2006). The second wave joins the existing cells, all of these OPCs are of ventral origin. After E18 the third wave arises from within the postnatal cortex and there is a reduction in the cells of ventral origin (Kessaris *et al.*, 2006). Migration of OPCs from their origin to their destined region is directed by growth factors and chemokines. When in their final position most OPCs differentiate into oligodendrocytes, whilst a subset remain as OPCs (Bradl & Lassmann, 2010).

1.1.7 Role of oligodendrocytes

Initially it was thought that oligodendrocytes were only responsible for the myelination of axons. However, it is becoming apparent that these cells play a greater role in the CNS by being involved in the maintenance and support of axons.

1.1.7.1 Myelination

Prior to myelination, oligodendrocytes must be correctly situated as mature cells are unable to move once differentiated. Myelination is the process of oligodendrocyte processes wrapping and insulating axon fibres. First the axon is contacted and the initial ensheathment of the axon occurs. This is followed by the wrapping of the axon fibre and the compaction of the membrane (Remahl & Hildebrand, 1982). One oligodendrocyte cell will contact and myelinate relatively few axons, approximately 20 - 60 (Chong *et al.*, 2012). The myelination of axons does not occur by chance and the axons to be myelinated are carefully selected by oligodendrocytes. These cells find axons that have a diameter greater than 0.2μm (Bradl & Lassmann, 2010), the desired axonal size is enough for myelination to begin. Larger diameter axons are myelinated prior to smaller diameter axons (Lee *et al.*, 2012a). Once myelination has been triggered it takes relatively few hours to produce the compacted myelin sheath (Simons & Nave, 2015).

Myelination can be triggered by the amount of neuronal differentiation which has occurred around the oligodendrocyte (Brinkmann *et al.*, 2008). It has also been established in a co-culture model that myelination can occur in a neuronal activity independent and dependent manner. The type of myelination is modulated by neuroregulin which can stimulate myelination through the action of NMDA receptors on oligodendrocyte precursors, which triggers the cells to

16

differentiate into myelinating oligodendrocytes (Lundgaard *et al.*, 2013). The effect of neuronal activity has been further investigated in brain slices and has found that the pattern of activity can elicit different responses from OPCs and can effect proliferation and differentiation of these cells (Nagy *et al.*, 2017).

1.1.7.2 Metabolism

Recently it has been discovered that oligodendrocytes have a wider role to play in the CNS than just the myelination of axons. Evidence has been found that suggests they are involved in axonal metabolism. Due to their close position with neuronal axons, oligodendrocytes are able to communicate with axons and can respond to axonal signals. Axons project far away from their cell body and those which are myelinated are insulated from contact with the extracellular space by their myelin sheath (Simons & Nave, 2015). Therefore, oligodendrocytes are in a more beneficial position to respond to axonal needs than the cell body itself and are able to transport metabolites directly to the axon. It is possible that oligodendrocytes may provide an extra step in the ANLS hypothesis since they express MCT1 which is able to export lactate (Lee *et al.*, 2012b). It has been suggested that lactate is shuttled from astrocytes to oligodendrocytes before it reaches its final destination in neurons, or that lactate may be directly transported from oligodendrocytes to neurons, in response to neuronal signals (Lee *et al.*, 2012b).

1.2 ISCHAEMIC STROKE

Stroke is the second leading cause of death in the world and causes 6.7 million deaths per year, accounting for approximately 12% of deaths worldwide (WHO, 2014). Strokes are most likely to occur during the perinatal period and in the elderly (Fernandez-Lopez *et al.*, 2014). Perinatal stroke has an incidence of approximately 1 in 4000 (Lynch & Nelson, 2001). Over the age of 75, one in five men and one in six women will have had a stroke, which is responsible for 1 in14 deaths (Stroke.org.uk, 2016). The main risk factor for ischaemic stroke is age and the chance of suffering a stroke doubles every decade after the age of 55 (Stroke.org.uk, 2016). There are many other well-known contributing factors that can increase the risk of stroke such as high blood pressure, diabetes, atrial fibrillation, high cholesterol, smoking and excessive alcohol consumption.

Ischaemic stroke usually occurs in the GM but insults can occur in WM, which result in lacunae infarcts (Fern, Matute & Stys, 2014). Infarcts that arise from GM insults are not restricted to this region and have the propensity to affect WM tracts as well. Therefore it is important to examine how all areas of the brain and all cell types are affected by ischaemic stoke. Cerebral ischaemic insults can occur in a global or focal manner. Global cerebral ischaemia is caused when the whole brain is starved of glucose and oxygen which is usually caused by other events such as cardiac arrest. Focal ischaemia occurs when cerebral blood supply is locally reduced to tissues and is usually caused by the obstruction of blood vessels by a clot or embolism (figure 1.1). Focal insults account for the majority of ischaemic stroke, which is approximately 85% of all strokes (Parpura *et al.*, 2017). The remaining 15% include haemorrhagic stroke and transient ischaemic attacks.
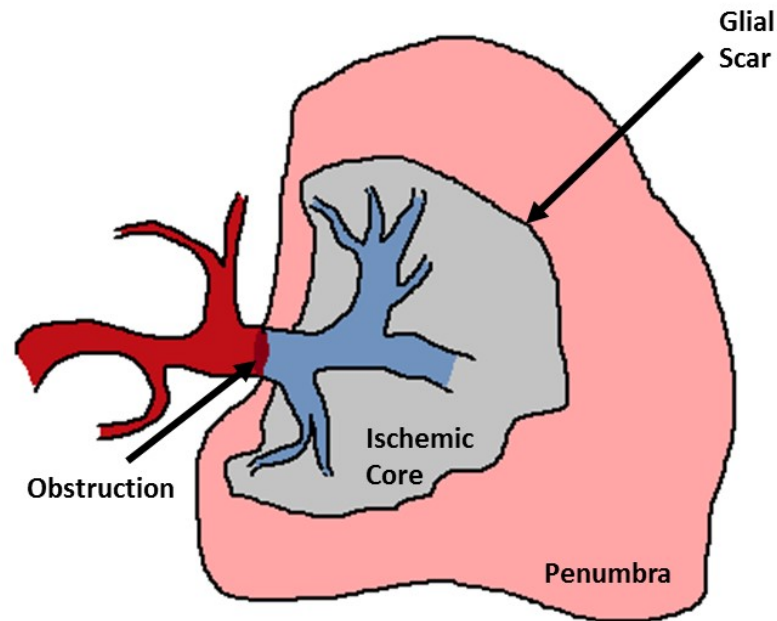
Figure 1.2 Schematic illustration of ischaemic infarct. The obstruction of the blood vessel prevents adequate blood flow causing the ischaemic lesion, which is formed of an ischaemic core where there is no blood flow and the penumbra where collateral blood flow may be retained. The glial scar forms around the ischaemic core to prevent damage to the penumbra.

The primary effect of cerebral ischaemic stroke is the withdrawal of the blood supply from a region of the brain due to a blood vessel occlusion. This deprives the affected area of oxygen and glucose, which are necessary for tissue to survive, causing the development of an ischaemic lesion (figure 1.2). The absence of the blood supply causes major disruption of homeostatic mechanisms, which in turn cause secondary insults such as oedema. Primary and secondary insults both contribute to the cell death and necrosis of tissues which is responsible for the injury seen in stroke patients. Different regions of the brain will be affected depending upon the location of the occluded blood vessel.

Astrocytes in the ischaemic core and a proportion in the penumbra succumb to cell death as opposed to reactive gliosis. Prior to soma loss

astrocytes undergo clasmatodendrosis, which is the shedding of their processes (Hulse *et al.*, 2001; Salter & Fern, 2008) and indicates that astrocytes are entering the cell death phase. Astrocyte cell death triggered by ischaemia occurs via apoptosis or necrosis, these pathways can occur simultaneously as a result of this injury (Cao *et al.*, 2010). Apoptosis occurs at the beginning of the insult but it is an energy intensive process and so ceases when the energy supply is depleted (Cao *et al.*, 2010). At this point necrosis becomes the predominant astrocyte cell death pathway. Necrosis is a spontaneous, un-programmed event which is ATP independent and thought to be mediated by calpains (Liu, Van Vleet & Schnellmann, 2004). Astrocyte cell death also occurs through cell swelling, an early response to ischaemic insult which is caused by the disruption of ion homeostasis (Gurer *et al.*, 2009). Cells which are severely swollen can lose membrane integrity and rupture thus dying due to bursting (Gurer *et al.*, 2009). There is evidence to suggest that as a result of ischaemic insult astrocyte cell death precedes neuronal death (Liu *et al.*, 1999). If astrocyte cell death can be understood and prevented, then neuronal cell death may be attenuated.

A great amount of damage is initially caused by the insult and subsequent development of the ischaemic lesion. Further damage is caused by reperfusion, when oxygenated blood returns to the area affected by stroke. The re-introduction of oxygen causes the production of free radicals and reactive oxygen species (ROS) (Lee *et al.*, 2000). These provide mechanisms of secondary injury which increase the amount of damage, by expanding the size of the initial infarct into previously uninjured tissue (Minnerup *et al.*, 2012).

Regardless of age, the hallmarks and potential results of ischaemia remain the same. There is the formation of an ischaemic lesion, consisting of an

ischemic core with a surrounding penumbra (Verkhratsky & Parpura, 2015). In the ischaemic core cell death is very high, as there is complete depletion of oxygen and glucose here. In the penumbra a proportion of cells are able to survive as this area is not completely deprived of blood flow by the insult and may be served by collateral vessels. The widespread tissue damage that occurs from ischaemic stroke can result in motor and memory deficits in patients and may even cause the development of some forms of dementia (Stroke.org.uk, 2016). Focal cerebral stroke can result in a variety of disabilities, many of which will have a major effect on patient life. When a hypoxic-ischaemic event occurs at birth, this can result in white matter injury which causes hemiplegic cerebral palsy, behavioural changes and many other conditions (Stroke.org.uk, 2016).

1.2.1 Current treatment strategies for ischaemic stroke

The available treatments administered for ischaemic stroke are few and have changed very little since the discovery of thrombolytic agents. Current treatments for stroke are limited, as the cause cannot be readily accessed. Preventative or prophylactic treatments would be difficult to administer as it cannot be predicted when a stroke will occur. Thrombolysis is the major treatment used to break down the clot and is achieved through the administration of tissue-plasminogen activator (tPA) (National Institute of Neurological & Stroke rt, 1995), the thrombus may also be surgically removed. The tPAs are serine proteases that cleave plasminogen to produce its active plasmin form, which then break down fibrin (Christophe *et al.*, 2017) thus destroying the clot. Thrombolytic treatment, in the form of tPA, can only be administered up to 4.5 hours after stroke onset. However, the quicker treatment can be received, the faster the blood supply can be re-established which provides a better outcome for the patient (Stroke.org.uk, 2016). In some cases

thrombolytic agents and surgery can be used in tandem to improve patient outcome (Berkhemer *et al.*, 2015).

After the initial treatment to remove the occlusion patients are then administered a variety of drug therapies to combat the resulting symptoms of ischaemic insult. For example, reducing pressure caused by oedema resulting from ischaemia. In some cases external cerebrospinal fluid (CSF) drainage is required to reduce the intracranial pressure (Kahle *et al.*, 2009). In severe cases, partial skull removal may be carried out in order to reduce overall cerebral pressure.

Recently, the reduction of cerebral temperature in improving outcome after ischaemic injury has been investigated. The use of hypothermia has been introduced and has been found to reduce damage from hypoxic brain injury caused by cardiac arrest (Hypothermia after Cardiac Arrest Study, 2002; Wu & Grotta, 2013). There are different cooling techniques that can be employed such as surface cooling or endovascular cooling (Vaity, Al-Subaie & Cecconi, 2015). There was a promising study carried out in rats where reducing brain temperature to 33°C caused a decrease in glutamate release (Busto *et al.*, 1989). Excess glutamate release and over-activation of GluRs is an important mechanism of neuronal cell death due to ischaemia, via a process termed excitotoxicity (Lucas & Newhouse, 1957; Pulsinelli, Sarokin & Buchan, 1993). Evidence from a number of studies suggests that endovascular cooling is the most effective method of achieving hypothermia and is most successful when combined with shivering suppression, shivering is a side effect of the reduced body temperature. This treatment has the potential to reduce damage in all cell types affected by ischaemia.

1.2.2 Future therapeutic strategies

The current treatments for stroke are few and have their limits in respect of the neurological functional outcome and time restrictions on administration. Thus, research is being carried out into areas beyond thrombolytic drugs. The main interests of current investigation include neuroprotection and reducing the size of infarct, in order to rescue more neurons. However, neurons are not the only cell type in the brain to be affected by ischaemia. Ischaemic insults affect all cell types including glial cells, which have many important roles in the CNS. These cells also need to be protected in the event of injury.

Many neuroprotective agents have provided positive results in a laboratory setting, both in cultured cells and in animal models. However, these compounds have failed to translate beneficial outcomes when it comes to patients in clinical trials (O'Collins *et al.*, 2006), in some cases they were found to be detrimental to stroke recovery. Ischaemia triggers a large biochemical cascade, which provides many options to potentially target. If these can be targeted as well as the initial insult then extensive cell death may be prevented.

1.3 ROLE OF GLIA IN ISCHAEMIA

It was previously mentioned that the majority of work investigating the cellular effects of ischaemia has focussed on neuronal response to injury and neuronal death. The important roles that glial cells have suggests that damage to these supporting cells will have an effect on neuronal response and sensitivity to ischaemia. Thereby linking neuronal survival to the surrounding astrocytes and oligodendrocytes.

1.3.1 Astrocyte response to ischaemic insult

During ischaemic insults one of the main cell types to respond are astrocytes, which become reactive and proliferate, a process termed astrogliosis. This complex process produces reactive astrocytes which arise from the existing population, these form a glial scar around the injury site (Faulkner *et al.*, 2004). This is a physical and biochemical barrier that prevents the migration of inflammatory and potentially infectious cells and factors from the infarct area to healthy tissue (Faulkner *et al.*, 2004; Voskuhl *et al.*, 2009). The formation of the scar also restricts the size of the infarct, containing the damaged tissue (Barreto *et al.*, 2011; Hayakawa *et al.*, 2010). The astrocytes which become reactive are from the surviving penumbral astrocytes, by doing so they enable the protection of unaffected tissue and promote tissue regeneration after damage (Takano *et al.*, 2009). The hallmarks of glial activation are the upregulation of glial fibrillary acidic protein (GFAP), hypertrophy of cells and cell proliferation (Wilhelmsson *et al.*, 2006).

Whilst astrocytes are reactive they release molecules to try to prevent damage and repair the CNS, including neuroprotective factors and those which control blood flow (Barres, 2008). However, the phenomenon of reactive gliosis has the potential to harm the CNS as much as it protects it. A number of the

factors released by reactive astrocytes have harmful effects on the CNS, such as chondroitin sulphate proteoglycans (CSPGs). CSPGs are inhibitory to axon extension and so can prevent axonal growth and regeneration after neuronal damage (Liu & Chopp, 2015). The downregulation of glutamate transporters as a result of injury contributes to the damage of surviving neurons (Allaman, Belanger & Magistretti, 2011). The lack of transporters allows extracellular glutamate to accumulate and so excitotoxicity can develop, which causes cytotoxic influx of calcium ions into neurons (Pulsinelli, Sarokin & Buchan, 1993).

The effects of ischaemic insult can cause irreversible cellular damage which leads to cell death (summarised in figure 1.3). Ischaemia induced astrocyte cell death occurs firstly via apoptosis which is the process of programmed cell death. During ischaemia the mitochondria intracellular calcium concentration can increase which causes membrane depolarisation and the release of cytochrome C (Sekerdag, Solaroglu & Gursoy-Ozdemir, 2018). This release causes the activation of caspases which leads to cell death. ER stress or the release of pro-apoptotic protein into the cytosol triggers the caspase cascade, which initiates apoptosis (Aoyama *et al.*, 2005). This mechanism of cell death also occurs in penumbral astrocytes where collateral blood supply remains (Astrup, Siesjö & Symon, 1981).

The lack of glucose and oxygen delivery to cells causes a switch in cell death programme as no energy can be produced to sustain apoptosis. Astrocyte cell death then occurs via necrosis (Gurer *et al.*, 2009; Lukaszevicz *et al.*, 2002), which accounts for the majority of astrocyte death, especially within the ischaemic infarct core. Necrosis can be triggered via many pathways. The prominent triggers of necrotic cell death include cell swelling, cytotoxic ion

influx, acidosis due to pH change and possibly an inability to utilize glycogen stores.

Necrotic cell death can be characterised by the loss of cell membrane integrity, cytoplasm vacuolation, loss of cell contents, and inflammation (Edinger & Thompson, 2004). In some cases the involvement of calpains are required for necrotic cell death to occur (Liu, Van Vleet & Schnellmann, 2004). Ischaemia induced astrocyte death can involve cytotoxic ion influx, leading to cell death. Cell swelling causes cell death by increasing osmotic pressure within the cell which strains cell membranes, resulting in rupture (Gurer *et al.*, 2009).

The mechanism of cell death also depends on the location of cells in relation to the injury. Those cells within the infarct core undergo necrotic cell death due to the drastic reduction in ATP production. However, those in the penumbral region still have a moderate energy supply and so apoptosis may be more common in this area.
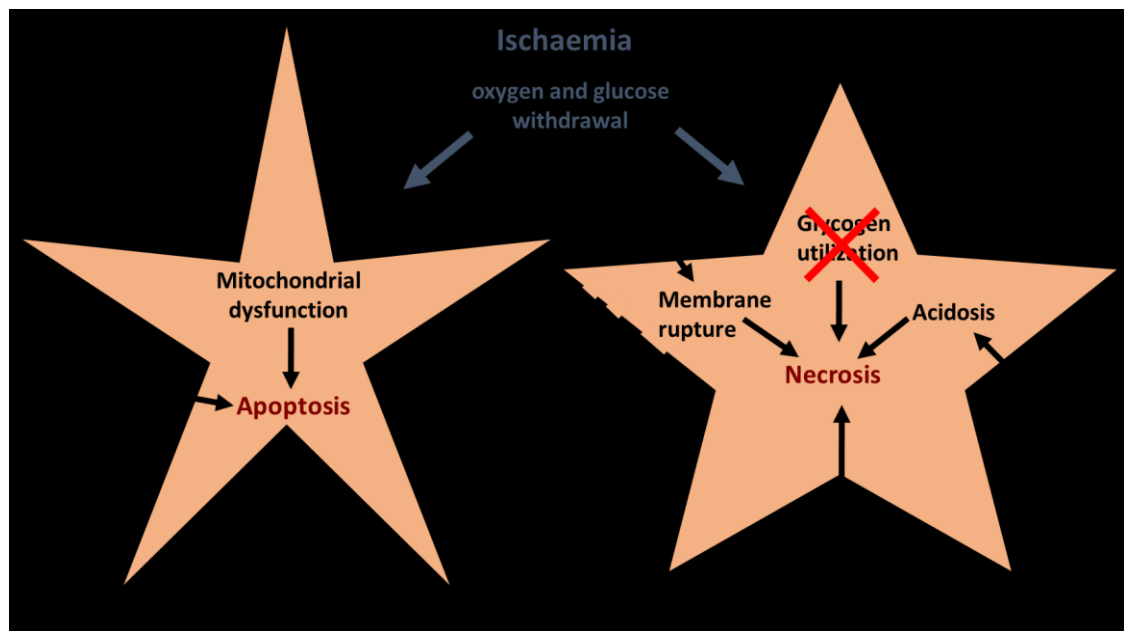
Figure 1.3: Astrocyte cell death mechanisms. Withdrawal of blood flow causes two cell death pathways to be triggered, either apoptosis or necrosis. Apoptosis occurs predominantly due to cellular distress, mitochondrial dysfunction and nitric oxide. Necrotic cell death results from the initial insults and subsequent effects of ischaemia such as cytotoxic ion influx, acidosis, lack of access to glycogen stores and increased water entry causing cell swelling.

1.3.2 Oligodendrocytes and ischaemic insult

Oligodendrocytes are naturally vulnerable to injury and insult due to the amount of membrane that they support and the metabolic demand they are under. They are particularly targeted in ischaemic stroke and periventricular leukomalacia, as WM can be just as much affected by ischaemia as GM is (Dewar, Underhill & Goldberg, 2003). Damage to oligodendrocytes can cause demyelination of neurons though loss or injury to myelin, which alters the ability of axons to function and may trigger degeneration. In mice without proteolipid protein, which is important for myelin formation, it was found that axonal swelling and degeneration occurred (Griffiths *et al.*, 1998). This shows that disruption to myelin is detrimental to neurons by causing structural changes to axons which will affect conduction of action potentials and the survival of neurons.

Oligodendrocytes are accepted as been very vulnerable to ischaemic insult. The main mechanism of oligodendrocyte injury and death is excitotoxicity (Matute *et al.*, 2002), a susceptibility they share with neurons. Excitotoxicity occurs via the over activation of glutamate receptors and the subsequent cytotoxic influx of calcium (Matute, Domercq & Sánchez-Gómez, 2006). Oligodendrocytes can be severely injured by oxidative stress and mitochondrial disruption (Mifsud *et al.*, 2014). These cells are also affected by ATP mediated toxicity (Domercq *et al.*, 2010), ischaemia triggers the release of ATP from other cells, such as astrocytes, causing the over-activation of purine receptors which contributes to cytotoxic calcium influx. Both oligodendrocyte processes and somas are vulnerable to ischaemic insult (Salter & Fern, 2005). Damage may occur to myelin processes, whilst the cell soma remains intact, however process loss usually occurs prior to cell death (McIver *et al.*, 2010), similar to astrocytes.

1.4 AIMS AND OBJECTIVES OF THIS THESIS

The aims and objectives of this body of work are: 1) determine whether regional sensitivity to acute ischaemic insult exists in adult astrocytes *in situ*. The hypothesis being that regional differences in ischaemia induced astrocyte cell death exist. 2) Investigate the mechanistic reasons behind any observed differences in astrocyte sensitivity to ischaemia. The second objective is split into three aims guided by previous work and evidence from the literature. These are; the role of astrocytic glycogen during ischaemia, the involvement of glutamate receptors in cytotoxic ion influx and sodium mediated astrocyte cell death via cell swelling (All mechanisms will be discussed further in relevant chapters).

1.4.1 Glycogen in OGD induced glial cell death (chapter 4)

Glycogen is utilized for many different processes throughout the CNS. Astrocytes are the major glycogen store in the brain and as such may be able to access this store in times of injury or insult to enable survival. The presence of glycogen stores has been determined to confer tolerance of ischaemic insult to astrocytes in optic nerve (Fern, 2015). The breakdown of glycogen results in lactate which can be exported and used as a metabolite by other cells such as neurons (Pellerin *et al.*, 1998). It has been found that lactate is critical for neuronal energy and for axonal function (Lee *et al.*, 2012b). We hypothesize that the presence of glycogen is required for astrocyte survival during ischaemic conditions.

1.4.2 Glutamate receptors and glial ischaemic injury (chapter 5)

The over-activation of glutamate receptors resulting in cytotoxic calcium influx is caused by ischaemia and is the predominant mechanism of neuronal

cell death (Coyle *et al.*, 1981; Lucas & Newhouse, 1957; Pulsinelli, Sarokin & Buchan, 1993). It is well known that astrocytes are resistant to excitotoxicity and so another mechanism is responsible for astrocyte ischaemic death. Astrocytes do express glutamate receptors, which have been found to be permeable to a variety of cations including sodium and potassium (Burnashev *et al.*, 1992; Matthias *et al.*, 2003). Therefore it is possible that adult astrocyte cell death occurs through the cytotoxic influx of a different ion. We hypothesize that glutamate receptors are involved in ischaemia induced astrocyte cell death.

1.4.3 Role of sodium influx on astrocyte swelling and death (chapter 6)

Ischaemic insults disrupt the ionic gradients which exist between the ECS and astrocytes. This dysregulation can result in ion influx followed by water, causing cell swelling. The increase in astrocyte volume strains the cell membrane leading to membrane rupture and cell death (Gurer *et al.*, 2009). Cell swelling and subsequent bursting is a major mechanism of ischaemic astrocyte cell death. It has been suggested that astrocyte cell swelling is mediated by sodium influx (Thomas *et al.*, 2004). Many transporters have been implicated in this mechanism of cell death, most notably the sodium-potassium-chloride co-transporter 1 (NKCC1) (Chen & Sun, 2005; Thomas *et al.*, 2004). Here we hypothesize that cytotoxic sodium influx plays a significant role in ischaemia induced astrocyte cell death.

Ischaemic injury is a complex event which causes a variety of effects on all CNS cell types. The mechanisms responsible astrocyte cell death are not fully understood and may depend on the physical location of astrocyte populations. Investigation into these mechanisms will provide further information about the effects of ischaemia on astrocytes and the sensitivity of astrocytes to insult. The

elucidation of these mechanisms may provide a suitable candidate which can be used to develop therapies to rescue surviving cells after stroke or even prevent the initial death of cells.

CHAPTER 2

2 MATERIALS AND METHODS

2.1 TRANSGENIC MOUSE MODELS

Throughout this work two transgenic mouse lines were maintained and used for experimentation these were GFAP-GFP mice for the study of astrocytes and PLP-GFP which were for the study of oligodendrocytes. Below is further information about these mice and how the two colonies were maintained.

2.1.1 GFAP-GFP mice

All astrocyte work was carried out using FVB/N-Tg(GFAPGFP) 14Mes/J transgenic mice. These mice have the hGFP-S65T form of EGFP, the expression of which is controlled by the human astrocyte specific, glial fibrillary acidic protein (GFAP) promoter (Zhuo *et al.*, 1997). This enables the expression of GFP to be achieved in astrocytes to allow easy detection and visualisation of this cell type. GFAP is an essential intermediate filament protein found in astrocytes, which has an important role in the cytoskeleton and maintaining cell structure (Middeldorp & Hol, 2011). The fluorescent cells can be seen when the GFP is excited at 470nm, with emission detected at 535nm.

2.1.2 PLP-GFP mice

Through the work on astrocytes, it became apparent that glial cells may be more affected by ischaemic insult than previously realised. Therefore, the sensitivity of oligodendrocytes to ischaemic insult was also investigated. For this work a different transgenic mouse line was used; PLP-GFP. In this model EGFP is ligated to the myelin proteolipid protein (PLP) promoter regulatory elements and the 3' untranslated region (UTR) of the PLP gene (Mallon *et al.*, 2002). This allows for the specific expression of fluorescent protein in oligodendrocytes.

PLP is a protein unique to oligodendrocytes and is the most abundant protein found in myelin (Mobius *et al.*, 2008). It has been found that PLP promoter activity is restricted to mature oligodendrocytes by P28 in the CNS (Michalski *et al.*, 2011), during development this promoter is active in many cell types, including some which are outside of the oligodendrocyte lineage. The excitation and emission was the same as for astrocyte GFP.

2.1.3 PCR Genotyping and agarose gel electrophoresis

Both mouse lines were maintained as heterozygous for the presence of the GFP gene and so for breeding purposes genotyping was required. This was achieved via polymerase chain reaction (PCR) in conjunction with agarose gel electrophoresis. The DNA to be tested was extracted from ear notch samples which were acquired exclusively for the purposes of genotyping.

PCR is the method of amplifying a region of DNA containing a gene of interest to see whether the gene is present within a chosen sample. Through cycles of heating and cooling the DNA strands separate allowing access by primers, re-annealing can then occur allowing the copying of the target region. Many cycles of this results in the target region being amplified which is then present in the PCR product. The PCR products are separated out from other DNA fragments via size with agarose gel electrophoresis.

2.1.3.1 Experimental Protocol

DNA extraction was carried out using the hotSHOT method which is outlined below (Truett *et al.*, 2000). This method uses two solutions for the DNA extraction which are: an alkaline lysis reagent containing NaOH 25mM, disodium EDTA (dissolved in H_2O) 0.2mM and a neutralising reagent Tris-HCL 40mM.

Single ear notches were placed in 0.5ml eppendorf tubes and 75µl alkaline lysis reagent was added. The samples were then heated at 95°C for 1.5 hours in a thermal cycler (MJ research PTC-100). These were then cooled to 4°C and 75µl of neutralising reagent was added and gently mixed.

The PCR master mix was then made for the required number of samples. PCR mix for one sample contained: 18.9µl ddH$_2$0, 2.5µL Dream Taq buffer

(Thermo Scientific), 0.15µl dNTP (Invitrogen), 0.15µl forward primer, 0.15µl

reverse primer (primer sequence 5'-GCGGATCTTGAAGTTCACCTTGATGCC,

both primers Sigma Aldrich) and 0.15µl Dream Taq polymerase (Thermo

Scientific). For each sample 3µl of extracted DNA was added to 22µl of PCR

mix added to give a total volume of 25µl. The samples were then mixed,

centrifuged and where placed in the PCR machine and the cycle was started

(BIORAD IQ PCR machine).

After completion of the PCR cycles, 4.2µl of 6x loading dye (Thermo

Scientific) was added to each sample. Next, 12.5µl of the sample was taken to

run on a 1% agarose gel in 1xTBE buffer (10 x TBE Invitrogen, Tris 1M, Boric

Acid 0.9M, EDTA 0.01M). The agarose gel contained 2µl of gel red (Biotium) per

50ml gel, this was used instead of ethidium bromide, so that the DNA bands can

be visualised. The gel was run for one hour at 130v and then imaged using a UV

gel imager.

2.2 LIVE IMAGING OF OPTIC NERVES AND BRAIN SLICES

To assess the regional sensitivity to ischaemia, a live imaging technique has been developed by the lab. This technique allows acute cell death caused by ischaemic conditions to be observed and recorded in real time, in live tissue preparations, either brain slices or optic nerve. Throughout this thesis the model of ischemia used is oxygen-glucose deprivation (OGD), during which glucose containing aCSF and oxygen are switched simultaneously and are replaced by sucrose containing aCSF and nitrogen, respectively.

2.2.1 Artificial cerebrospinal fluids (aCSF) and cutting solution

Below are all solutions used throughout this work for predominantly the live imaging. All chemicals used were obtained from Sigma Aldrich unless otherwise stated.

All aCSFs and cutting solutions were checked to ensure they had an osmolarity between 300 and 310 mOsm using a Wescor vapour pressure osmometer and were adjusted if required. The control solutions and cutting solutions were bubbled with 95% O_2/5% CO_2 for one hour prior to use and continued to be bubbled throughout experiments. The OGD solutions were bubbled in the same manner but with 95% N_2/5% CO_2.

aCSF and glucose free aCSF (OGD aCSF)

aCSF was made up to one litre with deionised water and then was split to form the normal and OGD solutions. The following was present at these concentrations; NaCl 126mM; KCl 4mM; $MgSO_4$ 2mM; Ca^{2+}(gluconate) 2mM; $NaHCO_3$ 25mM; NaH_2PO_4 2mM; Na^+ cyclamate 2mM. At this point solutions were split, one had 10mM glucose added, the other for OGD had 10mM sucrose added.

Zero sodium aCSF

This aCSF was used as a non-selective method to prevent the function of sodium transporters. The following was present at these concentrations; NMDG chloride 128mM; KCl 2mM; $MgSO_4$ 2mM; Ca^{2+} (gluconate) 2mM; Choline-HCO_3 25mM; KH_2PO_4 and either 10 mM glucose or sucrose.

Zero calcium aCSF

Zero calcium aCSF was used to assess calcium dependent and independent astrocyte cell death. The following was present at these concentrations; NaCl 126mM; KCl 4mM; $MgSO_4$ 2mM; EGTA 0.05 mM, $NaHCO_3$ 25mM; NaH_2PO_4 2mM; Na^+ cyclamate 2mM and glucose or sucrose at 10mM.

Modified HEPES cutting/holding aCSF

This cutting solution was used for preparation of brain slices and for holding them in a brain slice keeper. For one litre of solution the following was present at these concentrations; NaCl 92mM; KCl 2.5mM; NaH_2PO_4 1.2mM, NaHCO3 30mM; HEPES 20mM; Glucose 25mM; sodium ascorbate 5mM, thiourea 2mM, sodium pyruvate 3mM, $MgSO_4.7H_2O$ 2mM and $CaCl_2.2H_2O$ 2mM (Ting *et al.*, 2014). Made up to one litre with deionised water and pH adjusted to 7.3-7.4.

2.2.2 Optic nerve and brain slice tissue preparations

All animal procedures adhered to local ethical guidelines and were in accordance with British Home Office regulations, I obtained a HO personal licence in order to comply with regulations for the use of transgenic animals. For work on adult glial cells, mice of age P30 and over were used. For neonatal experiments (P10) mice of age P8-P12 were used. Adult mice were sacrificed

by schedule 1 via exposure to a rising concentration of carbon dioxide followed by exsanguination. Neonatal mice were sacrificed via cervical dislocation followed by decapitation.

Optic Nerves

The optic nerves (ON) were isolated from the head by first severing the nerve behind the eye ball and then removing the brain from the top of the skull with the nerves still attached. Brains were placed into cold oxygenated aCSF on ice and the ON were then removed at the optic chiasm and placed in ice cold oxygenated aCSF. The nerves were then separated by cutting the optic chiasm and were returned to ice cold oxygenated aCSF

Vibratome sectioning hemi-brains

For all live brain slices, the mice were sacrificed and the brain was dissected out as above and placed into oxygenated ice cold cutting/holding solution. After one minute, when cool, the brain was then hemi-sected using a scalpel and hemi-brains were placed in a mould and embedded in 0.5% low melting point agarose and was left to set on ice. The embedded hemi-brains were blocked; then the specimen and a support block (made of 4% agarose) were super glued to the cutting stage (figure 2.1) using cyanoacrylate glue (Loctite).
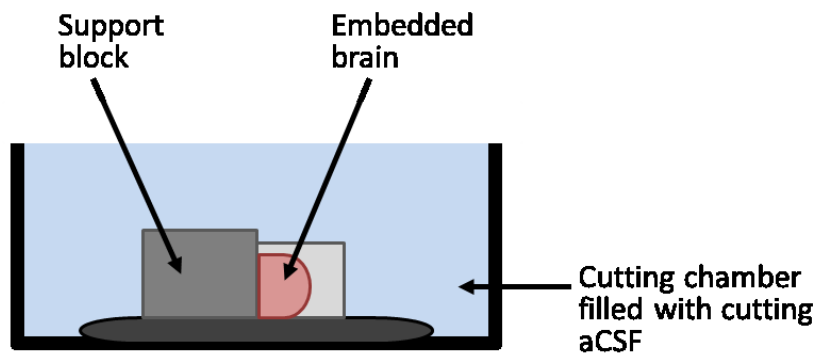
Figure 2.1: Schematic showing vibratome cutting chamber.

Coronal slices of hemi-brains were cut using a Leica VT1200 S vibratome with ordinary razor blades (Wilkinson Sword), in ice cold oxygenated cutting/holding aCSF, the temperature was maintained using ice around the cutting chamber. Slices were transferred to petri-dishes containing cold cutting/holding aCSF on ice, using a cut-off pipette. The cutting angle of the blade was set at 15°, which cut at a speed of 0.2 mm/s and 0.95mm amplitude, the slices obtained were between 160μm and 200μm thick. This depended on the region, as some regions were more delicate than others and so a thicker slice was required to keep the region of interest intact. Slicing was carried out for a maximum of 20 minutes to ensure the health of the slices obtained.

After cutting, slices were transferred to a brain slice keeper (BSK, Scientific Systems Design Inc.) containing oxygenated cutting/holding aCSF at 37°C for 30 minutes, temperature was maintained using a water bath. After this 30 minute recovery period (Ting et al., 2014) the BSK was left to cool to room temperature and slices were constantly oxygenated throughout, which maintained the slices for approximately five hours. Slices were then prepared for recording.

2.2.3 Live Imaging

ON

For live ON recording the nerve was mounted to the bottom of a plexi-glass perfusion chamber (Warner instruments), secured at each end with cyanoacrylate glue (Loctite) (figure 2.2). The perfusion chamber was sealed to a 22mm x 40mm glass cover slip with vacuum grease (Dow Corning).

Brain Slices

For live brain slices, recording occurred in the same chamber as for ON. A single brain slice was transferred from the keeper to the perfusion chamber using a cut-off Pasteur pipette and was kept in place using a slice anchor (Warner instruments).
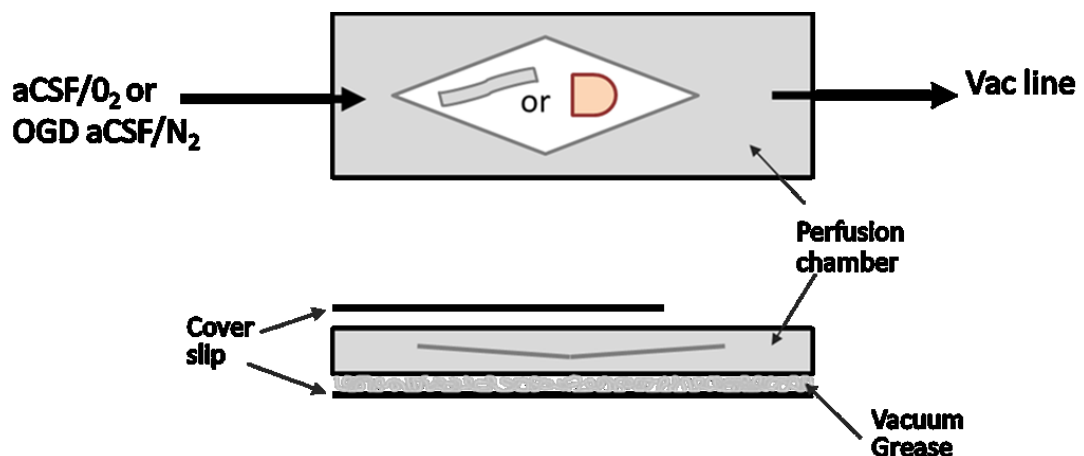
Figure 2.2: Schematic illustration of the recording chamber

In the chamber slices or nerves were continually perfused with aCSF heated to 37°C and were oxygenated, aCSF was removed via a vacuum line. The time-lapse recording of live tissue preparations was carried out as follows: recording lasted a total of 100 minutes. 0-10 minutes was the control period, with sections constantly perfused with aCSF at 1.5 - 2ml/min at 37°C and

$95\%O_2/5\%CO_2$ at approximately 0.1LPM. At 10-70 minutes was the OGD period, with glucose free aCSF perfusion and $95\%N_2/5\%CO_2$. 70-100 minutes was the reperfusion period where control conditions were restored. When changing conditions, the solution and gas were switched simultaneously. The recording chamber temperature was maintained at 37°C through the use of objective mounted heater.

Confocal and wide-field images were obtained using Nikon Eclipse TE2000-U inverted microscope with x40 oil immersion objective and spinning disc confocal unit (X-LIGHT, Crest Optics). The confocal unit was set to a 70µm aperture and the excitation of the GFP was achieved with 470nm LED and 535nm detection. MetaMorph software (version 7.8.9 Molecular Devices LLC, Cairn Research) was used to acquire images and run time-lapse image acquisition. Images were obtained every 60 seconds with a 2 second exposure. Images of 10 second exposure were also acquired for time 0 and time 100. For tissue preparations from PLP-GFP mice, the GFP expressed by the oligodendrocytes was much brighter than in astrocytes in GFAP-GFP mice and so shorter exposures of 50 milliseconds were used along with a lower intensity of light to avoid image saturation.

Mechanism of sensitivity

To investigate injury mechanisms during OGD, chemical inhibitors were added to the aCSFs during the standard experimental protocol. The possible mechanisms investigated in this work were cell death due to due to cytotoxic sodium influx, the role of astrocyte glycogen stores and the involvement of ionotropic glutamate receptors. The chemical inhibitors used were added to target particular aspects of the proposed mechanisms, such as transporters and

44

receptors (see table 1) and were applied either throughout the experiment or during OGD only.

Drug	Source	Target	Concentration	Solvent	Added
Bumetanide	Sigma-Aldrich	NKCC transporter	50µM	Ethanol	Throughout
Furosemide	Sigma-Aldrich	CCC transporters	5mM	DMSO	Throughout
DIOA	Abcam	KCC transporter	50µM	DMSO	Throughout
MK801	Tocris	NMDA glutamate receptors	10µM	DMSO	Throughout
NBQX	Tocris	non-NMDA, AMPA and Kainate receptors	20µM	DMSO	Throughout
Sodium Iodoacetate	Sigma-Aldrich	Glyceraldehyde-3-phosphate dehydrogenase	2mM	H_2O	OGD only
2 deoxy-glucose	Sigma-Aldrich	Block glycogenolysis	10µM	H_2O	OGD only

Table 1: Drugs employed during OGD experiments

2.2.4 Analysis of cell death

The images and time-lapse recordings were analysed off-line using Image J software, where cells and cell death events were counted manually. During the experiment the tissue can swell and distort, thereby altering the focal plane, only cells that were clearly visible throughout the experiment were counted. Astrocyte cell death was determined by the visual loss of fluorescence due to cell lysis which arises from membrane rupture and the release of fluorescent protein (Gurer *et al.*, 2009; Shannon, Salter & Fern, 2007). This same criteria was used to judge cell death of oligodendrocytes. Data from manual counts was processed and analysed using GraphPad Prism 6. To investigate the rates of cell death throughout this work, the time (t) at which cell death was half of the maximum was determined.

2.2.5 Statistical analysis

Throughout this work to compare the means of two groups the unpaired two-tailed T-test was used. This test is used when the populations follow normal distribution and it is assumed that the variance is the same for the two populations. If the variances differ then the Welch's T-test is used which

accounts for unequal variances and does not assume that the two populations have the same standard deviation (Motulsky, 2019).

For multiple comparisons one way ANOVA was used, which compares the means of three or more groups. This statistical test was used in conjunction with Tukey's multiple comparison follow up test, which compares every mean with every other mean. This test allows for any unequal sample sizes and accounts for the scatter of groups (Motulsky, 2019). In all cases a confidence interval of 95% was used and significance was set at $p < 0.05$. All graphs show standard error of the mean (SEM).

2.3 FIXING AND IMMUNO-STAINING OPTIC NERVE AND BRAIN SECTIONS

Tissue fixation was carried out using 4% paraformaldehyde (PFA) in PBS.10x PBS was made up with deionised water and then diluted for use, one litre contained 80g NaCl, 2g KCl, 26.8g Na_2HPO_4 and 2.4g KH_2PO_4. The pH was checked and adjusted to 7.4. For 4% PFA, 20g PFA was added to 450ml PBS and heated to 60°C whilst stirring until dissolved, the volume was then corrected to 500ml. When cool, the pH was checked and adjusted to 7.4. The PFA was then divided into 50ml and 15ml aliquots and stored at -20°. PFA was thoroughly defrosted before use.

2.3.1 ON Fixation

ON were dissected out into cold aCSF on ice before being transferred to 4% PFA in PBS for 30 minutes at room temperature. The fixed nerves were first rinsed in PBS before been placed in 30% sucrose PBS, which cryoprotected the tissue. This was carried out at room temperature until the nerves sank. The nerves were then embedded in OCT embedding medium (Thermo scientific) and frozen at -80°C.

2.3.2 Brain fixation

Brains were dissected out into cold aCSF on ice, and were then hemisected (as previously). The hemi-brains were placed in 4% PFA in PBS overnight at 4°C. Brain halves were then rinsed in PBS and cryoprotected in 30% sucrose PBS at 4°C until sinking. The halves were then dried off and embedded in OCT embedding medium (Thermo Scientific) and frozen at -80°C.

2.3.3 Cryosectioning and staining

The tissue block to be sectioned was removed from - 80°C and was left to warm to -20°C for one hour to allow the specimen to acclimatize to the

temperature in the cryostat. Optic nerves and brain halves were cryosectioned using a Leica CM1860 UV Cryostat at a temperature of around -22°C. Coronal sections of 20µm thickness were obtained and were mounted on Superfrost plus slides (Thermo Fisher). The sections were outlined using a hydrophobic pen (Sigma Aldrich) and washed in PBS for five minutes. The sections were then permeabilised and blocked in PBS containing 10% goat serum and 0.5% Triton-X-100 (PBGST) for two hours at room temperature. The primary antibody was diluted in PBGST and was added to the sections until they were well covered and incubated overnight at 4°C. After incubation, sections were washed three times with PBGST, each wash was for five minutes. The secondary antibody was diluted in PBGST and was applied to the sections as for the primary antibody. This incubation was for one hour at room temperature. Sections were then washed three times with PBGST for five minutes each time, followed by four PBS washes for five minutes each. Coverslips were then mounted using Citifluor (glycerol PBS Thermo Scientific) or Fluoromount (aqueous mounting medium, Sigma).

2.3.4 Double staining

For double staining the same protocol was carried out as for single staining until the washes after the first primary antibody. After the three, five minute washes the second primary antibody, diluted in PBGST, was applied as previously and left to incubate for two hours room temperature. The incubation was then followed by six, five minute washes with PBGST. Both secondary antibodies were diluted in PBGST and were incubated together with the sections for one hour at room temperature. The sections then underwent two, five minute washes with PBGST followed by four, five minute washes with PBS.

Coverslips were then mounted using Citifluor (glycerol PBS solution Thermo scientific) or Fluoromount (aqueous mounting medium, Sigma).

2.3.5 Antibodies

Other than for glycogen staining described below, the antibodies and the concentrations used were; rabbit anti-GFAP (Abcam) 1:500, Rabbit anti-Aldh1l1 (Abcam) 1:1000, Mouse anti-GFP (Abcam) 1:500. Secondary antibodies used at 1:1000: Goat anti-rabbit Alexa Fluor 568 (Life Technologies) and goat anti-mouse Alexa Fluor 488 (Life Technologies).

2.3.6 Image acquisition and processing

All immunofluorescence images were obtained using a Leica DM6000 inverted laser scanning confocal microscope and Leica LAS X software. Images were processed using Leica LAS X offline software and Image J software.

2.4 GLYCOGEN STAINING

2.4.1 Periodic Acid Schiff stain and protocol

The periodic acid Schiff (PAS) stain allows for the detection of glycogen by creating a pink colouration and involves a three step process. The first step oxidises any glycogen in the tissue to form aldehyde groups. The second step blocks the aldehyde groups which are not attached to glycogen molecules. Finally the third step is the reaction with the Schiff's reagent that reacts with the exposed aldehyde groups creating a pink stain showing the presence of glycogen in the tissue.

Following the absence of the blood supply, brain glycogen is quickly depleted and so the usual method of tissue fixation could not be used. Instead mice were sacrificed via Schedule 1 cervical dislocation and and then decapitated heads were immediately placed in liquid nitrogen. When frozen, the heads were removed and quickly embedded in OCT and were frozen again at -80°C. The embedded heads were placed in a -20°C freezer for one hour prior to cryosectioning to allow the heads to acclimatize to the temperature in the cryostat. Whole heads were then sectioned and 20µm thick coronal sections were obtained. The sections were mounted onto Superfrost plus slides (Thermo Fisher) and then were fixed with 4% PFA in PBS, 10mM glucose and 0.5% periodic acid for one hour at 4°C. After fixing the sections were rinsed with PBS and then were used for PAS stain. Fixing was carried out under these conditions to try and prevent any loss of glycogen from the fresh frozen sections prior to fixing.

Sections were incubated in 0.5% periodic acid for 10 minutes at room temperature which oxidises the sections (Newman, Korol & Gold, 2011). The

sections were rinsed in distilled water before been placed in a saturated solution of dimedone in distilled water for 30 minutes at 60°C (Gurer *et al.*, 2009). The sections were rinsed in distilled water and then were reacted with Schiff's reagent for 30 minutes at room temperature. The slides were then rinsed thoroughly in distilled water and further rinsed in tap water. Coverslips were mounted using Fluoromount (aqueous mounting medium, Sigma).

2.4.2 GFAP PAS co-stain

For co-staining, sections were fixed as described above for PAS staining and rinsed in PBS. Sections were then permeabilised and blocked in PBGST for two hours at room temperature. The PBGST was removed and sections were incubated with mouse anti-GFAP-CY3 conjugated monoclonal antibody (Sigma). The antibody was used at 1:400 dilution in PBGST and was incubated with sections overnight at 4°C. Sections were then washed in PBGST three times for five minutes and then in PBS three times for five minutes. PAS staining then proceeded as above. Sections were coverslipped and imaged the same day.

2.4.3 Imaging

Images were acquired using Nikon eclipse 80i microscope with colour and fluorescence cameras and x20 or x40 air objectives. The Cy3 conjugated antibody was excited using a TRITC filter set which provides a wavelength around 532nm. Corel PHOTO-PAINT X7 was used to process and overlay jpeg images obtained.

2.5 GLYCOGEN IMMUNOFLUORESCENCE

Due to limitations with the PAS stain an alternative method of visualising glycogen stores was pursued. Currently, there are no commercially available anti-glycogen antibodies and so we were kindly given an aliquot of an anti-glycogen IgM antibody, developed by Professor Hitoshi Ashida's group in Japan. The IgM antibody ESG1A9 has a high specificity (Nakamura-Tsuruta *et al.*, 2012) and has been shown to preferentially bind to higher molecular weight natural granules of glycogen (Oe *et al.*, 2016). The binding nature of this antibody means that is a useful tool for the quantification of glycogen stores within a region of interest (Nakamura-Tsuruta *et al.*, 2012). This IgM antibody was used to stain for glycogen in brain slices that had undergone the live imaging protocol in control, OGD and 2DOG (2-deoxy glucose) conditions.

2.5.1 Experimental Protocol

The live brain slices used for glycogen immunofluorescence (IF) were obtained as previously, however for IF 100µM thick slices were used. After cutting the slices underwent the 30 minute recovery step (as previously for live imaging slice preparation) and then were mounted in the recording chamber, although no images were obtained during the following protocol. The recovery step was important to replenish astrocyte glycogen stores that may have been depleted during dissection. Control slices were put on the rig for the length of the live imaging protocol (100 minutes) and were oxygenated and constantly perfused with aCSF. After this time period, slices were removed from the recording chamber and immediately placed in ice cold 4% PFA PBS for one hour at 4°C. For ischaemic conditions and OGD with 2DOG treatment slices underwent the live imaging protocol without the reperfusion period, as this may allow any surviving cells to replenish their glycogen stores. After 10 minutes of

control conditions and 60 minutes of OGD slices were removed from the recording chamber and treated as the control slices.

Once fixed, the free floating slices were washed thoroughly in PBS and then were incubated with the anti-glycogen IgM antibody. The antibody was diluted, 1:50, in PBS containing 0.1% Triton X-100 and was incubated with the slices for 24 hours at 4°C with gentle shaking (Oe *et al.*, 2016). A long incubation period was necessary for this antibody due to its nature as an IgM and because of the thickness of the sections.

The slices were then washed in PBS three times for five minutes and incubated with goat anti-mouse IgM Alexa-fluor 568 secondary antibody (Life Technologies). This was diluted 1:1000 in Triton PBS and was incubated with slices for one hour at room temperature, whilst shaking.

After the incubation slices were washed thoroughly in PBS, then mounted on slides and coverslipped using Permafluor mounting medium (Thermo Scientific).

2.5.2 Imaging and analysis

Z stack images of the slices were taken using a Leica DM6000 inverted laser scanning confocal microscope and Leica LAS X software using x40 oil immersion objective. The Z stacks averaged around 30µm with a step size of either 0.5µm or 1µm.

To quantify the presence and location of glycogen, Z stack images were analysed using ImageJ software. Stacks were loaded and the colour channels (green – GFP in astrocytes, red – glycogen labelled with Alexa-fluor 568 secondary) were merged and overlaid. The resulting stacks were put through the "RG2B localization plugin" (Christopher Philip Mauer 2004) via ImageJ. This software tool detects co-localised red and green pixels and converts them to

blue, saving the data in the blue channel and allowing the visualisation and quantification of glycogen present in astrocytes.

By drawing regions of interest around whole cells (soma and processes), the average pixel intensity (measured from 0 to 255) of the blue co-localisation was obtained. Figure 2.3 illustrates the process from the merged image and the conversion of the overlapping pixels to blue. The final panel shows a zoomed in image of the square depicted in the previous image and shows how the region of interest was drawn. Cells that were present in multiple planes were assessed for each plane they were present in. Background levels were obtained by taking co-localisation readings from planes beyond the cells. These values were then subtracted from those taken for glycogen levels to give a final value of co-localisation intensity. Statistical analysis was carried out as previously mentioned.
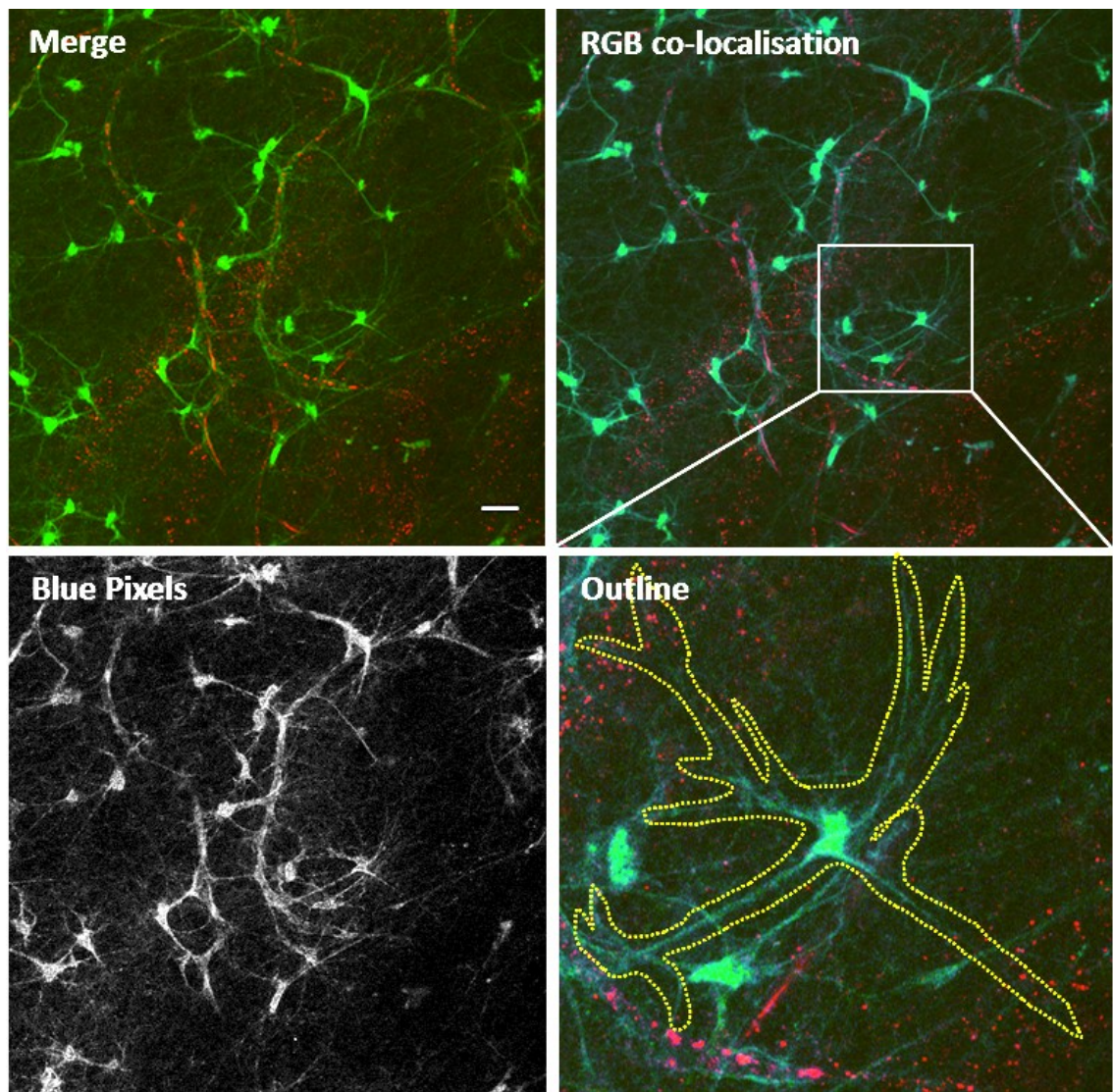
Figure 2.3: Measuring co-localisation. Merge - overlaid image green GFP, red glycogen. **RGB co-localisation** – image treated with ImageJ tool, co-localised pixels shown in blue. **Blue pixels** – image generated by the RG2B co-localisation tool showing the co-localised pixels. **Outline** – yellow line drawn around cell soma and processes to measure co-localisation intensity. Scale bar = 20μm

2.6 COBALT STAIN

Ionotropic glutamate receptors (iGluRs) are expressed by many cells in the CNS including glia (Seifert & Steinhauser, 2001). They are involved in the widely accepted mechanism of excitotoxicity that occurs in response to ischaemia, which results in cytotoxic calcium influx into neurons and neuronal death (Choi, 1987; Lucas & Newhouse, 1957; Pulsinelli, Sarokin & Buchan, 1993).

The cobalt stain allows for the visualisation of cells expressing receptors that are permeable to cations, such as calcium and sodium. Inhibition of glutamate receptors has been found to increase neuronal survival after OGD (Nishizawa, 2001). There is also the possibility that glutamate receptors may have a role to play in astrocyte response to ischaemic insult. Thus, it was necessary to determine whether they were being expressed by cells in our tissue preparations.

This cobalt stain involves stimulating the receptors of interest with an agonist (L-glutamate or kainic acid) in the presence of extracellular cobalt which then enters the cells through activated receptor pores. This is achieved by placing live tissue slices in a series of oxygenated solutions, after which they are fixed and treated to enhance the cobalt precipitate.

2.6.1 Experimental Protocol

The main solution used was the assay buffer which contained the following at these concentrations; NaCl 57.5mM; KCl 5mM, $NaHCO_3$ 20mM, glucose 12mM; sucrose 139mM; $CaCl_2$ 0.75mM and $MgCl_2$ 2mM. The assay buffer was adjusted to pH 7.4. This buffer was then used as a base to form the following staining solutions; the cobalt solution contained 5mM $CoCl_2$ and

agonist (L-glutamate) at 100mM; the ammonium sulphide solution contained 1.2% $(NH_4)_2S$ and the EDTA solution contained 2mM EDTA and was adjusted to pH 7.4.

For this procedure I used the protocol devised by Aurousseau et al (2012) as a guide. Mice were sacrificed and 250µm thick vibratome slices were obtained in ice cold cobalt cutting solution. The cutting solution used for the cobalt staining was slightly different to that used for the live imaging slices and contained the following at these concentrations; NaCl 125mM; KCl 2.5mM; NaH_2PO_4 1.25mM; $NaHCO_3$ 28mM; glucose 7mM, sucrose 223mM; sodium ascorbate; 0.88mM; sodium pyruvate 3mM; $CaCl_2$ 0.3mM and $MgCl_2$ 7mM. The slices were then allowed to recover in oxygenated cobalt cutting solution in the brain slice keeper for 30 minutes at room temperature. For the staining procedure all solutions needed to be freshly made (Albuquerque *et al.*, 2001) and constantly bubbled with (95%O_2/5%CO_2) (Aurousseau, Osswald & Bowie, 2012).

First the slices were incubated in assay buffer with cobalt chloride and agonist (100mM L-glutamate) for 30 minutes. This activated glutamate receptors and allowed cobalt entry into cells. The slices were then incubated with EDTA assay buffer for five minutes, this step chelated any remaining cobalt that had not entered cells. This was followed by a five minute wash in assay buffer only. The slices were then transferred to ammonium sulphide assay buffer for 10 minutes. This step precipitates the cobalt that has entered cells. The slices were then washed in assay buffer twice, for five minutes each time.

For staining with the use of glutamate antagonists the tissue specimens were incubated in assay buffer containing NBQX (20µM) and MK801 (10µM) for 30 minutes prior to the staining procedure. When investigating the effect of OGD

on cobalt uptake into cells, all solutions had glucose removed and were bubbled with nitrogen. Glutamate as an agonist was also excluded as during glucose deprivation exogenous glutamate can be used as a metabolite by astrocytes (Schousboe *et al.*, 2014). The staining procedure for OGD conditions was carried out at 37°C as room temperature is protective and cell death would not occur.

For all conditions the cobalt stained slices were then fixed in 4% PFA PBS for three hours at 4°C and cryoprotected in 30% sucrose PBS overnight. ON were also stained, these were dissected out as for live imaging and were allowed to recover for 30 minutes also. The same staining and fixing procedure was followed as for the brain slices.

2.6.2 Sectioning and silver enhancement

After cryoprotection the slices or nerves were embedded in OCT and frozen at -80°C. The tissue was left to thaw to -20°C and then 20µm thick cryosections of the slices and nerves were obtained and left to air dry. Silver enhancement of the cobalt precipitate then followed, this step develops the stain and fixes it so it can be viewed. A sliver enhancer kit was used (Sigma Aldrich), which contained solution A (silver nitrate), solution B (12-wolframosilicic acid) and sodium thiosulphate. The following protocol was supplied as a technical bulletin with the silver enhancer kit. First, immediately before use solutions A and B were mixed 1:1, 20µL of this mixture was then added to each section for 27 minutes. The slides were washed for five minutes in distilled water and then were placed in 2.5% sodium thiosulphate solution (3.9g sodium thiosulphate pentahydrate in 100ml distilled water) for three minutes to fix the enhanced precipitate. The slides were then thoroughly washed before mounting coverslips

using 10% glycerol PBS; coverslips were secured in place with clear nail varnish.

2.6.3 Imaging and analysis

The stained and enhanced sections were imaged using a Nikon eclipse 80i microscope. The acquired images were processed using ImageJ, where cobalt positive cells were manually counted. A minimum of 10 regions of interest were counted per tissue region from three animals for each condition. For statistical analysis GraphPad Prism 6 was used to carry out one way ANOVA.

.

CHAPTER 3

3 GLIAL SENSITIVITY TO ISCHAEMIA

3.1 INTRODUCTION

The recent change in focus of ischaemic research from neurons to glia has followed the discovery of the vital role that astrocytes play in the maintenance and functioning of the CNS. During times of injury and insult, astrocytes are pivotal to rescuing CNS function and for recovery. If astrocytes themselves are damaged this will have a detrimental effect on the CNS. The impact of astrocyte dysfunction on neurons and on the wider CNS is now beginning to be investigated. Studies carried out on ischaemic neurons *in vitro* have found that neuronal sensitivity to OGD is increased in the absence of astrocytes (Tanaka *et al.*, 1999), suggesting that astrocytes are vital for neuronal survival. Astrocyte-neuron calcium signalling is preserved in the penumbra, despite ischaemic insult (Choudhury & Ding, 2015), showing the importance of astrocyte interaction with neurons post injury.

3.1.1 Neuronal regional sensitivity

For many years it has been known that brain regions have different sensitivities to ischaemic insult as well as neuronal populations within regions showing varying regional vulnerability to ischaemia (Kirino, 1982). It is widely accepted that GM is very sensitive to ischaemia and that WM is more resistant (Marcoux *et al.*, 1982; Pantoni, Garcia & Gutierrez, 1996). Pulsinelli *et al.* (1982) found specific brain regions in which neurons were very sensitive to injury. They determined that the most sensitive neurons were those in the hippocampus, cortical neurons were the next sensitive followed by striatal neurons (Pulsinelli, Brierley & Plum, 1982). Orders of sensitivity also exist within these regions and differences were found between neurons within different cortical layers and

hippocampal regions. The model used by Pulsinelli *et al.* (1982) was global

ischaemia, achieved via four vessel occlusion, during which the carotid arteries

were transiently occluded and vertebral arteries were permanently blocked. It

was found that only 20 minutes of ischaemia was required to observe neuronal

damage in all of these regions (Pulsinelli, Brierley & Plum, 1982). This suggests

that only a relatively short period of ischaemia is necessary to cause irreversible

damage to neurons.

3.1.2 Astrocyte heterogeneity

Since the discovery of astrocytes, it has been accepted that there are two

general groups: fibrous, which are found in the WM, and protoplasmic found in

GM. The clear morphological differences seen between these two astrocyte

populations relate to their specialized functions (figure 2.1 and 2.2). WM fibrous

astrocytes have a smaller cell body and long reaching branched processes.

Fibrous astrocytes have been found to have minimal branching, with a

branching frequency of two to three in ON (Butt *et al.*, 1994), and not all

processes branch at all. The processes of these astrocytes interact with nodes

of Ranvier by partially encircling the nodes with other processes (Butt, Duncan

& Berry, 1994; Serwanski, Jukkola & Nishiyama, 2017). They also contact blood

vessels and project out to the pia where they terminate in the glial limitans. GM

protoplasmic astrocytes have a central cell soma from which project highly

branched and ramified processes. These processes are involved in neuronal

synapses and enable protoplasmic astrocytes to maintain and modulate the

area immediately surrounding them (Nedergaard, Ransom & Goldman, 2003),

thus dividing the GM into individual microdomains.

However, it is has been found that within these groups there may be

many different subtypes of astrocyte which vary depending upon their location

and individual function. Each region of the brain has its own microenvironment and so the cells within these regions are unique to that region and will be specialized through protein and receptor expression (Thoren *et al.*, 2005).

Astrocytes are a very heterogeneous population. This heterogeneity exists for different cellular aspects such as in morphology, density, expression profiles and strength of gap junction coupling. These are discussed below.

Investigation into astrocyte morphological heterogeneity found that differences existed between regions and these differences appeared to define structures of the brain (Emsley & Macklis, 2006). The regions that were defined corresponded to those seen when structures are determined by neuronal cell type. It has also been found that morphological heterogeneity also exists between astrocytes within the same brain region (Zhang & Barres, 2010).

Astrocytes do not only show regional variation in morphology but also in cell number. Differences in cell densities have been observed between many brain regions and a cell density map of the adult CNS has been produced by Emsley and Macklis (2006). They determined that astrocyte density varies across CNS regions and sub-regions. The astrocyte density recorded also depended upon the labelling method used either GFAP positive cells, GFP expressing cells under GFAP promoter or S100β (astrocyte marker). GFAP and S100β are not universal astrocyte markers, they both only detect subsets of the larger astrocyte population. In some regions the number of cells was similar regardless of the labelling method used such as in the substantia nigra pars compacta which contained approximately 80 positive cells mm^{-2} (Emsley & Macklis, 2006). Whereas, in regions such as the preoptic nucleus of the hypothalamus the density varied from 3-5 positive cells mm^{-2} with GFAP

labelling and GFP, to 15-20 positive cells mm^{-2} with S100β labelling (Emsley & Macklis, 2006).

The expression profile of specific astrocyte proteins varies between astrocytes across the CNS, which was discovered through the analysis of microarray data (Bachoo *et al.*, 2004). The variation in expression levels of intracellular proteins, membrane receptors and other factors will results in subpopulations of astrocytes having functions specialized to region in which they are situated and for their specific role.

A surprising way that astrocytes show heterogeneity is through the strength of gap junction connections. The astrocyte syncytium is a major feature of the CNS, but this has been found to show variation between subtypes of astrocytes. Lee *et al.* (1994) measured the strength of gap junction coupling via the diffusion of Lucifer yellow dye and found that the strength of coupling depended on region. The spinal cord showed weak coupling, whereas regions such as optic nerve and hippocampus showed strong gap junction interactions (Lee et al., 1994). Variation in the strength of gap junctions may affect the ability or speed of astrocyte signalling.

Due to this diversity, distinct populations may also show different tolerances to disease and insults such as ischaemia. It is well known that neurons have different sensitivities to ischaemia depending upon the region that they occupy (Pulsinelli, Brierley & Plum, 1982) and it would be logical to suggest that this is also the case for other CNS cell types.

3.1.3 Astrocyte sensitivity to ischaemia

Ischaemic insults affect all CNS cell types including astrocytes and astrocyte sensitivity to ischaemia has been debated. Any injury to astrocytes will

cause structural and functional deterioration to the affected CNS region. The majority of which occurs in the ischaemic core (Lukaszevicz *et al.*, 2002), where there is a high amount of necrosis. Ischaemia induced structural changes that have been observed include the breakdown of the BBB, widespread astrocyte cell death, astrocyte swelling and separation of myelin sheets (Pantoni, Garcia & Gutierrez, 1996). Breakdown of the BBB is caused through the death and swelling of astrocyte endfeet as well as an increase in permeability (Takata *et al.*, 2011). The swelling of endfeet causes changes to the basement membrane integrity (Kwon *et al.*, 2009), causing BBB disruption. Fragmented DNA in dead or dying glial cells was also identified (Petito *et al.*, 1998), showing the effect of ischaemia on glia.

Much of what is known about astrocyte sensitivity has been discovered through the study of astrocytes in culture. Although, it has been realised that *in vitro* astrocytes may behave and respond differently to those *in vivo* (Shannon, Salter & Fern, 2007). The *in vitro* studies that have been carried out do not account for the individual environments that are found in different brain regions. The physical position of these cells, the surrounding microenvironment and the presence of other cells such as neurons, oligodendrocytes and microglia will affect how astrocytes react to insults.

For some time it was believed that astrocytes were very resistant to ischaemia and long periods of OGD were required to cause cell death. However, it has subsequently been found that astrocytes and neurons vary little in their vulnerability to insult (Shannon, Salter & Fern, 2007). It has been discovered that in many cases astrocyte cell death may precede neuronal death (Liu *et al.*, 1999) and this glial cell death may also impact neuronal survival. Work carried out by Xu *et al.* (2001) used cells from neonatal animals for

primary cultures and allowed the cells to mature. They found that after 4 to 6 hours of OGD, astrocytes from the striatum were the most sensitive to ischaemia followed by hippocampal astrocytes and then cortical astrocytes (Xu, Sapolsky & Giffard, 2001). They did not examine WM regions and concentrated on astrocytes from GM regions. Another study found that hippocampal astrocytes cultured from embryos were very sensitive to OGD (Zhao & Flavin, 2000). Zhao and Flavin (2000), also suggested that astrocyte sensitivity to ischaemia may be coupled to neuronal sensitivity, whereby injury or damage to one directly affects the other.

Middle cerebral artery occlusion (MCAO) is one model, which gives a better representation of focal ischaemia and a truer depiction of astrocyte sensitivity as the cells are *in situ*. A limitation of this is that not all astrocytes experience the same amount of ischaemia as the technique aims to replicate an ischaemic lesion and so not all regions are affected. This model has been used to try to determine differences in astrocyte sensitivity to ischaemia. Lukaszevicz *et al.* (2002) used MCAO to investigate astrocyte sensitivity in GM and WM regions. In this study it is was found that cortical protoplasmic astrocytes were remarkably sensitive to ischaemia, with swelling and detrimental changes to cells seen within the first hour of ischaemia (Lukaszevicz et al., 2002).

An earlier group using MCAO in adult rats found visible astrocyte swelling in WM after just 30 minutes of ischaemia (Pantoni, Garcia & Gutierrez, 1996). Astrocyte damage increased as the period of ischaemia increased, after six hours of ischaemic conditions, some astrocyte processes had swollen to approximately 10μm diameter. This is a severe effect caused by the extended period of ischaemia and shows the kind of injury that can be sustained by astrocytes. Swelling will impair astrocyte function and if all cell types swell then

this will cause physical changes to the tissue. Pantoni *et al* (1996) found alterations in the oligodendrocyte population and concluded that WM is very sensitive to ischaemic insult. Here it was also observed that cells may die prior to any observation of physical evidence of damage. Changes were also observed in the nerve fibres themselves, which could inhibit the transmission of action potentials, thus causing further CNS dysfunction (Pantoni, Garcia & Gutierrez, 1996).

A preliminary study carried out by Shannon et al (2007) investigated regional differences in astrocyte sensitivity to OGD. For this work neonatal animals (postnatal day (P) 10) were used and the regions examined were optic nerve and hippocampal brain slices. At this age, it was found that ON astrocytes were more sensitive to OGD than the GM astrocytes. The model of ischaemia used here ensured that all regions were exposed to the same levels of OGD. This gave a more accurate reading of astrocyte sensitivity to ischaemia. The study of astrocytes *in situ* allows different CNS regions to be compared under the same conditions. We hypothesize that regional differences in astrocyte sensitivity to acute ischaemia exist. Astrocytes are not the only glial cell type that are affected by ischaemic insult. Oligodendrocytes also play an important role as the myelinating cell of the CNS.

3.1.4 Oligodendrocyte sensitivity to ischaemia

It is widely accepted and documented that oligodendrocytes experience high sensitivity to ischaemic insult. The literature shows that most oligodendrocyte cell death appears to occur during the reperfusion period, within three hours of the initial insult (Pantoni, Garcia & Gutierrez, 1996), with changes to oligodendrocytes occurring after just 30 minutes of MCAO. Physical damage to oligodendrocytes worsened as the length of MCAO was increased,

eventually leading to vacuolation of myelin. Widespread oligodendrocyte cell death has been achieved within nine hours after a relatively short period of ischaemia of just 30 minutes (Mifsud *et al.*, 2014). In most studies, samples of oligodendrocyte health are not obtained until many hours after the insult and establishment of reperfusion. This would suggest that the vulnerability seen is a result of secondary injury sustained during reperfusion of the tissue rather than the initial ischaemic insult.

It is not known whether oligodendrocytes exhibit regional sensitivities to ischaemia. However, from the description of oligodendrocytes by Del Rio-Hortega in 1921 we know that these cells are not homogeneous. He described interfascicular cells that are predominantly found in the WM and perineuronal cells that can be clearly seen in GM (Bunge, 1968). The perineuronal subtype of oligodendroglia are not explicitly connected to a myelin sheath (Ludwin, 1997). Ludwin (1997) proposed that these cells may assist with regulation of the neuronal microenvironment. The interfascicular oligodendrocytes are the cells which are closely associated with the myelin sheath. The appearance of these cells is that of a "string of pearls" and it is these cells which are responsible for the myelination of WM axons. Through the sequencing of RNA expression of ten brain regions, 13 different populations of oligodendrocytes have been described (Marques *et al.*, 2016). The heterogeneity that has been found suggests that these subpopulations of oligodendrocytes may have different roles in the CNS depending upon their location.

Petito *et al.* (1998) suggested oligodendrocytes may display regional susceptibility to ischaemic insult. They determined that GM oligodendrocytes were more sensitive to ischaemic injury than neurons. Although not as diverse as astrocytes, oligodendrocytes are a heterogeneous population that have

classically been divided into four subtypes (Butt *et al.*, 1994). They have been grouped according to their branching pattern and the number of myelin sheaths that they support (Butt *et al.*, 1994). This may have some bearing on their susceptibility to ischaemic insult. Those cells with more myelin sheaths have a greater amount of membrane to support. Thereby increasing the metabolic demands upon the cell and making then more susceptible to injury.

It was decided to investigate oligodendrocytes in the same manner as astrocytes to see the effect that our OGD protocol would have on oligodendrocyte cell death and to determine whether there would be regional sensitivity to ischaemia or whether this is just a phenomenon observed in astrocytes. In addition, to explore whether it was acute ischaemic injury which caused the observed widespread sensitivity of these cells.

3.2 RESULTS: PCR GENOTYPING

To maintain the health of both transgenic mouse colonies (GFAP-GFP and PLP-GFP) mice were genotyped to determine new breeding pairs. The DNA used was extracted from ear notch samples, obtained exclusively for genotyping. Figure 3.1 shows the typical result obtained for genotyping, the bright bands show the presence of the GFP transgene in the sample (black arrows) and thus the expression of GFP in the cells of interest. For both lines wild-type mice were crossed with heterozygous mice, meaning only half of the offspring would have the transgene present.

There are bands present in all lanes, however it was established that the brighter bands were indicative of animals which were positively expressing the GFP gene.
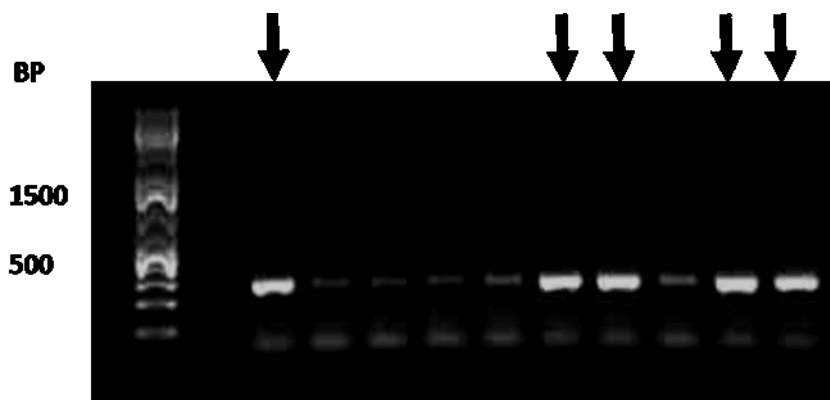
Figure 3.1: Representative image of agarose gel. Black arrows show animals positive for GFP. Gene ladder used was 1kb plus (Thermo Scientific).

3.3 Results: Green fluorescent protein (GFP) expression in astrocytes

The transgenic mice used for the following work specifically express GFP in astrocytes, under the GFAP promoter. Astrocytes expressing GFP are visible during live imaging and in fixed tissue (figure 3.2). Astrocytes seen during live imaging are marked with white arrows in the confocal images (figures 3.1A and B). The images in the first column are from the corpus callosum (CC), whilst those in the second column are from the dentate gyrus (DG)

First, it was determined whether the observed GFP was expressed in the correct cell type. Immunofluorescence staining was carried out on fixed frozen brain sections from adult mice (P30 and over) using an antibody against aldehyde dehydrogenase (ALDH1L1), which is an alternative marker for astrocytes. GFP (green) was observed in cells that morphologically had the appearance of astrocytes (figure 3.2C and D). ALDH1L1 (red) was detected in astrocyte cell bodies and processes (figure 3.2E and F). GFP expression in astrocytes was confirmed with the co-localisation of red and green signals, producing an orange colour (yellow arrows figure 3.2G-J).

Not all of the GFP expressing astrocytes present are positive for ALDH1L1; this is as ALDH1L1 is not a universal astrocyte marker and is only present in a subset of the astrocyte population. The expressed GFP is present in cells which display astrocyte morphology and characteristics such as long branched processes. These images also show the difference in the number of astrocytes seen in these two regions (CC and DG). In WM there are many more astrocytes than in GM, showing the heterogeneous nature of astrocytes that exists between regions (figures 3.2 and 3.3).
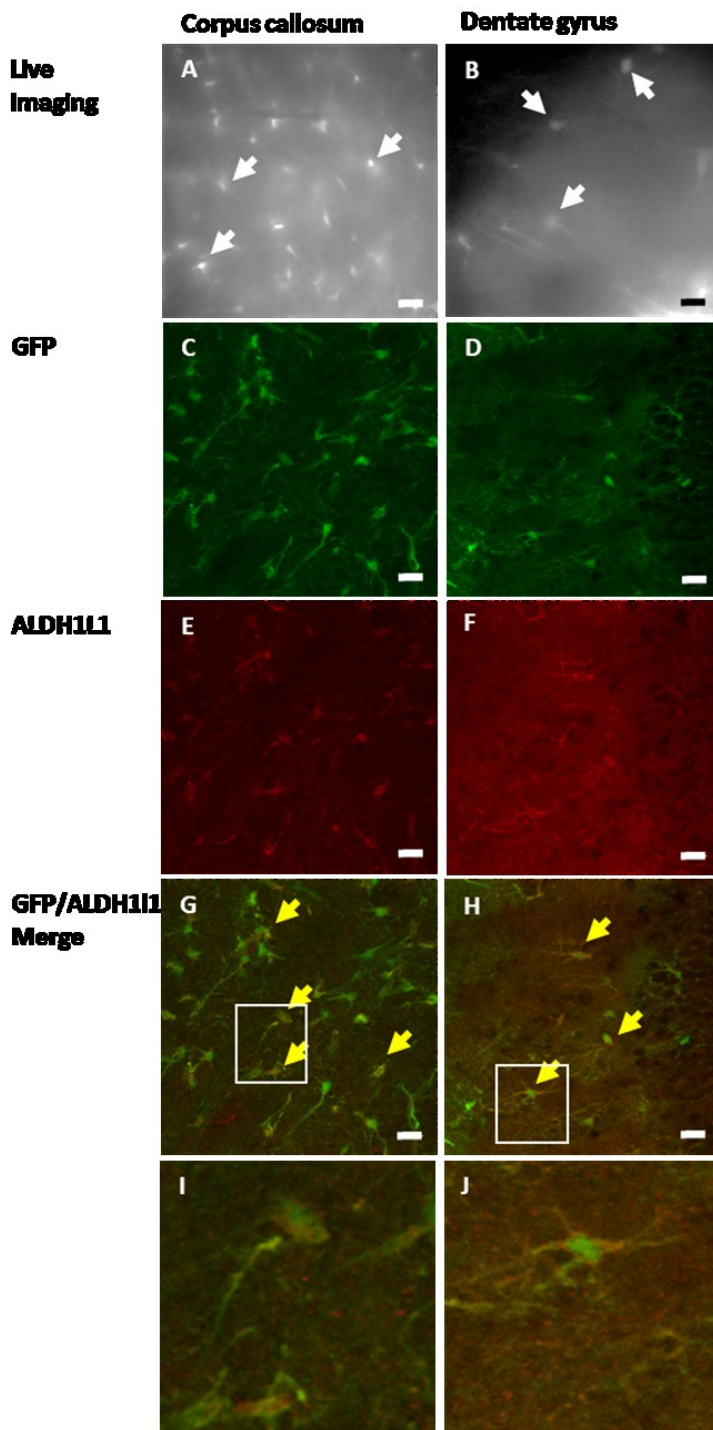
Figure 3.2: GFP expression in astrocytes. A + B: GFP expressed under the GFAP promoter in astrocytes as seen during live imaging. White arrows show representative astrocytes. **A, C, E, G + I:** CC, **B, D, F, H + J:** DG. **C – J:** are confocal maximum projections of Z stacks of fixed tissue sections. **C + D:** GFP in green. **E + F:** ALDH1L1 in red. **G + H:** merged image, yellow arrows show co-localisation of the green and red signals. **I** and **J:** show the area within boxes in images **G** and **H** respectively. Scale bars = 20µm.

3.4 RESULTS: GLIAL MORPHOLOGY

Investigation of glial cell sensitivity to acute ischaemic insult and the mechanisms behind ischaemic sensitivity were carried out using two transgenic mouse lines. These allowed astrocyte and oligodendrocyte cells to be visualised through the expression of green fluorescent protein (GFP), which was under the control of cell-type specific promoters (see below). Astrocyte and oligodendrocyte morphology in white matter (corpus callosum, CC) and grey matter (dentate gyrus, DG) in these two transgenic lines can be clearly seen in confocal images (figure 3.3 and 3.4) There is a clear difference between the long branched processes of the astrocytes and the more organised directed processes of the oligodendrocytes. The cell somas of these glial cell types also display differences; the oligodendrocyte cell bodies have a more regular shape when compared to astrocyte cell bodies and exist closer together often in lines. From figure 3.3 and 3.4 it can be seen that there are differences between glial cell types located in different regions. For example, astrocytes in the CC are arranged differently to those in the DG. The DG cells are further apart and are not overlapping as much as those in the CC. A major difference between the regions is the cell density. It is apparent that there are many more oligodendrocytes in the CC than the DG. The difference in density is similar for astrocytes.
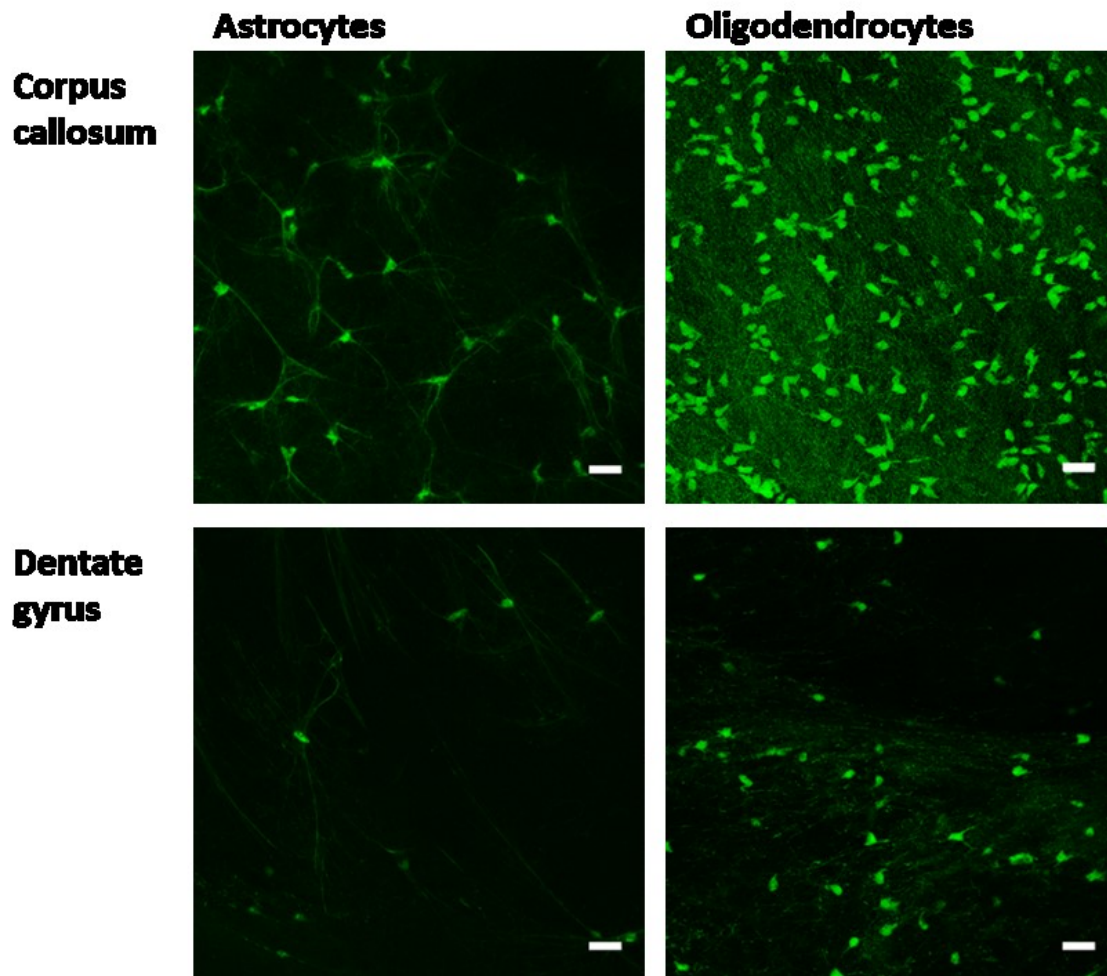
Figure 3.3: Astrocyte and oligodendrocyte morphology. Images show differences in cellular morphology between astrocytes and oligodendrocytes. Upper panel corpus callosum, lower panel dentate gyrus. The images are Z projections of confocal images taken from fixed brain slices (100μm thick). Scale bars = 20μm.
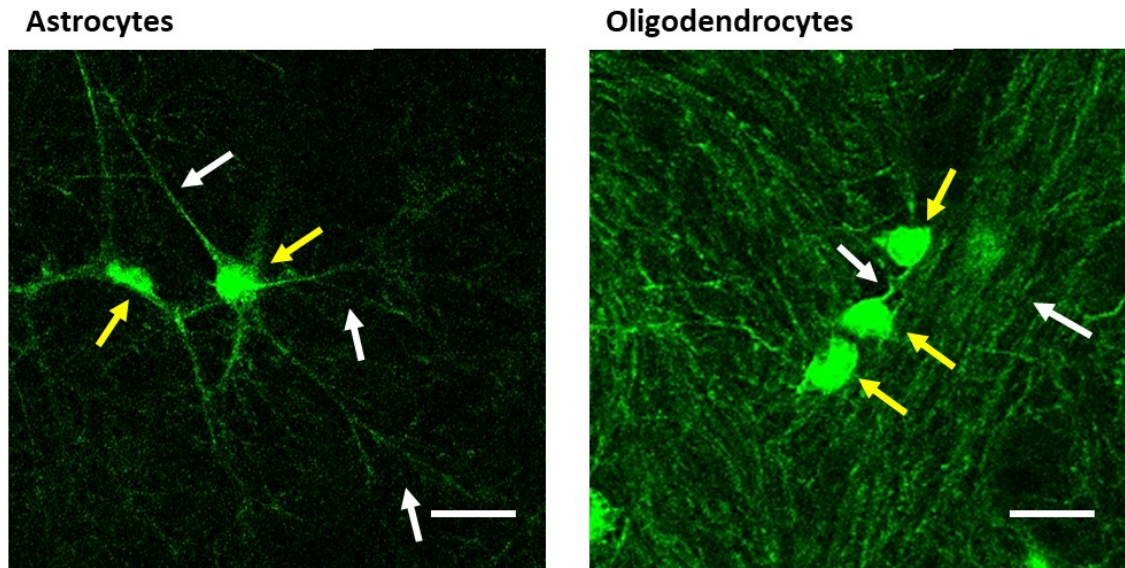
Figure 3.4: Glial morphological differences: Zoomed in confocal images of fixed brain slices, both are cells in CC. The white arrows depict examples of processes. The astrocyte process are far reaching and branched. Oligodendrocyte processes are more organised, less branched and show the direction of axons. Yellow arrows show cell bodies and how they are differently arranged in WM. The astrocyte cell bodies have irregular placement, whilst oligodendrocytes have regular placement and are close together. Scale bars = 20μm.

3.5 RESULTS: ASTROCYTE SENSITIVITY TO ISCHAEMIA

Next, it was determined which populations of astrocytes were most sensitive to OGD. Experiments lasted 100 minutes (figure 3.5A), the first 10 minutes were under control conditions with oxygen and aCSF perfusion. This period was followed by 60 minutes of OGD aCSF perfusion with nitrogen and the final 30 minutes was reperfusion, where aCSF and oxygen were re-introduced. The regions selected to be investigated were; corpus callosum (CC); optic nerve (ON); external capsule (EC); striatum (STR); hippocampal regions CA1 and dentate gyrus (DG); cortex, motor area (CTX (M)) and cortex, auditory/sensory (CTX (A/S)) (figure 3.5B). These regions were selected to give a variety of white and grey matter regions and to include those with known neuronal vulnerability. All regions showed no evidence of cell death under control conditions with aCSF perfusion only and oxygen.
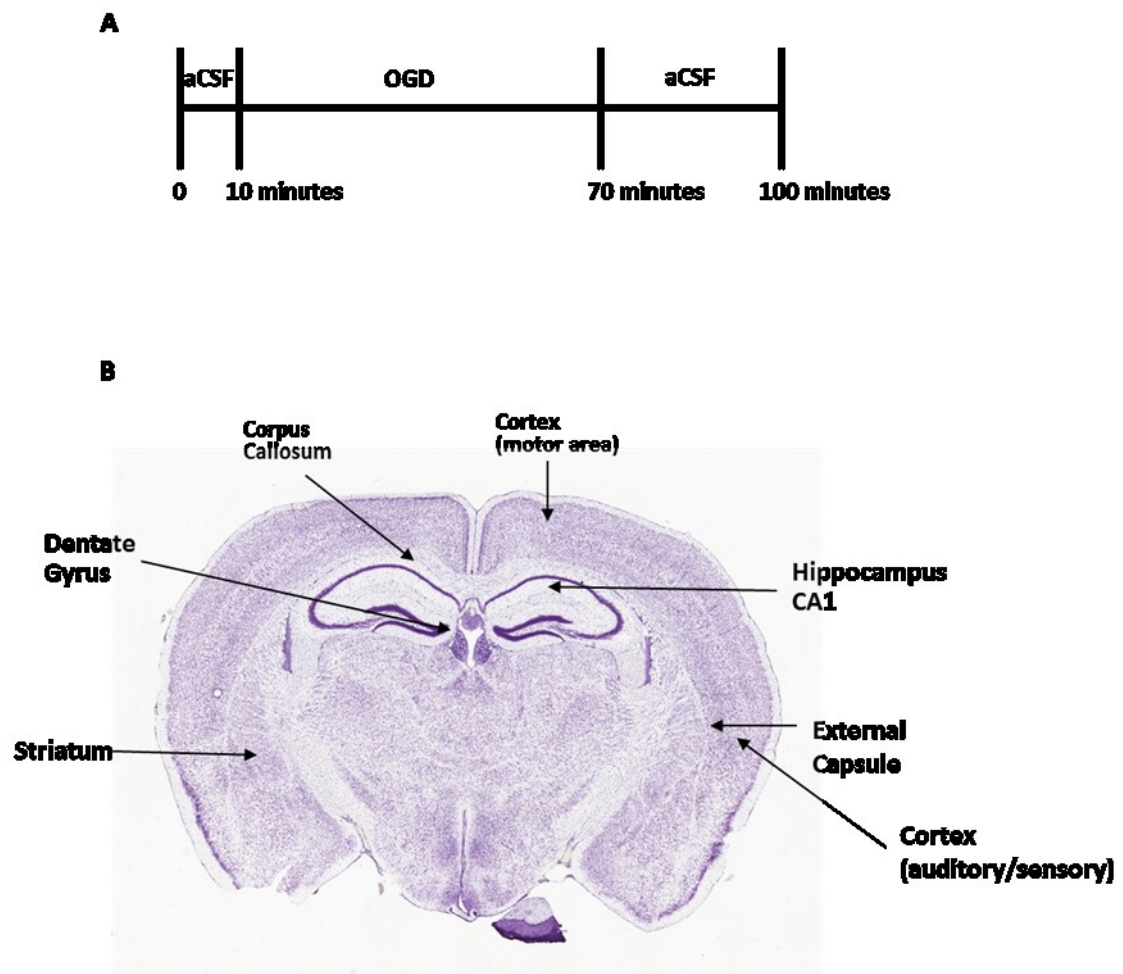
Figure 3.5: Experimental design and brain regions examined. A: Time points of live imaging protocol, 10 minutes of aCSF with oxygen, followed by 60 minutes of OGD with nitrogen and 30 minutes of reperfusion (aCSF with oxygen). Experiments lasted 100 minutes in total. **B:** Illustration of brain regions examined for astrocyte sensitivity to ischaemia (adapted from the Allen adult mouse reference brain atlas 2011).

3.5.1 Astrocyte cell death in response to OGD

Live confocal images of each region examined were obtained every minute in control and OGD conditions, shown at 0 minutes, 50 minutes and 100 minutes (end of the reperfusion period, figures 3.6 to 3.15). For all images, the white arrows illustrate the cells, which survive throughout the experiment. The yellow arrows depict the cells which died during the experiment due to OGD and reperfusion of the tissue.

3.5.1.1 White matter regional sensitivity

The ON astrocyte population showed tolerance to OGD with 33.54 ± 13.11% cell death by the end of the protocol (figure 3.6C). The majority of astrocytes that are present at the beginning of the experiment are therefore still present at 100 minutes (figure 3.6A). In these confocal images, the nerves are positioned across the field of view in both aCSF and OGD conditions.

The corpus callosum (CC) astrocytes were also resistant to OGD with cell death only reaching 31.95 ± 9.33% by the end of the protocol (figure 3.7C). It was observed that many astrocytes survived OGD and the reperfusion period (figure 3.7A) and that most astrocytes in this region do not lose membrane integrity during OGD. The cell death observed in these white matter tracts suggests that WM fibrous astrocytes are tolerant of acute ischaemic insult. The cell death profiles of the ON and CC showed that the t for half maximal cell death were similar, 68.36 ± 6.82 mins and 62.00 ± 2.32 mins respectively which suggests that these astrocyte populations behave in a similar manner (figures 3.6C and 3.7C).

The final WM tract investigated was the external capsule (EC, figure 3.8). This region produced a high degree of cell death, 75.11 ± 3.36% (figure 3.5C),

which was significantly higher compared to the other two WM regions (p=0.031). It is known that this region is often affected during haemorrhagic stroke (Chung *et al.*, 2000). This susceptibility may also predispose the region to be vulnerable to ischaemic stroke. The value for *t* for this region (figure 3.8C) was 57.83 ± 3.61mins showing the EC behaved more similarly to hippocampal and striatal astrocytes than the WM astrocytes.
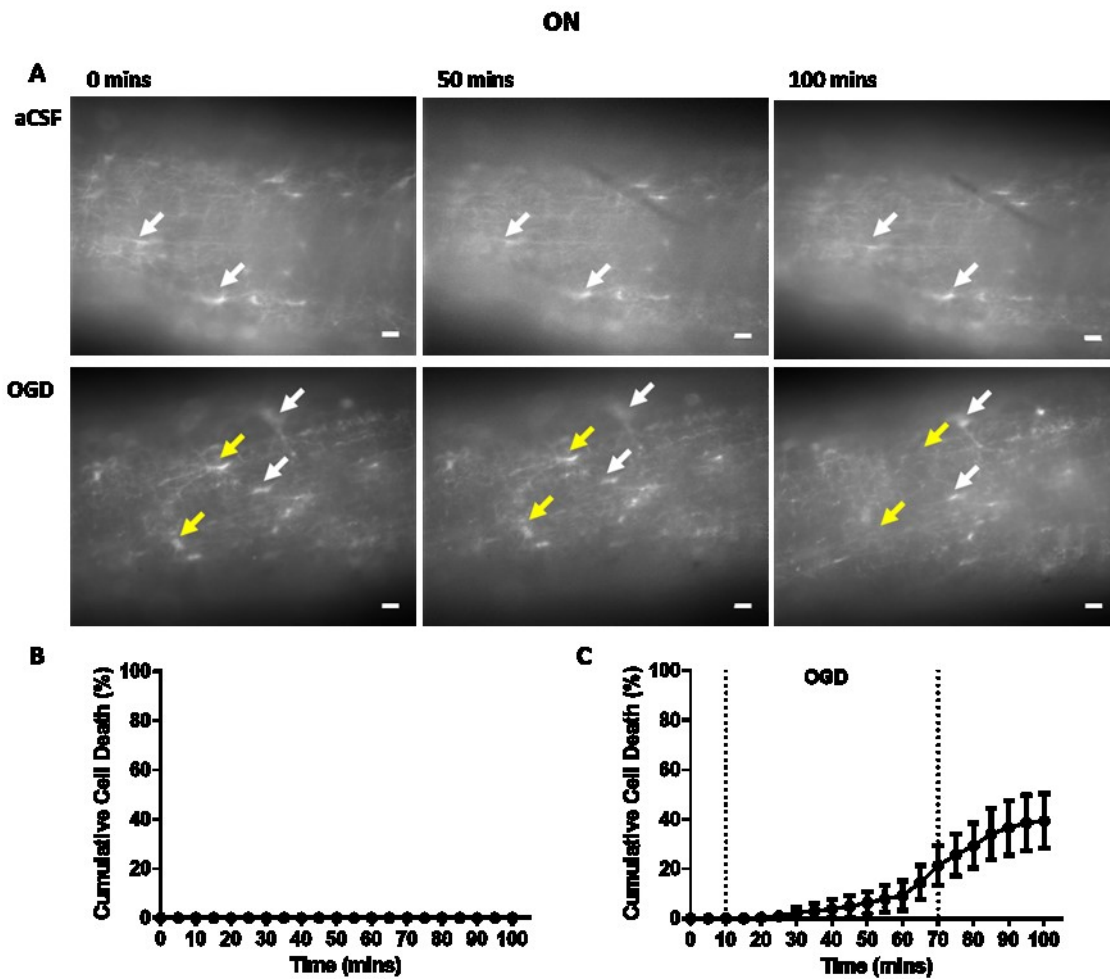
Figure 3.6: Astrocyte sensitivity to OGD in optic nerve (ON). A: Confocal images taken at 0, 50 and 100 minutes. Upper panel is control conditions with aCSF only, lower panel during experimental conditions with OGD. White arrows show cells present throughout experiments, yellow arrows show cells that died during OGD treatment. Scale bars = 20μM. **B + C:** Cell death over time with these treatments, **B:** aCSF n=35/2, **C:** OGD n=275/6 (n numbers = number of cells/number of nerves). Error bars = SEM.
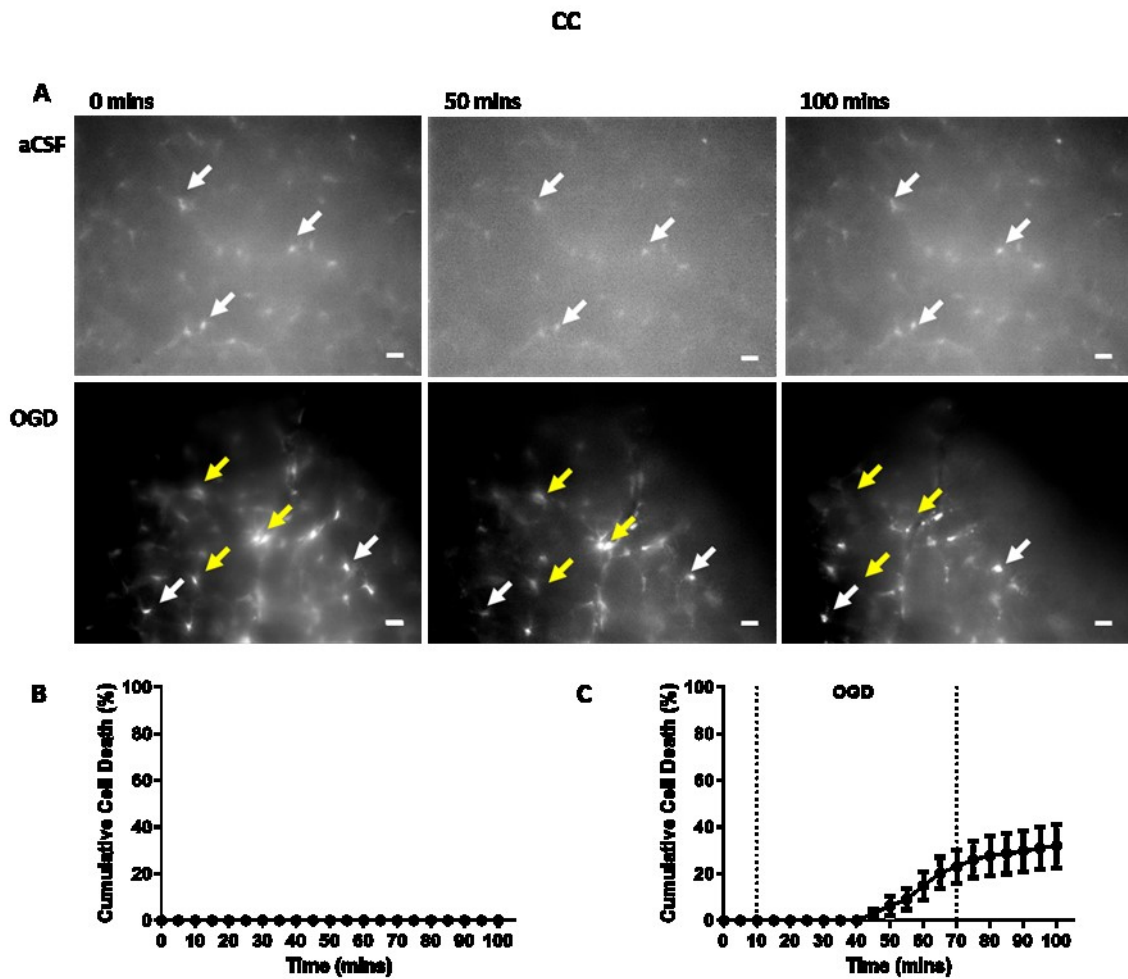
Figure 3.7: Astrocyte sensitivity to OGD in corpus callosum (CC). A: Confocal images taken at 0, 50 and 100 minutes. Upper panel is control conditions with aCSF only, lower panel during experimental conditions with OGD. White arrows show cells present throughout experiments, yellow arrows show cells that died during OGD treatment. Scale bars = 20μM. **B + C:** Cell death over time with these treatments, **B:** aCSF n=75/2, **C:** OGD n=193/6 (n numbers = number of cells/number of slices). Error bars = SEM.
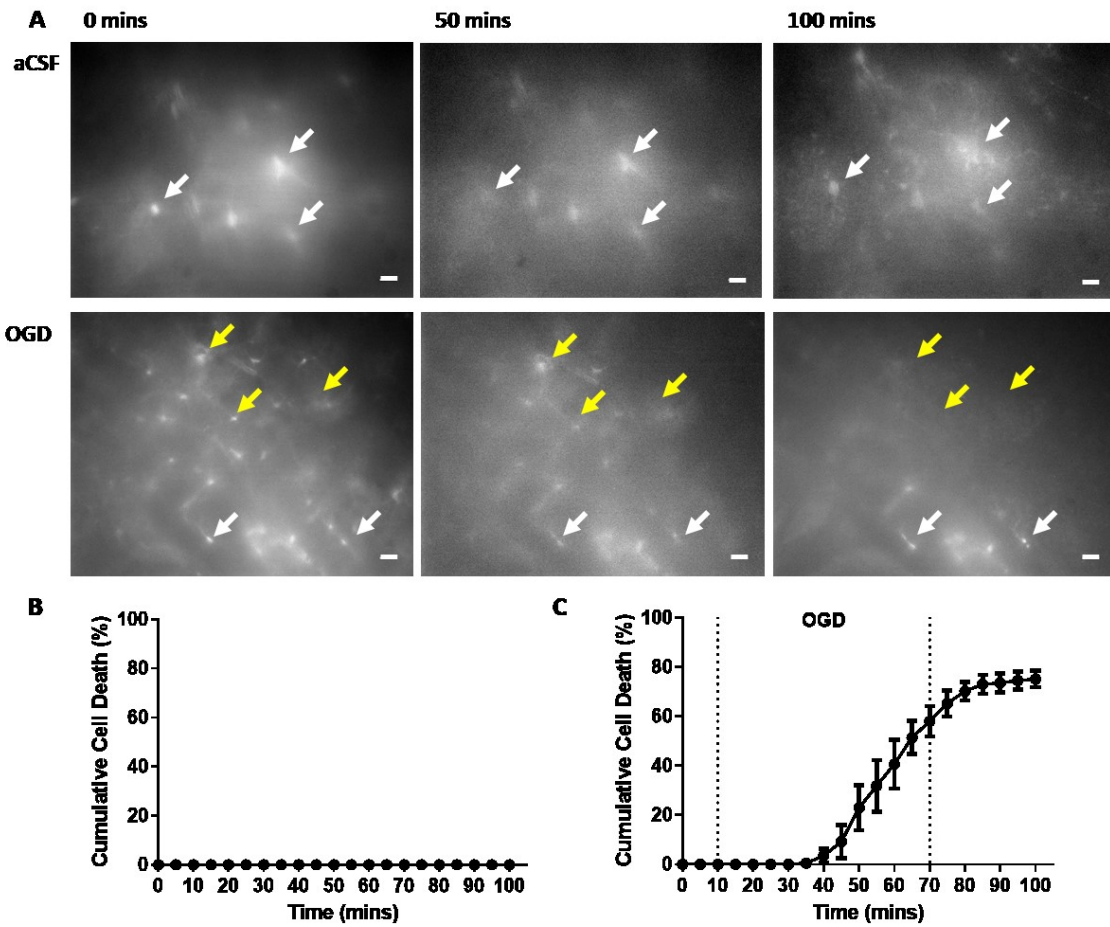
Figure 3.8: Astrocyte sensitivity to OGD in external capsule (EC). A: Confocal images taken at 0, 50 and 100 minutes. Upper panel is control conditions with aCSF only, lower panel during experimental conditions with OGD. White arrows show cells present throughout experiments, yellow arrows show cells that died during OGD treatment. Scale bars = 20μM. **B + C:** Cell death over time with these treatments, **B:** aCSF n=26/2, **C:** OGD n=184/6 (n numbers = number of cells/number of slices). Error bars = SEM.

3.5.1.2 Grey matter regional sensitivity

In the GM regions examined, it was generally observed that there were higher levels of astrocyte cell death. In the cortex (motor area) (CTX (M)), cell death reached 63.17 ± 6.59% (figure 3.9C). In the confocal images, the upper edge of the cortex is visible; this is the edge of the brain slice (figure 3.9A). On the pial surface are astrocytes, which are located on the edge of the cortex and project their processes down into the cortex.

To see whether this amount of cell death was unique to this region of the cortex, another cortical region was also examined, the auditory/sensory area (CTX (A/S)) (figure 3.10). In both aCSF and OGD images, the edge of the slice can be seen (figure 3.10A). In the OGD images cell death was observed, the yellow arrows depict cells which have died. The cell pointed out by the arrow in the upper right corner shows this well. This region showed high cell death in response to OGD of 81.33 ± 13.36% (figure 3.10C), which illustrates that cortical astrocyte populations are sensitive to acute ischaemic insult. The t half maxima for CTX (M) was 70.25 ± 2.98 mins and CTX (A/S) was 66.58 ± 3.77mins (figure 3.9C and 3.10C). These results suggest that astrocytes located in cortical regions have a comparable response to ischaemic insult.

The pial astrocytes would appear to be a subtype, if not a separate population of astrocytes. Their morphology is quite different from other protoplasmic astrocytes; their processes are not highly branched and they project down into the cortex and across the pial surface (figures 3.9A and 3.10A). Work carried out by the group has found that these pial astrocytes may be particularly vulnerable to ischaemia (unpublished). The relationship between cell distance from the cortex surface and time of cell death was therefore investigated (figure 3.11). A proportion of pial astrocytes died at 20 to 35

minutes ODG. There were pial astrocytes, which survived OGD and reperfusion (figures 3.9A and 3.10A). Most cortical astrocytes die towards the end of OGD and into the reperfusion period regardless of the distance from the surface (figure 3.11).

The astrocytes in different cortical layers were examined more closely, to see if astrocytes from the same layers died at a similar time point (figure 3.12). The number of cells to die at each time point was plotted for whole cortex (pooled results of the two cortical regions examined, figure 3.12A). Here, it shows that initial cell death occurs early after a short period of OGD. However, most cell death occurs after 30 to 40 minutes of OGD.

The cell death was examined for the individual cortical layers. The cell death of pial astrocytes on the surface almost depicts two populations (figure 3.12B). Those that are vulnerable to OGD and those that die towards the end of OGD and during reperfusion. This population behaves like other cortical astrocytes and show some tolerance. Astrocytes in layer 1 were located between 0 and 100μm from the surface (figure 3.12C). This layer contains no neuronal cell bodies and OGD induced cell death of astrocytes in this layer occurred in the late OGD period and during reperfusion. The astrocytes in layer 2, located over 100μm from the surface, responded to OGD in a similar manner as layer 1 (figure 3.12D). In these layers, most astrocyte death occurred after 30 to 40 minutes of OGD. There were significant differences between the total amounts of cell death seen in each layer (figure 3.12E). The lowest cell death was seen in layer 1, $14.51 \pm 3.57\%$, cell death of pial astrocytes was higher at $18.56 \pm 3.46\%$ (not significant). The highest amount of cell death was in layer 2 and over which achieved $37.74 \pm 4.76\%$ cell death. This was significantly higher than pial astrocyte cell death ($p=0.0047$) and layer 1 cell death

(p=0.0006). Overall, these findings suggest that for cortical astrocytes the distance from the surface does not affect the time at which OGD induced cell death occurs and that the majority of cell death occurs further from the surface of the cortex.
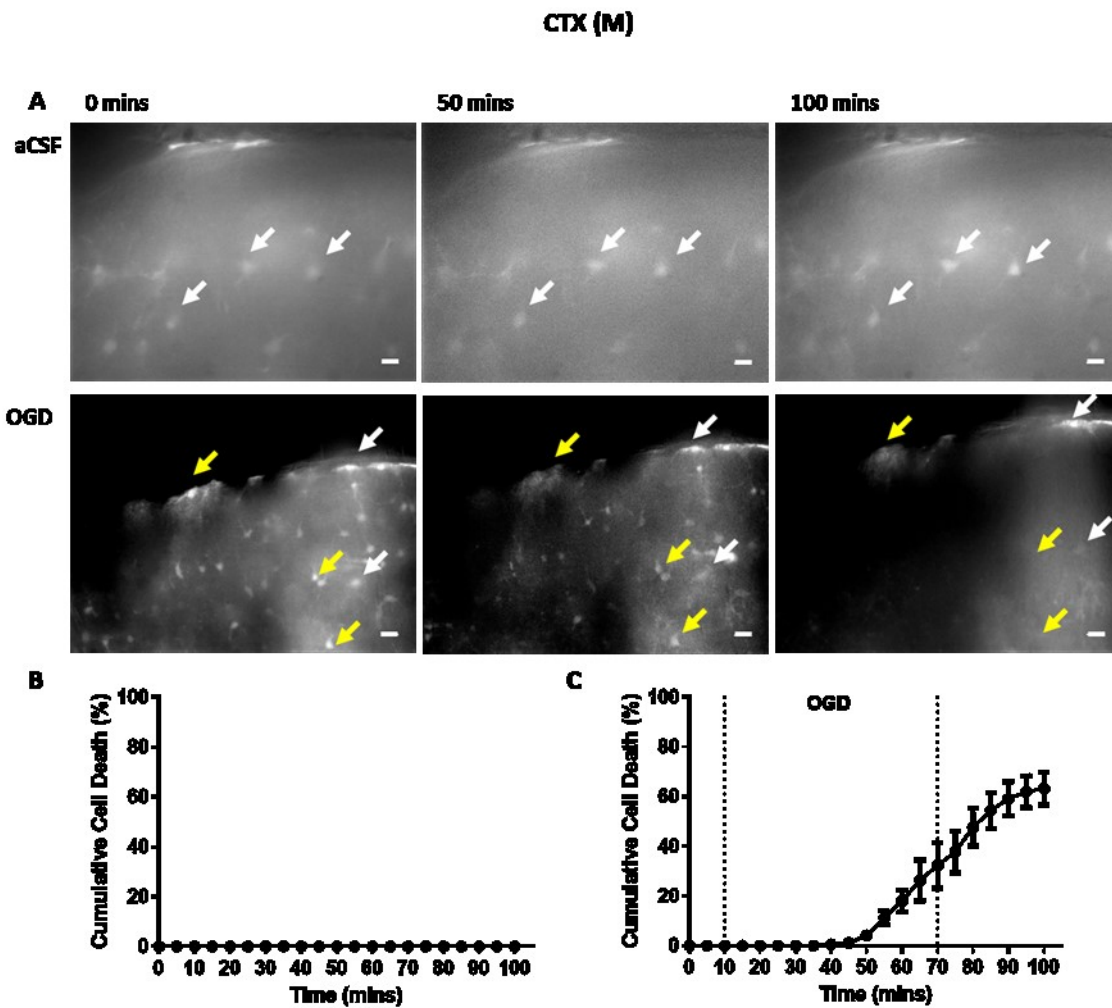
Figure 3.9: Astrocyte sensitivity to OGD in cortex, motor area (CTX (M). A: Confocal images taken at 0, 50 and 100 minutes. Upper panel is control conditions with aCSF only, lower panel during experimental conditions with OGD. In both panels the edge of the cortex can be seen. White arrows show cells present throughout experiments, yellow arrows show cells that died during OGD treatment. Scale bars = 20µM. **B + C:** Cell death over time with these treatments, **B:** aCSF n=23/2, **C:** OGD n=150/6 (n numbers = number of cells/number of slices). Error bars = SEM.
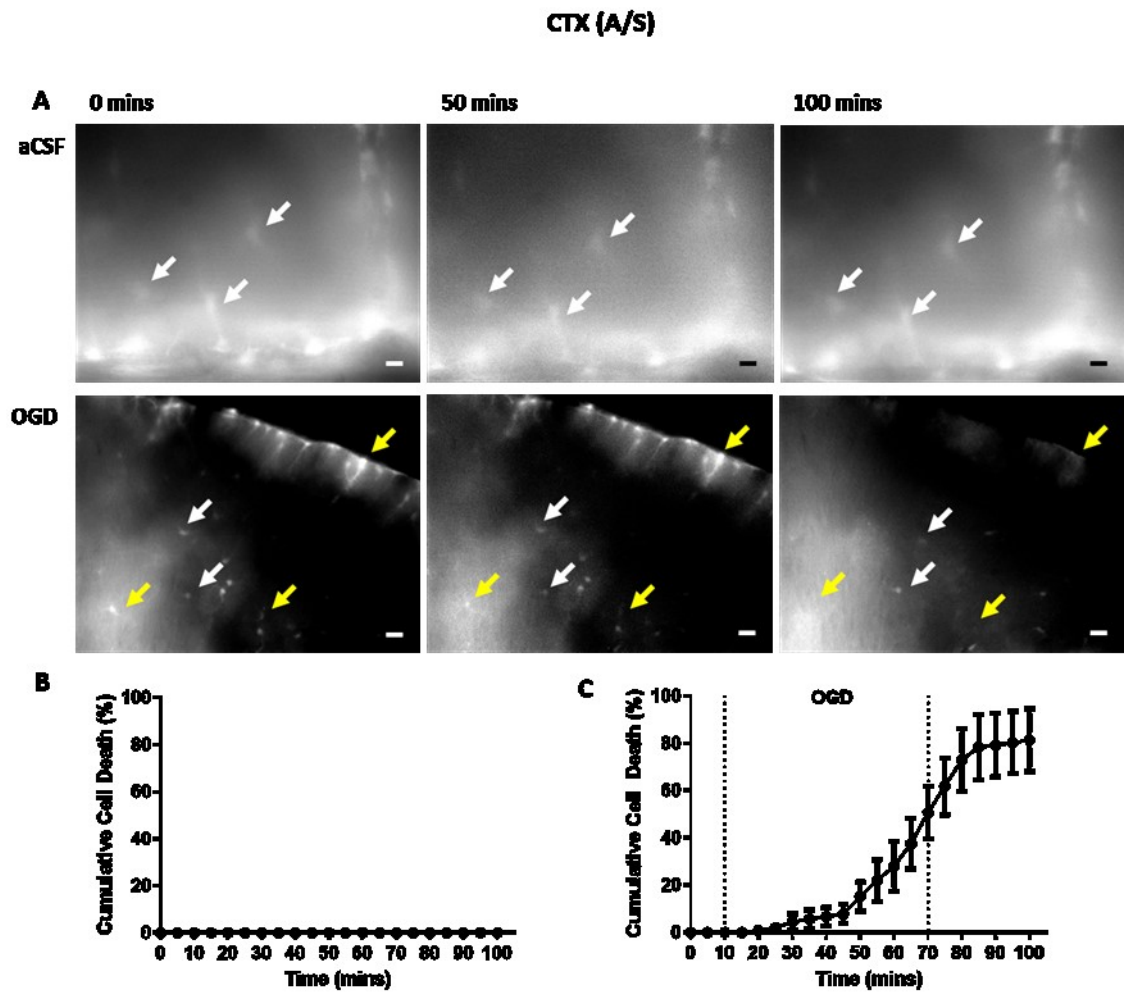
Figure 3.10: Astrocyte sensitivity to OGD in cortex, auditory/sensory area (CTX (A/S). **A:** Confocal images taken at 0, 50 and 100 minutes. Upper panel is control conditions with aCSF only, lower panel during experimental conditions with OGD. In both panels the edge of the cortex can be seen. White arrows show cells present throughout experiments, yellow arrows show cells that died during OGD treatment. Scale bars = 20µM. **B + C:** Cell death over time with these treatments, **B:** aCSF n=29/2, **C:** OGD n=195/6 (n numbers = number of cells/number of slices). Error bars = SEM.
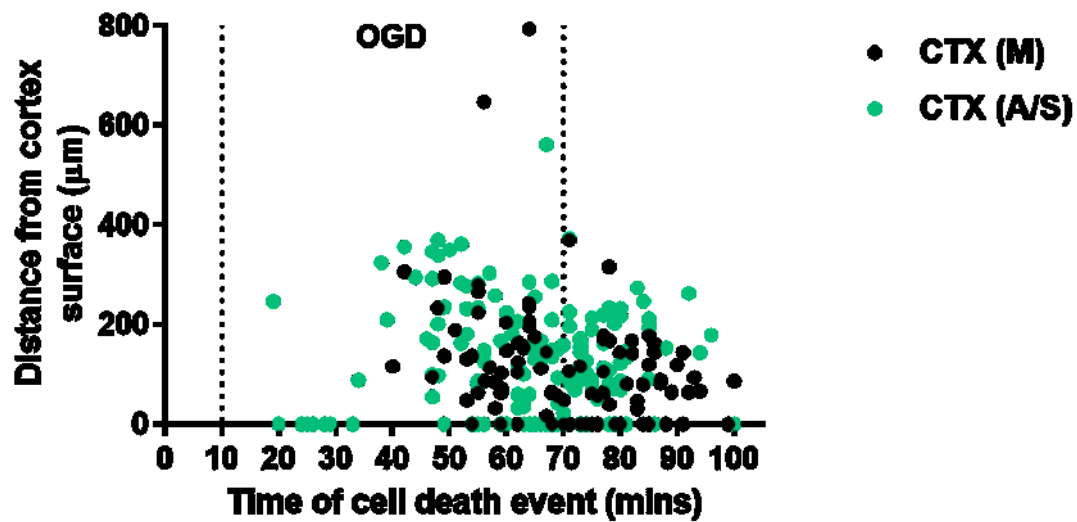
Figure 3.11: Effect of distance from cortex surface on OGD induced astrocyte cell death. Astrocytes from both cortex regions examined, CTX (M) n = 150/6, CTX (A/S) n = 195/6. Each point is one cell death event
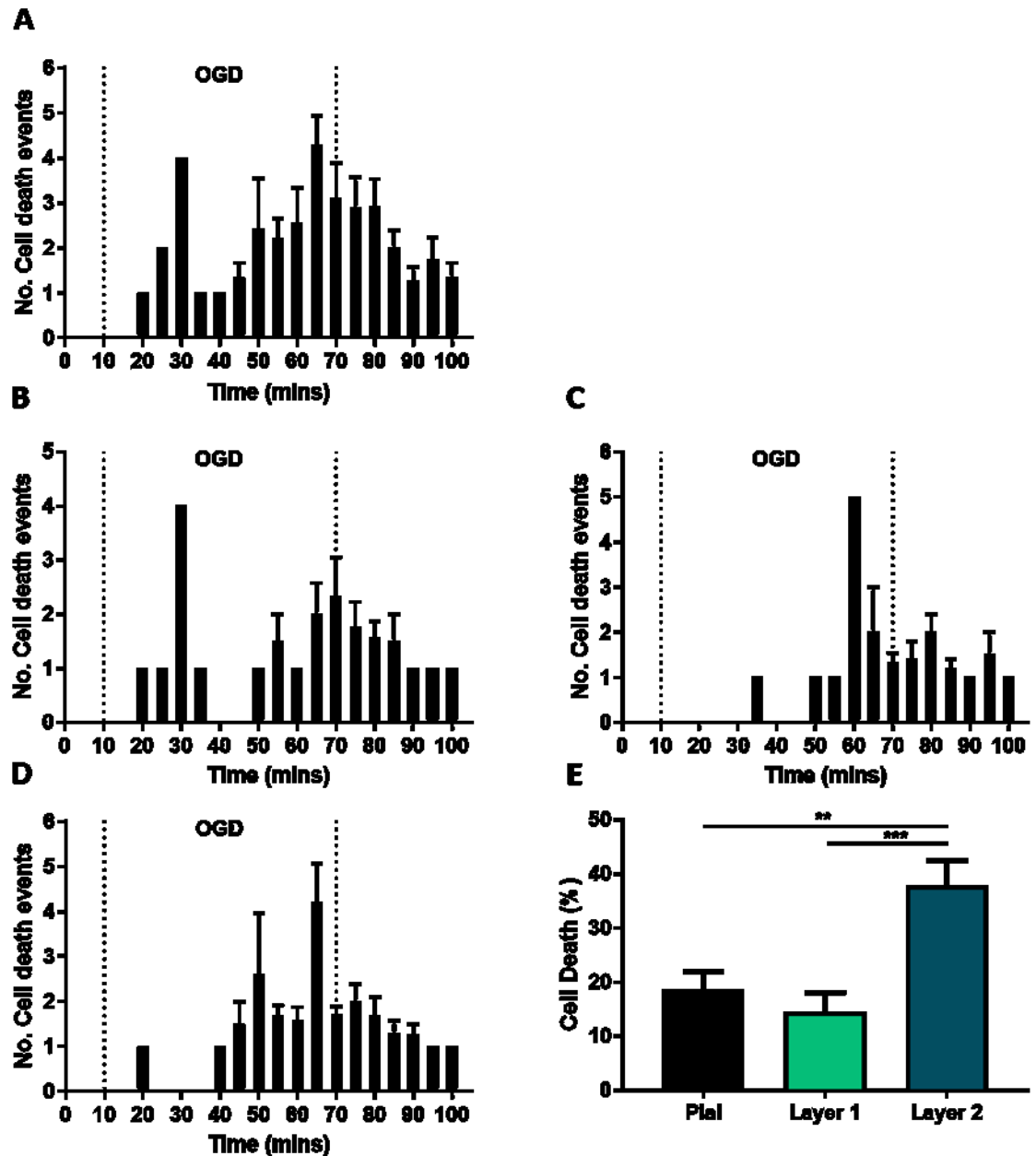
Figure 3.12: OGD induced astrocyte cell death in different cortical layers. A: Cell death events in each 5 minute period throughout cortex (pooled data). **B:** cell death events for pial astrocytes on cortex surface. **C:** cell death events for layer 1 astrocytes (within100μm from cortex surface). **D:** cell death events for layer 2 astrocytes and those situated over 100μm from the cortex surface. **E:** total astrocyte cell death in each layer. Error bars = SEM

The hippocampal astrocytes in the CA1 region and the dentate gyrus (DG) behaved in a similar manner to those in the cortex in response to OGD. The cell death recorded in these regions was approximately 94.04 ± 1.81% (figure 3.13C) for CA1 and 97.30 ± 1.24% for DG (figure 3.14C). In the OGD images for both regions clouds of GFP can be seen, this occurs after the cellular contents is released when cells rupture due to a loss of membrane integrity (figures 3.13A and 3.14A). In the aCSF confocal images, the edge of the dentate gyrus is running across the lower right corner of the images (figure 3.14A). The t half maxima achieved for these regions was 49.17 ± 4.99 mins for CA1 and 54.64 ± 3.3 mins for DG. These were the lowest values obtained for t which illustrates that cell death occurred rapidly in these regions.

Cell death caused by OGD in the striatum (STR) was similar to other GM regions and reached around 97.37 ± 1.19% (figure 3.15C). The structure present in the OGD panel of the confocal images is a blood vessel (figure 3.15A). The astrocytes that are wrapping the blood vessel are periventricular astrocytes. These periventricular astrocytes appear brighter than other astrocyte populations; it is unknown why this phenomenon occurs. The cell death rate in STR is similar to that for the hippocampal astrocytes (figure 3.15C). From these results, it would seem that striatal astrocytes have more in common with the populations that are found in CA1 and DG.
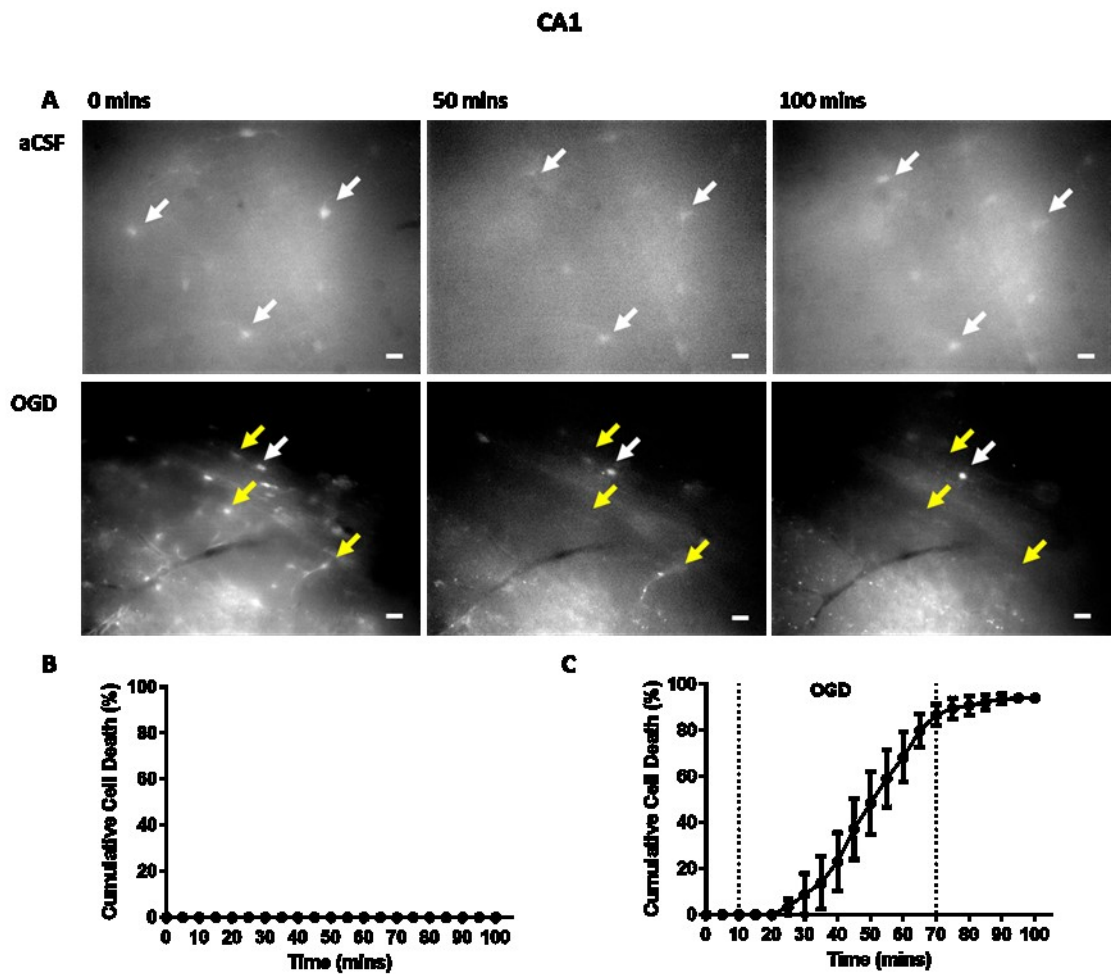
Figure 3.13: Astrocyte sensitivity to OGD in CA1 region of hippocampus (CA1). A: Confocal images taken at 0, 50 and 100 minutes. Upper panel is control conditions with aCSF only, lower panel during experimental conditions with OGD. White arrows show cells present throughout experiments, yellow arrows show cells that died during OGD treatment. Scale bars = 20μM. B + C: Cell death over time with these treatments, B: aCSF n=25/2, C: OGD n=222/6 (n numbers = number of cells/number of slices). Error bars = SEM.
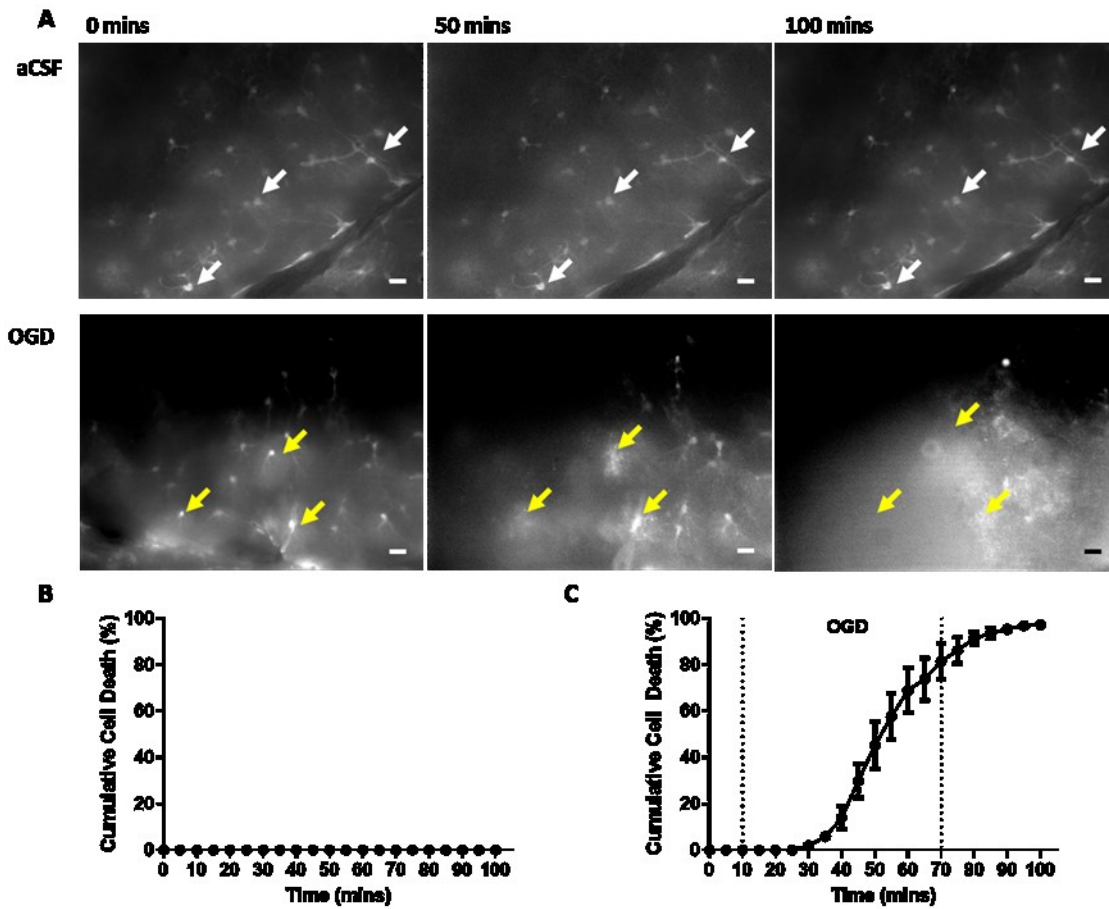
Figure 3.14: Astrocyte sensitivity to OGD in dentate gyrus of hippocampus (DG). A: Confocal images taken at 0, 50 and 100 minutes. Upper panel is control conditions with aCSF only, lower panel during experimental conditions with OGD. White arrows show cells present throughout experiments, yellow arrows show cells that died during OGD treatment. Scale bars = 20µM. **B + C:** Cell death over time with these treatments, **B:** aCSF n=85/2, **C:** OGD n=210/6 (n numbers = number of cells/number of slices). Error bars = SEM.
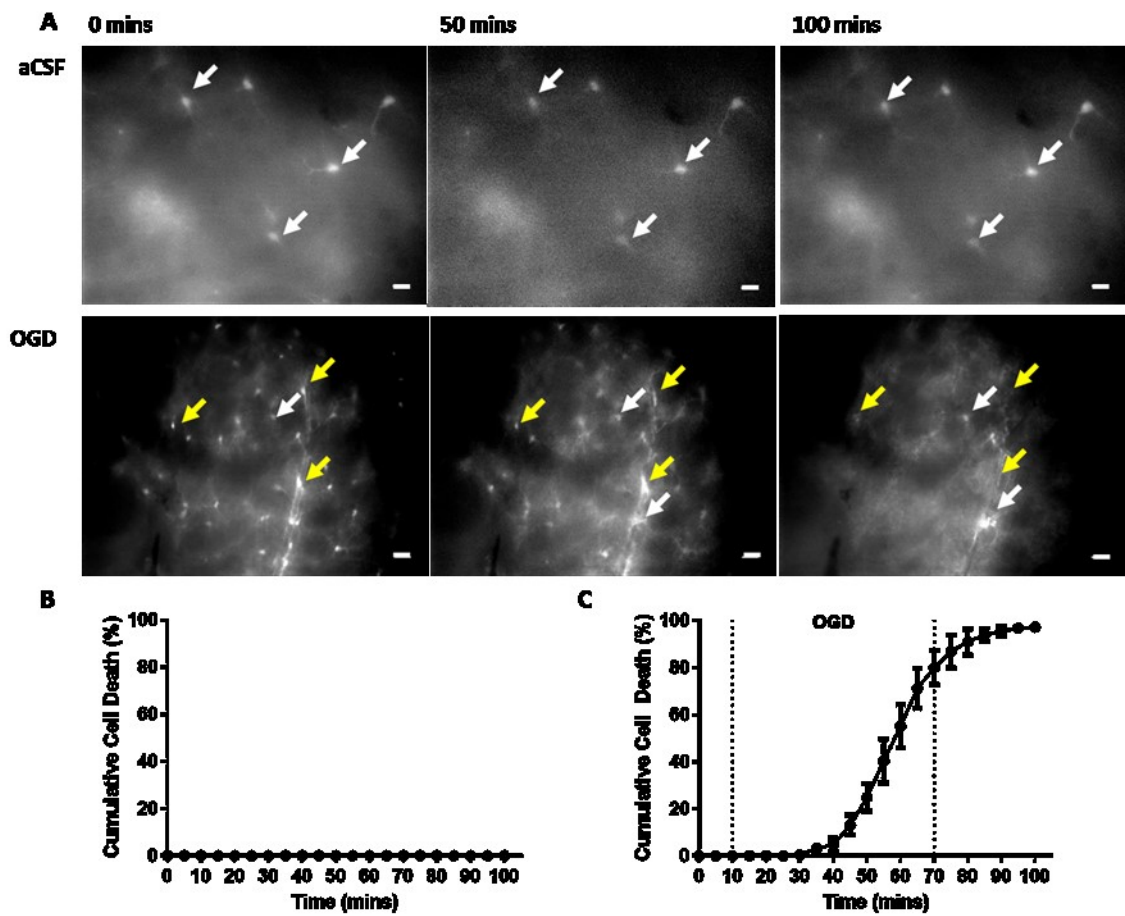
Figure 3.15: Astrocyte sensitivity to OGD in striatum (STR). A: Confocal images taken at 0, 50 and 100 minutes. Upper panel is control conditions with aCSF only, lower panel during experimental conditions with OGD. White arrows show cells present throughout experiments, yellow arrows show cells that died during OGD treatment. Scale bars = 20μM. **B + C:** Cell death over time with these treatments, **B:** aCSF n=28/2, **C:** OGD n=189/6 (n numbers = number of cells/number of slices). Error bars = SEM.

3.5.1.3 Comparison of regional sensitivity

To find which regions were most sensitive to OGD, the cell death for each region investigated was compared using one way ANOVA. First, OGD induced cell death for each region was compared to control conditions (aCSF only, figure 3.16A). This comparison confirmed that cell death was the result of OGD, as no cell death occurred during aCSF only conditions. Next, the amount of cell death was compared at the end of OGD to the end of reperfusion, for each region (figure 3.16B). It was seen that for most regions, the majority of cell death occurs during OGD and less occurs during reperfusion. The only exception is in the striatum where there was a significant increase in cell death from the end of OGD to the end of the reperfusion period (figure 3.16B, p=0.0141). This suggests that the high amount of astrocyte cell death in this region is due to reperfusion injury as well as the initial ischaemic insult.

These findings show that there were differences in the amount of astrocyte cell death, depending upon astrocyte location. The OGD induced cell death was then compared between regions, after OGD (figure 3.16C) and after the reperfusion period (3.16D). The main differences in amounts of cell death were between WM and GM astrocytes. The greatest difference at the end of OGD was between ON and CA1, ON and DG (p=<0.0001). There were significant differences between CC and both the hippocampal regions (CA1 and DG, p=<0.0001).These significant differences in the regions remained after the reperfusion period.

Differences in cell death were also observed between WM regions; significantly increased cell death is seen in EC when compared to ON and CC at the end of OGD (p=0.0310) and the end of reperfusion (p=0.0180). After OGD (figure 3.16C), significant differences in amounts of cell death were seen

between different GM regions, between the CTX (M) and the CA1 (p=0.0012) and the CTX (M) and DG (p=0.0047). Although these did not remain after the reperfusion period, the comparisons found that cell death in different GM regions was not significantly different.
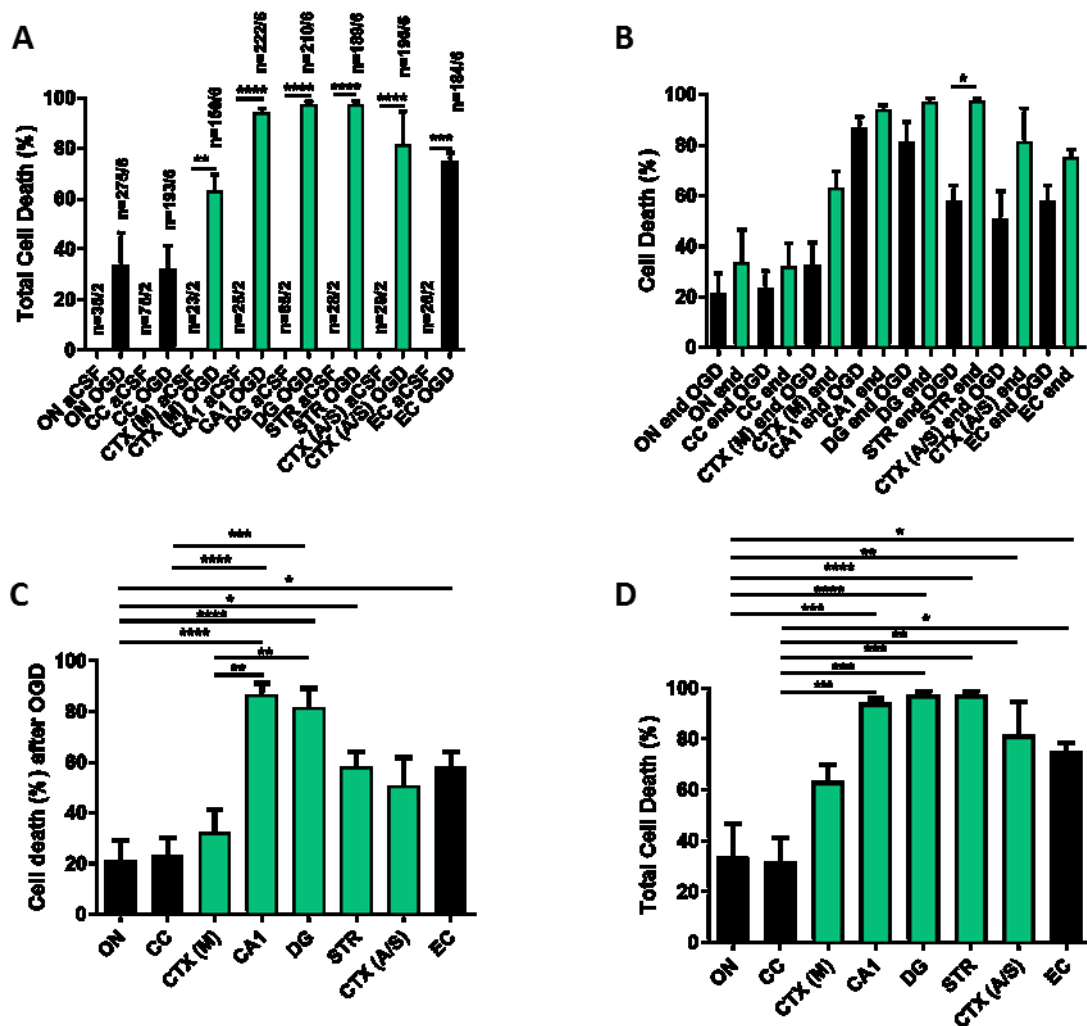
Figure 3.16: Astrocyte sensitivity to OGD varies between regions. A: total astrocyte cell death for each region in control (aCSF only) and OGD conditions. OGD compared to aCSF for that region only. N numbers = number of cells/number of slices. **B:** astrocyte cell death for each region after 60 minutes OGD (black bars) and at the end of reperfusion (green bars). Comparison made between these two time points for each region only. **C:** shows cell death after 60 minutes OGD. **D:** total astrocyte cell death after 60 minutes OGD and 30 minutes reperfusion. **C + D:** Each region compared to every other region, comparisons without bars not significant. Error bars = SEM. For p values, *=<0.05, **=<0.01, ***=0,001 and ****=<0.0001. **A, C + D** Black bars are white matter regions, green bars are grey matter.

The rate of cell death also shows some variance between WM and GM (figure 3.17). In all regions little cell death occurs before 30 minutes OGD, the highest observed was 23.01 ± 12.65% in CA1. The majority of astrocyte cell death occurred in the latter half of the OGD period, less cell death occurred during the reperfusion period (70-100 minutes). The WM regions exhibit similar rates of cell death, where t ranges from 62.00 ± 2.32 to 68.36 ± 6.82 mins, excluding the EC which had a slightly lower t of 57.50 ± 3.61 mins. The cortical regions had a steady progression of cell death throughout the experiment; this pattern was also observed in STR. Although, in this region the cell death was faster and greater. In CA1 and DG most cell death occurred after 30 minutes OGD, with less cell death occurring during the reperfusion period. The EC cell death profile was more similar to that of hippocampal astrocytes than the WM astrocytes, as mentioned previously.

Taken together these findings strongly suggest that astrocyte sensitivity to ischaemic insult depends upon the physical location of astrocyte populations within the CNS. It was determined that the CC was the region where astrocytes were most resistant to OGD, whereas DG contained astrocytes, which were most sensitive to ischaemia. These regions were taken forward to investigate the mechanisms behind the differences discovered in regional astrocyte sensitivity to OGD.
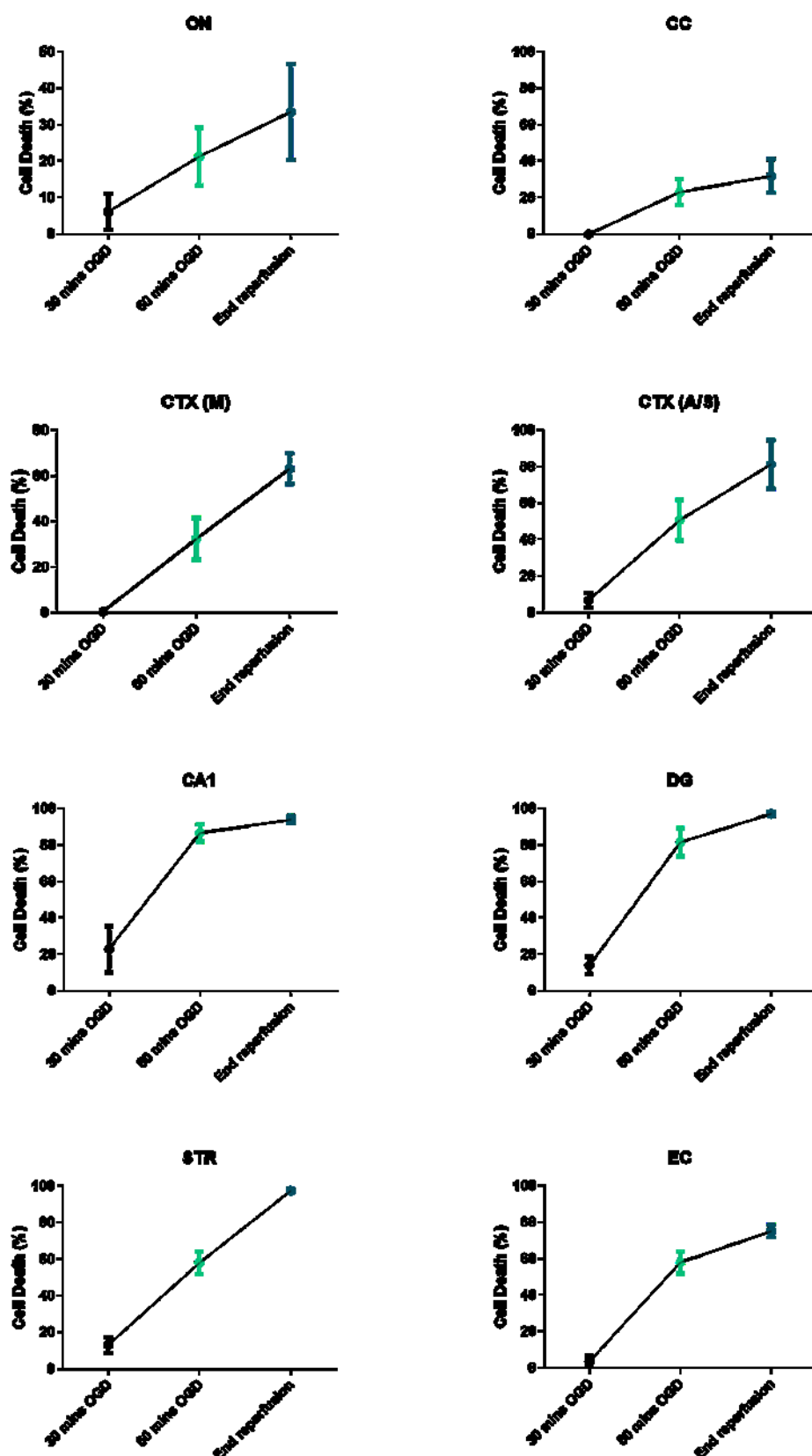
Figure 3.17: Astrocyte cell death region comparison. Graphs for each region showing the percentage of cell death after 30 minutes OGD, 60 minutes OGD and after reperfusion. Error bars = SEM.

3.5.2 Neonate astrocyte sensitivity to OGD

After establishing the presence of astrocyte regional sensitivity to OGD in adult brain slices, astrocyte sensitivity in neonatal (P10) brain slices was investigated. This was to see if neonates exhibited the same pattern of astrocyte sensitivity to ischaemia as was seen in adults. Previously, it had been found that neonatal GM astrocytes were more resistant to OGD than neonatal WM astrocytes (Shannon, Salter & Fern, 2007). Earlier work by the group found the amount of astrocyte cell death in neonate ON was 59.5% ± 5.2% (Fern, 1998).

There are a greater density of GFP expressing cells present in neonatal CC and DG than in the same regions in adults (figure 3.18A), only those showing clear astrocyte morphology were counted. The cell death profiles for each neonatal region (CC and DG) differ to those obtained for the same regions in adults (figures 3.18B and C). The t value for each region was higher than the same adult region. For CC t increased from 62.00 ± 2.32 for adult cells to 78.30 ± 5.33 mins in the neonate (p=0.0029) and for DG t was increased from 54.64 ± 3.30 mins to 68.50 ± 3.13 mins for the neonate (p=0.0033). This suggests that neonatal astrocytes display resistance to insult. The total amount of cell death in neonatal regions was significantly lower than that observed in adult regions (p=0.0112 for CC and p=0.0088 for DG, figure 3.18D). The neonate CC astrocyte cell death was 10.86 ± 3.10% and neonate DG cell death was 67.38 ± 12.21%. This suggests that neonatal astrocytes are much more resistant to ischaemic injury than adult astrocytes from the same region. The total cell death seen in neonate DG is significantly higher than that in the neonate CC (p=<0.0001, figure 3.18D), following the same pattern of sensitivity as the adult astrocytes in these regions.
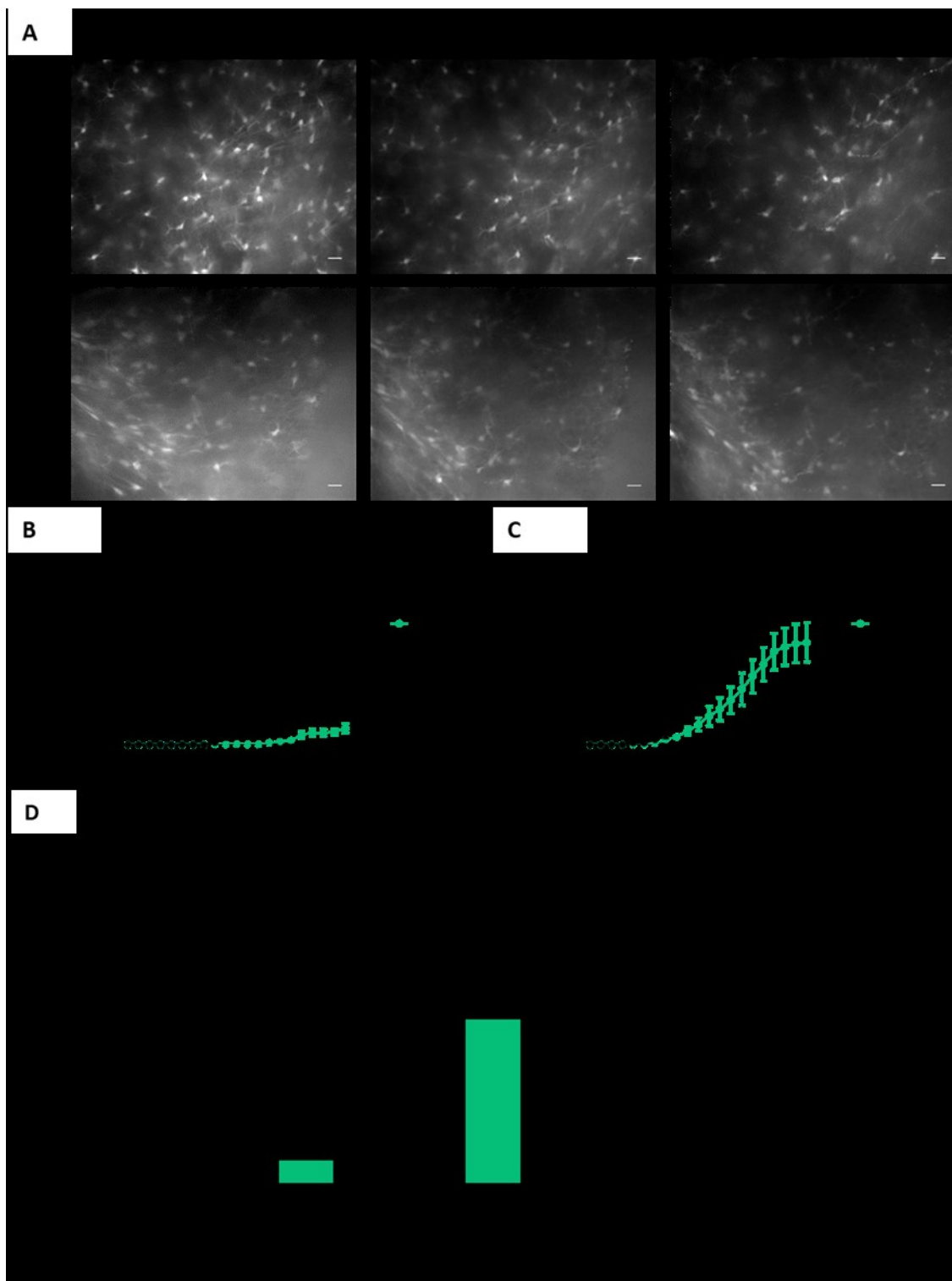
Figure 3.18: Neonatal astrocytes are more resistant to OGD than adult astrocytes: A: Confocal images of corpus callosum and dentate gyrus astrocytes taken at 0, 50 and 100 minutes. Scale bar = 20µm. **B + C:** neonate (green bars) and adult (black bars) astrocyte cell death over time in corpus callosum and dentate gyrus respectively. **D:** Comparison of total astrocyte cell death in neonate and adult brain regions after 60 minutes OGD and 30 minutes reperfusion. Error bars = SEM.

3.6 RESULTS: OLIGODENDROCYTE SENSITIVITY TO ISCHAEMIA

Astrocytes are not the only type of glial cell to interact with neurons and have a role in neuronal support (as previously discussed). Oligodendrocytes are also important for the correct function of neurons. The process of myelination puts oligodendrocytes in close proximity to neurons, allowing them to receive and respond to neuronal signals and provide metabolic support.

Due to the specific role that oligodendrocytes have, it was important to establish whether these cells were sensitive to acute ischaemic injury. Any injury to oligodendrocytes would be damaging to neurons and may impact neuronal survival during and after insult.

3.6.1 Oligodendrocytes are tolerant of OGD

To investigate oligodendrocyte sensitivity to ischaemia, oligodendrocytes in ON, CC and DG were observed. The same experimental protocol was followed as for investigation into astrocyte sensitivity. However, for oligodendrocyte experiments PLP-GFP transgenic mice were used. In these mice, oligodendrocytes express GFP under the promoter for proteolipid protein (Mallon *et al.*, 2002), which is specific to oligodendrocytes. There are numerous oligodendrocytes found in ON, these are interfascicular oligodendrocytes. In the confocal images the nerve is running across the field of view (figure 3.19A). In aCSF conditions, there was no cell death (figure 3.19B). Interestingly there was no OGD induced oligodendrocyte cell death in this region (figure 3.19C).

A similar pattern was seen in CC where it was found that there was very low OGD induced oligodendrocyte cell death (figure 3.20). The confocal images show the high density of oligodendrocytes in CC (figure 3.20A), due to white matter tracts containing myelinated axons. In the OGD 100 minutes image, it

appears as though there has been cell death. However, this is due to a change in the focal plane as the tissue preparation swells, distorting and moving the view of the cells. Only cells that were clearly visible throughout the experiment and not altered by the swelling of tissue were counted.

In the DG there are fewer oligodendrocytes present than in the WM (figure 3.21A) these are perineuronal oligodendrocytes. Again, in the OGD 100 minutes image it looks as though there has been death of oligodendrocytes, however this is due to the swelling of the surrounding tissue which alters the focus of the cells in view. In cases where cells could not be followed for the entirety of the experiment, they were disregarded and were not counted. The cell death profiles are given for control (aCSF, figure 3.21B) and OGD conditions (figure 3.21C). Even with OGD treatment GM oligodendrocytes still showed tolerance to insult as there was low cell death. All of the regions examined showed that oligodendrocytes are very tolerant to ischaemic insult. The low cell death achieved with ischaemic insult was not significantly different from control conditions (figure 3.22). When oligodendrocyte cell death was compared between regions, no significant differences were found. Taken together these findings suggest that oligodendrocytes in both GM and WM are very tolerant of acute ischaemic injury. This finding is in contrast with reports from the literature, where it is accepted that oligodendrocytes are extremely vulnerable to OGD.
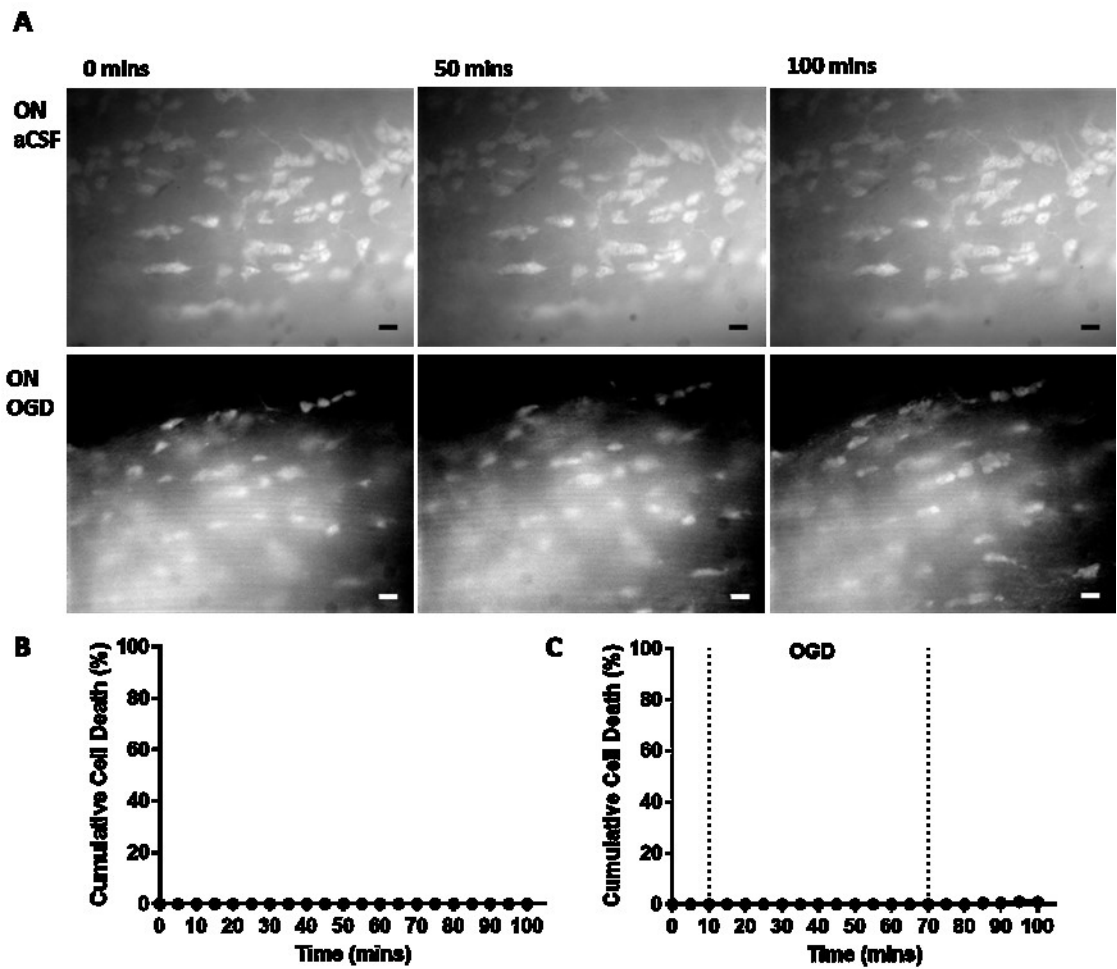
Figure 3.19: Oligodendrocyte sensitivity to OGD in optic nerve (ON). A: Confocal images of ON taken at time 0, 50 and 100 minutes. Scale bars = 20μm **B:** oligodendrocyte cell death over time control and **C:** OGD.
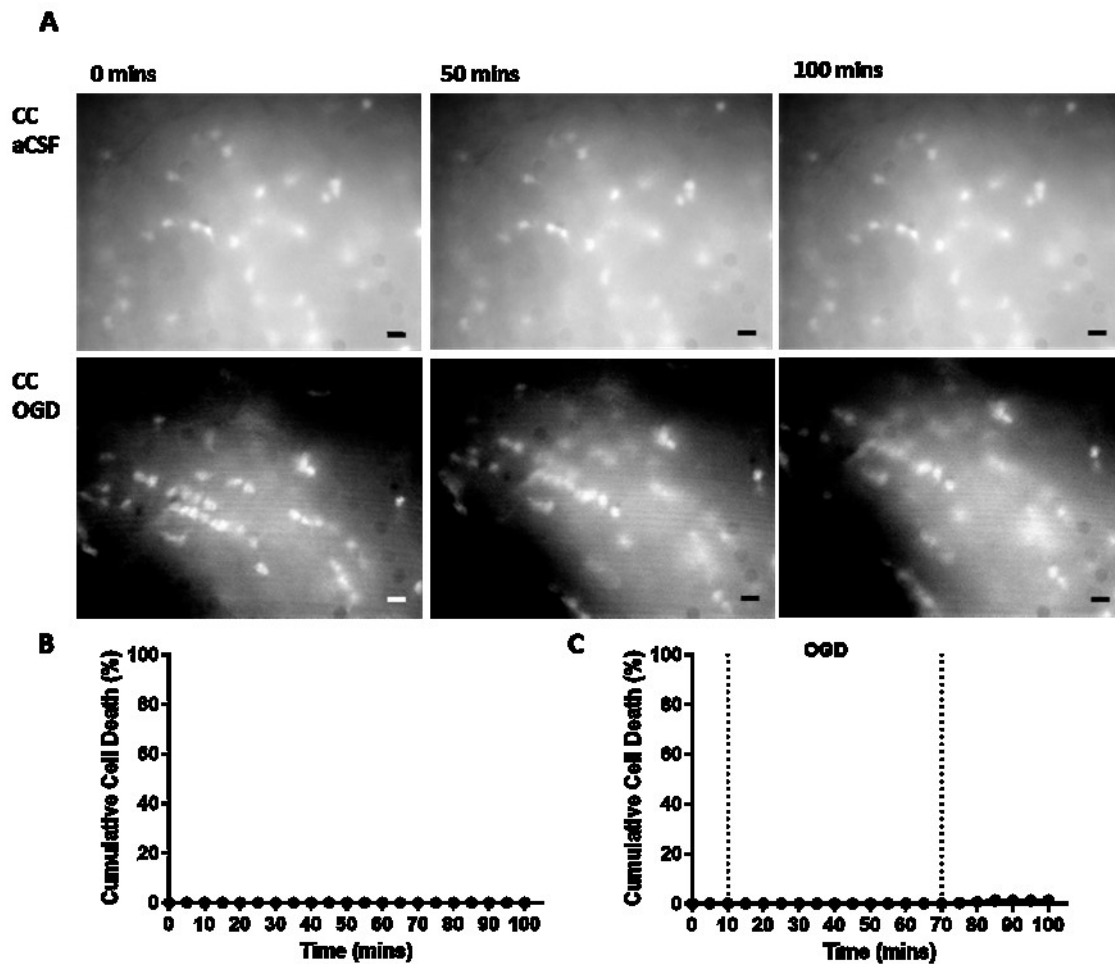
Figure 3.20: Oligodendrocyte sensitivity to OGD in corpus callosum (CC) A: Confocal images of CC taken at time 0, 50 and 100 minutes. Scale bars = 20µm B: oligodendrocyte cell death over time control and C: OGD.
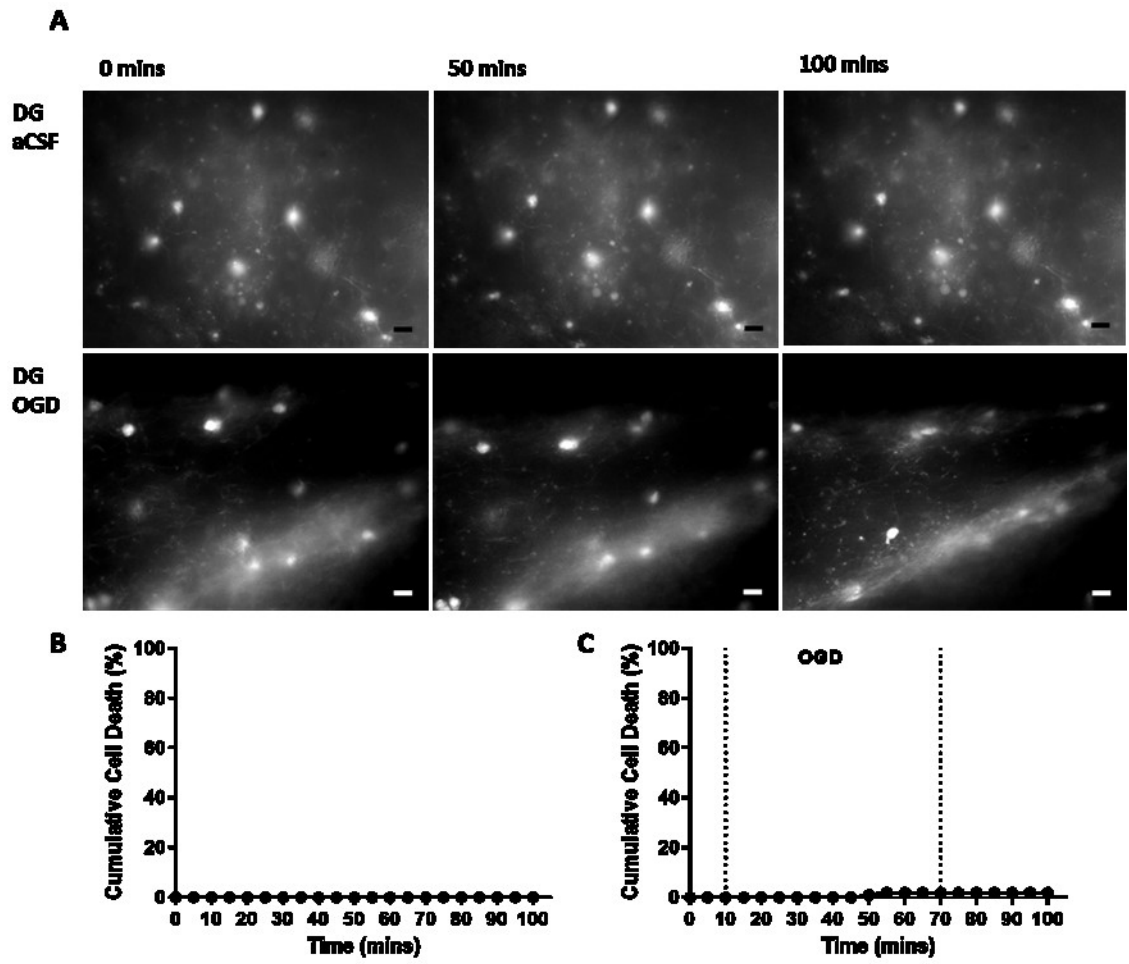
Figure 3.21: Oligodendrocyte sensitivity to OGD in dentate gyrus (DG) A:
Confocal images of DG taken at time 0, 50 and 100 minutes. Scale bars = 20µm
B: oligodendrocyte cell death over time control and **C:** OGD.
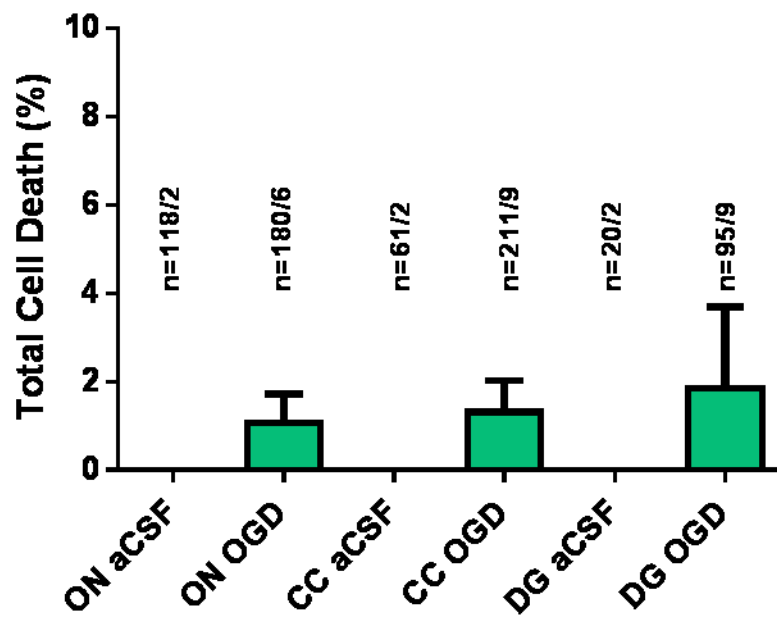
Figure 3.20: Oligodendrocytes are resistant to OGD. Graph of total oligodendrocyte cell death at 100 minutes. N numbers = number of cells/number of slices. Error bars = SEM.

3.7 COMPARISON OF GLIAL SENSITIVITY TO OGD

To see the differences in glial sensitivity to OGD the data from astrocytes and oligodendrocytes was compared for CC (figure 3.23 A and B), DG (figure 3.23 C and D) and ON regions (figure 3.23 E and F). For all regions examined, the cell death over time was very different between the two cell types, with astrocyte death generally increasing over time, whereas oligodendrocyte death remained low (figures 3.23A, C and E). When oligodendrocyte cell death did occur, it happened later during the OGD period than astrocytes cell death. In CC the OGD induced cell death that did occur was during reperfusion. There was a vast difference in the total amounts of cell death observed in each region between the two cell types (figures 3.23B, D and F). In CC and DG (figure 3.23B and D), there was the most dramatic difference in OGD induced cell death, with greater astrocyte cell death in both regions ($p=<0.0001$). In ON (figure 3.23F), astrocyte cell death in OGD conditions was higher when compared to oligodendrocyte death, however the significance was lower ($p=0.0231$). These results show that astrocytes are more sensitive to ischaemic injury than oligodendrocytes, even though it is accepted that oligodendrocytes are the population, which are more sensitive to ischaemic insult.
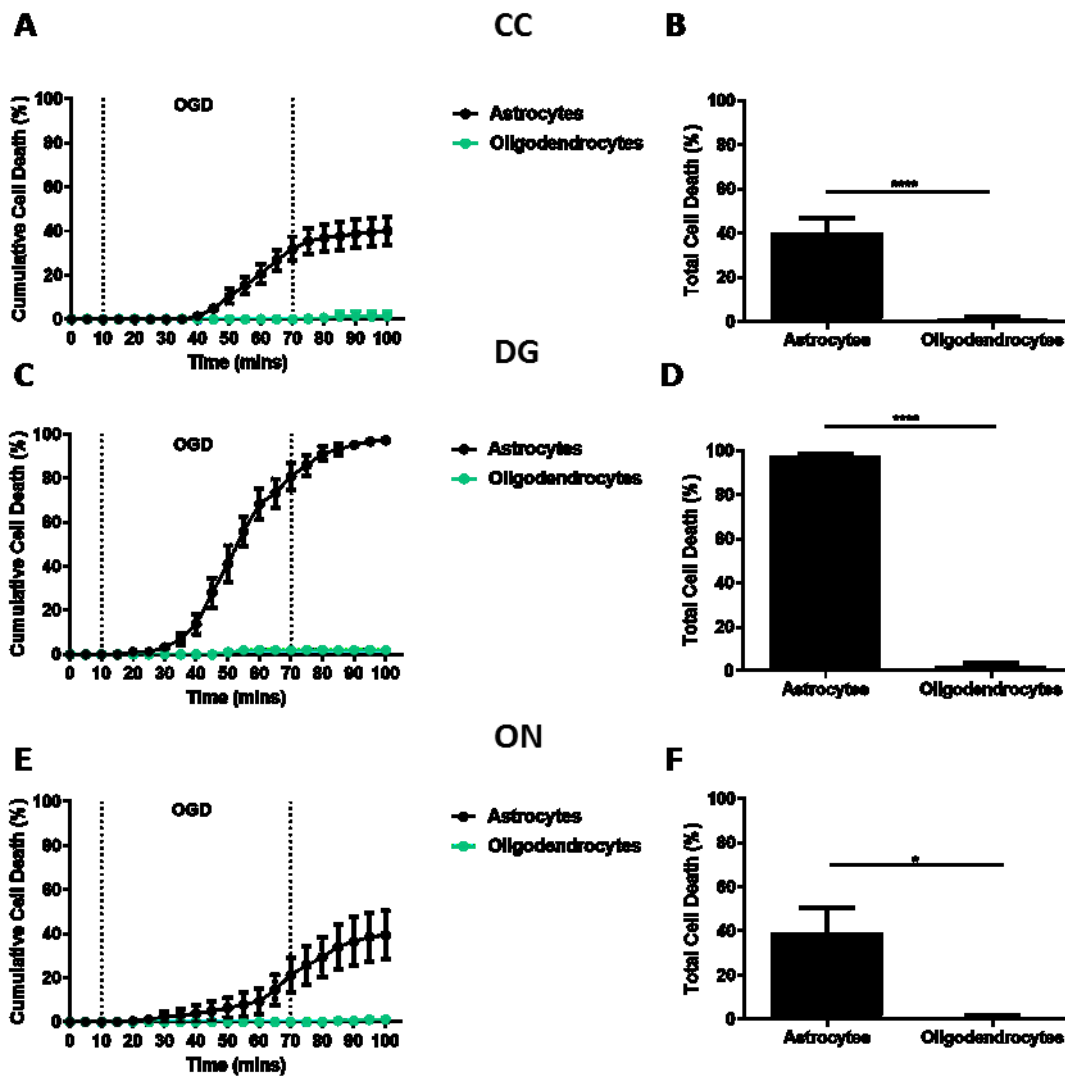
Figure 3.23: Astrocytes are more sensitive to OGD than oligodendrocytes. A, C + E: Astrocyte (black bars) and oligodendrocyte (green bars) cell death over time. **B, D + F:** total cell death at time 100 minutes for CC **(A+B)**, DG **(C+D)** and ON **(E+F)**. Error bars = SEM.

3.8 DISCUSSION: GLIAL SENSITIVITY TO OGD

Astrocytes and oligodendrocytes are both essential for the correct working of the CNS. Astrocytes are support cells to neurons and are responsible for the homeostatic regulation of the ECS as well as many other roles. Oligodendrocytes enable fast conduction of action potentials through the myelination of axons and have been implicated in axonal metabolic support. Due to the important roles these cells have, if either are damaged then this will have a detrimental effect on neuronal and CNS function. During ischaemic insult, all cell types within the ischaemic core and surrounding penumbra are affected. However, it is unknown how much the anatomical location of glial cells may determine their sensitivity to ischaemic insult. This work has established that regional sensitivity of astrocytes to OGD exists and it has been discovered that oligodendrocytes are resistant to acute ischaemic insult in the mature brain.

3.8.1 Astrocytes show regional sensitivity to OGD

First, the expression of GFP in astrocytes under the GFAP promoter was successfully confirmed through co-localisation with the astrocyte marker ALDH1L1 (figure 3.2). Not all astrocytes that were expressing GFP were positive for ALDH1L1, as ALDH1L1 does not detect all astrocyte populations and only identifies a certain subpopulation. The confocal images illustrate that the cells expressing GFP have definite astrocyte morphology, which also confirms that GFP was expressed in the correct cell type (figure 3.2).

This work has found that astrocyte sensitivity to OGD varies depending upon the physical location of the astrocyte population. Generally, astrocytes found in WM tracts were more resistant to ischaemic insult than cells found in GM matter regions (figure 3.16). The GM astrocyte populations were found to be very sensitive to OGD. The GM sensitivity to OGD found here is in

111

agreement with the literature where sensitive GM regions have been identified as cortex, hippocampus and striatum (Xu, Sapolsky & Giffard, 2001) Within GM regions, cell death began at slightly different time points and occurred at different rates (figure 3.16 and 3.17). However, when the total amount of OGD induced cell death was compared between GM regions, the variance was minimal. Investigation into cell death in different cortical layers found that there was not relationship between distance from the pial surface and time of astrocyte cell death event. However, it was noticed that layers that contained high neuronal density also showed astrocyte sensitivity to ischaemia. This suggests that astrocyte and neuronal survival are interlinked, which was previously posed by Zhao and Flavin (2000).

In the WM of the CC and ON, astrocytes behaved in a very similar manner and both displayed tolerance to acute ischaemic insult. Pantoni *et al*. (1996) found that WM astrocytes are physically affected after just 30 minutes of OGD, however there has been little further investigation into WM astrocyte sensitivity. Unlike the GM regions, the WM astrocyte population did show variance in the amount of OGD induced cell death achieved at the end of the experimental protocol. The EC was much more sensitive to OGD than the other WM regions investigated (figures 3.8 and 3.16). During ischaemia, the EC behaved more like a GM region such as CA1 or DG. This may be due the physical location of the EC, which is a relatively thin WM tract surrounded by large GM areas. It is known that this area is particularly susceptible to spontaneous intracerebral haemorrhage (Chung *et al.*, 2000), and so it may also be vulnerable to ischaemic stroke.

We have found that there are also differences in the sensitivities of neonatal (P10) astrocytes; those in CC (WM) are more resistant to ischaemic

insult than those in DG (GM) (figure 3.18). This follows the same pattern as for

the adult astrocytes, but is contrary to the findings of Shannon *et al.* (2007) who

found WM astrocyte more sensitive than GM. This may be as different WM

tracts were used, Shannon *et al.* (2007) studied ON astrocytes, whereas for the

current work CC was used. It is possible that astrocytes in different WM tracts

behave differently in neonates and so this requires further investigation. When

the total OGD induced astrocyte cell death from neonates and adults was

compared, it was found that the neonatal astrocytes were much more tolerant

than adult cells to ischaemia. During birth and development, the young

developing brain may undergo periods of ischaemia or suffer ischaemia like

conditions. Therefore it is important that developing and immature astrocytes

survive these stressful periods so as the cells can mature and take up their role

in the CNS. When these periods of ischaemia are more severe and longer

lasting, they often result in conditions such as cerebral palsy.

3.8.2 Oligodendrocytes show resistance to OGD

Unlike astrocytes, when oligodendrocytes were exposed to OGD it was

found that they were very resistant to acute ischaemic insult. All regions showed

less than 5% cell death (figure 3.22) which was significantly lower than the total

astrocyte cell death seen in the same regions (figure 3.23). In the literature, the

majority of studies demonstrate that oligodendrocytes are very sensitive to

ischaemic insult. It has been found that neonatal oligodendrocyte cultures are

particularly sensitive to OGD, with many cells dying after a short exposure. It

was reported that the majority of immature oligodendrocytes died within 30

minutes of OGD and after 60 minutes of OGD most of the cells present had died

(Fern & Moller, 2000). This study also showed that mature cultured

oligodendrocytes were very tolerant to OGD, 55 minutes of OGD resulted in

43.4 ± 5.3% cell death. The tolerance to insult has also been observed in whole mount ON preparations. P10 mouse ON oligodendrocytes were found to survive after 60 minutes of OGD, where only 30% cell death was seen at this time point (Salter & Fern, 2005). Oligodendrocyte resistance to OGD has been seen in CC slices where a minimum of one hour reperfusion was required for significant cell death to occur (Tekkok & Goldberg, 2001).

The resistance of oligodendrocytes to ischaemia has been demonstrated here. The majority of investigations which showed oligodendrocyte sensitivity, relatively short periods of ischaemia (10-30 minutes) were combined with longer periods of reperfusion (minimum of one hour). For this work interest lies in the acute injury of ischaemia and the initial effects of the insult. This evidence suggests that mature oligodendrocyte somas show resistance to ischaemic insult but are more sensitive to reperfusion. McIver *et al.* (2010) found that 24 hours after transient MCAO (60 minutes) there was not a significant loss of oligodendrocytes when compared to sham controls. Significant oligodendrocyte cell death was only observed 48 hours after insult (McIver *et al.*, 2010). This evidence confirms that mature oligodendrocyte cells are extremely tolerant to acute ischaemic insult and are more resistant than astrocytes. However, oligodendrocyte cell death was measured in the same manner as astrocyte cell death and so may not be representative of any oligodendrocyte injury that has occurred as a result of acute ischaemia. The *in situ* studies that have reported oligodendrocyte cell death have done so after long periods of reperfusion and not at the time of acute injury.

Oligodendrocyte cell somas express resistance to injury, however their processes and myelin are vulnerable to insult. Many studies have reported early defects and changes in oligodendrocyte processes after short periods of OGD,

such as Pantoni *et al.* 1996, who observed vacuolation and swollen processes after 30 minutes of MCAO. After six hours of MCAO, the myelin sheath had detached from the axolemma. Oligodendrocyte process loss has also been seen prior to cell soma loss (McIver *et al.*, 2010), here disintegration of proximal and distal processes was determined after 24 hours of reperfusion after 60 minutes ischaemia. The pathology observed in animal models has also been found in patients. In post-mortem samples, oligodendrocytes within the ischaemic infarct and in the penumbra displayed severe damage of distal processes and destruction of myelin (Aboul-Enein *et al.*, 2003).

The data in this chapter has demonstrated that astrocyte tolerance to modelled ischaemia varied significantly depending upon their physical location within the CNS. It has been determined that oligodendrocytes in brain slices and ON preparations are tolerant to acute ischaemic insult. Glial cells play such a pivotal role in the CNS that any damage or insult that occurs to them will not only be detrimental these cells but also to neurons and other cells in the CNS. By looking at how astrocytes and oligodendrocytes cope and respond to ischaemia will allow us to investigate the mechanisms of glial cell death. This will improve our understanding of the effect of ischaemic insults on the CNS and may provide possible therapeutic targets.

The CC was the least sensitive region to OGD ($31.95 \pm 9.33\%$ cell death), whilst the most sensitive was DG ($97.30 \pm 1.24\%$ cell death), as such these two regions were used to investigate the mechanisms behind the observed difference. There are many possible reasons as to why different astrocyte populations have varying sensitivities to OGD. The general astrocyte population is known to be heterogeneous; therefore, the differences that specialise them to a particular location may also determine their sensitivity to

ischaemia. From the literature and the previous work carried out by the group, it became apparent that there were three main areas, which may affect sensitivity to OGD. These were the role of glycogen stores, the role of glutamate receptors and sodium mediated cell swelling. Each of these have been investigated and discussed in the subsequent chapters.

CHAPTER 4

4 THE ROLE OF GLYCOGEN IN ISCHAEMIC INJURY OF GLIA

4.1 INTRODUCTION

Many processes carried out by astrocytes require energy, demand for which cannot always be satisfied by glucose from the circulation alone. The shortfall can be accounted for via the breakdown of astrocyte glycogen stores. Astrocytes are the major glycogen store in the brain and glycogenolysis can occur quickly to yield ATP during periods of high demand (Sickmann *et al.*, 2009), making it a useful energy reserve. A major product of glycogenolysis is lactate, which can be used by axons as an energy source, to survive and function during aglycaemia (Brown *et al.*, 2005; Fern, 2015; Ransom & Fern, 1997; Tekkok *et al.*, 2005; Wender *et al.*, 2000). Tekkok *et al.,* (2005) found that lactate was transported via monocarboxylate transporters (MCTs) from astrocytes to axons in mouse optic nerve (ON). It has been shown *in vitro* that lactate from glia is metabolized by axons (Funfschilling *et al.*, 2012), allowing axons to continue to function for a few minutes, when there is a lack of glucose.

Early studies into glial supply of metabolites were carried out in the honeybee drone retina. This preparation contains only two cell populations, photoreceptors (neuronal cells) and outer pigment cells (glial cells) (Coles & Tsacopoulos, 1981), making it ideal for the investigation of metabolite supply. The drone retina is highly compartmentalised, with glycolysis occurring in the glial cells only, whilst photoreceptors are the major site of oxygen consumption (Tsacopoulos *et al.*, 1988). The photoreceptors rely upon the glial cells, much like neurons rely upon astrocytes, for ionic homeostasis and buffering. In this model the glial cells are also responsible for metabolite supply to the photoreceptors and contain high levels of glycogen (Coles & Tsacopoulos,

1981). In these glial cells glucose and glycogen are converted into alanine which is released for use by the photoreceptors, where it is transaminated into pyruvate for use in the TCA cycle (Tsacopoulos *et al.*, 1994).

During ischaemia, it is thought that astrocytes in the penumbra may breakdown glycogen stores to produce lactate, which is released into the ECS for uptake by neurons. However, it is unknown if this energy store is used by astrocytes to maintain their own function during ischemia. A small glycogen store has been found in neurons, the cells examined were cultured from neocortex and hippocampus (Saez *et al.*, 2014). The glycogen levels determined were very low, just a fraction of the amount that is found in astrocytes. Saez *et al.* (2014) suggested that this store could be used during ischaemic insults to fuel neurons.

4.1.1 Astrocytes, glycogen and metabolism

The role of astrocytic glycogen has been found to be essential to the CNS. The lactate generated from glycogen breakdown can be used as a metabolic substrate, but is also utilized as a signalling molecule (Lauritzen *et al.*, 2014). During aglycaemic conditions, astrocytic glycogen is required for the survival of neurons in culture (Swanson & Choi, 1993). Involvement of glycogen in higher brain functions has been discovered and extends to processes such as memory consolidation, learning and the sleep/wake cycle (Gibbs, Anderson & Hertz, 2006; Naylor *et al.*, 2012; Suzuki *et al.*, 2011).

Initial work on lactate signalling was carried out in a neonatal chick learning model, where it was found that glycogenolysis was required for memory consolidation (Gibbs, Anderson & Hertz, 2006). The inhibition of glycogenolysis inhibited long term memory and was required for short term memory and recall

(Gibbs, Anderson & Hertz, 2006). The discovery of the expression of the lactate receptor GPR81 supported the role of lactate as a signalling molecule (Lauritzen *et al.*, 2014). This G-protein coupled receptor has been found to be expressed in cortex and hippocampus, particularly on synaptic membranes (Lauritzen *et al.*, 2014), which are regions of high neuronal activity. This receptor can exert an effect on numerous neurons by acting as a volume transmitter. Lactate signalling can respond to neuronal activity, via the inhibition of adenylyl cyclase (Lauritzen *et al.*, 2014). Lactate signalling has been shown to alter cerebral blood flow (Gordon *et al.*, 2008) and may be involved in other homeostatic processes such as osmoregulation, ventilation, glucose and sodium sensing (Magistretti & Allaman, 2018). Glycogen is utilized in the uptake and processing of glutamate (Sickmann *et al.*, 2009), which is further discussed below.

Glycogen is used for the active uptake of ions which is important for the maintenance of ionic gradients and for homeostasis. In particular, glycogenolysis is used to power the sodium/potassium ATPase (NKA) (Xu *et al.*, 2013). This transporter extrudes sodium whilst importing excess extracellular potassium, which can then be distributed throughout the astrocyte network to lower the extracellular concentration (Xu *et al.*, 2013). The NKA is activated by increases in extracellular potassium concentration, even small increases will stimulate the transporter and glycogenolysis (Hof, Pascale & Magistretti, 1988). These extracellular increases were seen by Xu *et al* (2013), who found they were required for glycogenolysis to occur. The levels of potassium in the extracellular space increase with neuronal activity (Xu *et al.*, 2013).

The utilization of glycogen under normal physiological conditions is associated with an increase in extracellular potassium concentration which

causes an increase in free intracellular calcium (Sotelo-Hitschfeld *et al.*, 2015). This triggers phosphorylase kinase, which phosphorylates and thereby activates the enzyme glycogen phosphorylase. Glycogen granules are broken down via glycogen phosphorylase and glycogen debranching enzyme, resulting in pyruvate which can be converted to lactate. Brain slice studies have found that depolarization and calcium influx can stimulate glycogen phosphorylase and trigger glycogenolysis (Ververken *et al.*, 1982). During times of high energy demand glucose can be trafficked between astrocytes through gap junctions, which has been observed in hippocampal astrocytes (Rouach *et al.*, 2008). These prior findings show that astrocytic glycogen is essential to the CNS and has a definite role during physiological conditions and times of low glucose.

4.1.1.1 Lactate as a neuronal metabolic substrate

It was discovered that astrocytes release lactate (Walz & Mukerji, 1988), however the reasons behind this release are unknown. It has been suggested that the lactate released is used as a metabolic substrate by neurons. This phenomenon has been summarised by the astrocyte-neuron lactate shuttle hypothesis (ANLS) as described by the Magistretti group (1994). There is evidence that neurons will use alternative metabolites in the absence of glucose and it has also been shown that neurons will use lactate to sustain excitability (Wyss *et al.*, 2011). The lactate that supports neuronal function was found to be derived from glycogen (Brown *et al.*, 2005). During aglycaemia, neuronal survival and function was enhanced by increasing astrocyte glycogen levels.

The ANLS hypothesis proposes that when required, astrocytes break down glycogen and convert it to lactate which is then transported to neurons (Pellerin & Magistretti, 1994). This is likely to occur during times of increased neuronal activity when glucose demand is high or under conditions of reduced

glucose delivery. There is some controversy about the ANLS hypothesis, even though there is evidence in the literature to support the movement of lactate from astrocytes to neurons the theory has not been directly proven. Astrocytes express monocarboxylate transporters (MCTS), specifically MCT1 and 4 and neurons express MCT2 (Bergersen, Rafiki & Ottersen, 2002; Pierre *et al.*, 2000). The location and affinities of these MCTs supports the release of lactate from astrocytes and the uptake by neurons. MCT2 expression has also been found on axons (Funfschilling *et al.*, 2012), as axons are covered in a myelin sheath then it would imply that metabolites may also be released by oligodendrocytes (Krasnow & Attwell, 2016). These metabolites are the result of oligodendrocyte glycolysis (Funfschilling *et al.*, 2012; Lee *et al.*, 2012b). It has been suggested that this occurs through a NMDA receptor dependent mechanism, which causes an increase in GLUT1 trafficking (Saab *et al.*, 2016), thereby increasing glucose transport into oligodendrocytes. This process of metabolite movement through oligodendrocytes shares similarities with the ANLS hypothesis (Krasnow & Attwell, 2016).

Mächler *et al.* (2015) have established the existence of a lactate gradient from astrocytes to neurons. This was determined through the investigation of MCT expression and the fact that neurons have lower levels of lactate but their MCTs have a higher affinity for the metabolite (Machler *et al.*, 2016), an analysis that supports the ANLS hypothesis. Astrocyte derived lactate has been shown to fuel ON axons, there is evidence to suggest that hippocampal neurons can metabolize lactate (Matsui *et al.*, 2017) and WM axons may also utilize this metabolite. Investigation into the role of lactate in mouse ON has also been carried out. Tekkok *et al.* (2005) first showed that during 60 minutes of aglycaemia lactate was utilized by ON and sustained compound action potential

(CAP) for 30 minutes. They found that CAP function was partially rescued by the administration of lactate. They also determined that lactate has a role in CAP function during physiological conditions, the absence of lactate increased the speed of nerve deterioration. This evidence suggests that exogenous lactate can support axonal function and is an additional energy substrate to glucose (Tekkok *et al.*, 2005).

Recently it was discovered that astrocytes contain a cytosolic lactate pool as well as glycogen stores (Sotelo-Hitschfeld *et al.*, 2015). This lactate pool can be quickly released when required, allowing time for glycogenolysis to occur to produce more lactate. This reservoir can be released against the lactate gradient and once released can be used by other cells. An increase in the extracellular potassium concentration causes the release of the lactate pool (Sotelo-Hitschfeld *et al.*, 2015). MCTs are not responsible for this lactate release, but it occurs through a novel and as yet unidentified anion channel which is permeable to lactate and chloride. The study also suggested that this astrocyte lactate pool may be utilized as a signalling molecule as well as a metabolite. The lactate receptor GPR81 is a G-protein coupled receptor which has been found to be expressed in synaptic regions, perivascular positions and on glia (Lauritzen *et al.*, 2014), this is consistent with the use of lactate as a signalling molecule. Lactate as a signalling molecule has been shown to reduce spontaneous activity in cultured cortical neurons (Bozzo, Puyal & Chatton, 2013), whilst in other regions it has caused neuronal excitement.

4.1.2 Glycogen and glutamate

Glycogen is frequently mobilised for the *de novo* synthesis of glutamine and is used throughout the glutamate-glutamine cycle. It has been shown that

glycogen is necessary for glutamatergic neurotransmission to occur (Sickmann *et al.*, 2009).

Glutamate cannot enter the brain from the circulation and so its formation has to occur *in situ*. Astrocytes are the only cells which are able to synthesize *de novo* glutamate. Pyruvate, resulting from glycogenolysis is a precursor for glutamate formation and is converted to α-ketoglutarate prior to glutamate and then glutamine (Gibbs *et al.*, 2007; Hertz & Rothman, 2017). Glutamine is produced by astrocytes for export to neurons, where it is converted into glutamate four use in neurotransmission. During times of high neuronal activity such as learning, glutamate levels are increased due to stimulation of glutamine synthesis (Gibbs *et al.*, 2007; Hertz *et al.*, 2003). Glutamate released by synapses is taken up by astrocytes. A proportion of this glutamate is lost to oxidative degradation (McKenna, 2013) as glutamate is converted into the TCA cycle intermediate α-ketoglutarate. This loss occurs for approximately 20% of glutamate that enters astrocytes (Hertz *et al.*, 2015). Glutamate is also recycled by astrocytes, the uptake of which requires glycogenolysis (Sickmann *et al.*, 2009). Once converted from glutamate to glutamine it is released from astrocytes for use by neurons.

The GM contains regions of high neuronal activity, where glycogen turnover is high during neuronal stimulation (Dienel & Cruz, 2003; Swanson, 1992). Glycogen is the preferred substrate for the formation of glutamine (Gibbs *et al.*, 2007) and so within GM astrocytes there is a constant turnover as glycogen stores are used to fuel neurotransmission and are replenished. An essential role for glycogen has been discovered during learning and the breakdown of glycogen is responsible for the increase in glutamate seen during learning activities (Gibbs *et al.*, 2007).

Many signalling molecules and neurotransmitters can stimulate glycogenolysis such as ATP, serotonin, noradrenaline, and adenosine (Hertz *et al.*, 2015). These all act to increase the intracellular calcium concentration which can activate glycogen phosphorylase and thus trigger glycogenolysis.

4.1.3 Oligodendrocytes and metabolism

Recently, a new role for oligodendrocytes in axonal metabolic support has been found. Close proximity to axons puts oligodendrocytes in the ideal position to assist with axon fuelling. It may not be feasible that neuronal cell somas can energetically supply axons, due to the distance that axons extend from the somata. The nature of the myelin sheath means it acts as a physical barrier around the axon preventing the uptake of metabolites from the extracellular space. Thus, axons must obtain metabolites from alternative sources. This new role for oligodendrocytes has been discovered along with their expression of MCT1 (Rinholm *et al.*, 2011) which can be used to export lactate from cells, corresponding with the neuronal expression of MCT2 for lactate import (Pierre *et al.*, 2000). Oligodendrocytes have been found to supply lactate to neurons via glycolysis (Funfschilling *et al.*, 2012). It has previously been mentioned that axons can be sustained by lactate when glucose is not available (Tekkok *et al.*, 2005). WM has particularly high glycolytic activity (Morland *et al.*, 2007), which will produce excess lactate in glial cells, which may be released for use by other cells.

The expression of MCT1 has been found in oligodendrocytes, specifically on the myelin processes that wrap axons (Rinholm *et al.*, 2011). MCT1 is essential for axon maintenance, knock out of the transporter causes axonal injury and neuronal loss (Lee *et al.*, 2012b). Oligodendrocytes form coupled networks with astrocytes, providing another route through which metabolites

can be distributed ultimately for use by axons. These two types of glial cells are coupled through gap junctions created from connexins (Orthmann-Murphy *et al.*, 2007). Oligodendrocytes express the connexins Cx47 and Cx32 which couple with the astrocyte connexins Cx43 and Cx30. It is thought that metabolites can pass through these mixed glia networks as they can in the astrocyte syncytium.

A recent study carried out on axonal metabolite preferences, found that CC axons preferentially use glucose delivered by oligodendrocytes (Meyer *et al.*, 2018). However, during aglycaemia lactate was found to partially recover axon compound action potentials (CAP). Full CAP recovery was only achieved with glucose administration. Meyer *et al* (2018) also determined that the metabolites used by axons are transferred from oligodendrocytes to neurons. CAP rescue was only seen when metabolites were directly loaded into oligodendrocytes but not astrocytes. This evidence suggests that only ON axons may exclusively use lactate as an alternative fuel. For this functional rescue of CC axons to occur, both GLUT1 and MCTs were required (Meyer *et al.*, 2018), which indicates that lactate has a role in axonal function but is not the sole substrate used in physiological conditions. Thus indicating that normally a mixture of glucose and lactate are used for ATP generation. However, when glucose is not available, lactate is able to partly sustain axon function for a short period of time. Many previous studies have found that in both WM and GM, lactate does have a role in supporting axonal function in the absence of glucose in the cortex, corpus callosum, optic nerve and hippocampus (Brown *et al.*, 2005; Lauritzen *et al.*, 2014).

Oligodendrocytes provide a link between glucose uptake, axonal activity and metabolic demand (Saab *et al.*, 2016). Neuronal activity is detected through the expression of glutamate N-methyl-D-aspartate receptors (NMDARs) on

oligodendrocyte processes (Saab *et al.*, 2016), facing the periaxonal space (Micu *et al.*, 2016). Activation of NMDARs recruits GLUT1 (glucose transporter 1) to the membrane to increase glucose transport into oligodendrocytes (Saab *et al.*, 2016). This has been described as a "power switch" through which the flow of metabolic substrates to neurons via oligodendrocytes can be controlled (Krasnow & Attwell, 2016).

4.1.4 Astrocyte metabolism during ischaemia

The core of the lesion caused by ischaemia suffers complete loss of blood supply, in the penumbra the blood supply is only reduced. In this region there is a degree of astrocyte survival as glucose and oxygen delivery is decreased, cells resort to other ways to produce energy. Penumbral astrocytes may be served by collateral vessels which are not affected by the occlusion. Here astrocytes can continue to function to maintain the working of the CNS and limit the damage caused by insult. The higher the tolerance of astrocytes to ischemia the more viable astrocytes to assist with regaining metabolic equilibrium and to ensure neuron survival after insult (Goss *et al.*, 1998; Li *et al.*, 2008).

During ischaemic insult all ion and metabolite concentration gradients are disrupted which in turn affects normal cellular processes. The disruption of the lactate gradient (Machler *et al.*, 2016) may contribute to neuronal cell death as neurons are unable to take up lactate, either due to injury or changes in the concentration gradients. The homeostatic disruption that occurs during ischaemia means that there is increased extracellular potassium, which causes release of lactate under physiological conditions (Sotelo-Hitschfeld *et al.*, 2015). The lactate that is released may be taken up by neurons if possible or may

function as a signalling molecule which can feedback to astrocytes to release more lactate.

It is possible that the lactate and glycogen produced by astrocytes may be used by astrocytes in the penumbra to increase their chances of survival during ischaemic insult. It has been found that during ischaemia astrocytic gap junctions are able to operate (Cotrina *et al.*, 1998), thus allowing the transfer of metabolites throughout the astrocyte network (Rouach *et al.*, 2008).

The therapeutic potential of lactate has been investigated and has been found to attenuate neuronal death when administered post insult (Berthet *et al.*, 2009). In cultured cells, increasing astrocyte glycogen content provided protection from hypoxic cell death (Hossain, Roulston & Stapleton, 2014). This would suggest that, at least in low oxygen conditions, astrocytes are able to utilize glycogen to promote their own and neuronal survival.

The evidence from the literature suggests that the location of neurons determines their metabolic preferences, which can be supplied by both astrocytes and oligodendrocytes (Meyer *et al.*, 2018; Rouach *et al.*, 2008) It is possible that the ANLS relates to the astrocyte support of neuronal cell bodies and to synapses whilst oligodendrocytes are responsible for the maintenance of axons.

In this chapter the role of astrocytic glycogen during acute ischaemia was investigated. Previous work by the group has found that the presence of glycogen stores conferred ischaemic tolerance in pre-myelinated white matter (Fern, 2015). In the following work the role of glycogen in preventing ischaemic astrocyte cell death was investigated in adult brain slices, to see if the findings would correspond with those for neonatal animals. By preventing the use of

astrocyte glycogen stores during OGD it can be determined whether the presence of these stores enables astrocytes to survive for longer during an ischaemic insult. Our hypothesis was that the presence of glycogen is required for astrocyte survival during ischaemic conditions. Glycogenolysis was prevented in two ways, firstly with the addition of sodium iodoacetate and secondly with 2-deoxy-glucose treatment.

4.2 RESULTS: SODIUM IODOACETATE INHIBITION OF GLYCOGEN STORES

During times of high energy demand astrocytes utilize their glycogen stores to ensure a supply of metabolic substrate (Sickmann *et al.*, 2009). Astrocytes can be prevented from utilizing their glycogen stores through treatment with sodium iodoacetate (IA) (figure 4.1). IA blocks the active site of glyceraldehyde-3-phosphate dehydrogenase, by binding to cysteine residues and stopping the function of the enzyme. Ultimately this prevents the production of pyruvate from glycogen sources and so the store cannot be used to fuel the cell. Under physiological conditions, IA would interrupt the utilization of glucose supplied to the cell. However, in the absence of external glucose, IA will selectively prevent access to the glycogen store.

Glycogen ⟷ Glucose

↓ ✗ IA
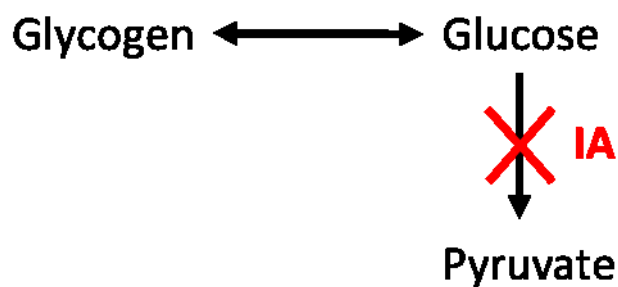
Pyruvate

Figure 4.1: Action of sodium iodoacetate (IA). Sodium iodoacetate prevents the production of pyruvate in the TCA cycle by blocking the enzyme glyceraldehyde-3-phosphate dehydrogenase. Under OGD this prevents the utilisation of the glycogen store.

4.2.1 IA affected OGD induced astrocyte cell death in CC and DG

The addition of IA had an effect on OGD induced astrocyte cell death in CC (figure 4.1). In the OGD with IA images the majority of astrocytes have died and at 100 minutes no cell bodies can be seen in the images (figure 4.2A),

which contrasts to OGD only conditions, where the majority of cells survive. In the OGD images a GFP "cloud" is often apparent after cells have lysed, this is a result of GFP release from astrocytes when the cells die. Treatment with IA had a highly significant effect in CC, where the t value was significantly decreased from 62.00 ± 2.32 to 42.25 ± 3.17 mins with IA, (p=0.0007, figure 4.2B). This suggests that cell death occurs more quickly as the time to reach half of the maximal cell death is reduced. The addition of IA caused cell death to increase from 40.17 ± 6.45% in OGD only conditions to 98.61 ± 1.39% (p=0.001,figure 4.2C).

IA treatment also increased the rate of OGD induced astrocyte cell death in DG (figure 4.3), the confocal images illustrate similar amounts of cell death in both conditions (figure 4.3A). The rate of cell death in DG was significantly decreased by the addition of IA. The t for DG was 54.64 ± 3.30 mins, this was reduced to 38.13 ± 4.89 mins with IA (p=0.018, figure 4.3B). The total amount of cell death in DG was only slightly increased from 97.61 ± 1.01% to 100 ± 0% (not significant), with the addition of IA (figure 4.3C). Comparison of the DG cell death profile with that for CC, found that IA treatment made both regions behave in the same manner as there was a similar increase in the rate of cell death. These findings suggest that glycogen has an important role to play in ischaemic insult tolerance in astrocytes.

Astrocyte cell death at different time points throughout the experiment were compared for each region (figure 4.4). From this it can be seen that for CC astrocytes the amount of cell death is consistently higher at each time point with IA treatment (figure 4.4A). After 30 minutes, OGD induced cell death was increased from 0 ± 0% to 38.21 ± 11.51% (p=0.0025). At the end of OGD, astrocyte death with IA treatment was increased from 23.11 ± 7.12% to

98.61±1.39% (p=<0.0001). This significant increase was present at the end of

the reperfusion period (p=<0.0001). For DG astrocytes cell death with IA

treatment was only significantly higher after 30 minutes OGD, where astrocyte

death was increased from 14.04 ± 7.77% to 55.85 ± 16.09% (p=0.0009). Taken

together the findings show an increase in the rate of cell death in both fibrous

and protoplasmic astrocytes.
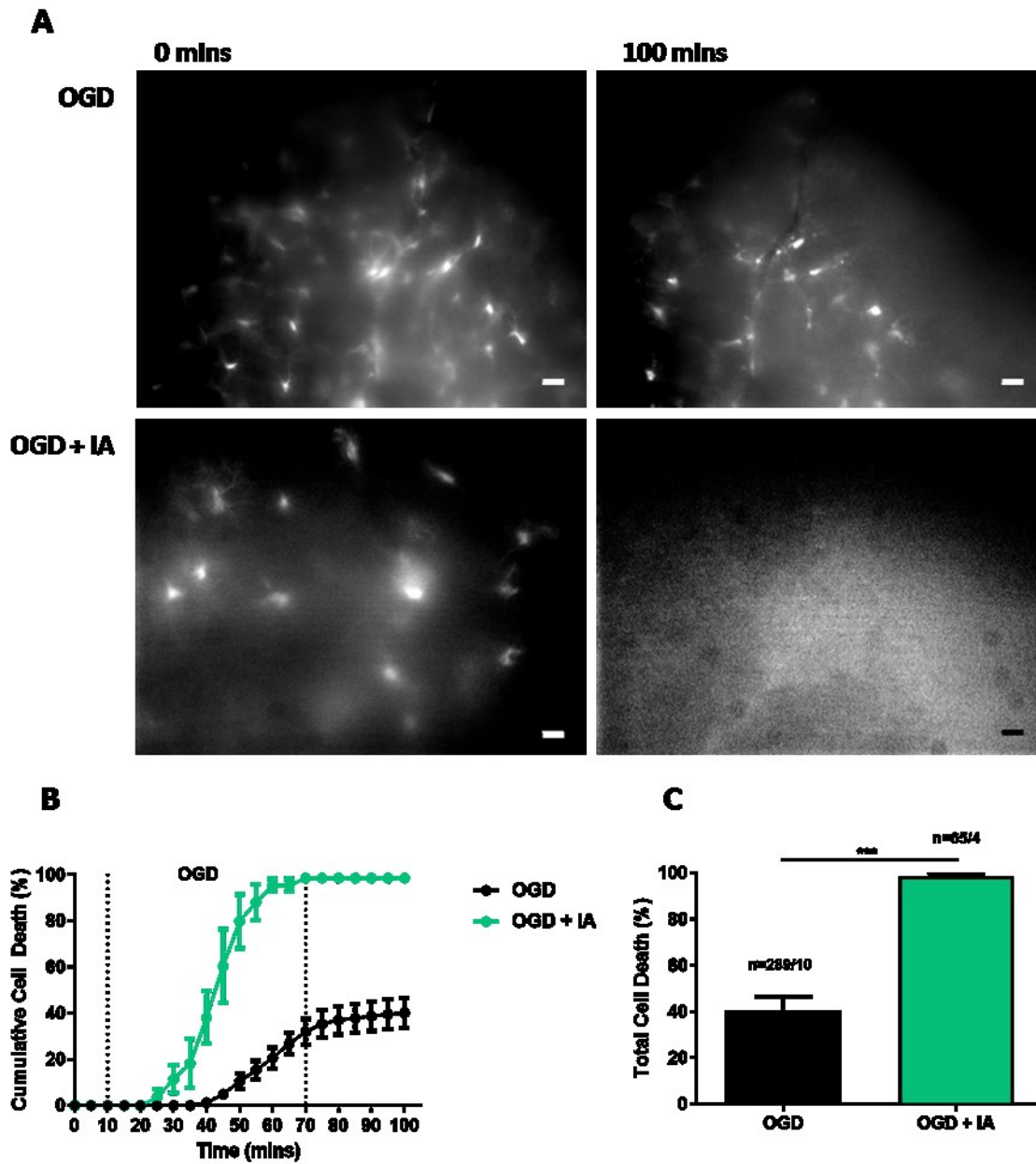
Figure 4.2: Sodium Iodoacetate (IA) treatment (2mM) increased OGD induced astrocyte cell death in corpus callosum (CC). **A:** Confocal images during OGD (upper panel) and OGD with IA treatment (lower panel). Images taken at 0 and 100 minutes. Scale bar =20 μm. **B:** Astrocyte cell death over time. **C:** total cell death at time 100 minutes, OGD only (black bar) and OGD with IA (green bar). Error bars = SEM. N numbers = number of cells/number of slices. IA added during OGD (10-70 mins).

Figure 4.3: Sodium Iodoacetate (IA) treatment (2mM) affected the rate of OGD induced astrocyte cell death in dentate gyrus (DG). **A:** Confocal images during OGD (upper panel) and OGD with IA treatment (lower panel. Images taken at 0 and 100 minutes. Scale bar =20 μm. **B:** Astrocyte cell death over time. **C:** total cell death at time 100 minutes, OGD only (black bar) and OGD with IA (green bar). Error bars = SEM. N numbers = numbers of cells/number of slices. IA added during OGD (10-70 mins).

Figure 4.4: Effect of IA on OGD induced cell death at defined time points in CC and DG. Astrocyte cell death after 30 and 60 minutes OGD and at the end of reperfusion with OGD only (black bars) and OGD with IA treatment (green bars). **A:** corpus callosum. **B:** dentate gyrus. Error bars = SEM.

4.3 RESULTS: 2-DEOXY-GLUCOSE TREATMENT OF ASTROCYTES AND

OLIGODENDROCYTES

2-deoxy-glucose (2DOG) is a glucose analogue and once inside the cell is phosphorylated by glucose hexokinase which normally phosphorylates glucose. This yields 2-deoxy-glucose-6-phosphate, the phosphorylation prevents the molecule from leaving the cell (SOLS & CRANE, 1954). The presence of phosphorylated 2DOG is mistaken by cells for a supply of glucose and so the glycogen stores are preserved and not used (figure 4.5).

Figure 4.5: Action of 2-deoxy-glucose (2DOG). 2-deoxy-glucose is a glucose mimic and is phosphorylated by the same hexokinase that phosphorylates glucose, preserving glycogen stores.

4.3.1 2DOG affects OGD induced astrocyte cell death in CC and DG but not in the ON

The presence of 2DOG increased astrocyte death in CC (figure 4.6). Fewer astrocytes were visible at the end of the reperfusion period in the presence of 2DOG than in OGD alone (figure 4.6A). Treatment with 2DOG also altered the cell death profile (figure 4.6B). The t value was reduced from 62.00 ± 2.32 mins to 47.33 ± 5.74 mins (p=0.029), showing the addition of 2DOG

137

increased the rate of cell death. Total astrocyte cell death in CC was significantly higher at the end of the perfusion period with 2DOG treatment, 77.71 ± 8 .73%, than OGD alone, 40.17 ± 6.45% (p=0.0035, figure 4.6C).

In DG, the images obtained with 2DOG treatment (figure 4.7A lower panel) are similar to those for OGD (figure 4.7A upper panel). The addition of 2DOG did not significantly alter the *t* value, which for DG was 54.64 ± 3.30 mins and with 2DOG was 45.42 ± 3.92 mins (figure 4.7B). The presence of 2DOG increased total cell death from 97.61 ± 1.01% to 99.12 ± 0.88% (not significant, figure 4.7C).

ON OGD induced astrocyte cell death was examined in the presence of 2DOG, as another WM tract, to compare to the results obtained for CC (figure 4.8). ON astrocytes remain tolerant of the ischaemic insult with 2DOG treatment (figure 4.8A). The rate of cell death was similar for both conditions, the *t* values obtained were similar under both conditions (figure 4.8B). The t for ON was 68.36 ± 6.82 mins and with 2DOG was 63.42 ± 6.03 mins (not significant). The total amount of astrocyte cell death was increased with 2DOG treatment, from 39.42 ± 11.03% to 56.67 ± 9.49% (not significant, figure 4.8C). These findings indicate that astrocyte glycogen stores may have a different role in the ON than in other regions.

By comparing the cell death at different time points, it can be seen at which phase astrocyte cell death is most affected. 2DOG treatment significantly increased OGD induced cell death at each time point in CC (figure 4.9A). After 30 minutes OGD, 2DOG treatment increased cell death from 0% to 32.38 ± 15.35% (p=0.019). At the end of OGD, cell death was significantly increased from 23.11 ± 7.12% to 64.38 ± 10.38% with 2DOG treatment (p=0.0091). This accounts for the majority of cell death in this region in the presence of 2DOG.

For DG the 2DOG treatment caused significantly increased cell death during early OGD (figure 4.9B). After 30 minutes OGD, 2DOG increased cell death from 11.01 ± 4.03% to 32.67 ± 11.40% (p=0.396). In ON, OGD induced astrocyte cell death was not significantly altered by 2DOG treatment (figure 4.9C). These results suggest that the presence of 2DOG increases astrocyte sensitivity to OGD in both CC and DG.

A

B

C
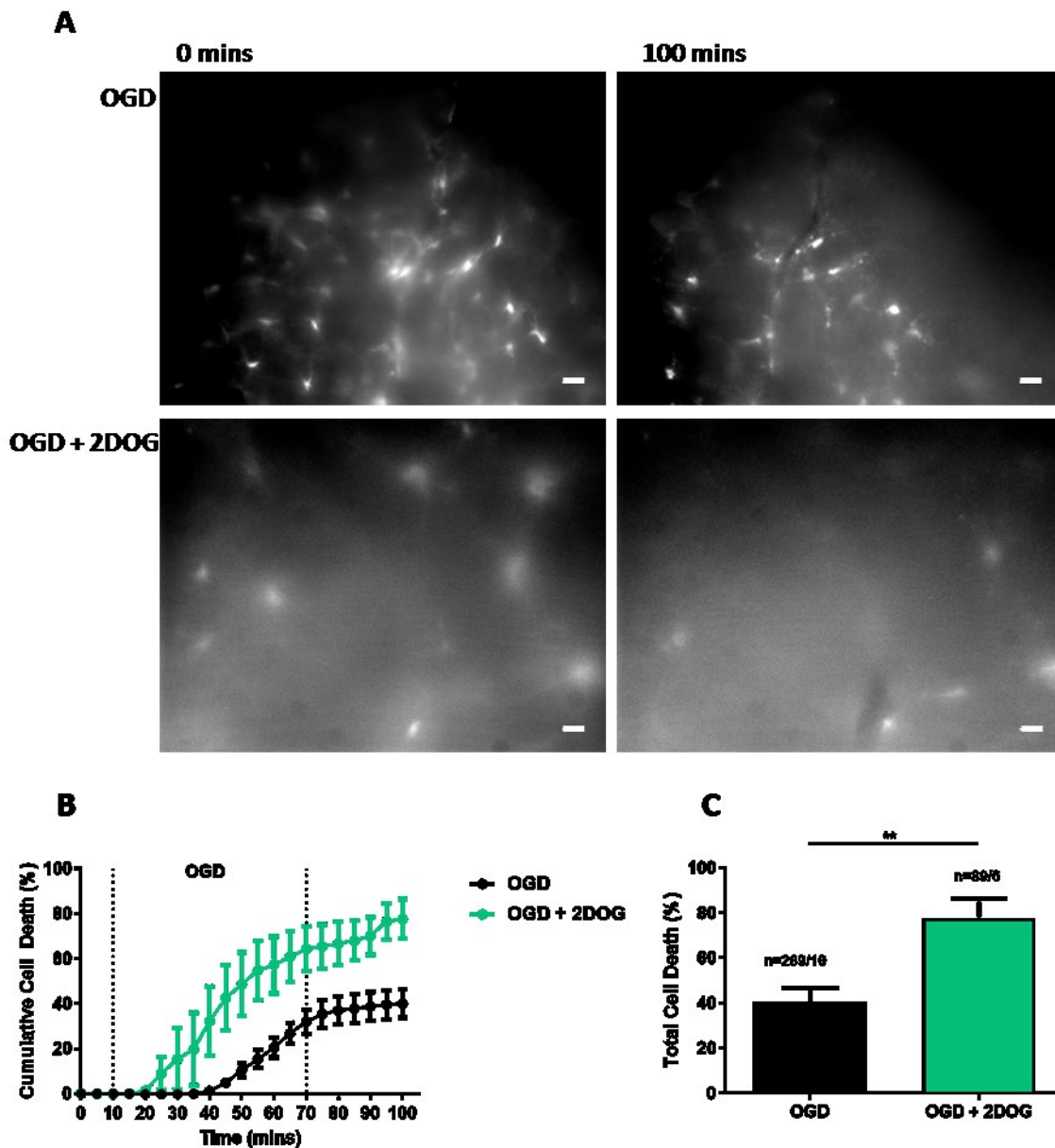
Figure 4.6: 2-deoxy-glucose (2DOG) treatment (10µM) increased astrocyte cell death in corpus callosum (CC). **A:** Confocal images of during OGD (upper panel) and OGD with 2DOG treatment (lower panel). Images taken at 0 and 100 minutes. Scale bar =20 µm. **B:** astrocyte cell death over time. **C:** total cell death at time 100 minutes, OGD only (black bar) and OGD with 2DOG (green bar). Error bars = SEM. N numbers = number of cells/number of slices. 2DOG added during OGD (10-70 mins)
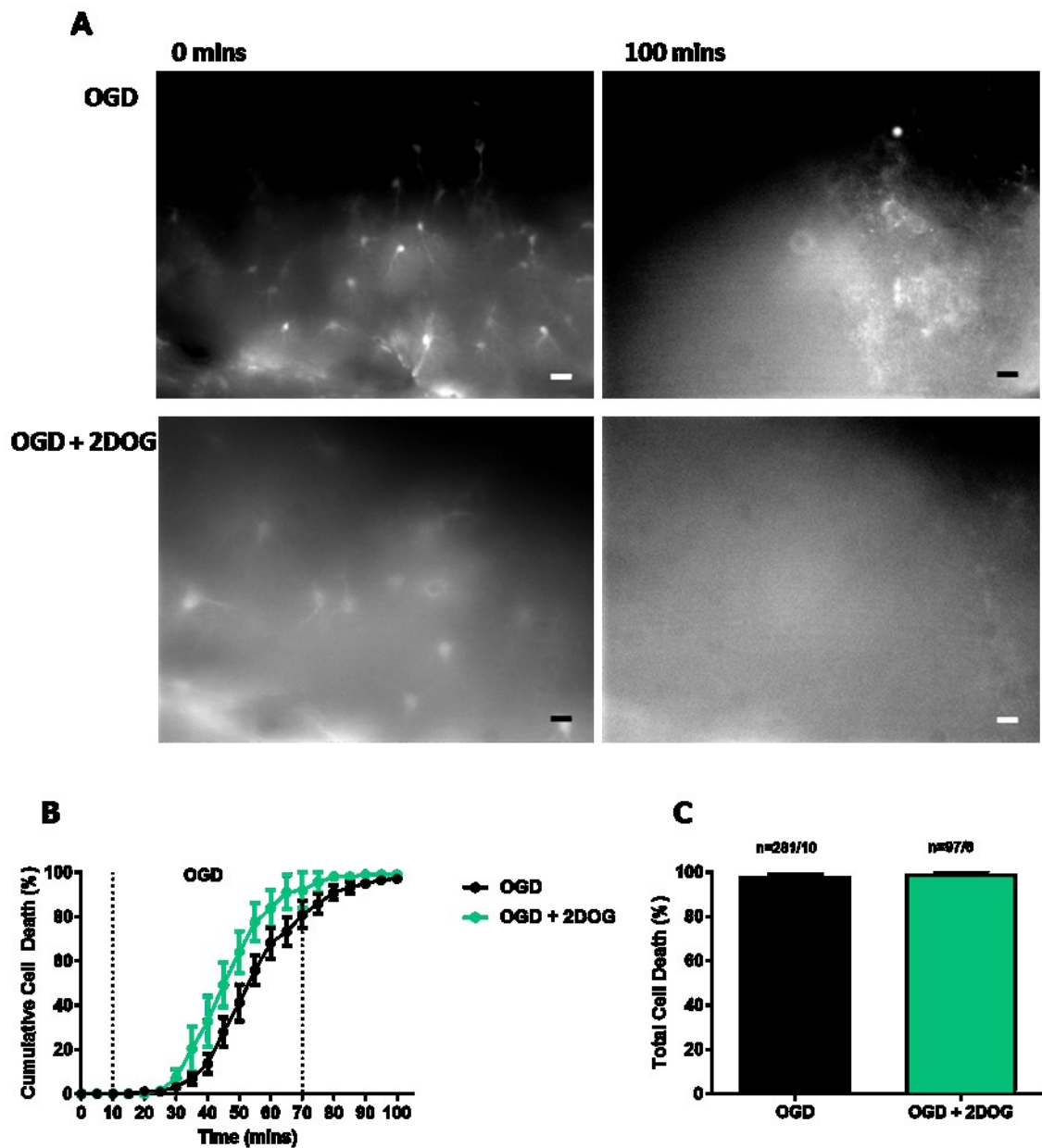
Figure 4.7: 2-deoxy-glucose (2DOG) treatment (10µM) had no effect on astrocyte cell death in dentate gyrus (DG). A: Confocal images of during OGD (upper panel) and OGD with 2DOG treatment (lower panel). Images taken at 0 and 100 minutes. Scale bar =20 µm. **B:** astrocyte cell death over time. **C:** total cell death at time 100 minutes, OGD only (black bar) and OGD with 2DOG (green bar). Error bars = SEM. N numbers = number of cells/number of slices. 2DOG added during OGD (10 -70 mins)
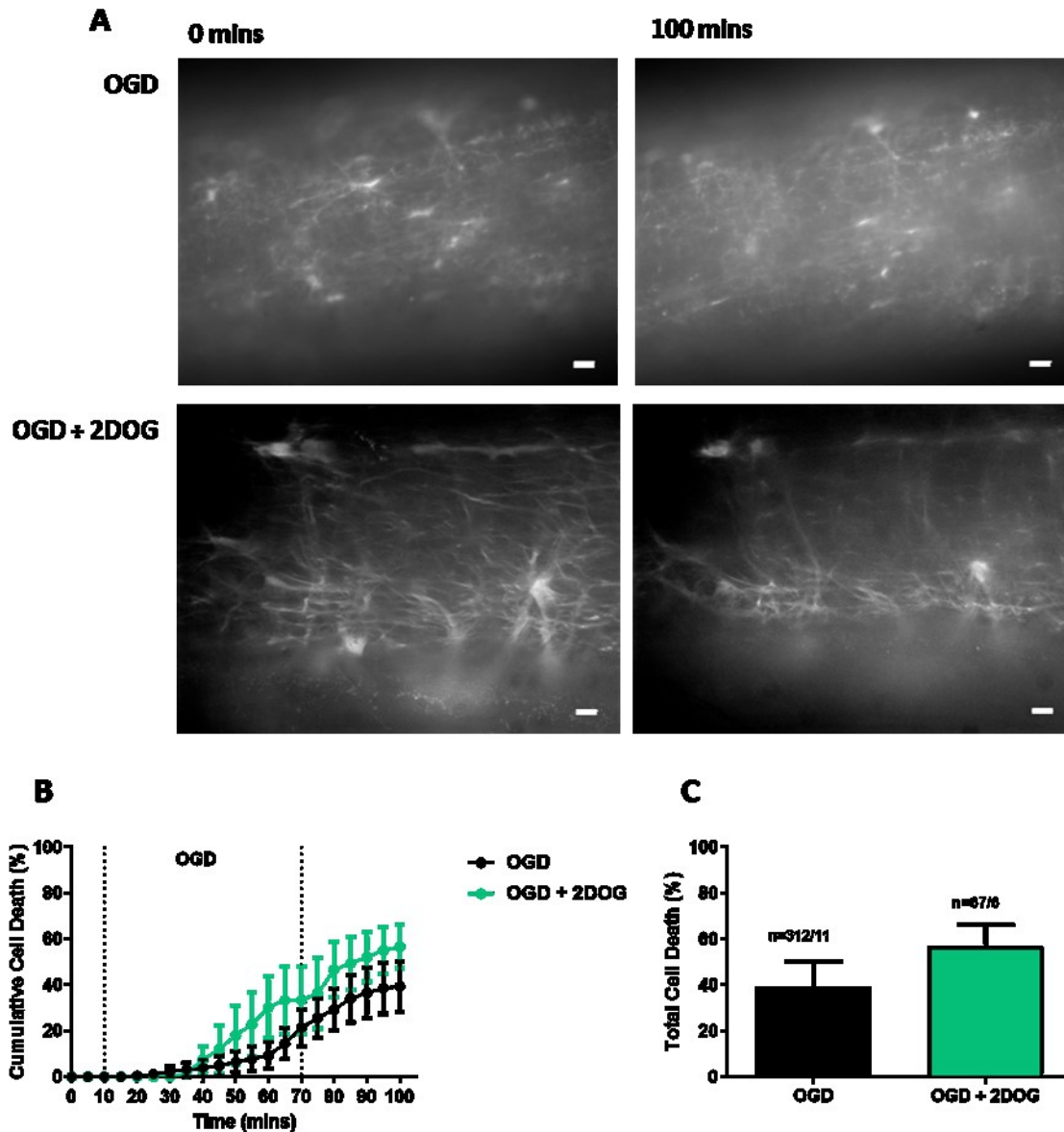
Figure 4.8: 2-deoxy-glucose (2DOG) treatment (10μM) had little effect on OGD induced astrocyte cell death in optic nerve (ON). A: Confocal images of during OGD (upper panel) and OGD with 2DOG treatment (lower panel). Images taken at 0 and 100 minutes. Scale bar =20 μm. B: astrocyte cell death over time. C: total cell death at time 100 minutes, OGD only (black bar) and OGD with 2DOG (green bar). Error bars = SEM. N numbers = number of cells/number of slices. 2DOG added during OGD (10-70 mins)
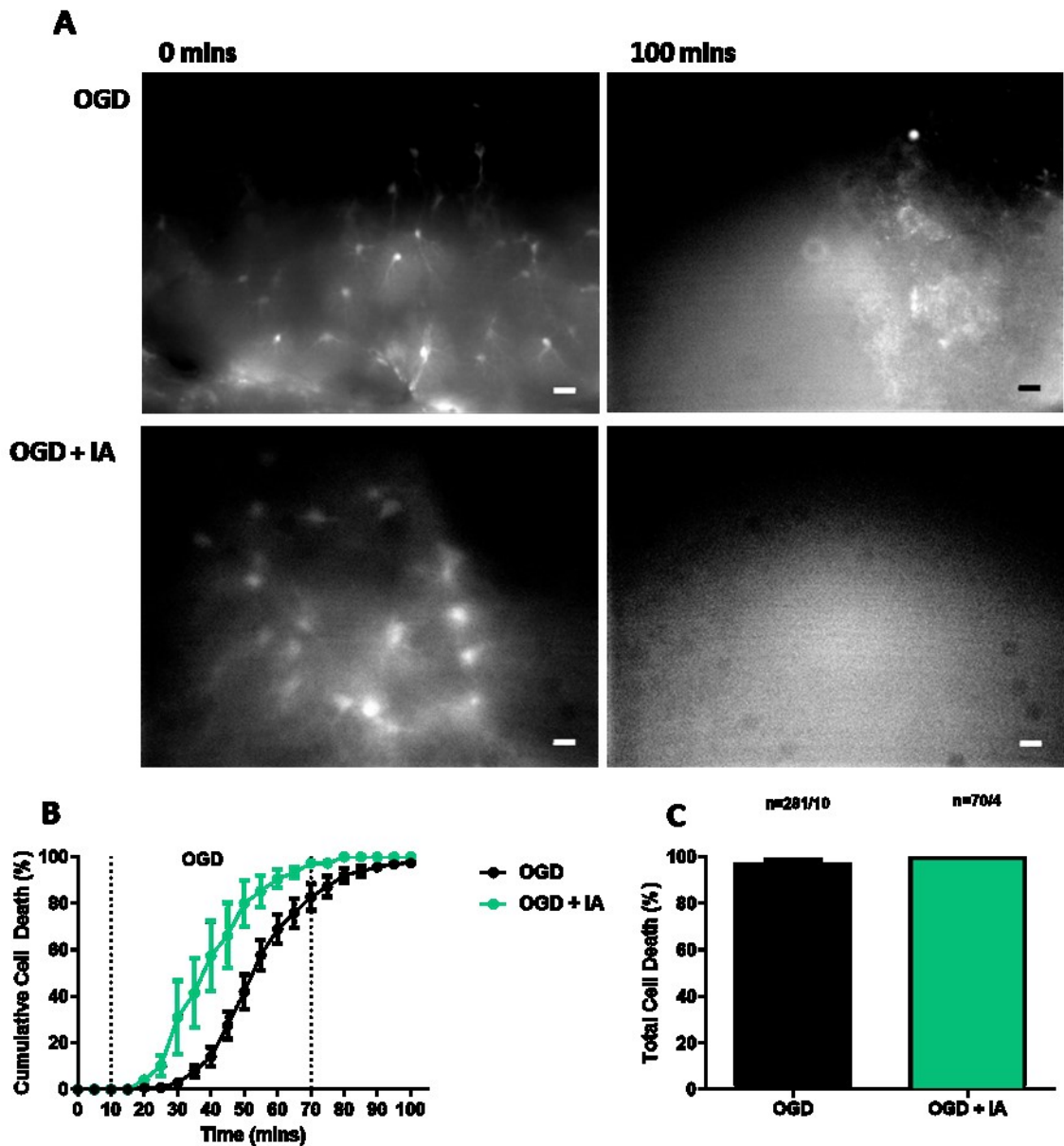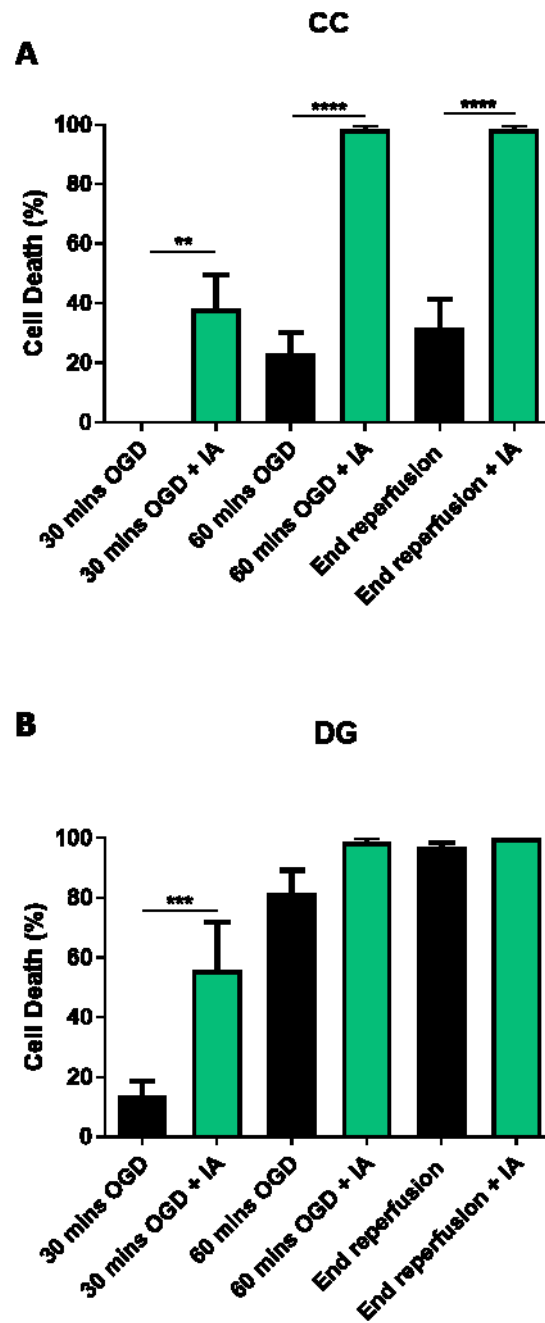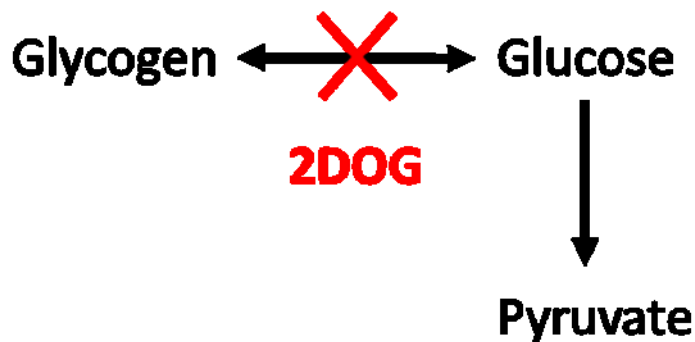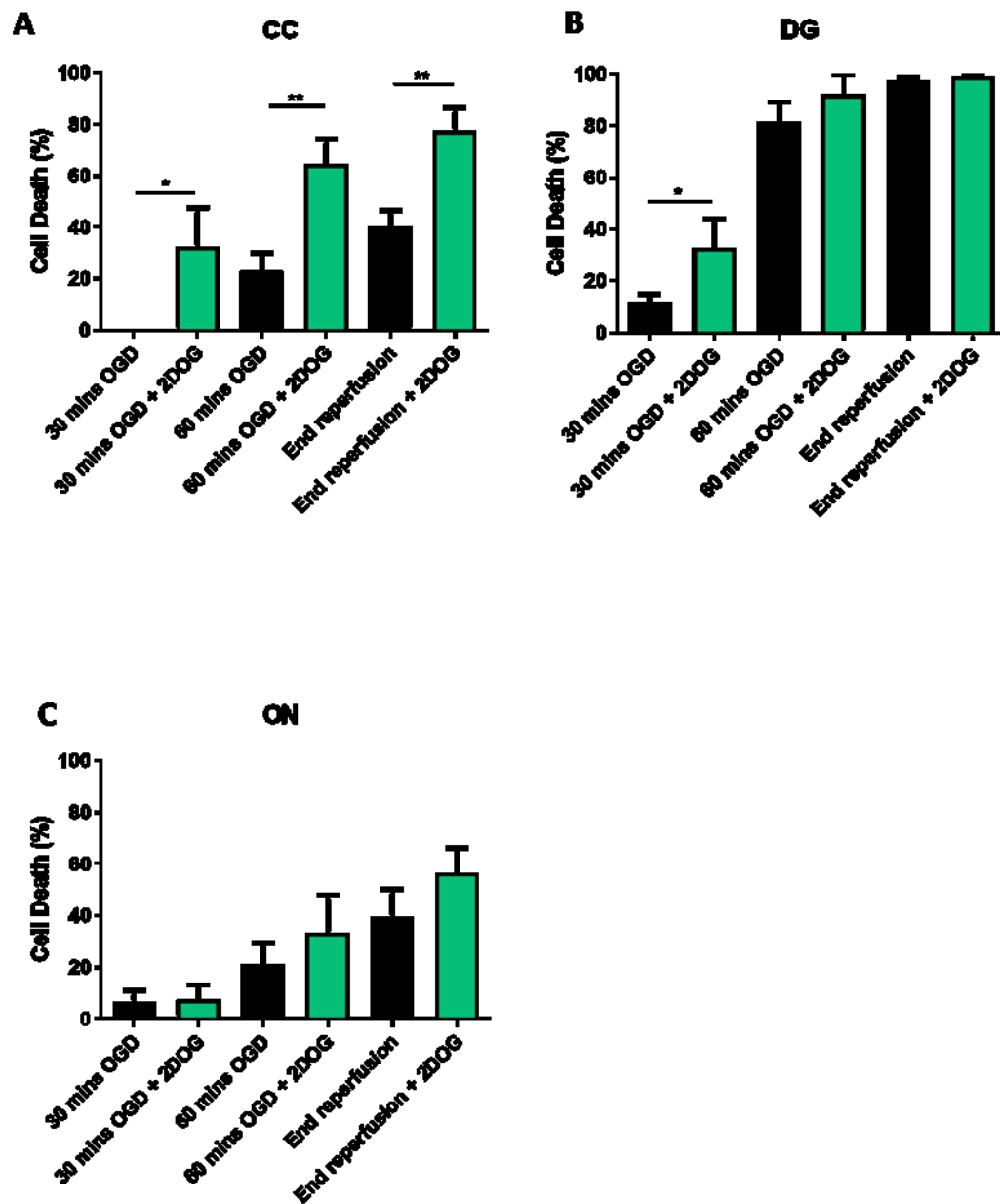
Figure 4.9: Effect of 2DOG on OGD induced astrocyte cell death at defined time points in CC, DG and ON. Astrocyte cell death after 30 and 60 minutes OGD and at the end of reperfusion, with OGD only (black bars) and OGD with 2DOG (green bars) treatment. **A:** corpus callosum. **B:** dentate gyrus. **C:** optic nerve. Error bars = SEM

4.3.2 2DOG treatment had no effect on OGD induced oligodendrocyte cell death

Astrocytes are not the only glial cells which are affected by ischaemic insult; oligodendrocytes are also susceptible to injury. It was investigated whether preventing the breakdown of astrocyte glycogen stores impacted oligodendrocyte cell death during OGD.

The presence of 2DOG did not alter oligodendrocyte cell death in CC (figure 4.10). Oligodendrocytes survived the length of the experiment under both conditions, OGD and OGD with 2DOG (figure 4.10A). The cell death profile with 2DOG treatment is very similar to that for OGD only conditions (figure 4.10B). The addition of 2DOG did not increase OGD induced oligodendrocyte cell death (figure 4.10C). Total cell death with was decreased from $1.31 \pm 0.71\%$ to 0% with 2DOG treatment (not significant).

In DG, the resilience of oligodendrocytes to acute ischaemia remained even with 2DOG treatment (figure 4.11). Most oligodendrocytes survive OGD and OGD with the addition of 2DOG (figure 4.11A). Again, in these images (as previously mentioned) some cells in the OGD panel appear that they have died, however they have gone out of the focal plane due to the swelling of the tissue. The addition of 2DOG has only slightly altered the cell death profile in this region (figure 4.11B). Total oligodendrocyte cell death was increased from $1.83 \pm 1.83\%$ to $3.70 \pm 3.70\%$ (not significant, figure 4.11C).

2DOG treatment during OGD had no effect on OGD induced oligodendrocyte cell death in ON (figure 4.12). All oligodendrocytes monitored survived for the duration of the experiment, with the focal plane altering slightly (figure 4.12A). The cell death profile is unchanged with the administration of

2DOG (figure 4.12B). The presence of 2DOG did not cause significant oligodendrocyte cell death to occur (figure 4.12C). The total cell death achieved was $1.06 \pm 0.67\%$ in OGD conditions and 0% with 2DOG treatment. Taking these findings into consideration it can be seen that 2DOG treatment, preventing the utilization of glycogen stores, has no effect on OGD induced oligodendrocyte cell death.
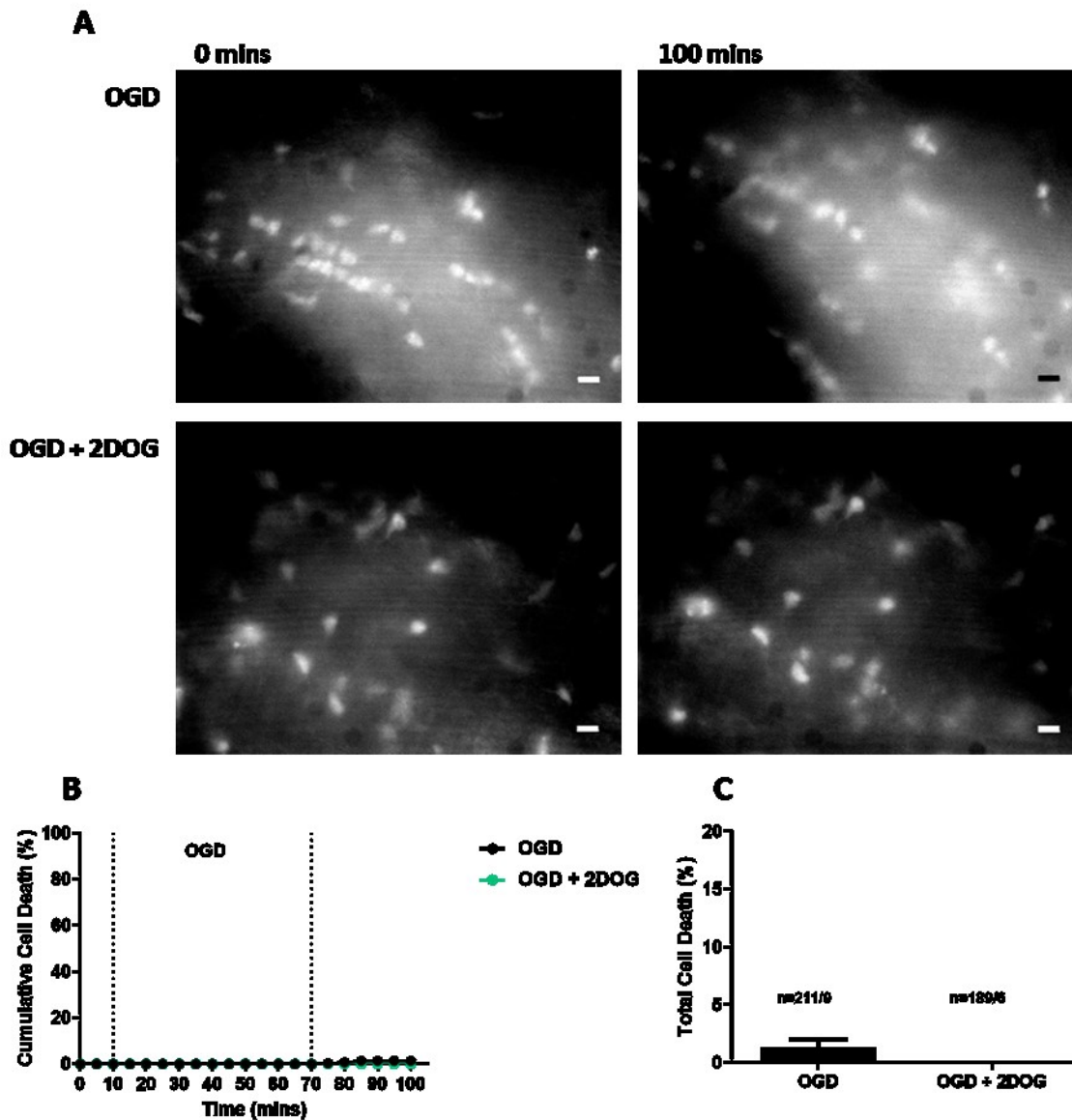
Figure 4.10: 2-deoxy-glucose (2DOG) treatment (10µM) had no effect on OGD induced oligodendrocyte cell death in corpus callosum (CC). **A:** Confocal images during OGD (upper panel) and OGD with 2DOG treatment (lower panel). Images taken at 0 and 100 minutes. Scale bar =20 µm. **B:** oligodendrocyte cell death over time. **C:** total cell death at time 100 minutes, OGD only (black bar) and OGD with 2DOG. Error bars = SEM. N numbers = number of cells/number of slices. 2DOG added during OGD (10-70 mins)
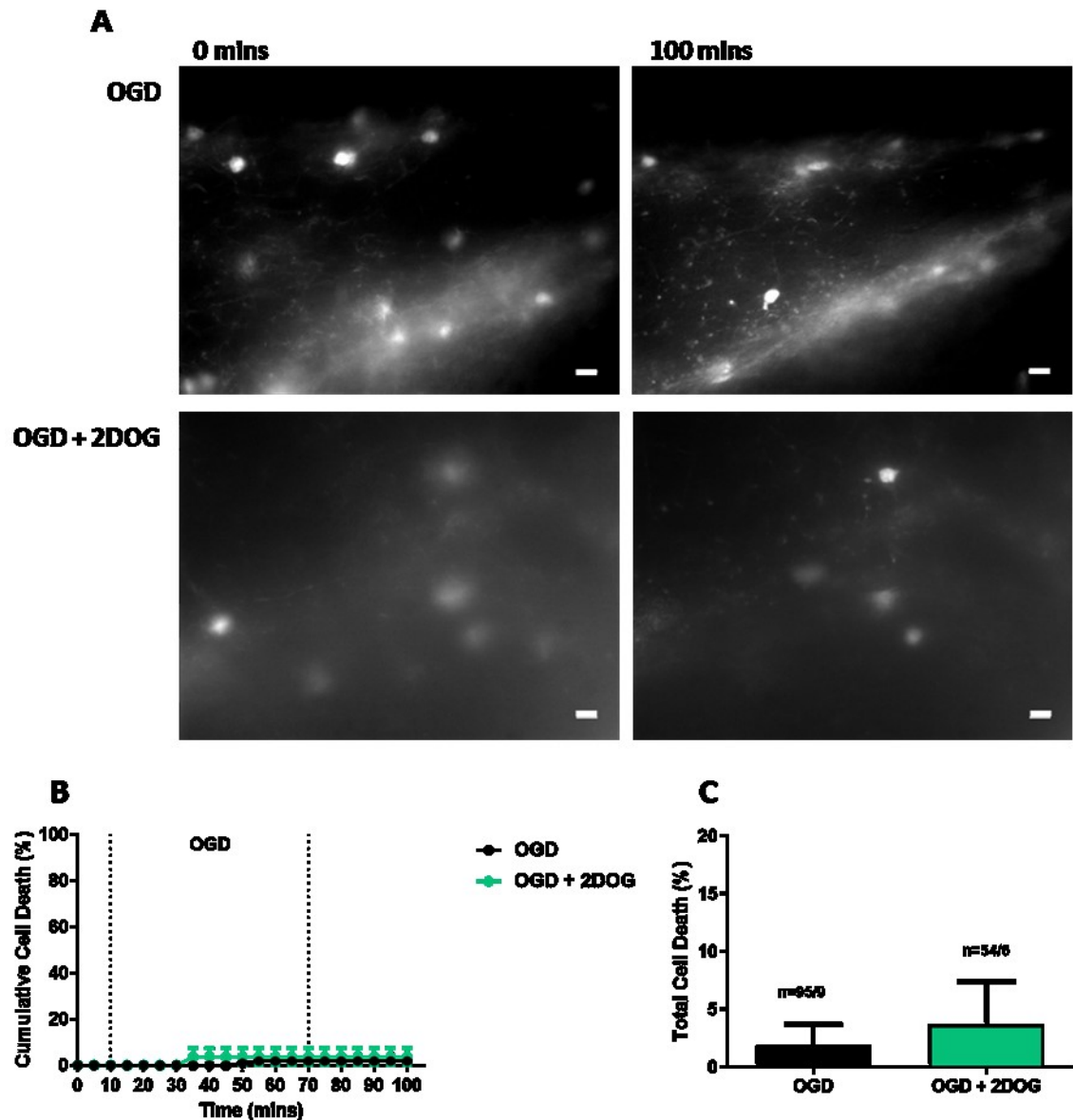
Figure 4.11: 2-deoxy-glucose (2DOG) treatment (10µM) had no effect on OGD induced oligodendrocyte cell death in dentate gyrus (DG). A: Confocal images during OGD (upper panel) and OGD with 2DOG treatment (lower panel). Images taken at 0 and 100 minutes. Scale bar =20 µm. B: oligodendrocyte cell death over time. C: total cell death at time 100 minutes, OGD only (black bar) and OGD with 2DOG (green bar). Error bars = SEM. N numbers = number of cells/number of slices. 2DOG added during OGD (10-70 mins)
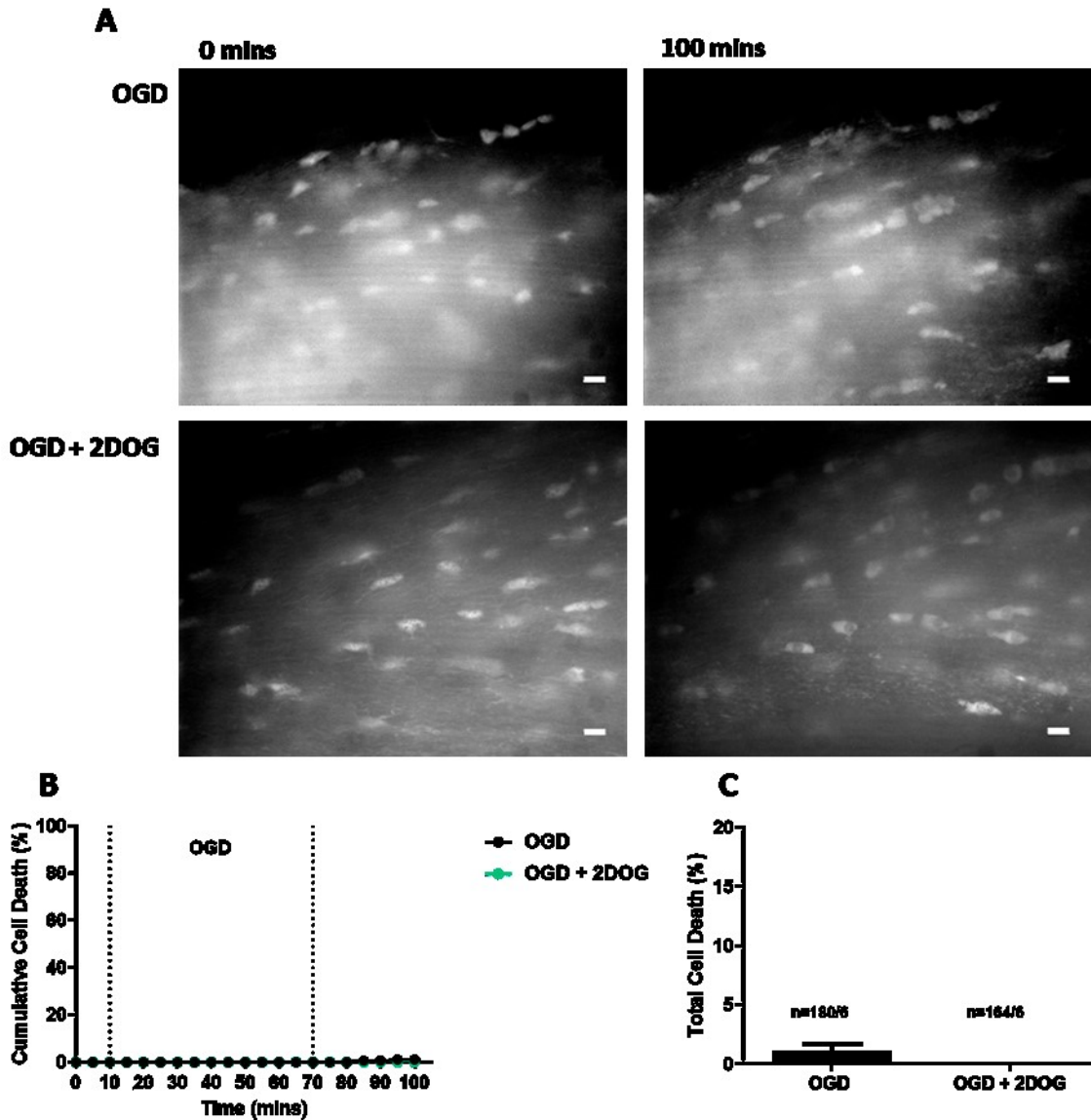
Figure 4.12: 2-deoxy-glucose (2DOG) treatment (10µM) had no effect on OGD induced oligodendrocyte cell death optic nerve (ON). **A:** Confocal images during OGD (upper panel) and OGD with 2DOG treatment (lower panel). Images taken at 0 and 100 minutes. Scale bar =20 µm. **B:** oligodendrocyte cell death over time. **C:** total cell death at time 100 minutes, OGD only (black bar) and OGD with 2DOG. Error bars = SEM. N numbers = number of cells/number of slices. 2DOG added during OGD (10-70 mins)
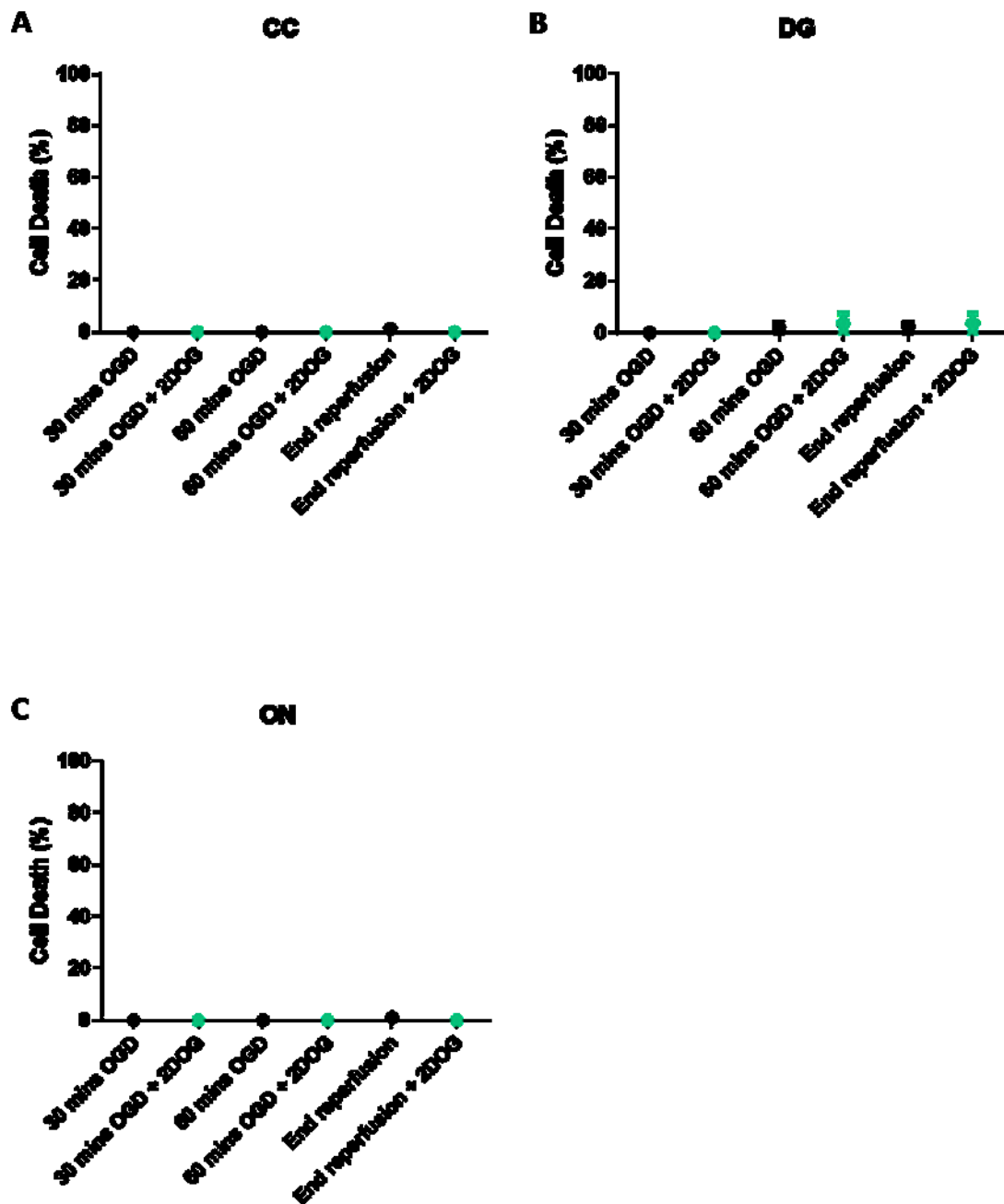
Figure 4.13: 2DOG treatment had no effect on OGD induced oligodendrocyte cell death at defined time points in CC, DG and ON. Oligodendrocyte cell death after 30 and 60 minutes OGD and at the end of reperfusion with OGD only (black) and OGD with 2DOG treatment (green). A: corpus callosum. B: dentate gyrus. C: optic nerve Error bars = SEM.

4.3.3 Results: Comparison of 2DOG treatment on glial cells

Oligodendrocyte cell death at defined time points was compared to see the effects of 2DOG treatment (figure 4.13). Comparisons were carried out for each region and found that the presence of 2DOG during OGD did not significantly alter oligodendrocyte cell death, in any region (CC figure 4.13A, DG figure 4.13B and ON figure 4.13C).

When comparing the effects of 2DOG treatment on each glial cell type, it was found that 2DOG had a greater effect on astrocyte cell death (figure 4.14). For each region the total astrocyte cell death was significantly higher than the total oligodendrocyte cell death. In CC, the difference in total cell death was from $77.71 \pm 8.73\%$ in astrocytes to 0% in oligodendrocytes, (p=<0.0001, figure 4.14A and B). In DG, astrocyte cell death was $99.12 \pm 0.88\%$, whilst oligodendrocyte cell death was only $3.70 \pm 3.70\%$, (p=<0.0001, figure 4.14C and D). In ON, the astrocyte cell death with 2DOG treatment was $56.67 \pm 9.49\%$, whereas oligodendrocyte death was 0%, (p=0.0001, figure 4.14E and F). These findings show that blocking glycogenolysis had a much greater effect on OGD induced astrocyte cell death than on oligodendrocyte cell death.
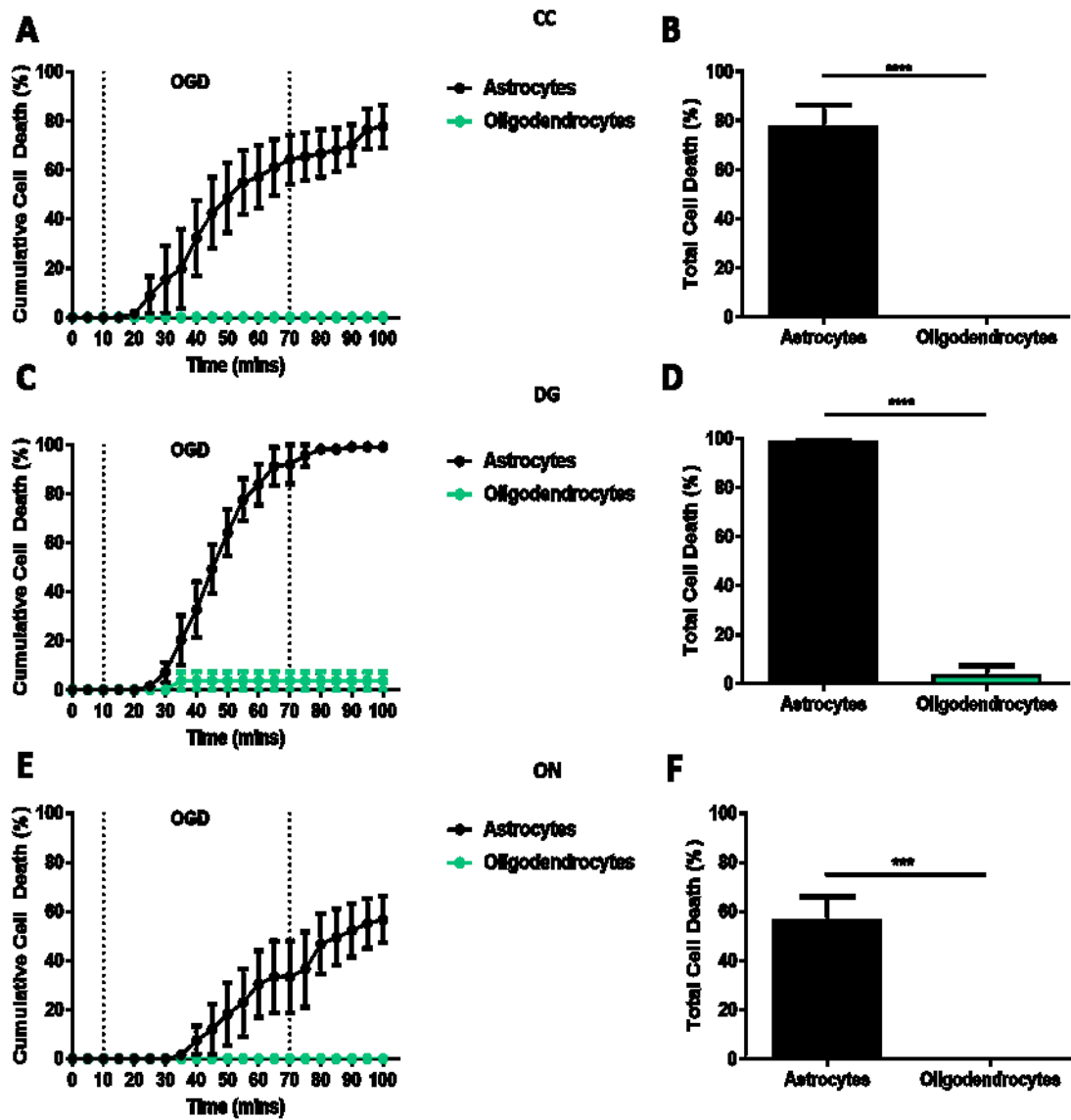
Figure 4.14: 2-deoxy-glucose (2DOG) treatment (10µM) increased OGD induced astrocyte cell death only. A: corpus callosum, OGD induced cell death over time. B: corpus callosum, total OGD induced cell death. C: dentate gyrus, OGD induced cell death over time. D: dentate gyrus, total OGD induced cell death. E: optic nerve, OGD induced cell death over time. F: optic nerve, total OGD induced cell death. Error bars = SEM. Astrocytes (black), oligodendrocytes (green)

4.4 RESULTS: GLYCOGEN STAINING – PERIODIC ACID SCHIFF STAIN

At first this method of staining seemed quite promising, however it soon became apparent that the white matter was heavily stained, whereas the grey matter was not stained to the same extent. The pink staining was also found to be widespread throughout the region (WM) and did not appear to be restricted to astrocytes (figure 4.15). It would have been expected that the staining would be confined to astrocytes as they are the major glycogen store of the brain. From this and reports in the literature it was clear that this is not a reliable method to visualise glycogen stores in astrocytes. Recently is has been proposed that the PAS stain may in fact stain for glycoproteins as well as cellular glycogen, therefore resulting in widespread staining.

Due to the limitations that were discovered using this stain an alternative method needed to be found. There are no commercially available glycogen antibodies. However, we were able to obtain an aliquot of an anti-glycogen IgM courtesy of Professor Hitoshi Ashida's group in Japan. This antibody has been found to bind to larger molecular weight glycogen granules.
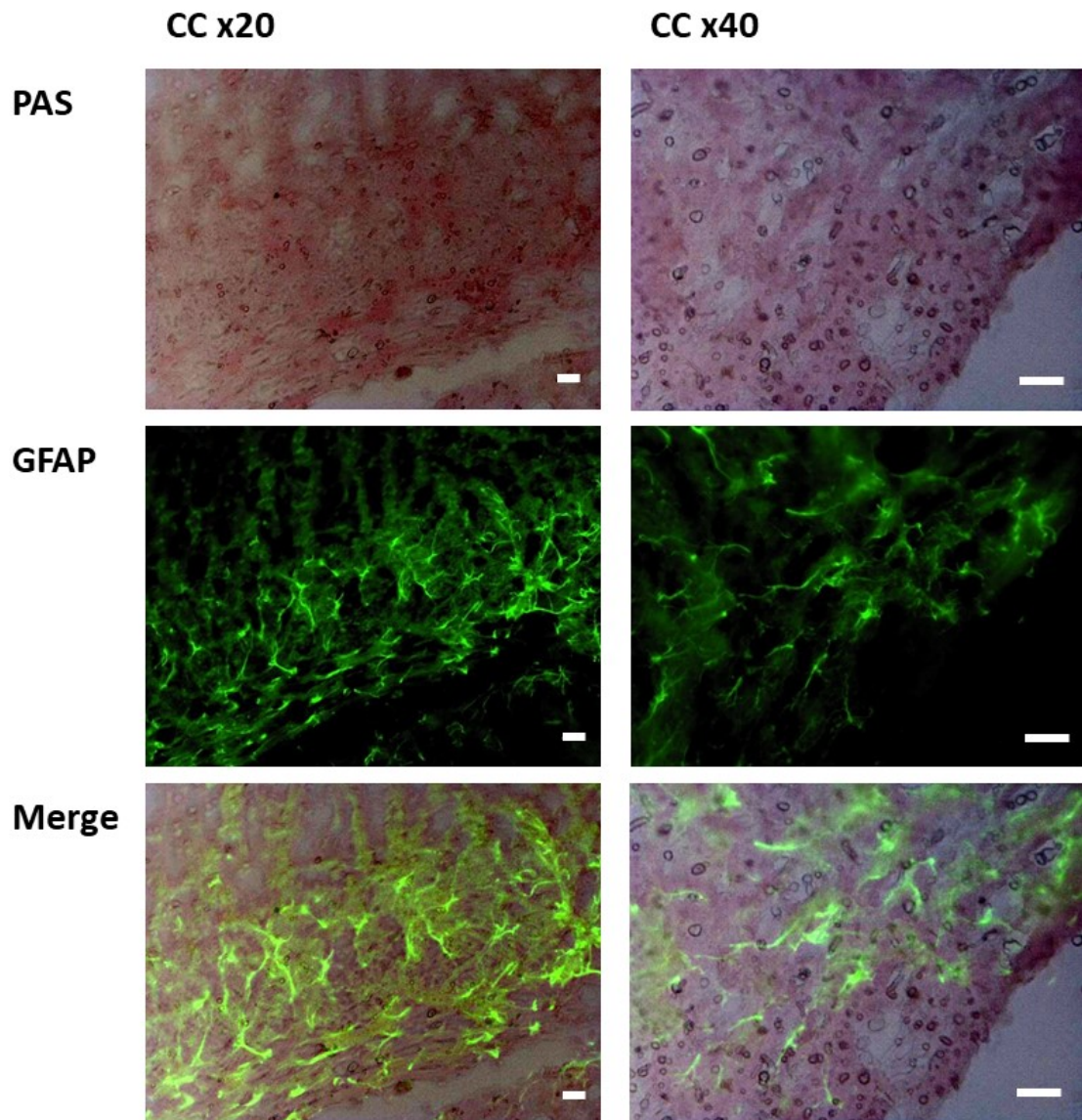
Figure 4.15: Example of PAS stain and co-staining with GFAP. Upper panel images taken with x20 objective. Lower panel taken using x40 objective. Both panels show images of the corpus callosum. Pink colouration is the product of the PAS stain, green is GFAP, merge shows overlay of the two images. Grey matter regions were very weakly stained. Scale bars = 20µM.

4.5 RESULTS: GLYCOGEN STAINING – ANTI-GLYCOGEN ANTIBODY

After observing the effects of IA and 2DOG on astrocyte cell death during OGD, astrocyte glycogen levels were examined in each region (CC and DG) during OGD, OGD with glycogenolysis block and aCSF only conditions. This was achieved using fixed brain slices which were incubated with an anti-glycogen IgM antibody. The slices were fixed after undergoing OGD, OGD with 2DOG or aCSF only.

The confocal images of CC stained for glycogen are Z projections of fixed sections (figure 4.16A). The upper panel shows control slices (aCSF), the central panel shows OGD slices and the lower panel shows OGD slices treated with 2DOG. In the first column GFP expressed by astrocytes is green, glycogen granules are shown in red in the second column and the third column is the merged image (GFP and glycogen). In the final column images have undergone "RG2B co-localization" in which co-localised red and green pixels are displayed as blue. Quantification of co-localised pixels was carried out by measuring the intensity of co-localised pixels, given in arbitrary units (AU) (figure 4.16B).

In CC, after OGD the amount of astrocytic glycogen is significantly reduced in surviving cells from 7.08 ± 0.25 AU in control (aCSF) to 5.49 ± 0.28 AU after OGD, ($p=0.0014$, figure 4.16B). The presence of 2DOG preserves the astrocyte glycogen stores, which is visible in those cells which have survived OGD. 2DOG treatment maintained glycogen levels which were 7.06 ± 0.47 AU after OGD. This was significantly higher than levels seen after OGD ($p=0.0139$) and was not significantly different from control levels. These findings show the presence of viable astrocytes after OGD and suggests that in CC, 2DOG is effective at preventing glycogenolysis which maintains the glycogen stores in viable cells.

Confocal images of DG astrocyte glycogen levels were obtained as for CC astrocytes (figure 4.17A arranged as for figure 4.17A). Quantification of astrocyte glycogen was carried out and was as co-localised pixel intensity (figure 4.17B). After OGD, astrocyte glycogen levels in DG astrocytes were reduced from 10.32 ± 0.39 AU in control (aCSF) to 9.34 ± 0.73 AU (not significant) in surviving cells. The addition of 2DOG caused DG astrocyte glycogen levels to be significantly reduced when compared to control (p=0.0077). Here, astrocyte glycogen dropped to 7.83 ± 0.85 AU. This region had fewer viable astrocytes after OGD and after OGD with 2DOG treatment and so measurements were limited to the surviving cells.

The amount of astrocyte glycogen co-localisation was compared for the two regions (figure 4.18). It was found that the DG contained significantly more astrocyte located glycogen than the CC (p=<0.0001). The levels seen in CC were 7.08 ± 0.25 AU, whereas in DG levels were higher at 10.32 ± 0.39 AU. These findings suggest that DG astrocytes naturally have larger glycogen stores than CC astrocytes. The evidence shows that for both regions glycogen stores are depleted after one hour of OGD in surviving astrocytes. However, it would seem that 2DOG is more successful at inhibiting glycogenolysis in CC than in DG.
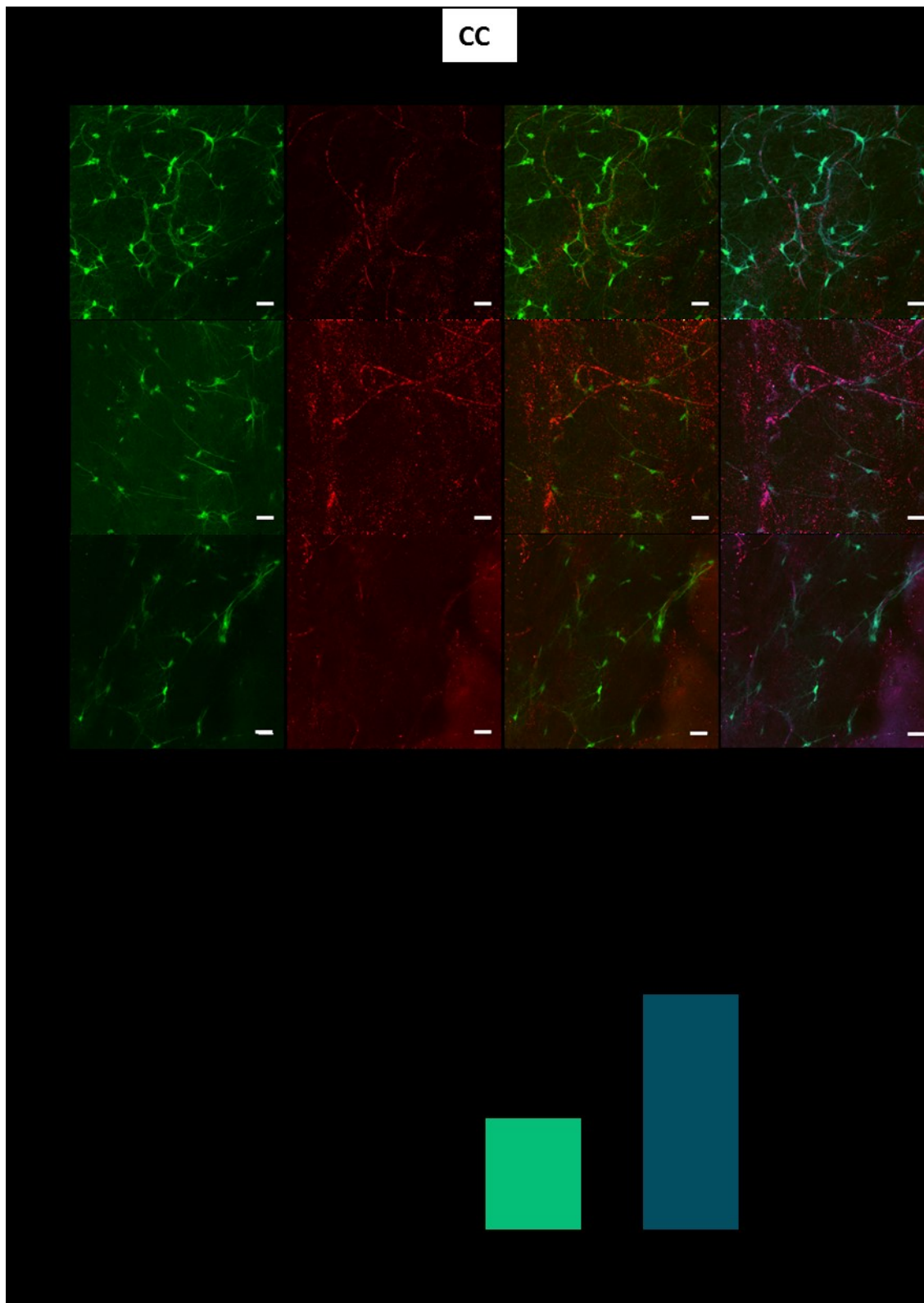
Figure 4.16: Changes in astrocyte glycogen levels in different conditions in corpus callosum (CC). A: confocal images of Z projections from fixed frozen sections showing glycogen staining. Green is GFP, red is glycogen, "RG2B co-localization" shows co-localised pixels in blue. Scale bars = 20µm. **B:** quantification of glycogen staining in whole cells. Error bars = SEM. N numbers = number of cells/number of regions of interest.
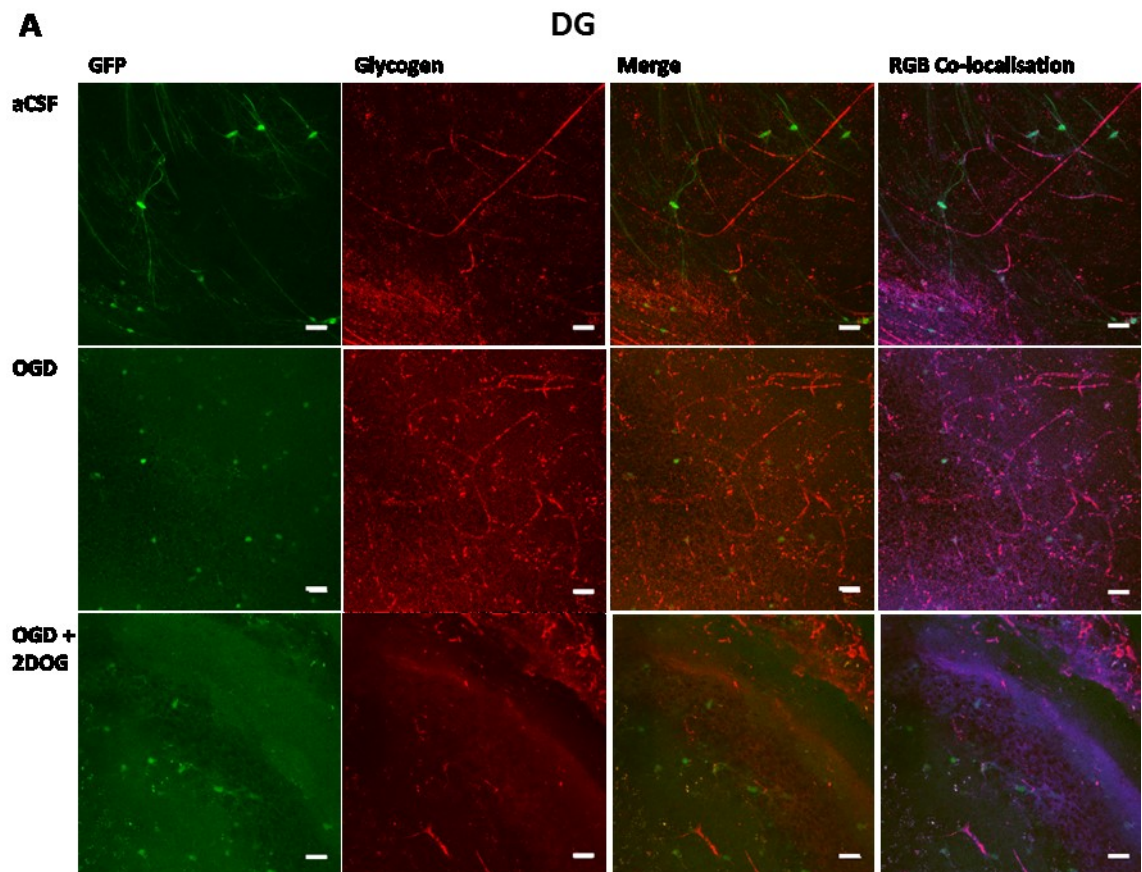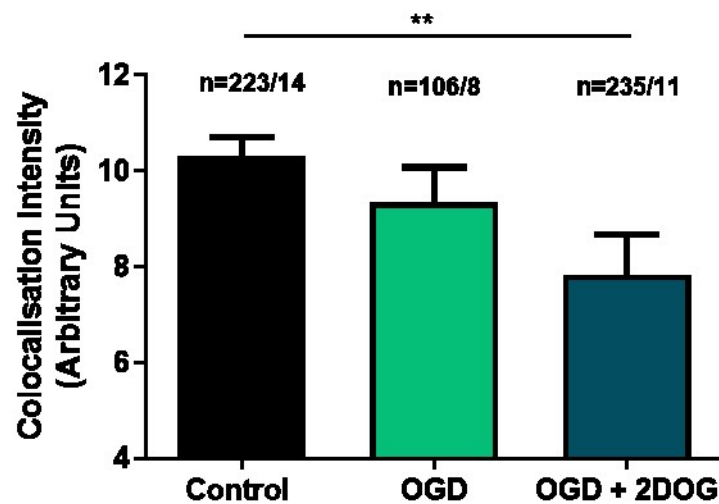
Figure 4.17: Changes in astrocyte glycogen levels in different conditions in dentate gyrus (DG). A: confocal images of Z projections showing glycogen staining. Green is GFP, red is glycogen, "RG2B co-localization" shows co-localised pixels in blue. Scale bars = 20µm. B: quantification of glycogen staining in whole cells. Error bars = SEM. N numbers = number of cells/number of regions of interest.
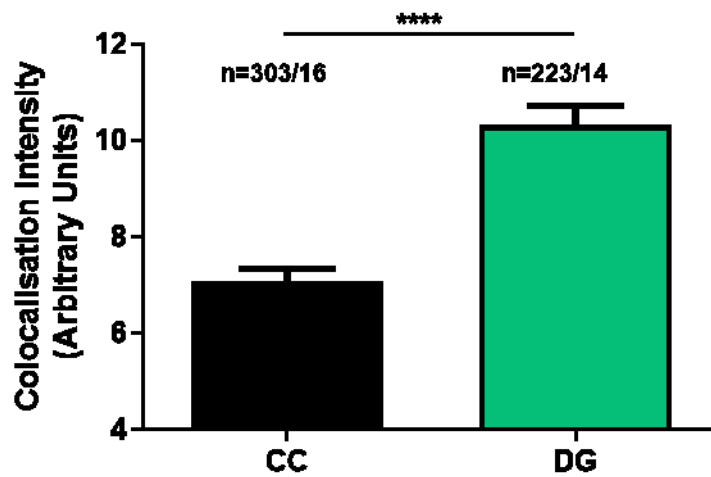
Figure 4.18: Higher levels of glycogen are found in DG. Comparison of glycogen co-localisation in CC (black bar) and DG (green bar) found significantly more astrocytic glycogen in DG. Error bars = SEM.

4.6 Discussion: Role of astrocytic glycogen in ischaemia

In this chapter the role of astrocytic glycogen stores during acute ischaemic insult was examined. I also investigated whether these stores affected glial survival during and after injury. The presence of astrocytic glycogen is known to promote neuronal survival (Swanson & Choi, 1993), however the role that glycogen may play in glial response to insult has not been widely investigated in adult models. Fern (2015) found in neonatal WM that the presence of glycogen increased tolerance to ischaemic injury. It is possible that astrocytes use glycogen to extend their own survival for a limited time, during ischaemia.

4.6.1 Glycogen stores contribute to astrocyte survival.

The inhibition of glycogenolysis with IA or 2DOG significantly increased OGD induced astrocyte cell death (p=0.0001) in CC (figures 4.2 and 4.6). Blocking access to glycogen stores caused astrocytes in this WM region to behave like GM astrocytes and experience extensive cell death. The use of IA achieved a more dramatic effect in CC than in DG (figure 4.2B and C), while 2DOG had no significant effect upon DG astrocyte death (figure 4.7C). This may be due to fact that the maximum amount of cell death in DG is already achieved with OGD, thus limiting any effect of the metabolic block upon cell death. In support of this interpretation, block of glycogen utilization in the DG resulted in cell death beginning significantly earlier time point (figure 4.3 and 4.7) in the presence of IA or 2DOG. In ON, the addition of 2DOG treatment increased OGD induced cell death, although this was not significant and was not to the same extent in the CC. This suggests a lesser role for glycogen in ON and that the tolerance of these cells to ischaemia may be due to other mechanisms. The lack of astrocyte cell death in the presence of 2DOG illustrates the heterogeneous

nature of the astrocyte population. The ON was examined as previous work had been carried out on pre-myelinated ON (P0-P2), which found that glycogen was necessary for axonal function during ischaemic conditions (Fern, 2015).

The evidence here shows that the glycogenolysis and the utilization of the resulting metabolites is required for CC astrocyte survival during acute ischaemic insult. In DG, the presence of glycogen stores delays OGD induced cell death, however even with functioning glycogenolysis these cells remain very sensitive to ischaemic injury. In the adult ON, glycogen does not appear to be significant for astrocyte survival in ischemic conditions.

4.6.2 Glycogen levels vary between regions and conditions

Immunofluorescence staining of brain sections allowed the levels of astrocyte glycogen in CC and DG to be visualised and quantified. The effect of OGD and OGD with 2DOG on astrocyte glycogen levels in these regions was investigated in the surviving cells.

When the co-localised glycogen levels were compared in CC and DG, it was found that DG contained significantly more (p=<0.0001) astrocytic glycogen than CC (figure 4.18). This finding corresponds with the literature, where it has been found that the highest amounts of glycogen are in the hippocampus (Oe *et al.*, 2016). The DG is a region of high energy demand which will need to utilize these larger glycogen stores for synthesis of glutamine, during which pyruvate derived from glycogen is preferred (Gibbs *et al.*, 2007). Glycogenolysis is also utilized for glutamate uptake through the fuelling of the NKA (Xu *et al.*, 2013) for sodium extrusion which is the driving force for glutamate uptake. The discovery that glycogen is involved in memory and learning (Gibbs, Anderson & Hertz, 2006) also explains the high levels that are seen in the hippocampus. However,

it is interesting that higher levels of glycogen seen here in the DG does not correspond to ischaemic protection, even though preventing access to glycogen stores increased cell death in CC. This suggests the presence of glycogen does not equate to cell survival during ischaemia.

In CC there was significant decrease (p=0.0014) in astrocyte glycogen levels after one hour OGD (figure 4.16). Glycogen was present in viable astrocytes at the end of OGD, these cells had retained their morphology and had not lost their cytoplasmic GFP despite the ischaemic insult. This would suggest that not only are CC astrocytes tolerant to insult but that there is a role for glycogen during ischaemic insult. When 2DOG was administered in CC, the glycogen stores were effectively protected in surviving astrocytes, showing that glycogenolysis was successfully inhibited during OGD (figure 4.16B). It is possible that surviving astrocytes are able to utilize stores before cell death due to the resilience of cells and glycolytic nature of astrocytes (Supplie *et al.*, 2017).

The changes in DG astrocyte glycogen levels after OGD and OGD with 2DOG differed to those seen in CC. In DG, astrocyte glycogen levels were reduced in surviving astrocytes after OGD, however this was not significant when compared to control conditions (figure 4.17B). This suggests that DG astrocyte glycogen stores are not accessed to the same extent as CC astrocyte glycogen stores, which may be due to the sensitivity of DG astrocytes to ischaemia. The significant reduction in the surviving astrocyte glycogen levels seen in the presence of 2DOG may be due to the catastrophic cell death that occurs under these conditions. The lack of viable cells after injury results in a loss of astrocyte glycogen in the region, even if glycogenolysis was successfully inhibited. The addition of 2DOG seemed to stress DG astrocytes and greatly

161

increased the sensitivity of these cells to ischaemia. This caused widespread cell death, which resulted in few surviving cells.

The evidence obtained suggests that glycogen is used to aid astrocyte survival during and after ischaemic insult in the CC.. The finding of higher glycogen levels in the DG is consistent with the high metabolic demand that exists in this region as glycogen is required for glutamatergic transmission (Sickmann *et al.*, 2009). The higher levels of glycogen in DG astrocytes did not prevent ischaemic induced cell death. This would suggest that there are differences in cell death mechanisms between regions. Also the glycogen in this region must have a specific role, such as neurotransmitter synthesis.

4.6.3 Glycogen stores are not utilized by oligodendrocytes

The discovery that oligodendrocytes show tolerance to acute ischaemic insult has raised questions as to how they are able to survive acute ischaemic injury. Thus, the role of glycogen in oligodendrocyte survival was investigated. When astrocytic glycogen stores were inhibited, the lack of access to lactate had no effect on oligodendrocyte ischaemic cell death (figures 4.10-4.13). This suggests that metabolic products from glycogenolysis are not used by oligodendrocytes during ischaemic insults and their tolerance to ischaemic injury is due to a different mechanism. When investigating the role of glycogen store inhibition on oligodendrocytes only 2DOG was used as this fully prevented the breakdown of glycogen stores. Whilst IA prevents the utilization of the stores after their breakdown, via the inhibition of the enzyme responsible for the sixth step of glycolysis.

CHAPTER 5

5 GLIA AND GLUTAMATE RECEPTORS

5.1 INTRODUCTION

It has been shown that astrocytes and oligodendrocytes can express both NMDA and AMPA/kainate ionotropic glutamate receptors (GluRs) (Burnashev, 1996; Conti *et al.*, 1996). Binding of glutamate to the GluRs produces opening of the receptor pore, allowing the influx of cations and triggering intracellular increases in ion concentrations and depolarization. The influx of ions through NMDA GluRs may be prevented through endogenous magnesium block, which occludes the pore opening, this block is voltage dependent (Mayer, Westbrook & Guthrie, 1984; Nowak *et al.*, 1984). Regional variability in astrocyte GluR expression levels has been suggested (Dzamba *et al.*, 2015), which would result in location dependent amounts of GluR mediated ion influx.

The subunit arrangement of GluRs affects the permeability of receptor pore to various ions (Dzamba, Honsa & Anderova, 2013). Investigation of these subunits determined that the GluRs expressed by glial cells are more permeable to calcium ions that other GluRs (Burnashev, 1996), and those expressed by astrocytes have low calcium permeability (Kirischuk, Parpura & Verkhratsky, 2012; Palygin *et al.*, 2010). GluRs are also permeable to cations such as sodium and potassium (Dzamba, Honsa & Anderova, 2013). Sodium influx into astrocytes is involved in physiological and cytotoxic cell swelling which precedes ischaemic cell death and will be further discussed in the next chapter.

5.1.1 Astrocytes and glutamate receptors

Astrocytes express both NMDA and AMPA/kainate receptors (Burnashev, 1996; Conti *et al.*, 1996). This has triggered further investigation

into the role of glial GluRs. The known involvement of GluRs in ischaemia induced neuronal cell death via excitotoxicity (Coyle *et al.*, 1981; Lucas & Newhouse, 1957; Pulsinelli, Sarokin & Buchan, 1993), identified GluRs as a suitable target to examine for a role ischaemic astrocyte cell death.

Both NMDA and AMPA/kainate receptors are permeable to calcium and other ions. Under physiological conditions this contributes to the astrocyte homeostatic maintenance of the extracellular space (ECS). For AMPA/kainate receptors, the amount of GluR2 subunits incorporation into the receptor determines the receptor permeability to calcium, a lower level of expression results in increased permeability (Hollmann, Hartley & Heinemann, 1991; Jonas & Burnashev, 1995). The AMPA/kainate receptor channels are also permeable to sodium and potassium ions allowing more of these ions to pass through when the receptor is activated (Citri & Malenka, 2008).

The presence of GluRs on astrocytes suggests they have a physiological role to play. The important role that has been discovered for GluRs is involvement in neuron to glia signalling. There are two possible routes that two-way communication can occur, through the ectopic release of neurotransmitters (Araque, Carmignoto & Haydon, 2001) or via gap junction connections (Alvarez-Maubecin *et al.*, 2000).

The activation of AMPA/kainate and NMDA receptors triggers an increase astrocyte intracellular calcium concentration (Kim, Rioult & Cornell-Bell, 1994; Müller *et al.*, 1993). In astrocytes this calcium increase can be transmitted to other astrocytes via gap junctions, producing calcium waves across the astrocyte syncytium (Charles *et al.*, 1991; Cornell-Bell *et al.*, 1990; Dani, Chernjavsky & Smith, 1992). This will then inform and direct astrocyte responses to neuronal communication. Cortical NMDA receptors have been

found to be more sensitive to glutamate than AMPA receptors (Lalo *et al.*, 2006). Lalo *et al.* (2006) determined the glutamate EC_{50} for each receptor in cortical astrocytes, for NMDA receptors the EC_{50} was $1.9 \pm 0.5\mu M$ and for AMPA receptors the EC_{50} was $52.1 \pm 14.06\mu M$. This suggests that astrocytes can detect different concentrations of extracellular glutamate, also that different concentrations of glutamate may elicit diverse responses from astrocytes. Glutamate can be utilized as a metabolite, when converted into α-ketoglutarate which can then enter the TCA cycle to generate ATP (McKenna, 2007). Approximately 20% of glutamate taken up by astrocytes is converted and lost to the TCA cycle (Hertz *et al.*, 2015; McKenna, 2013).

It is widely accepted that astrocytes are resistant to excitotoxicity. However, it has been found that over activation of AMPA receptors can be severely damaging to neocortical astrocytes (David *et al.*, 1996), showing that immature astrocytes have an increased sensitivity to higher glutamate levels than mature cells, which are resistant to excitotoxicity. It has been reported that a transient increase in glutamate concentration can cause astrocyte cell swelling and longer exposures caused oxidative stress in cells, which goes on to trigger cell death (Chen, Liao & Kuo, 2000).

5.1.2 Oligodendrocytes and glutamate receptors

Oligodendrocytes were initially thought to only express AMPA/kainate receptors (Gallo *et al.*, 1994; Patneau *et al.*, 1994). These receptors are involved in CNS development and in pathological oligodendrocyte damage. It has now been shown that NMDA receptor expression is normal for WM oligodendrocytes (Karadottir *et al.*, 2005). The receptors found on oligodendrocytes have a specific subunit composition, containing mainly NR1, NR2C and NR3 subunits (Karadottir *et al.*, 2005). The binding of glutamate to

oligodendrocyte located GluRs causes intracellular increase of calcium, either by influx of calcium across the cell membrane (Willard & Koochekpour, 2013) or release from internal calcium stores (Micu *et al.*, 2016). Further investigation found that NMDA receptors are predominantly localised to oligodendrocyte processes and are involved in ischaemic injury via calcium influx and accumulation, triggered by excitotoxicity (Micu *et al.*, 2006; Salter & Fern, 2005). Recently, the group has established that axonal vesicular glutamate release is the source of glutamate responsible for excitotoxic myelin damage (Doyle *et al.*, 2018). It was also determined that injury was mediated by NMDA receptors containing GluN2C/D subunits.

In oligodendrocytes, GluRs are used for neuron to glia signalling and myelin located receptors are in a perfect position to respond to axonal glutamate release. During development axons use glutamate to signal to oligodendrocyte precursor cells via AMPA/kainate receptors (Kukley, Capetillo-Zarate & Dietrich, 2007), which may allow the identification of axons. Glutamate activation of NMDA receptors on precursor cells initiates their differentiation into myelinating oligodendrocytes via the (Lundgaard *et al.*, 2013). Recently it has been discovered that signalling occurs between neuronal axons and the covering myelin sheath (Micu *et al.*, 2016). This kind of axonal signalling has been implicated in communicating axonal metabolic demand to glial cells (Funfschilling *et al.*, 2012).

5.1.3 Glutamate receptors involvement in ischaemic glial injury

The main mechanism of acute ischaemic neuronal cell death is excitotoxicity, whereby increased concentrations of glutamate over-activate GluRs causing a cytotoxic influx of calcium (Coyle *et al.*, 1981; Lucas & Newhouse, 1957; Pulsinelli, Sarokin & Buchan, 1993). The increase in

intracellular calcium also causes accumulation of calcium within mitochondria. This increase depolarizes the mitochondrial membrane triggering the release of apoptotic factors (Matute, 2006). This cell death mechanism is also responsible for oligodendrocyte cell death after ischaemic insult. Initially, oligodendrocyte excitotoxicity was thought to be caused by AMPA/kainate receptors (Matute *et al.*, 2002). However, with the discovery of oligodendrocyte NMDA receptor expression, it has now been suggested that the different kinds of receptors may be responsible for different kinds of injury.

Salter and Fern (2005) found that over-activation of NMDA receptors caused process loss in P10 ON oligodendrocytes and suggested that there may be differential expression of GluRs (Salter & Fern, 2005). They also suggested that NMDA receptors are responsible for injury to processes after insult, whilst AMPA/kainate receptors may be responsible for cytotoxicity (Salter & Fern, 2005). Excitoxicity is not only responsible for process loss and cell death but also causes damage and vacuolation to myelin (Pantoni, Garcia & Gutierrez, 1996). The excessive activation of particularly AMPA/kainate receptors was found to cause widespread death of cultured cortical astrocytes (David *et al.*, 1996). Increased levels of glutamate can cause astrocyte cell swelling and prolonged exposure caused cell death, most likely via oxidative stress (Chen, Liao & Kuo, 2000).

Previous work has found that in P2 mice, astrocyte cell death was due to cytotoxic influx of calcium (Fern, 1998). However, the mechanism of ischaemic astrocyte cell death changes with age of the animal and the point of development. In P10 mice it was found that cell death was the result of sodium influx, which was suggested to occur via the sodium-potassium-chloride co-transporter 1 (NKCC1) (Salter & Fern, 2008; Thomas *et al.*, 2004). In this

chapter the involvement of calcium and GluRs were investigated to see their effect on glial cell death and to determine whether the mechanism for adult ischaemic cell death is different to that for P10 animals. Here the hypothesis being that glutamate receptors are involved in ischaemia induced astrocyte cell death.

5.2 RESULTS: ZERO CALCIUM CONDITIONS INCREASED OGD INDUCED ASTROCYTE CELL DEATH

Studies investigating ischaemia induced neuronal death have established that it is a calcium dependent process. First, it was examined whether calcium was required for OGD induced astrocyte cell death. Slices that underwent OGD did so with either normal calcium or calcium-free OGD aCSF. Calcium-free OGD aCSF contained a calcium chelator (EGTA 0.05mM), thereby lowering extracellular calcium during the OGD period and reduces calcium influx into cells.

Contrary to the effect seen on neuronal cell death previously reported, zero calcium conditions increased OGD induced astrocyte cell death in CC (figure 5.1). Few astrocytes survive in the confocal images of OGD with zero calcium (figure 5.1A). The use of calcium-free aCSF caused a significant reduction in the t value from 62.00 ± 2.32 mins to 48.58 ± 2.81 mins (p=0.0034, figure 5.1B). This suggests a lack of external calcium increased the rate of OGD induced cell death. The total amount of cell death was significantly higher with OGD and zero calcium conditions, cell death was increased to 97.17 ± 1.91% from 40.17 ± 6.45 (p=<0.0001, figure 5.1C).

In DG cell death was already high at 97.61 ± 1.01%, with zero calcium this was increased to 99.28 ± 0.73% (not significant, figure 5.2C). The removal of calcium from the aCSF caused a decrease in t value from 54.64 ± 3.30 mins to 40.83 ± 3.12 mins (p=0.012, figure 5.2B). The DG confocal images show little difference between astrocytes that underwent OGD only and those that experienced OGD without calcium, widespread cell death is seen under both conditions (figure 5.2A).

The OGD induced astrocyte cell death was compared between the two conditions for each region at defined time points throughout the experiment (figure 5.3). For CC the removal of calcium from the aCSF caused OGD induced cell death to be significantly increased at each time point (figure 5.3A). After 30 minutes OGD cell death was increased from $0 \pm 0\%$ to $22.54 \pm 8.74\%$ without calcium (p=0.0476). The significance of increased cell death was greater as the experiment progressed. At 60 minutes OGD cell death increased from $22.11 \pm 7.12\%$ to $93.06 \pm 4.10\%$, (p=<0.0001) whereas at the end of reperfusion cell death had increase from $40.17 \pm 6.45\%$ to $97.17 \pm 1.91\%$ (p=<0.0001). This suggests that a lack of calcium increased CC astrocyte sensitivity to OGD.

For DG, only one time point was significantly increased, this was after 30 minutes OGD (figure 5.3B). Here, cell death was increased from $14.04 \pm 4.77\%$ to $49.59 \pm 10.89\%$ (p=0.0006). Zero calcium conditions caused DG astrocytes to become very sensitive to the initial ischaemic insult. Taken together these results suggest that ischaemia induced CC and DG astrocyte cell death occurs in an external calcium independent manner. The removal of calcium did not provide protection to astrocytes and worsened OGD induced cell death.

Figure 5.1: Zero Calcium conditions increased OGD induced astrocyte cell death in corpus callosum (CC). A: Confocal images of during OGD (upper panel) and OGD with 0 Ca (lower panel). Images taken at 0 and 100 minutes. Scale bar = 20 μm. **B:** Astrocyte cell death over time. **C:** Total cell death at time 100 minutes, OGD only (black bar) and OGD with $0Ca^{2+}$ (green bar). Error bars = SEM. N numbers = number of cells/number of slices.

A

B

C
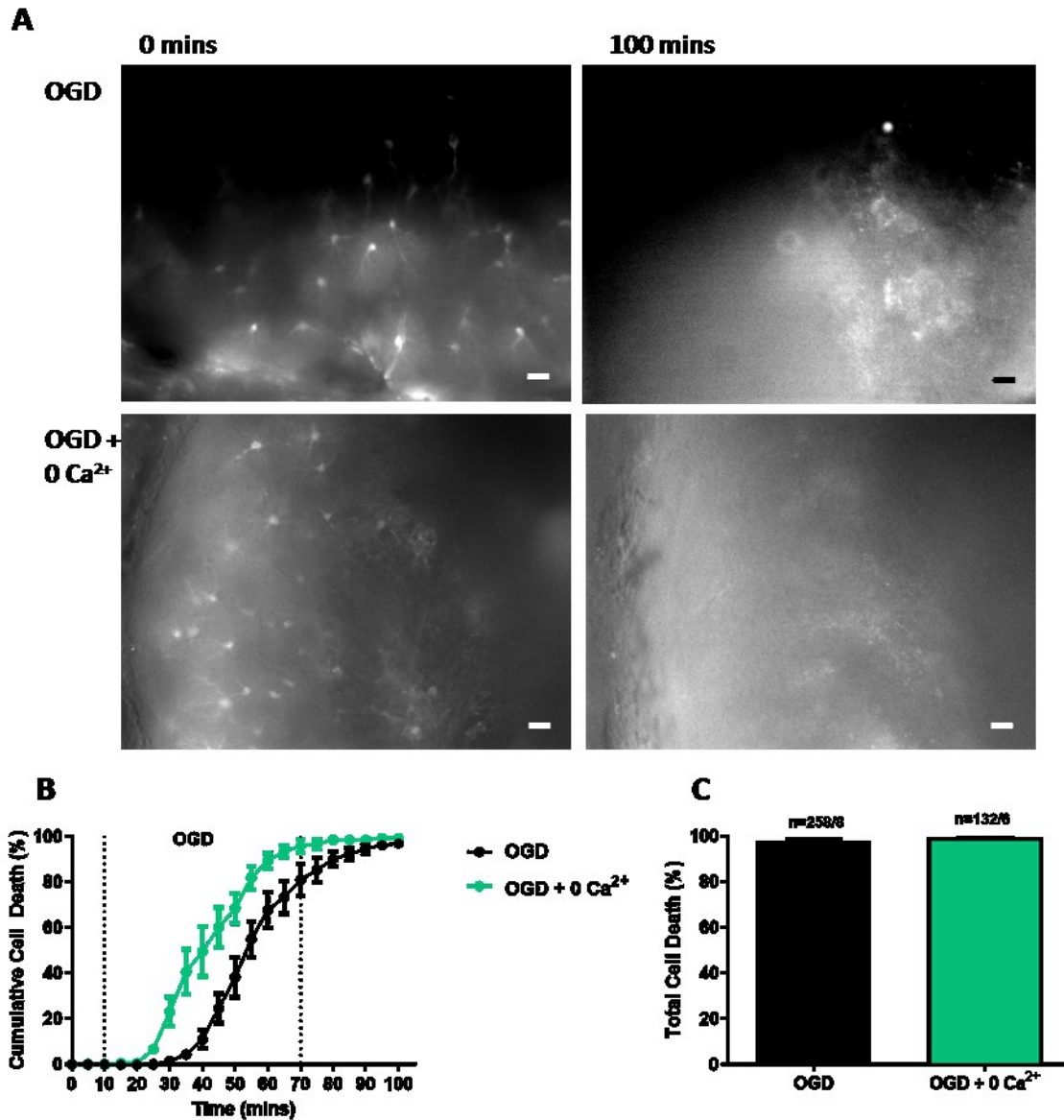
Figure 5.2: Zero Calcium conditions increased the rate of OGD induced astrocyte cell death in dentate gyrus (DG). **A:** Confocal images of during OGD (upper panel) and OGD with 0 Ca (lower panel). Images taken at 0 and 100 minutes. Scale bar = 20 µm. **B:** Astrocyte cell death over time. **C:** Total cell death at time 100 minutes, OGD only (black bar) and OGD with $0Ca^{2+}$ (green bar). Error bars = SEM. N numbers = number of cells/number of slices.
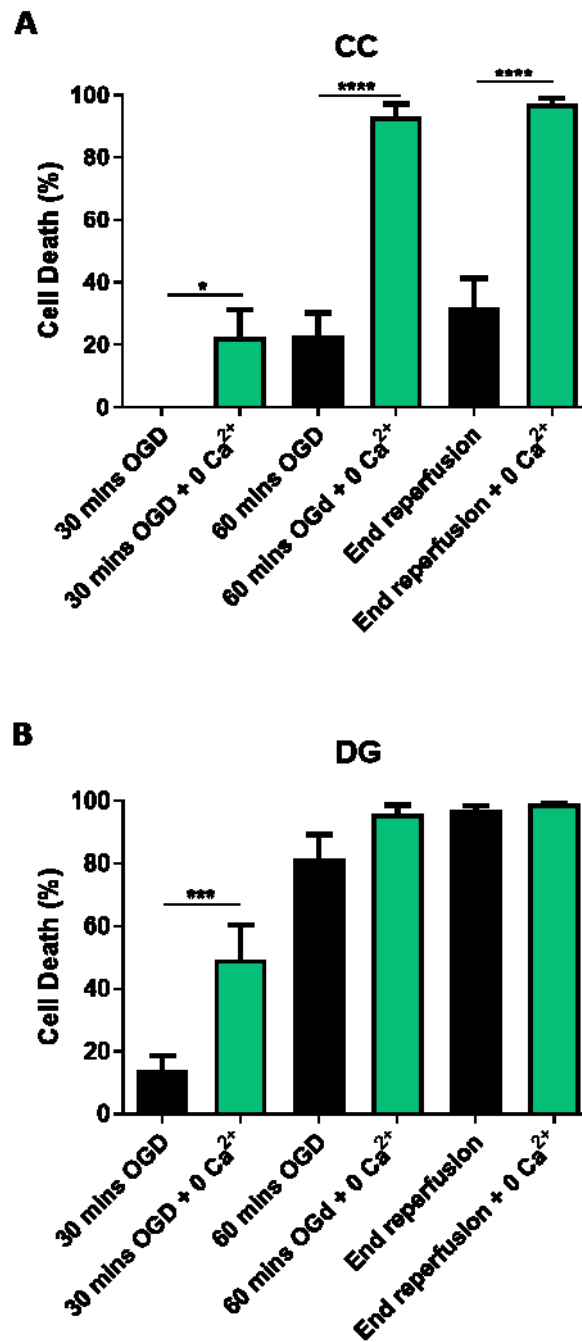
Figure 5.3: Zero calcium conditions altered cell death at defined time points. A: corpus callosum, **B:** dentate gyrus. Cell death at 30 and 60 minutes OGD the end of reperfusion, with (black bars) and without calcium (green bars). Error bars = SEM.

5.3 RESULTS: EFFECT OF GLUTAMATE RECEPTOR INHIBITORS ON GLIAL CELL DEATH

Glutamate receptor antagonists have been found to increase neuronal survival during ischaemic insults (Pulsinelli, Sarokin & Buchan, 1993). Astrocytes and oligodendrocytes also express GluRs and so it was investigated whether inhibiting these receptors would have an effect on OGD induced glial cell death. The inhibitors used were NBQX (2,3-dioxo-6-nitro-1,2,3.4-tetrahydrobenzo[*f*]quinoxaline-7-sulfonamide) which blocks AMPA receptors and MK801 ((5*S*,10*R*)-(+)-5-methyl-10,11-dihydro-5*H*-dibenzo[*a,d*]cyclohepten-5,10-imine maleate) which blocks NMDA receptors. Brain slices were incubated with these inhibitors for 20 minutes prior to OGD exposure, to allow the inhibitors to penetrate the slices.

5.3.1 Results: Glutamate receptor inhibitors NBQX and MK801 increased OGD induced astrocyte cell death in CC

Inhibiting AMPA and NMDA GluRs increased OGD induced astrocyte cell death in CC (figure 5.4). In the confocal images, the effect of the addition of NBQX and MK801 shows there are fewer surviving astrocytes (figure 5.4A). The presence of the antagonists had no effect on the rate of cell death, as the *t* values for both conditions were similar (figure 5.4B). For CC the t value was 62.00 ± 2.32 mins, whilst with antagonists the value was 55.42 ± 2.63 mins (not significant) The total amount of cell death was significantly increased from $40.17 \pm 6.45\%$ to $67.93 \pm 4.86\%$ with the addition of antagonists, p=0.0093 (figure 5.4C).

In DG treatment with GluR inhibitors caused no significant change in OGD induced astrocyte cell death (figure 5.5). The addition of NBQX and

MK801 increased the resistance of some astrocytes to OGD, illustrated by the confocal images (figure 5.5A). The t value with the addition of inhibitors was found to be similar to that for OGD only, 55.38 ± 6.60 mins and 54.64 ± 3.30 mins respectively (figure 5.5B). The total cell death achieved with the use of GluRIs was lower than that for OGD alone, 92.49 ± 3.44% and 97.61 ± 0.01% respectively (not significant, figure 5.5C). The addition of NBQX and MK801 caused a rise in OGD induced cell death to occur in CC, whereas in DG, OGD induced cell death was reduced.
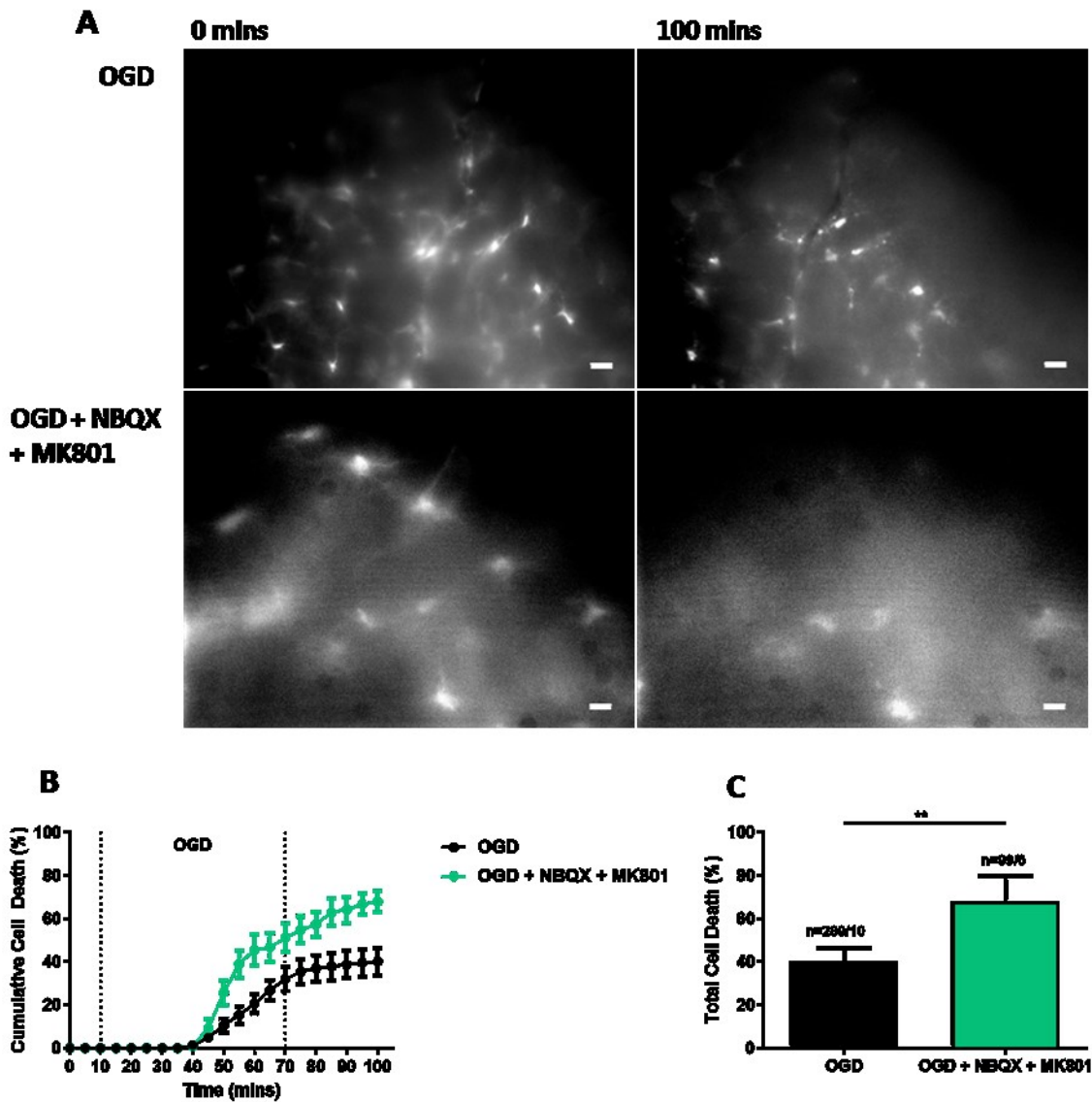
Figure 5.4: Glutamate receptor inhibitors NBQX (20µM) and MK801 (10µM) increased OGD induced astrocyte cell death in corpus callosum (CC). A: Confocal images during OGD (upper panel) and OGD with NBQX and MK801 (lower panel). Images taken at 0 and 100 minutes. Scale bar = 20 µm. B: Astrocyte cell death over time. C: Total cell death at time 100 minutes, OGD only (black bar) and OGD with NBQX and MK801 (green bar). Error bars = SEM. N numbers = number of cells/number of slices

Figure 5.5: Glutamate receptor inhibitors NBQX (20µM) and MK801 (10µM) had no effect on OGD induced astrocyte cell death in dentate gyrus (DG). A: Confocal images during OGD (upper panel) and OGD with NBQX and MK801 (lower panel). Images taken at 0 and 100 minutes. Scale bar = 20 µm. B: Astrocyte cell death over time. C: Total cell death at time 100 minutes, OGD only (black bar) and OGD with NBQX and MK801 (green bar). Error bars = SEM. N numbers = number of cells/number of slices.

5.3.2 Results: MK801 alone increased OGD induced astrocyte cell death in CC

To determine whether the cause of this increase cell death during OGD in the CC was due to NMDA or AMPA receptors, slices were treated with MK801 alone. MK801 selectively inhibits NMDA receptors, leaving AMPA GluR free to be activated. Previous work investigating oligodendrocytes has determined that AMPA receptors may be responsible for cytotoxic injury (Matute *et al.*, 1997; Micu *et al.*, 2006; Salter & Fern, 2005). The addition of MK801 increased OGD induced astrocyte loss in CC, which can be seen in the confocal images (figure 5.6A). NMDA GluR inhibition caused a significant reduction in t value from 62.00 ± 2.32 mins to 50.67 ± 2.02 mins (p=0.004, figure 5.6B). The total amount of cell death obtained by using MK801 was significantly increased from 40.17 ± 6.45% to 94.49 ± 2.61% (p=<0.0001, figure 5.6C).

In the DG, the presence of MK801 during OGD resulted in widespread astrocyte death as seen in the confocal images (figure 5.7A). By inhibiting NMDA GluRs the cell death profile was shifted and there was a significant reduction in t value. For DG, this was 54.64 ± 3.30 mins and with MK801 this was decreased to 39.75 ± 3.53 mins (p=0.0105, figure 5.7B). The total amount of cell death achieved with MK801 was increased from 97.61 ± 1.01% with OGD and 100 ± 0% with MK801 (not significant, figure 5.7C).Taken together these findings suggest that NMDA GluRs may have a protective role in cytotoxic astrocyte cell death, as increased cell death was observed when NMDA receptors were inhibited, with the greatest effect seen in WM.
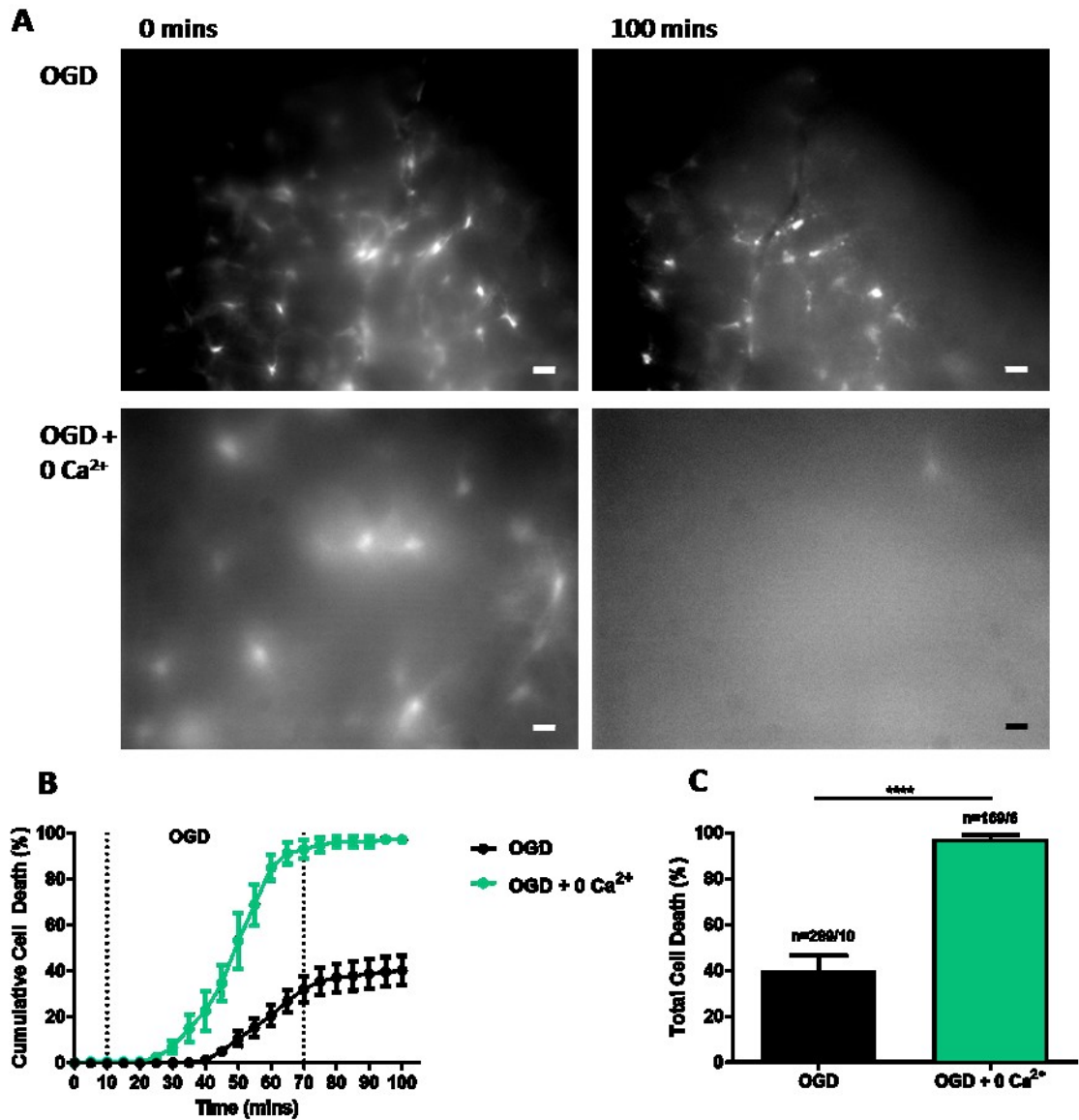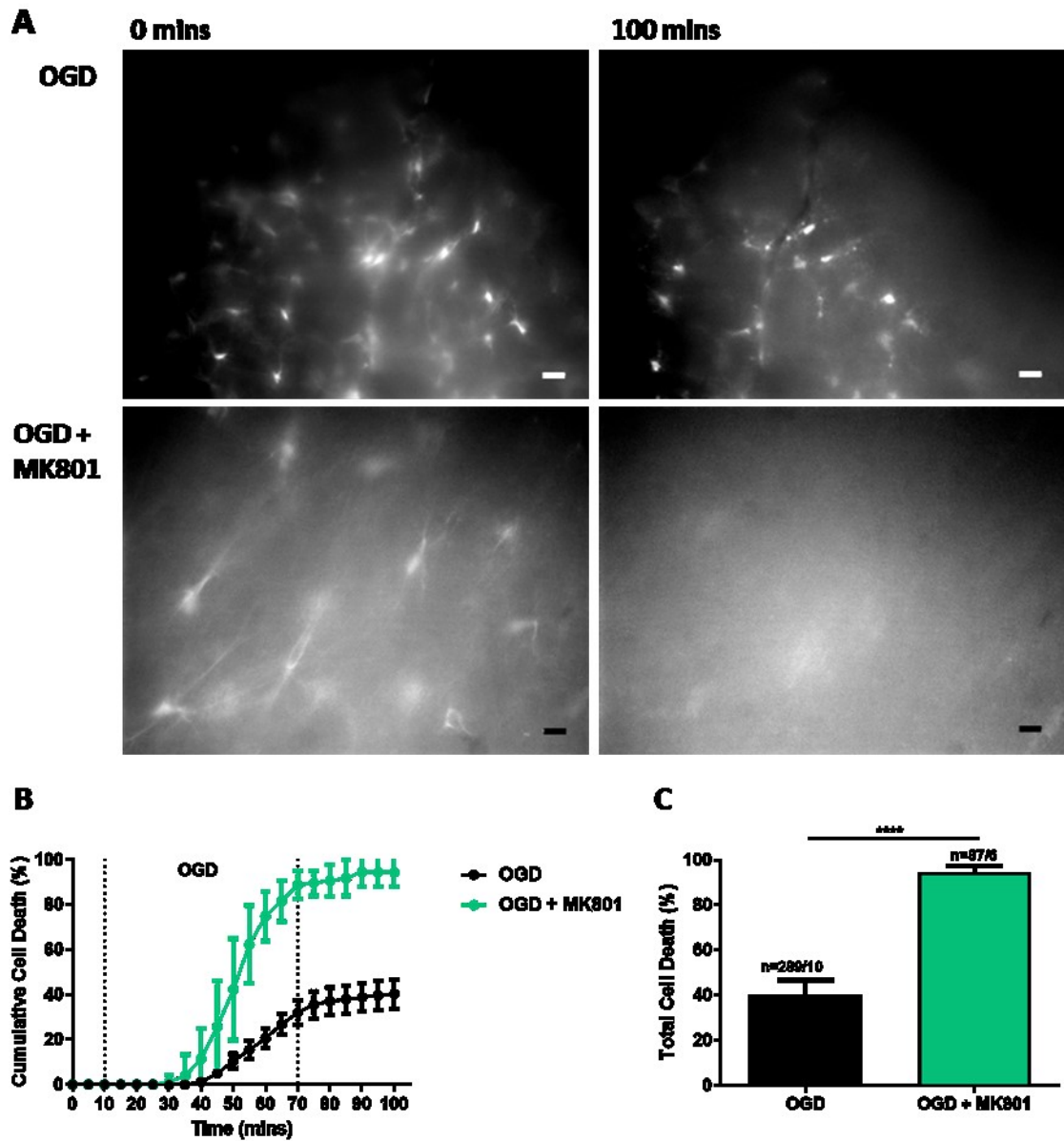
Figure 5.6: MK801 treatment increased OGD induced astrocyte cell death in corpus callosum (CC). A: Confocal images during OGD (upper panel) and with MK801 (lower panel) Images taken at 0 and 100 minutes. Scale bars = 20µm. B: Astrocyte cell death over time. C: Total cell death at 100 minutes, OGD only (black bar) and OGD with MK801 (green bar). Error bars = SEM. N numbers = number of cells/number of slices

DG
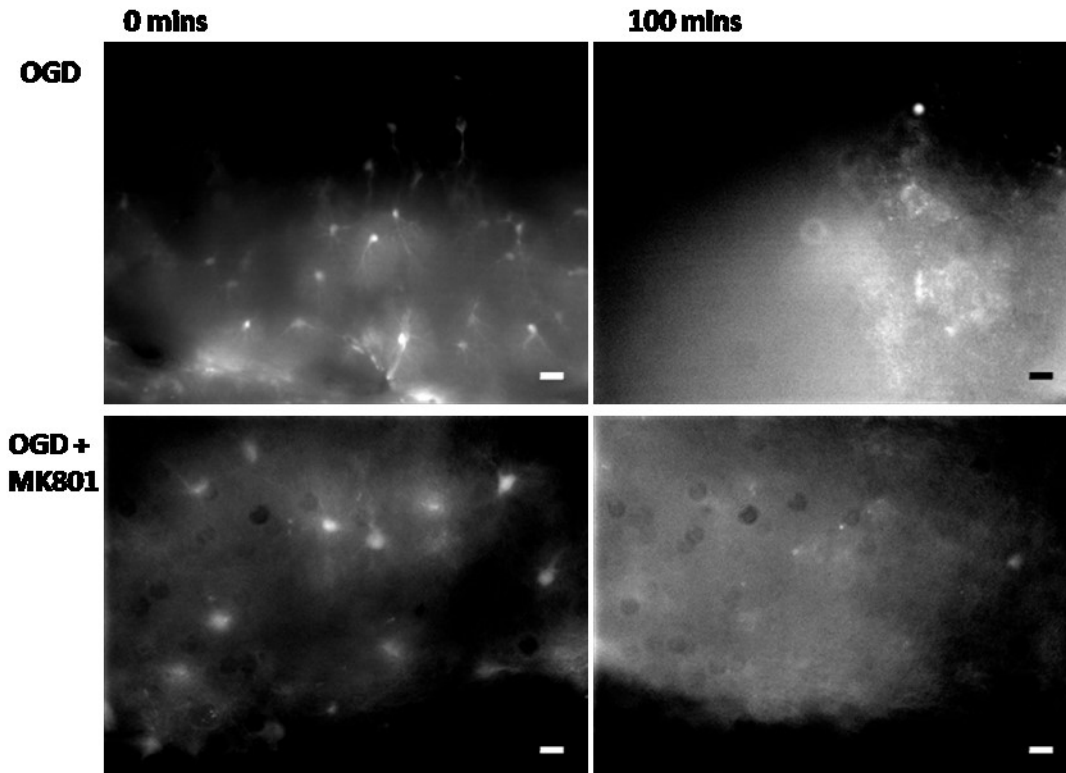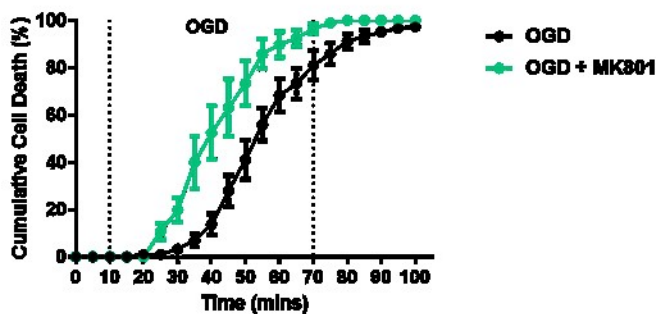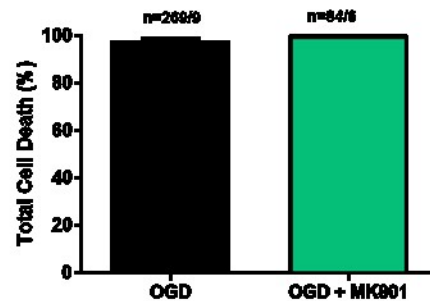
Figure 5.7: MK801 treatment had no effect on OGD induced astrocyte cell death in dentate gyrus (DG). A: Confocal images during OGD (upper panel) and with MK801 (lower panel) Images taken at 0 and 100 minutes. Scale bars = 20µm. B: Astrocyte cell death over time. C: total cell death at 100 minutes, OGD only (black bar) and OGD with MK801 (green bar). Error bars = SEM. N numbers = number of cells/number of slices.

### 5.3.3 Results: Comparison of glutamate receptor inhibitor combinations

The effect of the combinations of GluR antagonists used was compared to determine the potential role of AMPA receptors in astrocyte cell death (figure 5.8). In CC, inhibiting NMDA receptors caused cell death to occur at a similar rate to the inhibition of both receptors, the t values been 55.42 ± 2.63 mins and 50.67 ± 2.02 mins (not significant, figure 5.8A). The use of MK801 alone resulted in significantly increased cell death in CC of 94.49 ± 2.61%, when compared with that achieved with both inhibitors 67.93 ± 4.86% (p=0.0007, figure 5.8C). The comparison of different time points found that in CC, there were no significant differences in cell death after 30 minutes OGD (figure 5.8E). However, after 60 minutes OGD the use of both inhibitors significantly increased astrocyte death when compared to OGD from 23.11 ± 7.12% to 51.21 ± 6.46% (p=0.0092, figure 5.8E) and using MK801 further increased this to 88.72 ± 2.35%.(p=<0.0001, figure 5.8E). At the end of reperfusion (100 minutes) the use of inhibitors caused significantly higher cell death when compared to OGD alone, p=0.0075 with NBQX and MK801 and p=<0.0001 with MK801 only (figure 5.8E).

In DG the cell death profiles were found to be similar (figure 5.8B), although MK801 treatment caused cell death to begin earlier at 20 minutes rather than 35 minutes with NBQX and MK801. The t value obtained from MK801 only treatment was significantly lower than that for both inhibitors, 39.75 ± 3.53 mins and 55.38 ± 6.60 mins respectively (p=0.021). The total cell death achieved using MK801 was significantly higher than when both inhibitors were used (p=0.0246, figure 5.8D). The comparison of cell death at defined time points revealed that at 30 minutes, OGD with MK801 resulted in significantly

higher cell death when compared to values for OGD only, 52.46 ± 11.43% with

MK801 and 14.64 ± 4.77% with OGD, (p=0.0334, figure 5.8F). The only other

significant difference seen was at the end of reperfusion where MK801

treatment resulted in greater cell death than the presence of both inhibitors, 100

± 0% and 92.49 ± 3.44% respectively, (p=0.0156, figure 5.8F). These findings

would suggest that there is a role for AMPA receptors in OGD induced astrocyte

cell death, as the inhibition of NMDA receptors caused increased cell death in

WM and GM.
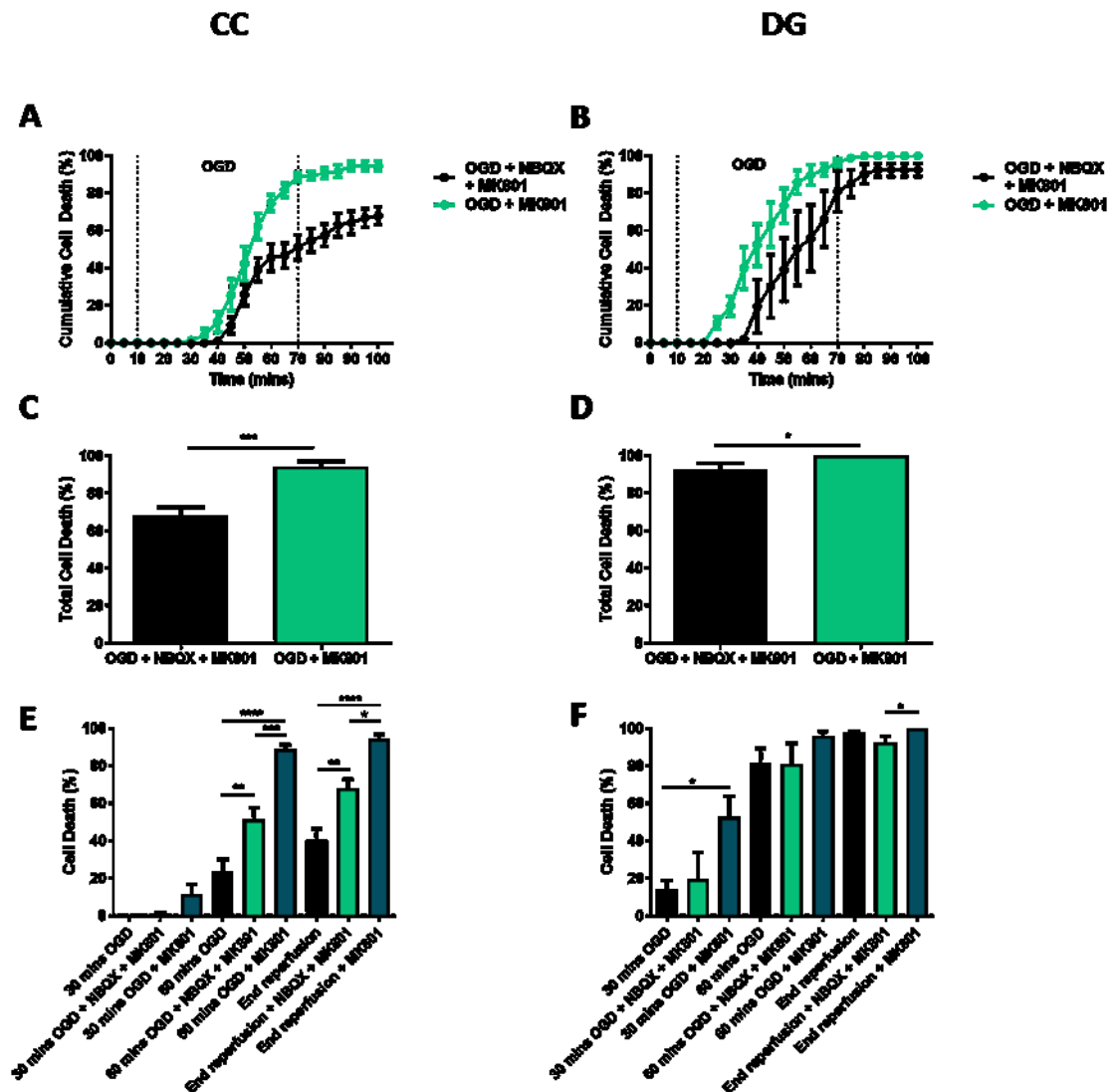
Figure 5.8: Blocking only NMDA receptors increased OGD induced astrocyte cell death. A + B: Astrocyte cell death over time with glutamate receptor inhibitors, NBQX and MK801 (black) and MK801 only (green), **C + D:** astrocyte cell death at time 100 minutes, OGD with NBQX and MK801 (black bar) OGD with MK801 only (green) and **E + F:** astrocyte cell death at defined time points, OGD only black bars, OGD with NBQX and MK801 (green bars) and OGD with MK801 only (blue bars). **A, C + E:** corpus callosum, **B, D + F:** dentate gyrus. Error bars = SEM

5.3.4 Results: Glutamate receptor inhibitors did not affect OGD induced oligodendrocyte cell death.

Astrocytes are not the only glial cells to express GluRs, they are also found on oligodendrocytes. GluRs are involved in ischaemic cell death via excitotoxicity, which oligodendrocytes are sensitive to (Karadottir *et al.*, 2005; Matute *et al.*, 2002; Matute, Domercq & Sánchez-Gómez, 2006). Here it was investigated whether using GluR inhibitors would confer the same effect on oligodendrocyte cell death as for astrocytes, or whether the inhibitors would prevent cell death. It was found that the presence of NBQX and MK801 did not affect OGD induced oligodendrocyte cell death in CC (figure 5.9). The confocal images illustrate that after OGD and OGD in the presence of the antagonists there was very little change and few cells were lost (figure 5.9A). The cell death profiles for both conditions are very similar and were unaffected by the presence of GluRIs (figure 5.9B). The total OGD induced oligodendrocyte cell death achieved with GluRIs was reduced from $1.31 \pm 0.71\%$ with OGD alone to $0.89 \pm 0.89\%$ (not significant, figure 5.9C).

The presence of NBQX and MK801 had no significant effect on DG oligodendrocytes (figure 5.10A). The treatment with GluRIs had little effect on the cell death profile (figure 5.10B). The addition of GluRIs did reduce OGD induced DG oligodendrocyte cell death. Total cell death with OGD only conditions was $1.85 \pm 1.85\%$, the addition of NBQX and MK801 cell death was $0 \pm 0\%$ (figure 5.10C). These findings suggest that GluRIs may prevent OGD induced oligodendrocyte cell death. However, oligodendrocyte cell death was very low after 60 minutes OGD and 30 minutes reperfusion and so any prevention of cell death was not statistically significant.
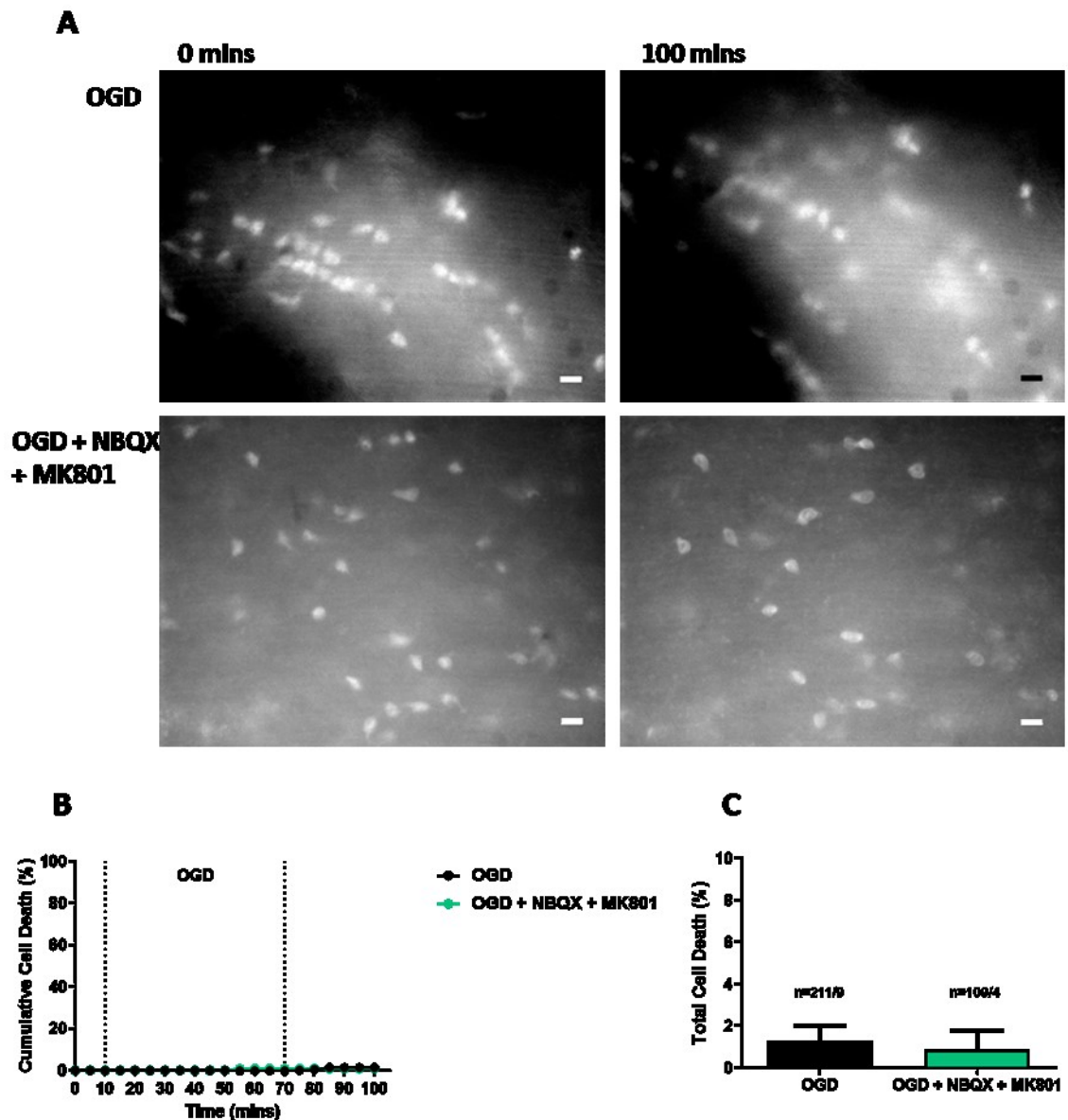
Figure 5.9: Glutamate receptor inhibitors NBQX (20µM) and MK801 (10µM) had no effect on OGD induced oligodendrocyte cell death in corpus callosum (CC). A: Confocal images during OGD (upper panel) and glutamate receptor inhibitors (lower panel). Images taken at 0 and 100 minutes. Scale bars = 20µM. B: Oligodendrocyte cell death over time. C: total cell death at 100 minutes, OGD only (black bar) and OGD with NBQX and MK801 (green bar). Error bars = SEM. N numbers = number of cells/number of slices.
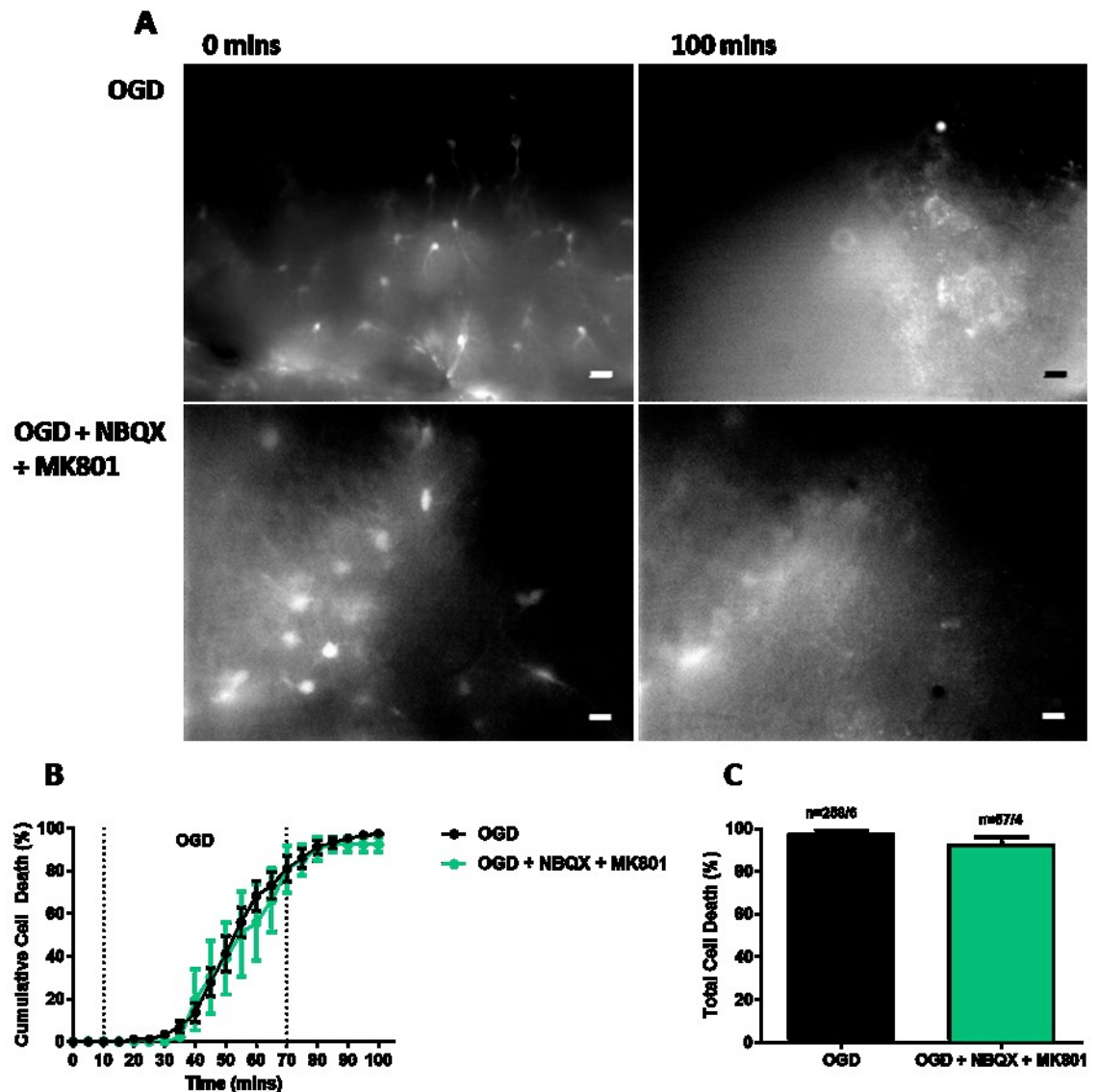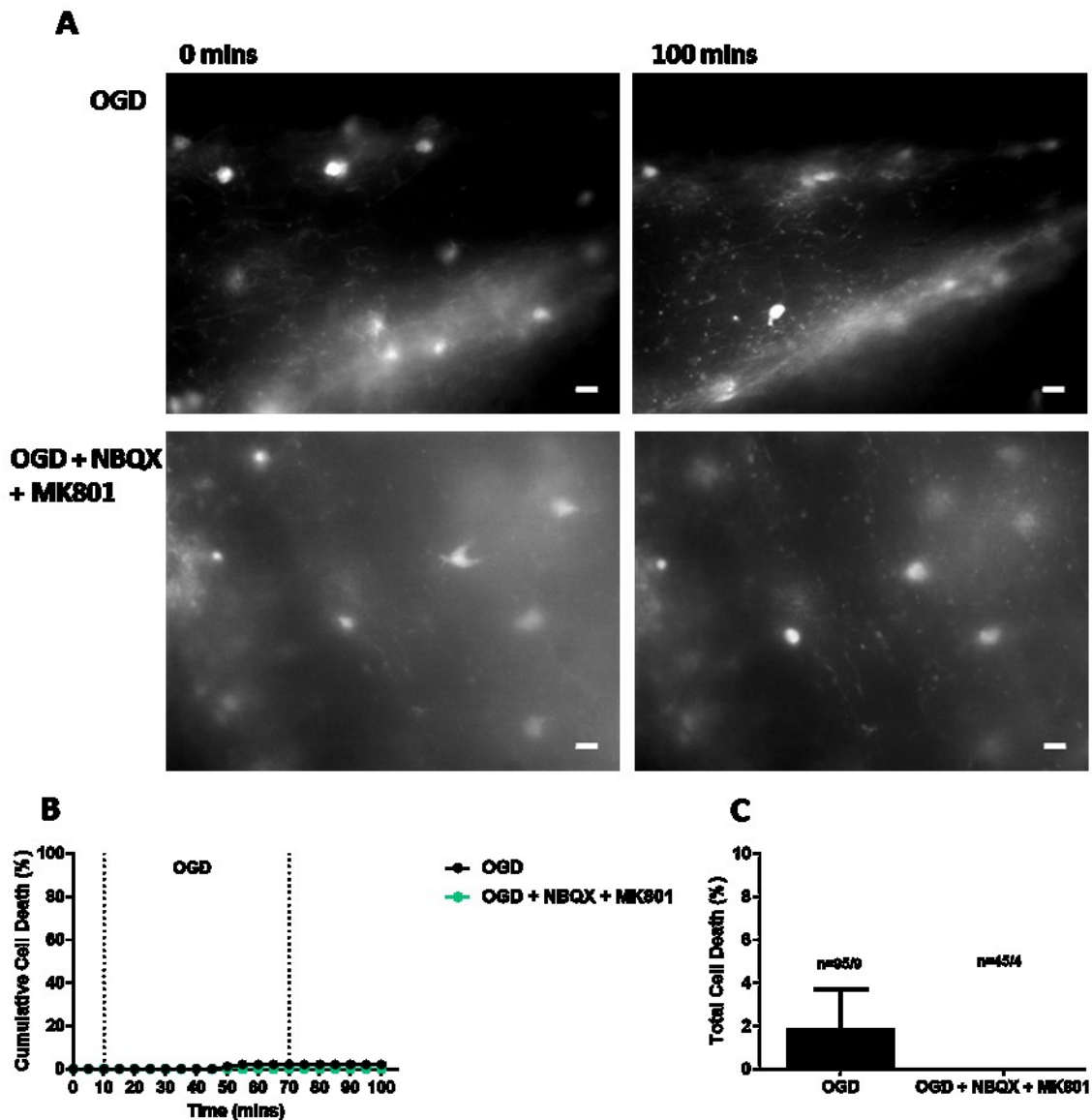
Figure 5.10: Glutamate receptor inhibitors NBQX (20μM) and MK801 (10μM) had no effect on OGD induced oligodendrocyte cell death in dentate gyrus (DG). A: Confocal images during OGD (upper panel) and glutamate receptor inhibitors (lower panel). Images taken at 0 and 100 minutes. Scale bars = 20μM. B: Oligodendrocyte cell death over time. C: total cell death at 100 minutes, OGD only (black bar) and OGD with NBQX and MK801. Error bars = SEM. N numbers = number of cells/number of slices.

5.4 RESULTS: COBALT STAIN VISUALISATION OF DIVALENT CATION ENTRY INTO CELLS

During ischaemia ionic gradients are disrupted and cytotoxic influx of ions can occur. One route for ions to enter cells is through activated GluRs, which are permeable to divalent cations such as calcium. Calcium is required for neuronal and oligodendrocyte ischaemic cell death, however we have found that removal of extracellular calcium increases OGD induced astrocyte cell death (figures 5.1 and 5.2), indicating that calcium may also be beneficial to cell viability.

Cobalt is a divalent cation which is able to enter neural cells through activated GluR pores (Albuquerque *et al.*, 2001; Aurousseau, Osswald & Bowie, 2012; Pruss *et al.*, 1991). Cobalt staining thus allows the visualisation of cation entry into all cells in live tissue preparations and reveals the presence of activated GluRs. Cobalt staining of live tissue was carried out for three regions (ON, CC and DG) under different conditions which were, aCSF with agonist (first panel), aCSF with GluR inhibitor and agonist (central panel) and OGD (final panel, figure 5.11A). The GluR agonist used throughout the cobalt staining was L-glutamate to ensure activation of GluRs. However, the agonist was not added during OGD since I am looking at receptor gating by ischaemic glutamate release. Also glutamate can be converted into the TCA cycle intermediate α-ketoglutarate which may act as an energy source (McKenna, 2007). The evidence of cobalt entry is shown through the presence of a black precipitate in cells and can be seen in neurons, astrocytes and oligodendrocytes. The treatment of tissue preparations with GluRIs prevented the entry of cobalt into cells, illustrating that cobalt entered cells via activated GluRs. Under OGD conditions, cobalt staining will be limited to those cells which survived OGD. The

cells which experienced cobalt entry under OGD show that this is due to activated GluRs on OGD tolerant cells. Quantification of the cobalt positive cells in the tissue regions of interest was carried out (figure 5.11B). Under physiological conditions the most cobalt positive cells were seen in DG, in this brain region there are a high number of neuronal cell bodies which account for this. Fewer positive cells were seen in the WM tracts, as these contain only axons, oligodendrocytes and astrocytes. The use of GluRIs significantly reduced the cobalt entry into cells in all regions ($p=<0.0001$), thus also reducing the cation entry into cells. The number of cobalt positive cells in all regions was significantly reduced under OGD conditions ($p=<0.0001$). Under these conditions some cells do survive and can be seen (figure 5.11A final panel, ON and CC). It is likely that the cells that do survive are glial cells as they display tolerance to ischaemic insult. These findings show that cation entry occurs through GluRs as cobalt entry is prevented in the presence of GluR antagonists.
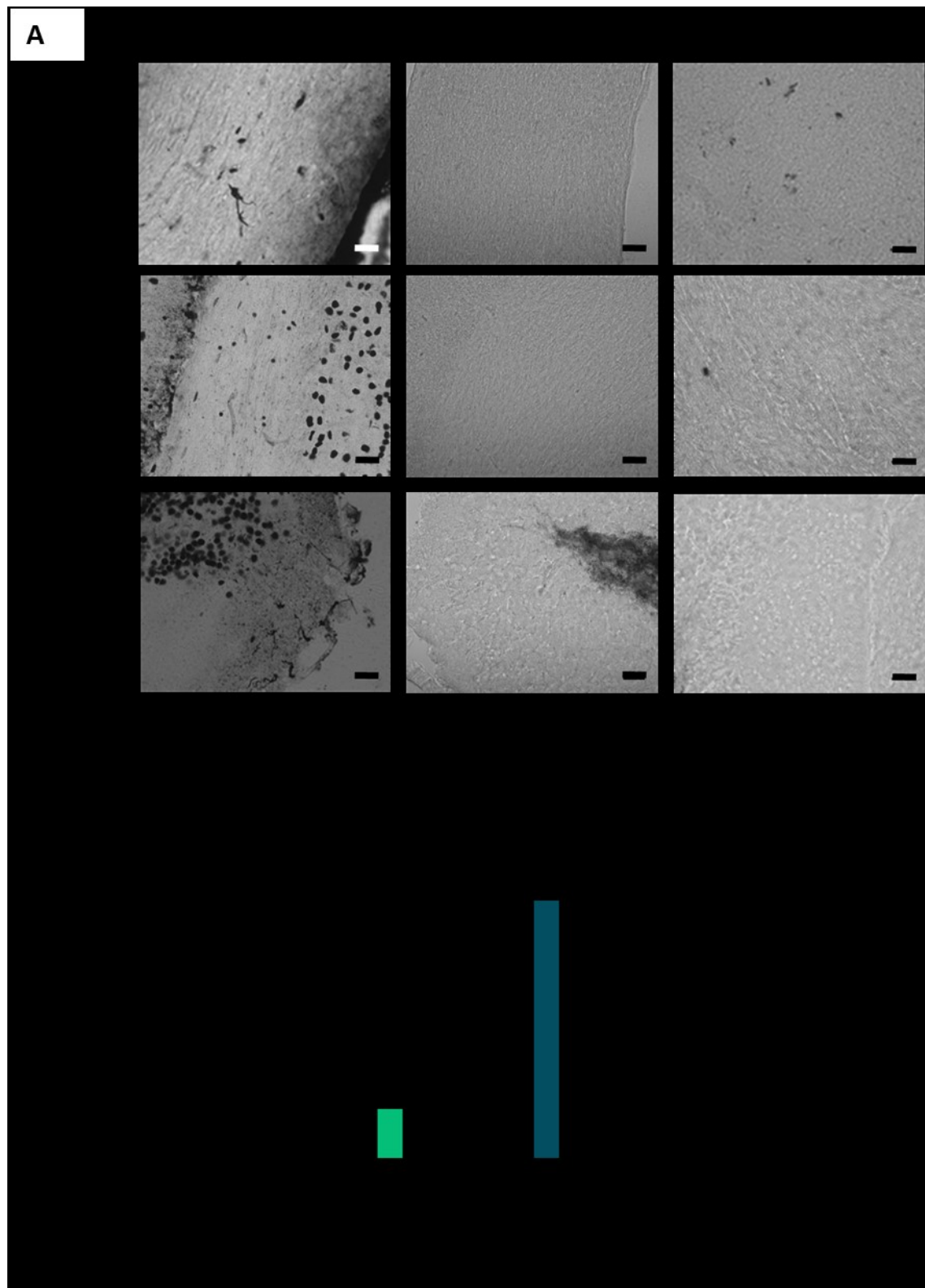
Figure 5.11: Cobalt staining of divalent cation entry into cells in different conditions. A: Representative images of cobalt positive cells in optic nerve (ON), corpus callosum (CC) and dentate gyrus (DG). In physiological conditions (aCSF), use of glutamate receptor inhibitors (GluRI) and oxygen glucose deprivation (OGD). Scale bars = 50μm. **B:** Quantification of number of cobalt

positive cells in each region (ON black, CC green and DG blue) and condition. Error bars = SEM.

5.5 DISCUSSION: ROLE OF CALCIUM AND GLUTAMATE RECEPTORS IN GLIAL ISCHAEMIC INJURY

The over-activation of GluRs in response to an ischaemic challenge is, termed excitotoxicity and results in cytotoxic calcium influx in neurons, oligodendrocytes and immature astrocytes (Coyle *et al.*, 1981; David *et al.*, 1996; Lucas & Newhouse, 1957; Pantoni, Garcia & Gutierrez, 1996; Salter & Fern, 2005). This has a detrimental effect on cells and leads to the triggering of cell death mechanisms (Matute, 2006). This chapter aimed to investigate whether calcium influx and GluRs have a role to play in ischaemic cell death of adult mature glia *in situ*.

5.5.1 OGD induced astrocyte cell death is not mediated by calcium influx

Cytotoxic calcium influx and excitotoxicity have a role to play in neuronal ischaemic cell death (Coyle *et al.*, 1981; Lucas & Newhouse, 1957; Pulsinelli, Sarokin & Buchan, 1993). Previous work has found that in P0-P2 mice, calcium influx is responsible for astrocyte cell death (Fern, 1998), however this was not so for P10 mice (Salter & Fern, 2008; Thomas *et al.*, 2004). This work has found that in adult mice, ischaemic astrocyte cell death occurs independently of external calcium influx. Interestingly, removing calcium caused earlier and significantly increased cell death in CC (p=<0.0001) and earlier, more rapid cell death in DG (figures 5.1 and 5.2). In DG, cell death was increased but not significantly, due to the high levels of cell death that exist in this region during OGD. The effect observed under calcium free conditions would suggest that calcium may have a role in protecting astrocytes during OGD and that cytotoxic calcium influx is not responsible for adult astrocytic cell death (Thomas *et al.*, 2004).

The ion concentrations surrounding astrocytes can affect cell survival (Bondarenko & Chesler, 2001). The phenomenon of zero calcium conditions increasing cell death was previously observed by Thomas et al (2004) and Salter and Fern (2008). There is evidence that zero calcium conditions are also detrimental to neurons (Goldberg & Choi, 1993). Calcium is required by astrocytes for volume regulation (O'Connor & Kimelberg, 1993).The absence of calcium may cause cell death as astrocytes are not able to combat the effect of ischaemia induced swelling. Calcium is used by astrocytes for glial communication via waves which transmit across astrocytes and the syncytium (Cornell-Bell *et al.*, 1990). A reduction in the calcium may result in the disruption of glial signalling and astrocyte communication with neurons, thus disrupting any potential survival signal. There is evidence to suggest that calcium is involved in cell survival as this ion is required for the regulation of several cellular processes (Chiesa *et al.*, 1998). A lack of calcium can cause changes in astrocyte function, a reduction in calcium can itself act as an apoptotic signal (Chiesa *et al.*, 1998). In a model of traumatic brain injury, zero extracellular calcium also caused increased astrocyte cell death (Rzigalinski *et al.*, 1997), suggesting the reduction of calcium can trigger apoptosis. The increase in cell death shows how the mechanism of astrocyte cell death changes as the cells mature and corresponds with the findings of Thomas *et al* (2004).

5.5.2 Glial glutamate receptor inhibition and OGD induced cell death

Inhibition of GluRs has been found to provide to protection to neurons that experience ischaemic insult (Pulsinelli, Sarokin & Buchan, 1993), thus the effect of the inhibitors, NBQX and MK801, on astrocyte cell death was investigated. The only significant change in OGD induced astrocyte cell death produced by GluR block was seen in CC (p=0.0093), where cell death was

increased (figure 5.4). Whilst a decrease in DG astrocyte cell death was seen, it was not significant (figure 5.5). The results show that simultaneous block of both NMDA and AMPA GluRs tends to potentiate injury in adult WM astrocytes and would indicate that astrocytes in different regions may have different mechanisms of cell death in response to ischaemic injury.

The selective NMDA receptor blocker MK801 caused a significant increase in CC astrocyte death during OGD (p=<0.0001, figure 5.6) when applied alone. In DG, MK801 treatment caused ischaemic cell death to occur earlier and increased the amount of cell death, although not significantly (figure 5.7). These findings suggest that ionotropic GluR generally and NMDA receptors specifically are protective against ischaemic cell death in mature astrocytes. The inhibition of NMDA receptors may affect astrocytes by preventing NMDA receptor initiated cell survival signals. There is evidence in the literature which suggests that NMDA receptors trigger the activation of transcription factors and anti-apoptotic factors which encourage cell survival and neuroprotection (Papadia *et al.*, 2005; Soriano & Hardingham, 2007). This pro-survival signalling can cause post-translational modification of proteins and initiate gene expression (Papadia *et al.*, 2005; Soriano & Hardingham, 2007). A study carried out in neurons has found that NMDA receptor inhibition results in increased cell death during injury, due to the prevention of survival signals (Ikonomidou, Stefovska & Turski, 2000; Tashiro *et al.*, 2006). The process of pre-conditioning cells to develop resistance to ischaemic insult is thought to occur via NMDA receptor signalling (Mabuchi *et al.*, 2001). The exact role for astrocyte NMDA receptors is unknown and so it is possible that their presence on astrocytes is for pro-survival signalling. If astrocyte NMDA receptors have a role in cell survival, then the inhibition with MK801 will lead to an increased

amount of cell death due to the lack of survival signals. The inhibition of neuronal NMDA receptors may also prevent the communication of cell survival signals from neurons to astrocytes.

There are previous studies which have reported that over activation of glutamate receptors can damage astrocytes (Matute *et al.*, 2002). It is known that AMPA receptors are more permeable to sodium ions (Citri & Malenka, 2008), which have been found to contribute to ischaemic cell death in P10 mice (Thomas *et al.*, 2004). The over excitation of AMPA receptors may cause influx of sodium ions and result in sodium dependent cell death. The role of sodium is further discussed and investigated in the next chapter. It would appear that there is a role for GluRs in astrocyte ischaemic cell death, via influx of other ions apart from calcium and further investigation is required.

Inhibition of GluRs had no effect on OGD induced oligodendrocyte cell death (figures 5.9 and 5.10). In OGD conditions, oligodendrocyte cell death was already very low and so any protective effect may not be detectable. Excitotoxicity is thought to be a major mechanism of ischaemic oligodendrocyte cell death (Leuchtmann *et al.*, 2003), thus it would be expected that inhibition of GluRs would prevent cell death. It is possible that the use of GluRIs does protect oligodendrocytes, however it has been found that cell death is not seen until at least one hour after insult (Pantoni, Garcia & Gutierrez, 1996) and widespread oligodendrocyte cell death has been documented nine hours after insult (Tekkok & Goldberg, 2001). Also the observable effect of GluR inhibition may be limited due to the low amount of OGD induced oligodendrocyte cell death that occurs. This work is concerned with the acute ischaemic injury and so pathological oligodendrocyte cell death has not yet occurred.

5.5.3 Cobalt staining of cation entry

Activated GluRs are permeable to divalent and monovalent cations such as calcium, sodium and potassium. Cobalt is a divalent cation, which is able to enter cells via GluR channels. The cobalt staining method used here has shown that cobalt permeable GluRs are present in ON, CC and DG (figure 5.11). When tissue preparations were treated with GluRIs, cobalt was prevented from entering which confirmed that NMDA and AMPA GluRs are the major route of calcium entry in the presence of the agonist (L-glutamate). Under OGD conditions cobalt was able to enter some cells but not to the same extent as under normoxic conditions in the presence of the agonist. The cells that did show staining after OGD had survived the insult and displayed glial morphology. The data confirm that the influx of calcium during OGD, together with the findings from the calcium removal experiments highlights the differing protection that this event confers. The calcium influx via GluR under ischaemic conditions in astrocytes is therefore a form of glutamate excito-protection, contrasting to the well-established excitotoxicity found in neurons and oligodendrocytes.

This chapter has shown that external calcium influx is not responsible for OGD induced astrocyte cell death in either CC or DG, however cell death could result from calcium release from internal stores and further work is required to establish whether this source of calcium is a possible ischaemia induced cell death mechanism. This supports previous findings that showed sodium influx and not calcium was responsible for astrocyte cell death in P10 mice (Thomas et al., 2004). AMPA receptors may be responsible for astrocyte cell death as inhibition of NMDA receptors caused widespread astrocyte death, possibly due to sodium influx which causes cytotoxic cell swelling. The role of sodium in ischaemic astrocyte cell death is investigated in the next chapter.

CHAPTER 6

6 ROLE OF SODIUM AND ASTROCYTE SWELLING

6.1 INTRODUCTION

Sodium has an important role in the CNS, where it is utilized for several processes, including signalling and the maintenance of ionic gradients. Transmembrane sodium movement generally obeys the established ionic concentration gradient and occurs through a variety of transporters and ion channels, which include sodium-hydrogen exchanger (NHE), sodium-calcium exchanger (NCX), sodium-bicarbonate co-transporter (NBC) and voltage-insensitive sodium channels (N_x). Astrocytes express voltage gated sodium channels (Verkhratsky & Steinhäuser, 2000), although expression levels are generally lower than in neurons or some populations of oligodendroglia (Káradóttir *et al.*, 2008). The expression of these channels by astrocytes *in vivo* is still being discussed (Rose & Verkhratsky, 2016), however it has been shown in spinal cord that in the event of sodium channel blockade they can serve as pathway for sodium entry (Rose, Ransom & Waxman, 1997). Sodium can also enter astrocytes through receptor pores such as ionotropic glutamate receptors (iGluRs), which are permeable to ions when activated. iGluR ion permeability is determined by their subunit expression (discussed in the previous chapter). Another route for sodium entry is via cation chloride co-transporters (CCC), which includes the sodium-potassium-chloride co-transporter 1 (NKCC1). This transporter has been implicated in astrocytic cell swelling. A major route for sodium extrusion occurs via the action of the sodium/potassium ATPase. During times of CNS injury or insult ionic gradients are disrupted and homeostatic maintenance breaks down, altering cell function and leading to changes in cell volume that can be fatal to the cell.

6.1.1 Sodium homeostasis

Under normal physiological conditions, astrocytes regulate the ECS sodium concentration and contribute to the maintenance of the large inwardly directed sodium gradient. The energy contained within this sodium gradient is harnessed to transport other ions and molecules across the cell membrane, via expression of several sodium-dependent transporters. There is also a natural flow of sodium into cells, as some channels such as neurotransmitter receptor pores generate sodium currents (Lalo *et al.*, 2011). These pores are permeable to cations and so sodium is the major cation which enters cells (Kirischuk, Parpura & Verkhratsky, 2012; Lalo *et al.*, 2011).

High extracellular sodium concentration or increases in sodium concentration, will trigger sodium uptake by astrocytes. This increases astrocyte intracellular sodium levels which can dissipate throughout the astrocyte syncytium via gap junctions, which lowers the intracellular sodium concentration (Rose & Ransom, 1997; Rouach *et al.*, 2008). It has been determined that the conduction of gap junctions is not uniform and alterations to conductance change how sodium is distributed throughout the syncytium (Rouach *et al.*, 2008). The homeostatic control of sodium is not an independent process and is tightly linked to potassium homeostasis and pH regulation.

6.1.2 Sodium transporters

A variety of channels and transporters are involved in sodium influx and efflux (figure 6.1). Below are brief descriptions of the roles of the main sodium transporters expressed in astrocytes with particular interest shown for CCCs, of these the NKCC1 and KCC (potassium-chloride co-transporter) were specifically examined. Most of these channels are driven by the inward sodium

gradient that is generated between the extracellular space and the intracellular space, which involves the sodium/potassium pump.
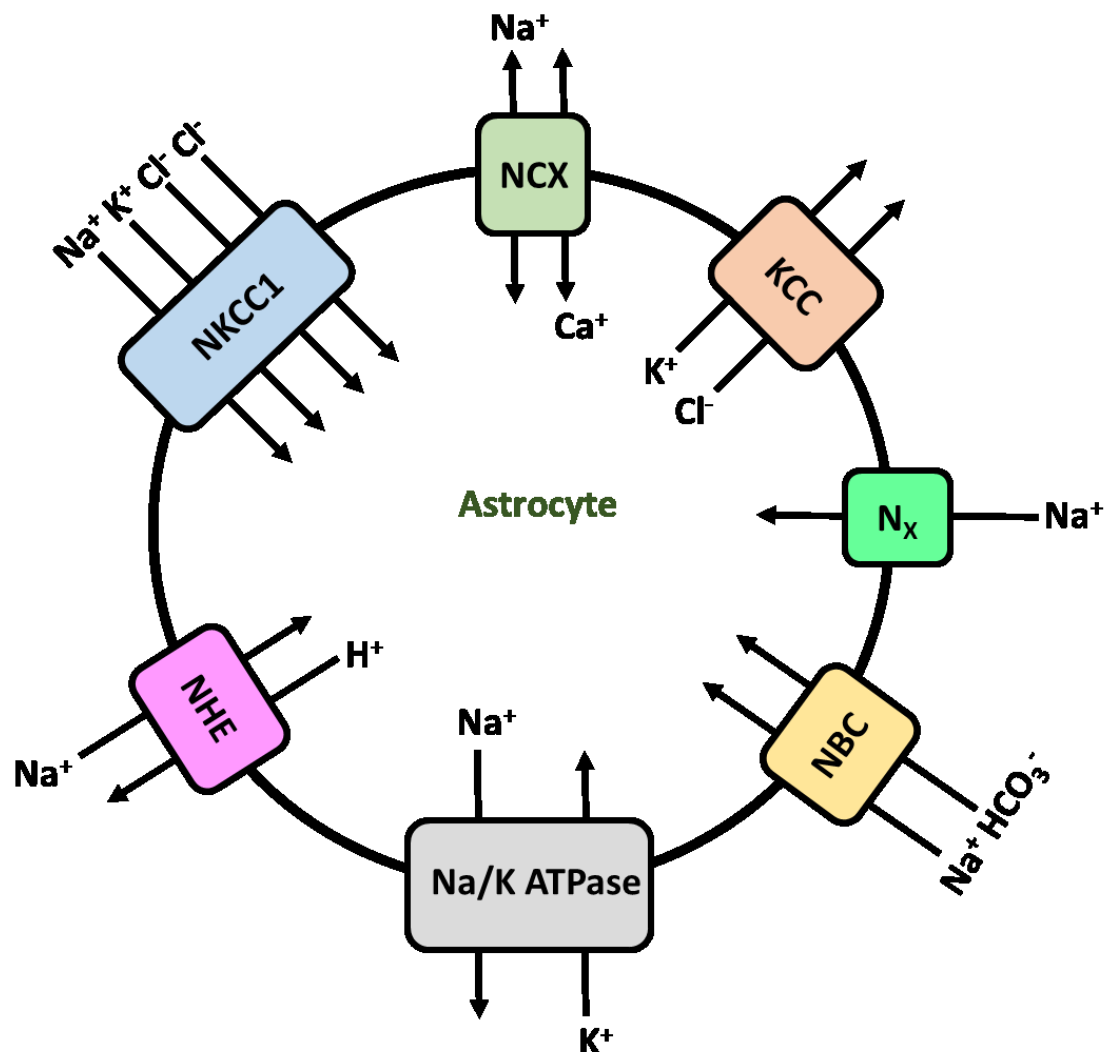
Figure 6.1: Key sodium transporters expressed by astrocytes. Sodium transporters and the direction of movement. NCX – sodium/calcium exchanger, KCC – potassium-chloride co-transporter, N_x – sodium channel, NBC – sodium-bicarbonate co-transporter, Na/K ATPase – sodium/potassium ATPase, NHE – sodium/hydrogen exchanger. NKCC1 – sodium-potassium-chloride co-transporter.

There is a concentration of sodium transporters and iGluRs on astrocyte perisynaptic processes (Kirischuk, Parpura & Verkhratsky, 2012). The interaction of these processes with synapses allows astrocytes to respond to neuronal activity. The transporters in this location include NCX and glutamate transporters (Minelli *et al.*, 2007). The NCX can function in both forward and

reverse modes, the working direction of the exchanger is determined by both the intracellular and extracellular sodium and calcium concentrations, as well as the membrane potential (Kirischuk, Parpura & Verkhratsky, 2012). The NCX reversal potential is close to the membrane resting potential (Kirischuk, Kettenmann & Verkhratsky, 1997) and so changes in the membrane potential will alter the direction of the exchanger. Therefore the NCX fluctuates between forward and reverse directions as activity levels change (Rojas, Ramos & Dipolo, 2004).

Under physiological conditions, the sodium/potassium ATPase (NKA) extrudes sodium from cells in exchange for potassium and is the main exporter of sodium and a major energy consumer (Erecińska & Silver, 1994). The NKA accounts for approximately 50% of cellular ATP hydrolysis (Astrup, Sørensen & Sørensen, 1981) and the high energy usage links the process of homeostasis to cellular metabolism (Silver & Erecińska, 1997). Any loss of function of this transporter can cause neurological disorder symptoms, such as aspects of parkinsonism and Alzheimer's disease (Moseley *et al.*, 2007). The NKA is sensitive to changes in both sodium and potassium concentration (Walz & Hertz, 1982), and even small rises in extracellular potassium concentration trigger activation of the transporter (Dinuzzo *et al.*, 2012). The presence of NKA on perisynaptic processes associates it with synaptic activity and it has been established that glutamate uptake and accompanying sodium influx triggers NKA activity (Pellerin & Magistretti, 1997). Co-assembly of aquaporin 4 (AQP4) and NKA has been found on astrocyte process endfeet, implicating NKA activity with water movement (Illarionova *et al.*, 2010).

Astrocyte N_x channels are sensitive to extracellular increases in sodium concentration, but are insensitive to changes in voltage (Noda & Hiyama, 2005).

Activation of N_x causes intracellular increase in sodium, which activates NKA to extrude the accumulated sodium. The N_x mediated stimulation of NKA causes glycolysis and subsequent lactate release, linking extracellular sodium increases with metabolite export (Rose & Verkhratsky, 2016).

The sodium-potassium-chloride co-transporter 1 (NKCC1) is widely expressed in astrocytes and has been confirmed in cortex, corpus callosum, hippocampus, cerebellum and optic nerve (MacVicar *et al.*, 2002; Yan, Dempsey & Sun, 2001a). During physiological conditions this transporter directs the movement of sodium, potassium and chloride ions into the cell, by utilizing the inwardly directed sodium gradient (Jayakumar & Norenberg, 2010). NKCC1 can be activated by an increase in the extracellular potassium concentration (Su *et al.*, 2002). The movement of chloride ions into astrocytes by NKCC1 can lead to the intracellular accumulation of chloride, triggering the influx of water which causes an increase in cell volume and swelling (Su *et al.*, 2002). Normal increases in cell volume can be corrected via regulated volume decrease. The genetic ablation of NKCC1 reduced cell swelling, which indicates a role for NKCC1 in volume regulation (Su *et al.*, 2002). NKCC1 may also contribute to pathology and has been implicated in cytotoxic cell swelling (Chen & Sun, 2005; Jayakumar & Norenberg, 2010).

The regulation of pH is partly achieved with the activation of the sodium-bicarbonate co-transporter (NBC) which is sensitive to increases in the extracellular potassium concentration, arising from neuronal activity (Rose & Verkhratsky, 2016). NBC activation can stimulate the glycolysis regulatory enzyme phosphofructokinase, which triggers glycolysis (Ruminot *et al.*, 2011) and links neuronal activity to astrocyte metabolism. Sodium-hydrogen exchangers (NHE) work in conjunction with NBCs to achieve pH regulation,

through sodium export and proton import. This transporter is also important for sodium extrusion. The absence of NHE increased astrocyte tolerance to OGD (Kintner *et al.*, 2004), suggesting a role in ischaemic injury.

The uptake of neurotransmitters and precursors utilizes the sodium gradient. Therefore glutamate or γ-aminobutyric acid (GABA) movement by excitatory amino acid transporters 1 and 2 (EAAT1 and 2), is accompanied by sodium ions (Schousboe, 2003). This results in transient increases in intracellular sodium concentration mainly within astrocyte processes, however more general cell wide increases can occur (Chatton, Marquet & Magistretti, 2000).

6.1.3 Role of astrocytic sodium in the CNS

Sodium transporter, receptors and channels have been found to be concentrated on astrocyte perisynaptic processes (Kirischuk, Parpura & Verkhratsky, 2012). These processes are in a unique location to interact with synapses. From this position astrocytes can detect the size and duration of neuronal activity and respond accordingly. Fluctuations in sodium levels allow astrocytes to regulate many physiological processes and link sodium concentration with homeostasis and metabolism. The resting concentration of astrocyte intracellular sodium concentration is approximately 15mM (Rose & Verkhratsky, 2016) which is in part maintained through passive sodium entry into cells, during resting conditions (Rose & Ransom, 1996).

Calcium is the predominant astrocyte signalling molecule, however it has been found that astrocytes are also sensitive to changes in sodium concentrations and produce sodium fluctuations (Verkhratsky *et al.*, 2013). Astrocyte calcium responses induced by synaptic activity are short acting,

whereas astrocyte sodium transients are more prolonged and can outlast synaptic transmission (Kirischuk, Kettenmann & Verkhratsky, 2007; Verkhratsky *et al.*, 2013). This indicates that astrocytes have the capability to produce different responses to neuronal stimuli through the use of different signalling molecules. Astrocyte sodium signals are proportional to synaptic activation and can differ in both time course and amplitude (Rose & Verkhratsky, 2016). The sodium transients generated in perisynaptic processes can spread throughout the astrocyte and trigger propagating waves that spread throughout the astrocyte network (Bernardinelli, Magistretti & Chatton, 2004). The sodium waves transmit across the astrocyte syncytia in a similar manner to calcium waves, predominantly through hemi-channels that form gap junctions with neighbouring cells (Langer *et al.*, 2012).

Sodium signalling can trigger a variety of homeostatic responses based upon the levels of neuronal activity (Kirischuk, Parpura & Verkhratsky, 2012). Sodium signals can function independently, direct calcium signals or work in conjunction with calcium signals. For example, increases in sodium concentration can cause rapid transient calcium increases within astrocyte microdomains (Kirischuk, Parpura & Verkhratsky, 2012), which occur due to the reversal of the NCX. There are many signalling functions of sodium, which require further investigation.

The neurotransmitter shuttles for glutamine/glutamate and glutamate/GABA are modulated by sodium, via direct regulation of glutamine synthetase (Benjamin, 1987). Sodium increases can dictate the speed and direction of GABA and calcium transport (Kirischuk, Parpura & Verkhratsky, 2012) which occurs via sodium dependent GABA transporters (GATs). GABA release can be triggered by changes in intracellular sodium concentration

(Kirmse & Kirischuk, 2006), which also regulate glutamate uptake (Chatton, Marquet & Magistretti, 2000).

The homeostatic regulation of potassium is a complex process involving sodium, in which many systems and transporters cooperate. Sodium increases trigger activation of the NKA and NKCC1, both of which allow entry of potassium into the astrocytes thereby lowering the extracellular concentration (Kirischuk, Parpura & Verkhratsky, 2012). Inwardly rectifying potassium channels, which are involved in lowering the extracellular potassium concentration, can be inhibited by increases in intracellular sodium concentration (Rose & Verkhratsky, 2016), thereby disrupting potassium homeostasis. The sodium concentration is used to modulate transporters involved in intra and extracellular pH homeostasis (Deitmer & Rose, 2010). The main transporters involved to achieve this are the NHE and NBC, thus regulating the movement of protons, hydroxide and bicarbonate ions to maintain the pH. The transmembrane sodium gradient is also utilized for the scavenging of reactive oxygen species (ROS) by ascorbic acid (Rose & Verkhratsky, 2016).

Sodium has an impact on metabolic regulation, activation of the NKA can stimulate glycolysis which produces lactate, possibly for the ANLS hypothesis (Pellerin & Magistretti, 1994). Intracellular sodium increases stimulate glucose uptake in astrocyte process endfeet (Voutsinos-Porche *et al.*, 2003), which partly provides substrate for the increase in glycolysis. Mitochondria can also respond to sodium signals through increases in intra-mitochondrial sodium concentration (Bernardinelli, Azarias & Chatton, 2006). This regulates astrocyte mitochondrial metabolism and can result in further lactate production by stimulating glycolysis (Azarias *et al.*, 2011).

Cell swelling occurs in response to extracellular increases in sodium and potassium concentration and is thought to be predominantly mediated by several transporters including NKCC1, NBC and KCC (Florence, Baillie & Mulligan, 2012; Payne *et al.*, 2003). The KCC is part of the same solute carrier family as NKCC1 (Mercado, Mount & Gamba, 2004) and is able to function bi-directionally (Dunham & Ellory, 1981). The sodium dependent transmembrane movement of ions generates an osmotic gradient, which triggers the movement of water (Brookes, 2005) into astrocytes via aquaporin channels, (Brookes, 2005; Nielsen *et al.*, 1997; Payne *et al.*, 2003), water efflux can also occur through these pores. Under physiological conditions, increases in cell volume are corrected via active volume regulation. The KCC can be stimulated to reduce cell volume (Brookes, 2005) through the export of potassium and chloride ions. Astrocyte cell volume is also regulated by the NHE which works alongside anion exchangers to maintain the correct volume of the cell (Brookes, 2005).

In some cell populations sodium can act as a regulator of protein activity by physically binding to the protein channel. Some of the channels that have been found to be regulated in this manner are NMDA receptors (Yu & Salter, 1998), voltage gated calcium channels, G-protein gated potassium channels (Blumenstein *et al.*, 2004) and sodium dependent potassium channels (Bhattacharjee & Kaczmarek, 2005).

6.1.4 Sodium influx, transporters and ischaemia

The maintenance of ionic gradients and ion homeostasis is an energy intensive process. During ischaemia, the reduced energy and oxygen supply disrupts ionic gradients causing cellular dysfunction. A major mechanism of ischaemia induced astrocyte cell death is via cytotoxic cell swelling. Astrocytes

are susceptible to cell swelling due to their role in glutamate uptake and potassium clearance, both of which utilize the sodium gradient (Boscia *et al.*, 2016). The disruption of ions during ischaemia and over-activation of transporters and receptors allows the influx of sodium, potassium and chloride into astrocytes. Movement of water into cells follows this influx due to osmotic overload, this increases cell volume and results in astrocyte swelling (Su *et al.*, 2002; Su, Kintner & Sun, 2002). Cell swelling can occur to such an extent that it becomes cytotoxic, cell membranes lose integrity and burst (Gurer *et al.*, 2009). Under physiological conditions any swelling can be corrected via regulated volume decrease. This process requires energy and cannot occur during ischaemia as ATP is unavailable and so astrocytes succumb to injury.

Previous work by the group has established that in P10 ON, ischaemic injury is sodium dependent (Thomas *et al.*, 2004). This study suggested that ischaemic injury was mediated by NKCC1. Further evidence from the literature suggests that NKCC1 has a role in ischaemic injury, due to its role in ion movement. Pharmacological inhibition of NKCC1 has been found to protect neurons from ischaemic injury (Yan, Dempsey & Sun, 2001b), possibly by preventing the swelling induced release of glutamate and reducing excitotoxicity, the main mechanism of ischaemic neuronal death. The inhibition of NKCC1 has also been found to reduce oedema and the size of ischaemic infarct (O'Donnell *et al.*, 2004; Yan, Dempsey & Sun, 2001b).

Ischaemia causes an increase in extracellular potassium, which can stimulate NKCC1 activity and induce astrocyte swelling, increasing cell size by approximately 20% (Su *et al.*, 2002; Su, Kintner & Sun, 2002). This swelling was prevented through the inhibition of NKCC1 or the absence of chloride or sodium (Su, Kintner & Sun, 2002). Su *et al* (2002) determined that astrocyte NKCC1

remains active during cell swelling, implying that during ischaemia the transporter may remain open, thereby exacerbating injury. It has been suggested that there may be a feed forward effect, whereby NKCC1 is further stimulated by cell swelling (Mongin *et al.*, 1994). During ischaemia volume regulation mechanisms are inhibited, which is detrimental to the cell (Mongin & Kimelberg, 2005).

Reperfusion after ischaemic insult has been found to reactivate NKCC1 which may be responsible for a proportion of reperfusion injury (Kintner *et al.*, 2007; Kintner *et al.*, 2004; Lenart *et al.*, 2004). The reintroduction of blood flow can also activate the NHE, causing sodium entry (Kintner *et al.*, 2004). It has been found that NKCC1 can also be activated via phosphorylation of the transporter (Flemmer *et al.*, 2002; Lenart *et al.*, 2004). Once stimulated NKCC1 has the ability to activate the reverse mode of NCX, due to the increase in intracellular sodium. In this chapter the role of sodium and CCCs in astrocyte ischaemic injury has been investigated. In order to study the potential involvement of these transporters inhibitors were used to block the transporter of interest. Here bumetanide was used to specifically inhibit NKCC1, DIOA was used to selectively inhibit KCC and furosemide was used as a non-specific CCC inhibitor (figure 6.2). In this chapter we investigated the hypothesis that cytotoxic sodium influx plays a significant role in ischaemia induced astrocyte cell death.
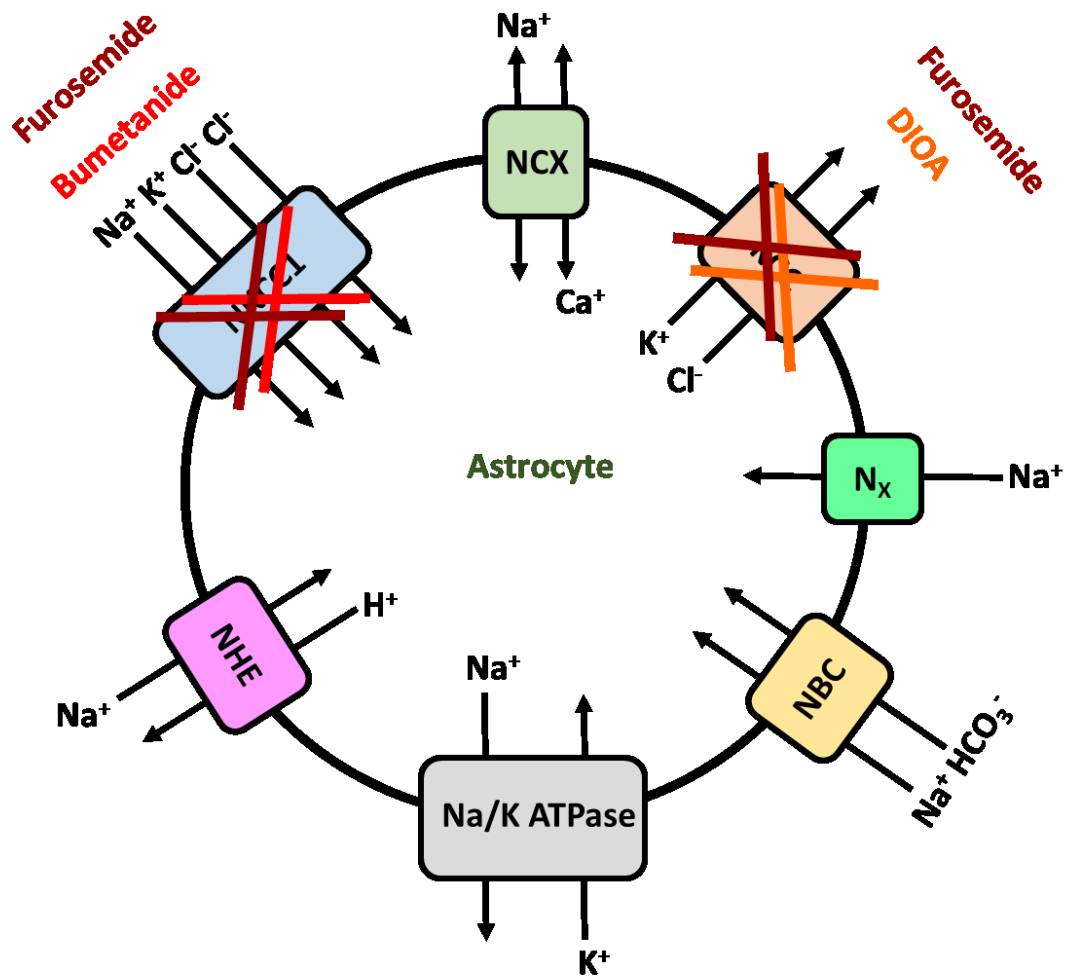
Figure 6.2: Action of CCC inhibitors. Furosemide inhibits all CCCs, Bumetanide specifically inhibits NKCC1 and DIOA inhibits KCC.

6.2 RESULTS: SODIUM DEPENDENT ASTROCYTE CELL DEATH IN DENTATE GYRUS.

Sodium influx has been implicated in ischaemic astrocyte swelling and death in P10 rat optic nerve (Thomas *et al.*, 2004). To investigate the role of sodium in ischaemic injury, sodium was removed from the aCSF during OGD and was replaced with NMDG chloride (128mM). This was to determine whether ischaemic injury of adult astrocytes was sodium dependent in the CC and the DG.

In CC, the confocal images show that many astrocytes survive the period of OGD in both the presence and absence of sodium (figure 6.3A). The lack of sodium caused a significant increase in *t* value from 62.00 ± 2.32 mins to 71.25 ± 3.52 mins (p=0.0455, figure 6.1B), which suggests a slower rate of cell death. When sodium was removed from the aCSF, the total cell death was decreased from 40.17 ± 6.45% to 31.79 ± 8.41% (not significant, figure 6.3C).

In DG, the removal of sodium had a profound effect upon OGD induced cell death (figure 6.4). The confocal images show that in the absence of sodium, GM astrocytes can survive the ischaemic insult and reperfusion (figure 6.4A, lower panel). The *t* values were not significantly different between the two conditions, for DG this was 54.64 ± 3.30 mins and without sodium was 64.92 ± 3.48 mins (figure 6.4B). By removing sodium GM astrocytes behaved in a similar manner to those in WM. The overall cell death achieved without sodium was decreased from 97.61 ± 1.01% to 37.70 ± 9.80% (p=<0.0001, figure 6.4C). These results suggest that sodium influx during OGD accounts for the higher injury sensitivity of DG astrocytes compared to CC cells.

A

B

C
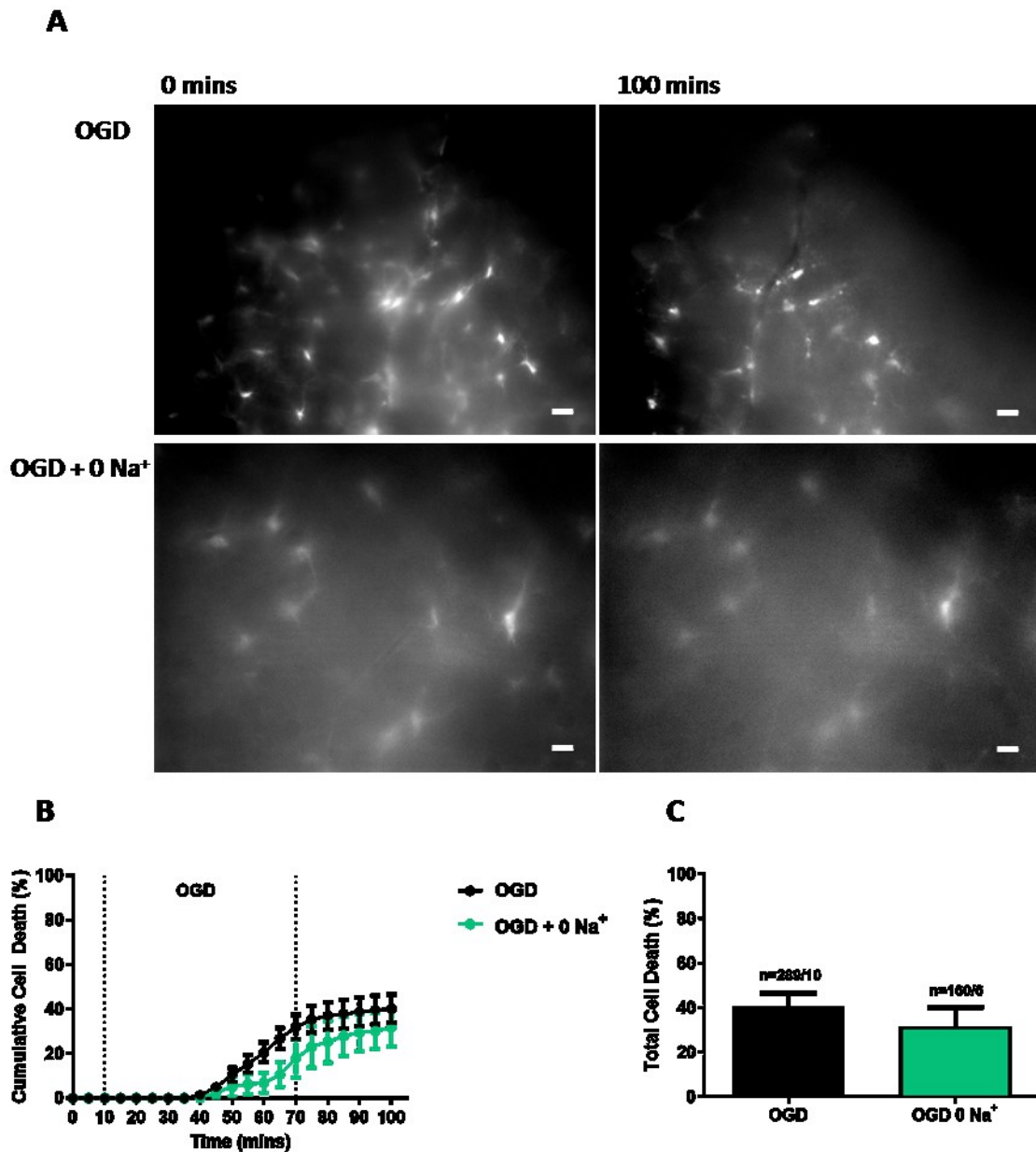
Figure 6.3: Zero Sodium conditions had no effect on OGD induced astrocyte cell death in corpus callosum (CC). A: Confocal images during OGD (upper panel) and OGD with 0 Na (lower panel). Images taken at 0 and 100 minutes. Scale bar = 20 μm. B: Astrocyte cell death over time. C: total cell death at time 100 minutes, OGD only (black bar) and OGD with 0Na$^+$ (green bar). Error bars = SEM. N numbers = number of cells/number of slices.
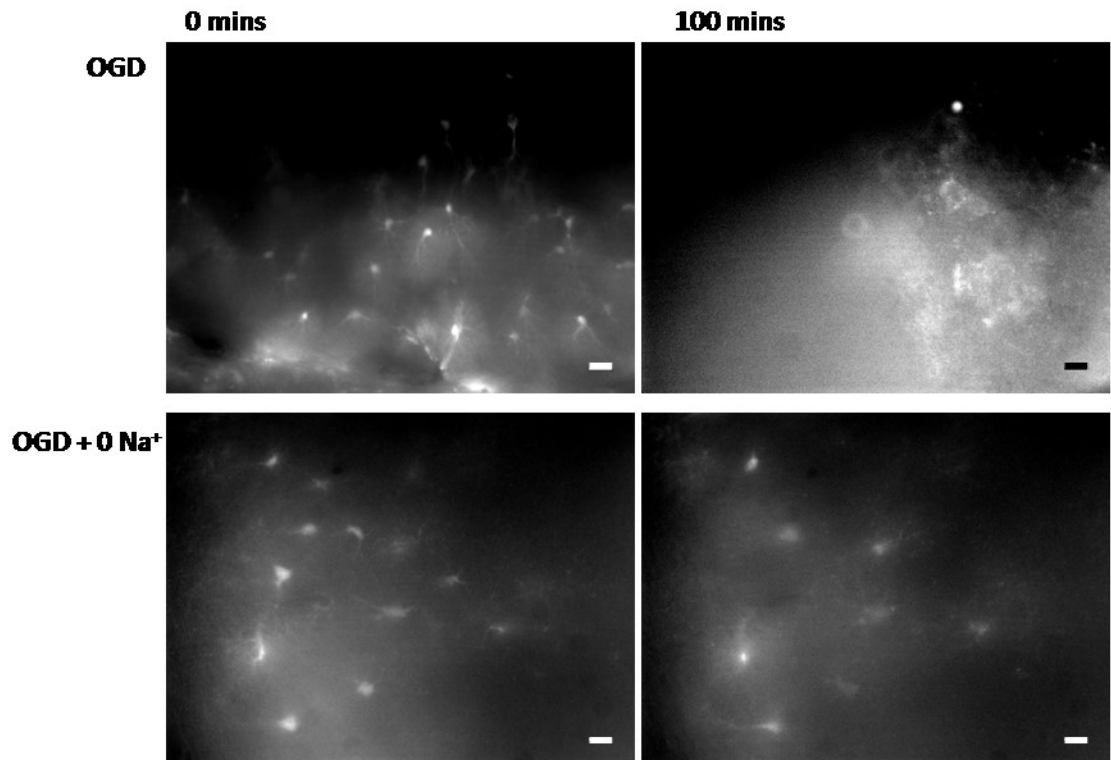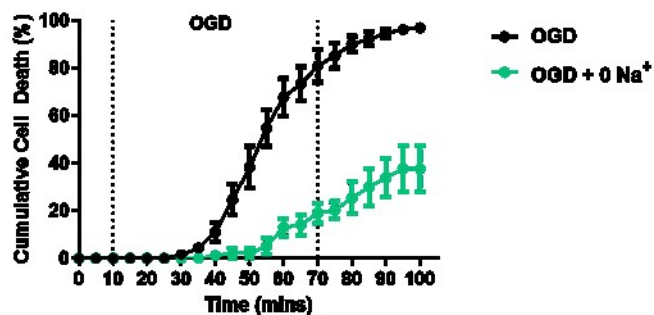
Figure 6.4: Zero Sodium conditions decreased OGD induced astrocyte cell death in dentate gyrus (DG). A: Confocal images during OGD (upper panel) and OGD with 0 Na (lower panel). Images taken at 0 and 100 minutes. Scale bar = 20 μm. **B:** Astrocyte cell death over time. **C:** total cell death at time 100 minutes, OGD only (black bar) and OGD with 0Na$^+$ (green bar). Error bars = SEM. N numbers = number of cells/number of slices.

6.3 Results: Role of NKCC1 in ischaemic astrocyte cell death

The NKCC1 is known to play a role in astrocyte cell swelling (Su, Kintner & Sun, 2002), which contributes to OGD induced cell death. The involvement of this transporter in ischaemic astrocyte cell death was examined by inhibiting the NKCC1 with bumetanide. Bumetanide is a well-known and widely used distal loop diuretic and is a specific inhibitor of the NKCC1 at the concentration used (50μM).

6.3.1 Results: Effect of NKCC1 inhibition on OGD induced astrocyte death in adult slices

The inhibition of NKCC1 increased OGD induced astrocyte cell death in CC (figure 6.3). The confocal images illustrate the difference in cell death between OGD only and OGD in the presence of bumetanide (figure 6.5A). The addition of bumetanide did not cause a significant change in t value, which was 62.00 ± 2.32 mins for CC and 58.92 ± 2.39 mins for CC with NKCC1 inhibition (figure 6.5B). The total amount of cell death achieved with OGD and bumetanide was significantly higher than that seen in OGD only conditions (figure 6.5C). The inhibition of NKCC1 caused cell death to increase from 40.17 ± 6.45% to 92.65 ± 2.64 % (p=<0.0001), which is similar to the amount of OGD induced cell death seen in GM astrocytes.

In DG, the presence of bumetanide did not affect OGD induced astrocyte cell death (figure 6.6). Exposure to OGD either in the presence or absence of the drug caused the majority of astrocyte to die as seen in the confocal images (figure 6.6A). The t value was not significantly altered by the addition of bumetanide, the t for DG was 54.64 ± 3.30 mins and with inhibitor was 52.58 ± 2.63 mins, suggesting that the presence of bumetanide had very little effect

216

(figure 6.6B). The inhibition of NKCC1 did not alter the total amount of OGD induced astrocyte death, 97.61 ± 1.01% with OGD and 97.69 ± 1.73% with OGD and bumetanide (not significant, figure 6.6C). Taken together these results suggest that NKCC1 has different roles in CC and DG during ischaemic insult. The inhibition of the transporter had a greater effect in CC showing that there is a potential role for the NKCC1 in astrocyte survival.

A

B **C**
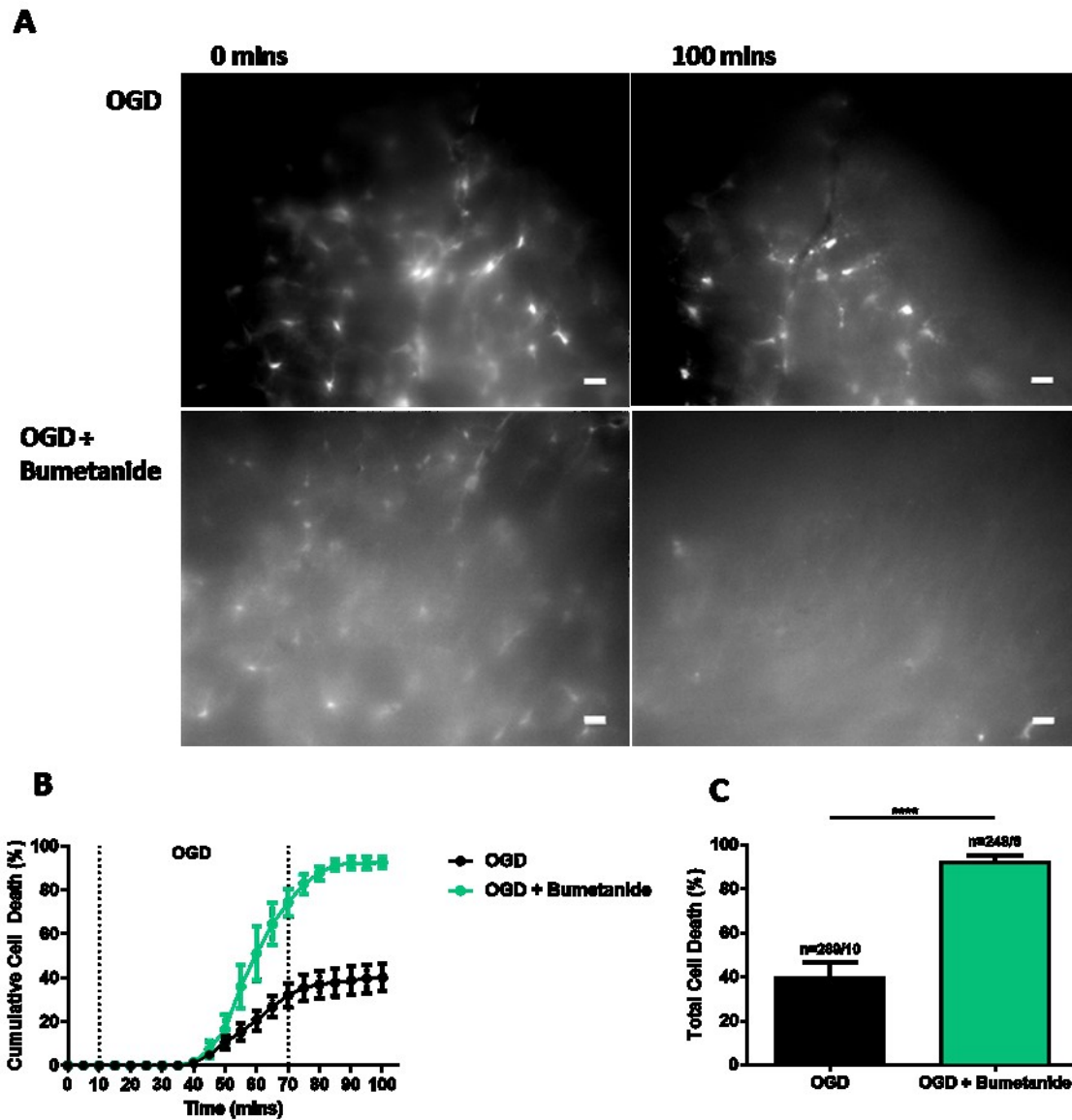
Figure 6.5: NKCC1 inhibitor bumetanide (50µM) increased OGD induced astrocyte cell death in corpus callosum (CC). **A:** Confocal images during OGD (upper panel) and OGD with bumetanide treatment (lower panel). Images taken at 0 and 100 minutes. Scale bar = 20 µm. **B:** Astrocyte cell death over time. **C:** total cell death at time 100 minutes, OGD only (black bar) and OGD with bumetanide (green bar). Error bars = SEM. N numbers = number of cells/number of slices.
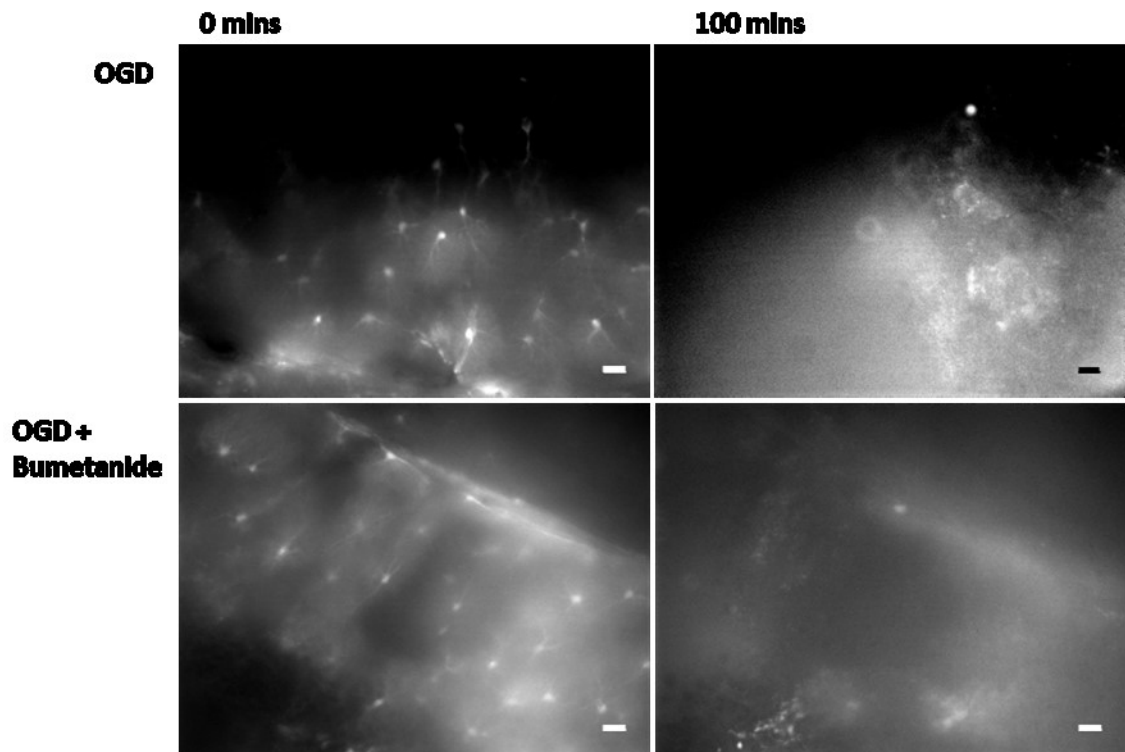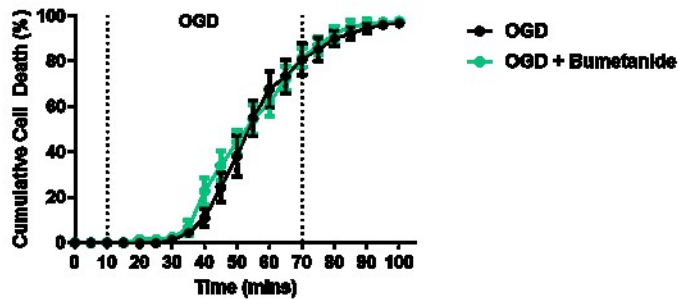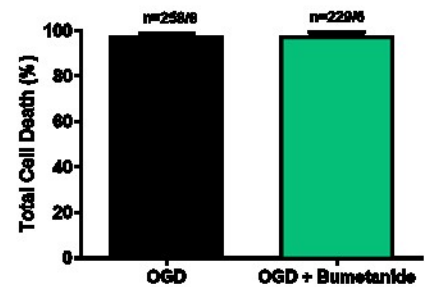
Figure 6.6: NKCC1 inhibitor bumetanide (50μM) has no effect on OGD induced astrocyte cell death in dentate gyrus (DG). A: Confocal images during OGD (upper panel) and OGD with bumetanide treatment (lower panel). Images taken at 0 and 100 minutes. Scale bar = 20 μm. B: Astrocyte cell death over time. C: total cell death at time 100 minutes OGD only (black bar) and OGD with bumetanide (green bar). Error bars = SEM. N numbers = number of cells/number of slices.

6.3.2 Results: NKCC1 inhibition and the effect on OGD induced cell death in neonatal astrocytes

It was previously established that mechanisms of ischaemic astrocyte death change with age, from a calcium dependent mechanism in P2 ON to sodium dependent in P10 ON (Fern, 1998; Thomas *et al.*, 2004). The previous section investigated NKCC1 inhibition in adult brain slices. Here the effect of bumetanide on neonatal astrocytes (P10) was examined to see if there were any differences in the mechanism of cell death at this age. In CC, the presence of bumetanide significantly increased astrocyte cell death from 10.86 ± 3.10% to 38.69 ± 4.80%, p=0.0007 (figure 6.7C). The confocal images illustrate the increased astrocyte sensitivity to OGD that occurs with the addition of bumetanide (figure 6.7A). However, inhibition of NKCC1 did not cause a significant change in t value, which for neonate CC was 78.30 ± 5.33 mins and 75.75 ± 5.13 mins with bumetanide (figure 6.5B).

The neonatal DG astrocytes behaved differently to neonatal CC astrocytes. Inhibiting NKCC1 in DG significantly reduced astrocyte cell death from 67.38 ± 12.79% to 34.09 ± 4.36%, (p=0.0335, figure 6.8 C). The confocal images depict the tolerance of DG astrocytes in the presence of bumetanide compared with OGD only, where cell breakdown and death can be seen (figure 6.8A). NKCC1 inhibition did not cause a significant change in *t* value, for neonate DG this was 68.50 ± 3.13 mins and with bumetanide was 73.42 ± 1.91 mins (figure 6.8B). The addition of bumetanide had differing effects in each region investigated, suggesting that the mechanism of ischaemic cell death depends upon the region in which astrocytes are located. The results for the neonatal CC astrocytes were similar to those for the adult CC astrocytes, where NKCC1 inhibition increased sensitivity to OGD. However, for neonate DG

astrocytes, bumetanide treatment was protective and increased tolerance to ischaemic insult.
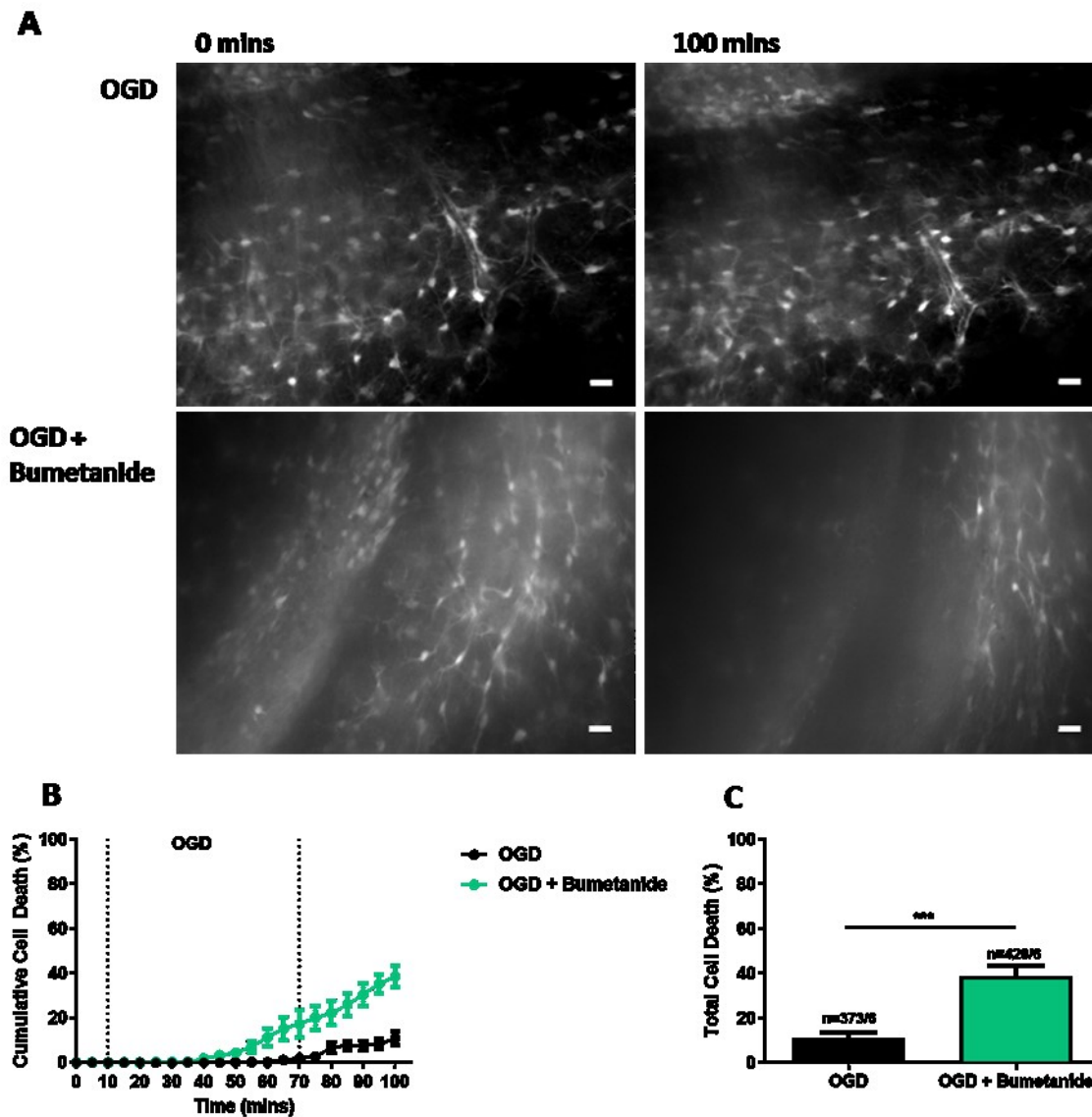
Figure 6.7: Bumetanide treatment (50µM) increased OGD induced astrocyte cell death in neonatal corpus callosum (CC). A: Confocal images taken during OGD (upper panel) and during OGD with bumetanide treatment (lower panel). Images taken at 0 and 100 minutes. Scale bars = 20µM. B: Astrocyte cell death over time. C: cell death at time 100 minutes, OGD only (black bar) and OGD with bumetanide (green bar). Error bar = SEM. N numbers = number of cells/number of slices.
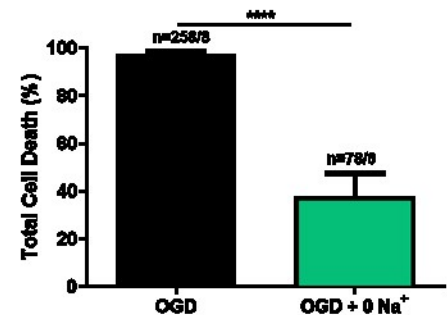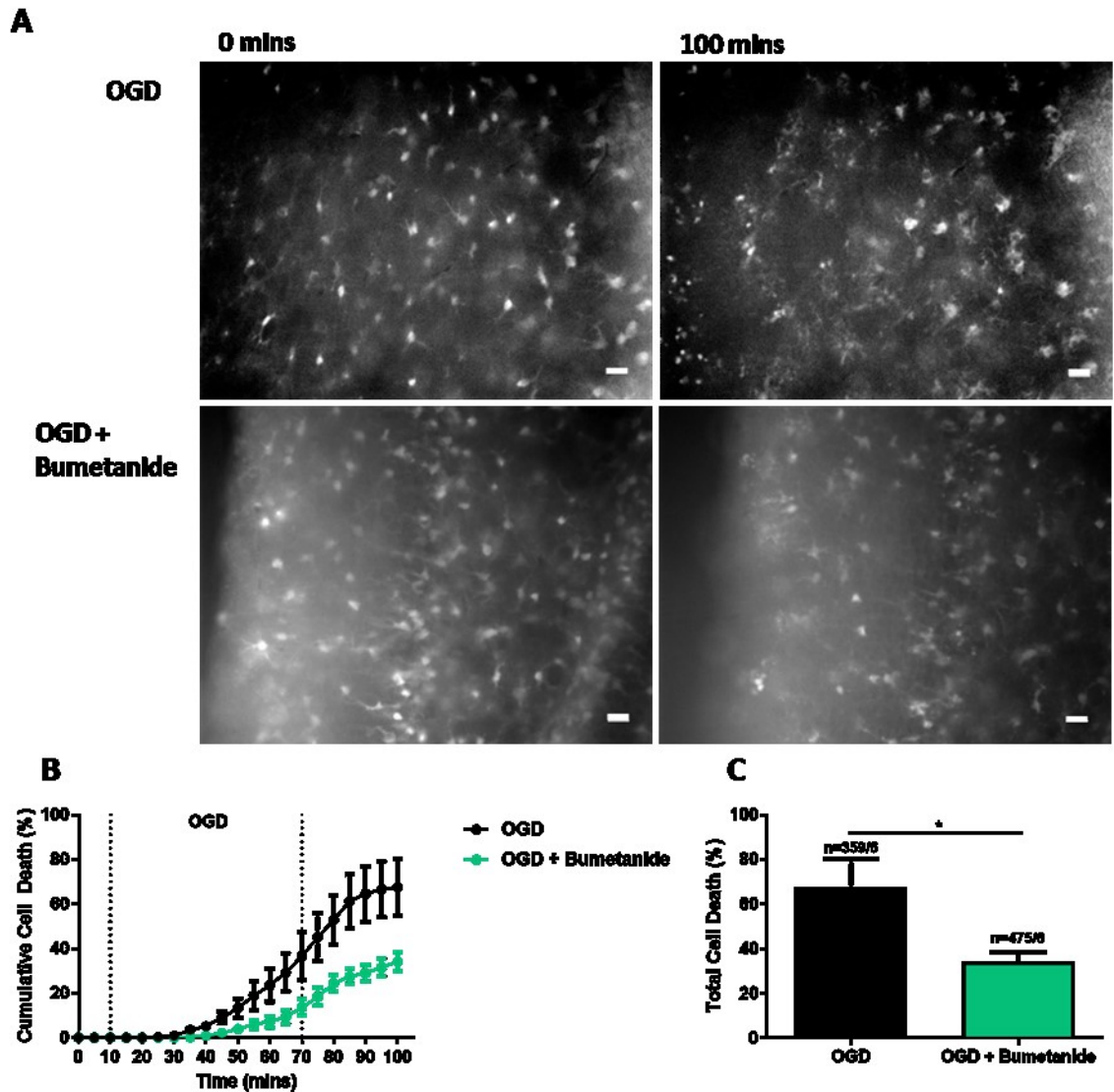
Figure 6.8: Bumetanide treatment (50µM) decreased OGD induced astrocyte cell death in neonatal dentate gyrus (DG). **A:** Confocal images taken during OGD (upper panel) and during OGD with bumetanide treatment (lower panel). Images taken at 0 and 100 minutes. Scale bars = 20µM. **B:** Astrocyte cell death over time. **C:** cell death at time 100 minutes, OGD only (black bar) and OGD with bumetanide (green bar). Error bar = SEM. N numbers = number of cells/number of slices.

6.4 RESULTS: ROLE OF KCC IN ISCHAEMIC ASTROCYTE CELL DEATH

The NKCC is not the only CCC expressed by astrocytes, the KCC was selected for investigation due to its transportation of chloride ions and involvement in astrocyte cell swelling (Ringel & Plesnila, 2008). Ringel and Plesnila (2008) found that the inhibition of KCC increased cell volume, suggesting dysfunction of this transporter may contribute to ischaemic astrocyte death. The KCC was selectively inhibited by the addition of 50µM DIOA (2-[[(2S-2-butyl-6,7-dichloro-2-cyclopentyl-1-oxo-3H-inden-5-yl]oxy]acetic acid).

In CC, the selective KCC inhibitor caused a significant increase in astrocyte OGD induced cell death from 40.17 ± 6.45% to 61.93 ± 4.87% (p=0.0332, figure 6.9C). The confocal images illustrate the loss of astrocytes due to OGD in the presence of DIOA (figure 6.9A). KCC inhibition caused a change in the rate of cell death as the t values were significantly different. The CC t value was 62.00 ± 2.32 mins and with the addition of DIOA was 48.08 ± 2.19 mins (p=0.0012, figure 6.9B).

The presence of DIOA decreased OGD induced astrocyte death in DG from 97.61 ± 1.01% to 88.19 ± 10.25% (not significant, figure 6.10C). The total cell death for slices treated with DIOA had more variability and so the reduction in cell death was not significant. The confocal images depict extensive cell death in both conditions (6.10A). The inhibition of KCC caused little change to the cell death profile and the t values were not significantly different, for DG this was 54.64 ± 3.30 mins and with DIOA was 49.08 ± 2.58 mins (figure 6.10B). The inhibition of the KCC neither protected nor caused widespread cell death, which would suggest that this transporter has a less prominent role in OGD induced astrocyte cell death.

A

B

C
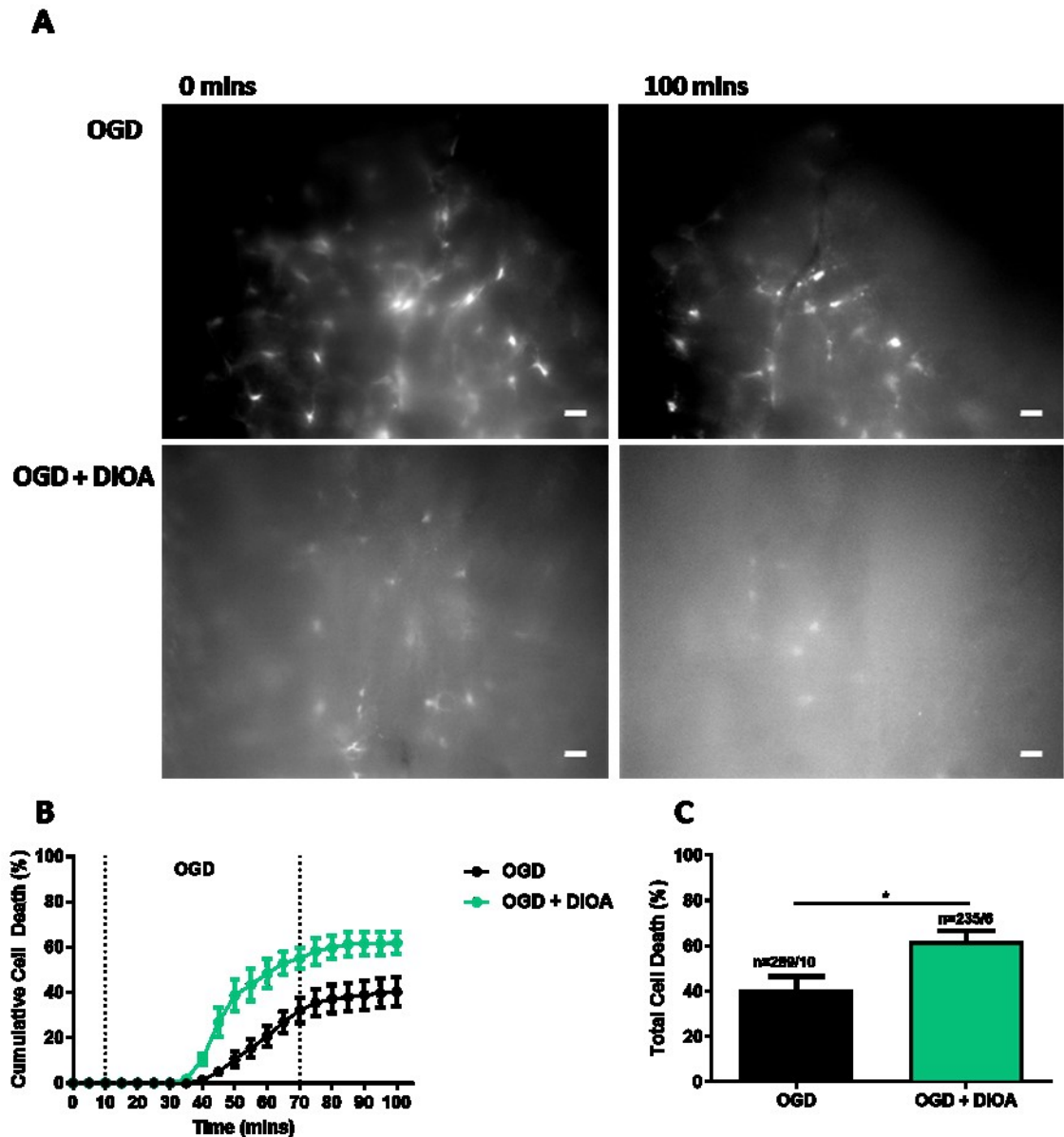
Figure 6.9: DIOA treatment (50μM) increased OGD induced astrocyte cell death in corpus callosum (CC). A: Confocal images during OGD (upper panel) and OGD with DIOA treatment (lower panel). Images taken at 0 and 100 minutes. Scale bar =20 μm. B: Astrocyte cell death over time. C: total cell death at time 100 minutes, OGD only (black bar) and OGD with DIOA (green bar). Error bars = SEM. N numbers = number of cells/number of slices.
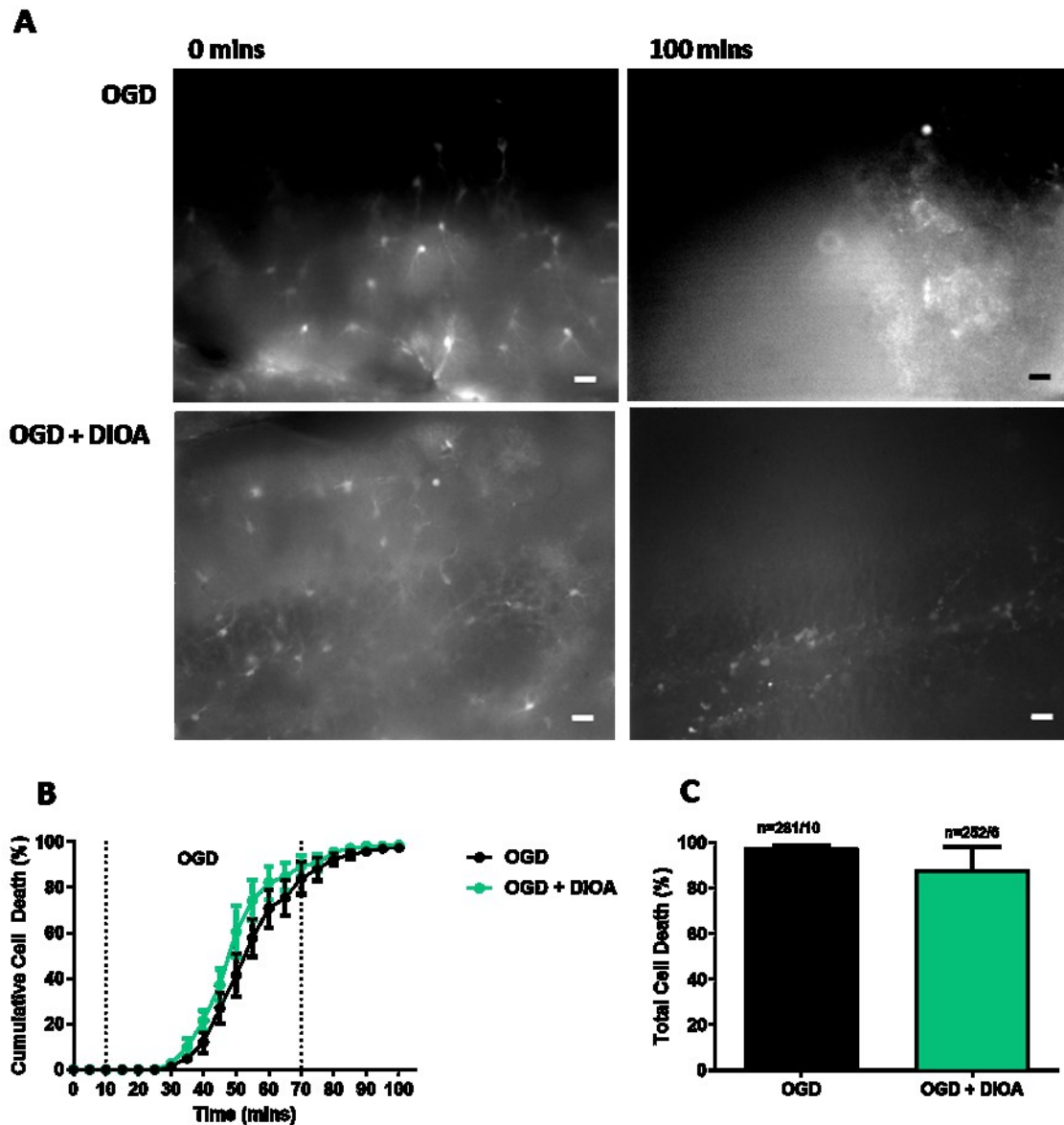
Figure 6.10: DIOA treatment (50μM) had no effect on OGD induced astrocyte cell death in dentate gyrus (DG). **A:** Confocal images during OGD (upper panel) and OGD with DIOA treatment (lower panel). Images taken at 0 and 100 minutes. Scale bar =20 μm. **B:** Astrocyte cell death over time. **C:** total cell death at time 100 minutes, OGD only (black bar) and OGD with DIOA (green bar). Error bars = SEM. N numbers = number of cells/number of slices.

## 6.5 RESULTS: BROAD-SPECTRUM INHIBITION OF CCCS REDUCED GM ASTROCYTE CELL DEATH

The selective inhibition of NKCC1 and KCC had varying impacts on OGD induced astrocyte cell death in WM and GM. To investigate the role of all CCCs slices were then treated with furosemide, another widely used distal loop diuretic which at 5mM concentration will non-selectively inhibit the majority of CCCs.

In CC, the addition of furosemide did not affect OGD induced astrocyte cell death when compared to OGD only conditions (figure 6.11). The confocal images illustrate that CC astrocytes were tolerant to OGD under both conditions (figure 6.11A). The inhibition of CCCs with furosemide slowed the rate of cell death and resulted in an increase in t value, however this was not significant (figure 6.11B). The t values for CC with and without furosemide were 70.25 ± 5.60 mins and 62.00 ± 2.32 mins respectively. The presence of furosemide did not affect the total amount of OGD induced cell death (figure 6.11C). The astrocyte death in the presence of furosemide was 39.07 ± 6.78% and was 40.17 ± 6.45% with OGD only (not significant).

In DG, the presence of furosemide slightly increased astrocyte tolerance to ischaemia (figure 6.12). The confocal images show that inhibition of CCCs provided protection and resulted in astrocytes that survive OGD (figure 6.12A). Furosemide did not alter the rate of cell death as shown by the t value, which was 54.64 ± 3.30 mins for DG only and 62.00 ± 2.04 mins with inhibitor (figure 6.12B). Inhibition of CCCs caused cell death to significantly decrease from 97.61 ± 1.01% to 89.89 ± 2.75% (p=0.0073, figure 6.12C). The addition of furosemide had a greater effect on GM astrocytes, suggesting that CCCs have a greater role in OGD induced astrocyte death in DG than in CC.

A

B

C
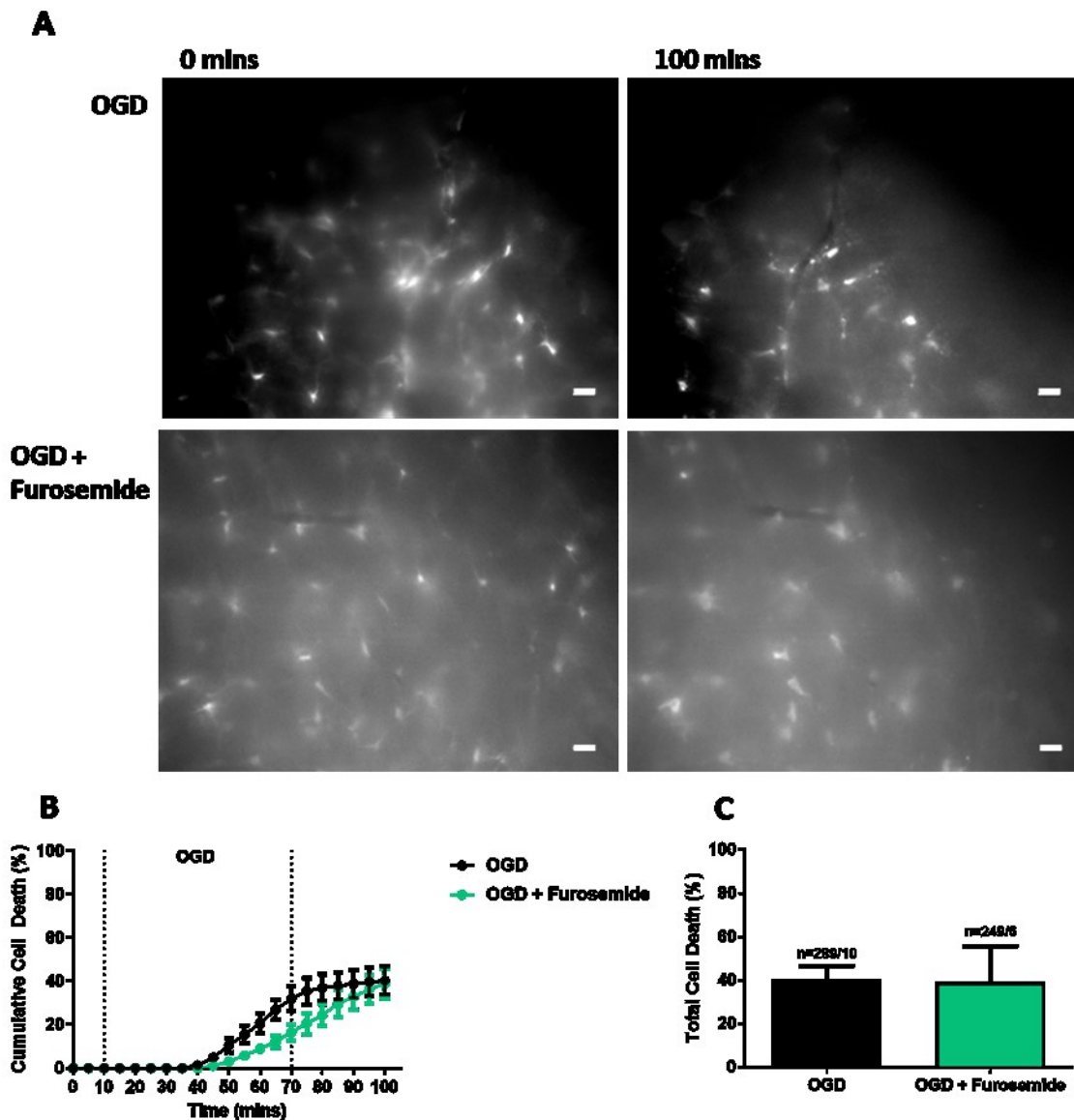
Figure 6.11: Furosemide treatment (5mM) had no effect on OGD induced astrocyte cell death in corpus callosum (CC). **A:** Confocal images taken during OGD (upper panel) and OGD with furosemide treatment (lower panel). Images taken at 0 and 100 minutes. Scale bar =20 μm. **B:** CC astrocyte cell death over time. **C:** total cell death at time 100 minutes, OGD only (black bar) and OGD with furosemide (green bar). Error bars = SEM. N numbers = number of cells/number of slices.
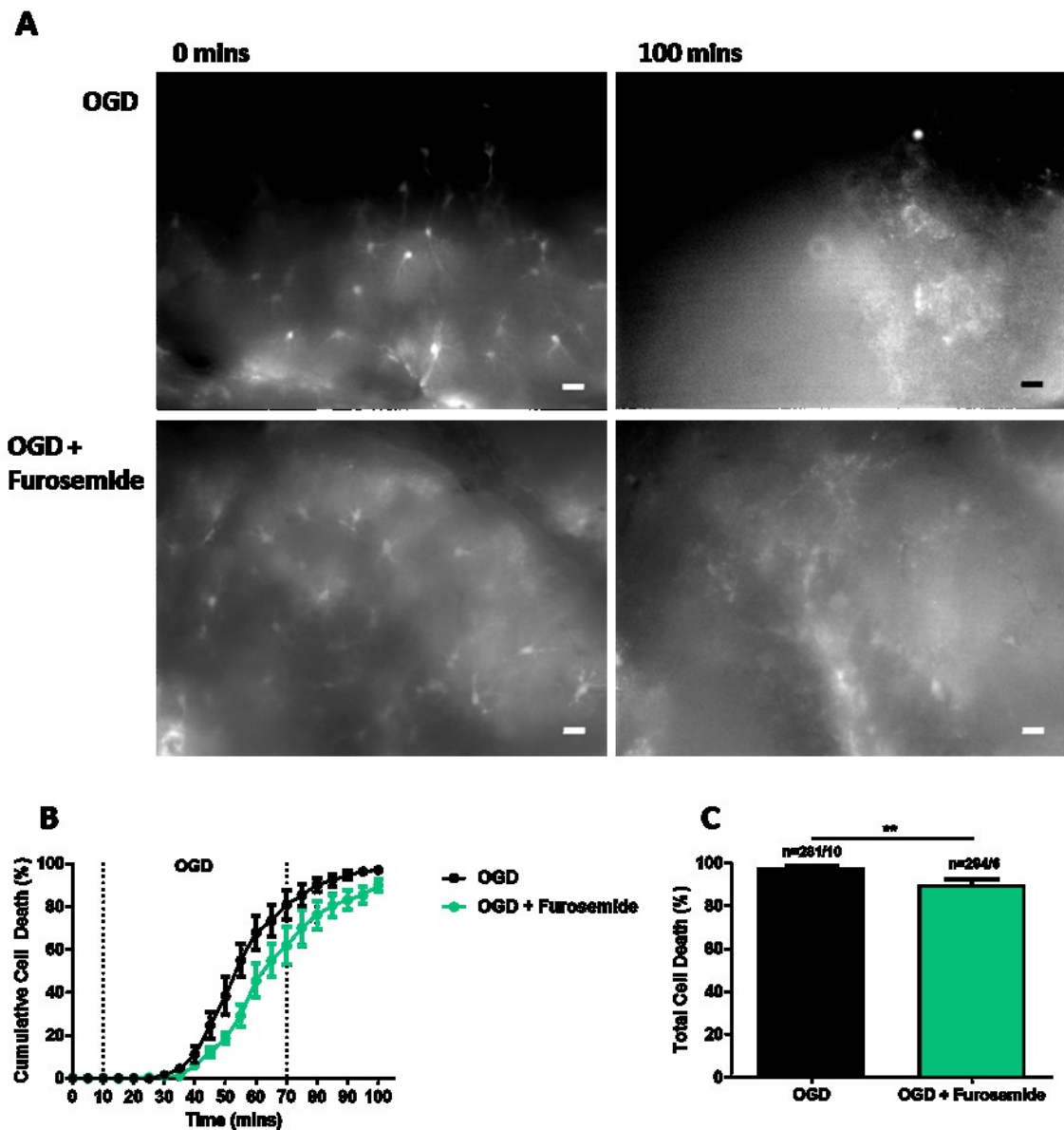
Figure 6.12: Furosemide treatment (5mM) decreased OGD induced astrocyte cell death in dentate gyrus (DG). **A:** Confocal images taken during OGD (upper panel) and OGD with furosemide treatment (lower panel). Images taken at 0 and 100 minutes. Scale bar =20 μm. **B:** CC astrocyte cell death over time. **C:** total cell death at time 100 minutes, OGD only (black bar) and OGD with furosemide (green bar). Error bars = SEM. N numbers = number of cells/number of slices.

6.6 RESULTS: COMPARISON OF CCC INHIBITORS

To determine the effect of inhibiting CCCs on OGD induced astrocyte cell death, the regions were compared for each condition, (CC figures 6.13A, C, E and G, DG figures 6.13B, D, F and H) over time (figures 6.11A and B) and at selected time points (figures 6.13C-H). In CC, the results demonstrate that inhibition of NKCC1 with bumetanide had the greatest effect on OGD induced astrocyte cell death (figure 6.13A). The presence of bumetanide significantly increased CC cell death after 60 minutes OGD from 23.11 ± 7.12% to 73.35 ± 5.60% (p=<0.0001, figure 6.13 E). Throughout the reperfusion period cell death was increased, this increase remained at the end of the experiment (figure 6.13G). The addition of DIOA, to inhibit KCC, increased OGD induced cell death but to a lesser extent than in the presence of bumetanide. After 30 minutes of OGD, astrocyte death was increased from 0% to 10.91 ± 2.16% (p=<0.0001) and after 60 minutes OGD, DIOA increased cell death from 23.11 ± 7.12% to 55.08 ± 4.67%, (p=0.0044, figures 6.13C and E). These results suggest that the inhibition of KCC increased sensitivity to ischaemic insult in CC astrocytes. The other inhibitors used did not significantly affect OGD induced astrocyte cell death. The data indicate that NKCC1 acts as an important protector of astrocytes in adult WM, which largely accounts for the ischaemia tolerance of these cells.

The inhibition of NKCC1 did not affect OGD induced cell death in DG, where astrocytes behaved in a similar manner to those under OGD only conditions (figure 6.13B). In this region the most significant decrease in OGD induced cell death was seen in sodium free conditions, this reduced DG astrocyte sensitivity to OGD. After 60 minutes of insult, cell death dropped from 81.61 ± 7.66% to 19.02 ± 4.17% with the absence of sodium (p=<0.0001, figure

6.13F). The reduction in cell death was maintained throughout the reperfusion period (p=<0.0001, figure 6.13H). The only other inhibitor which delayed cell death was furosemide (figure 6.13B). The CCC inhibitor did reduce cell death at each time point, however, this was not significant (figure 6.13D, F and H). The DG is very sensitive to OGD and widespread cell death is seen in this region, which limits the detection of increased sensitivity to OGD induced injury. The absence of any significant effect of drugs upon the rate of astrocyte cell death during OGD argue against a role for any of the CCC in the reduction of injury in this cell population.

Sodium free conditions applied during OGD had a highly protective effect on DG astrocytes suggesting ischaemic cell death in GM is sodium dependent, whereas in CC sodium removal had little effect. The findings highlight the significant cellular injury pathways that operate in these two populations of astrocytes.
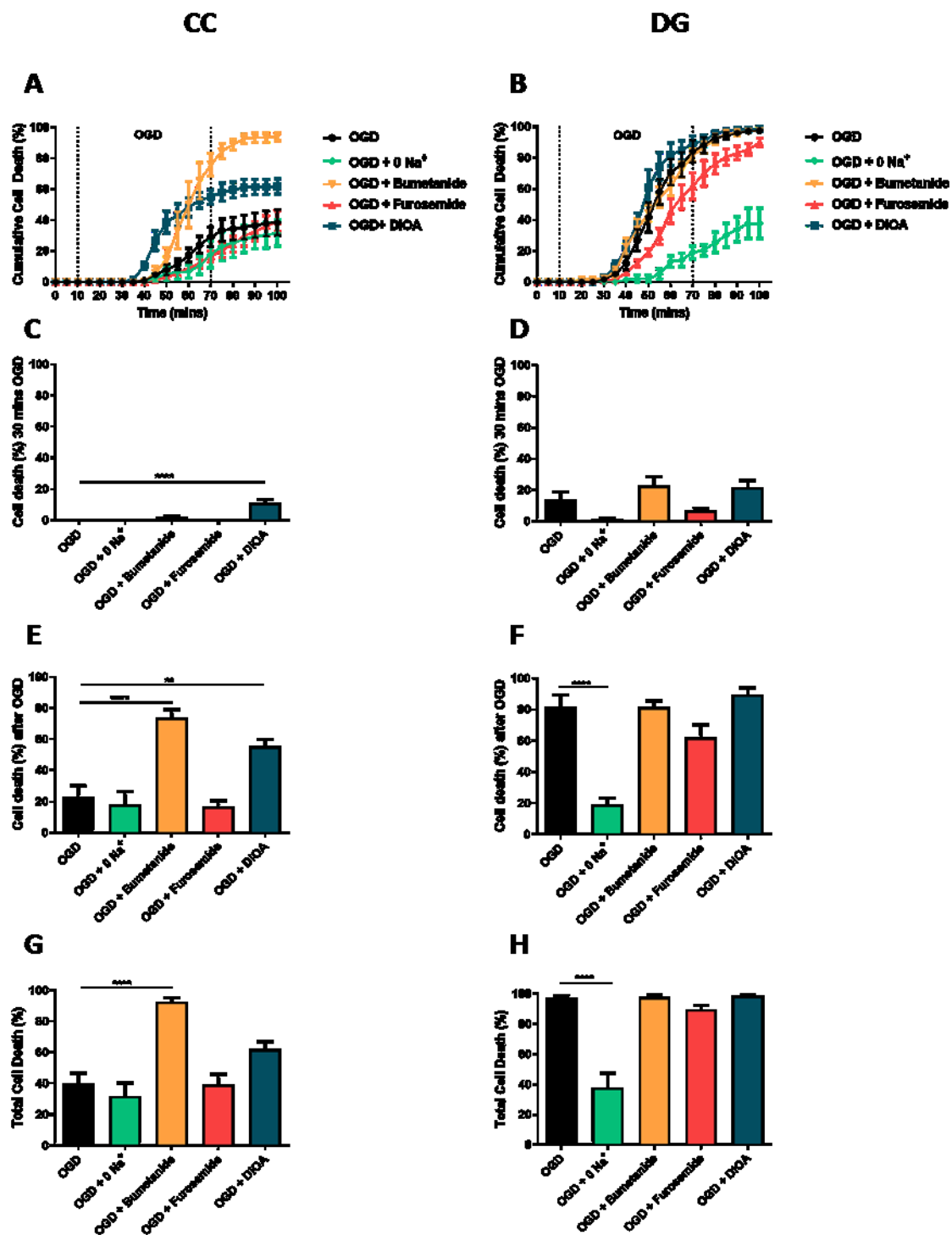
Figure 6.13: Comparison of sodium transporter inhibition. A + B: Cell death over time with OGD only and for each inhibitor. **C + D:** Astrocyte cell death after 30 minutes OGD for each inhibitor. **E + F:** Astrocyte cell death after 60 minutes OGD for each inhibitor, **G + H:** Total astrocyte cell death after reperfusion period. **A, C, E + G:** CC, **B, D, F + H:** DG. Error bars = SEM. Comparison via ANOVA, inhibitors compared to OGD.

6.7 Discussion: Sodium and CCCs in OGD induced astrocyte cell death

Previously, it was established that ischaemic insult causes cytotoxic cell swelling and astrocyte death, which is thought to be mediated by CCCs such as NKCC1, and that ischaemic injury is sodium dependent (Thomas *et al.*, 2004). My data shows that this picture is too simplistic and that cellular mechanism of acute ischaemic injury differ significantly between astrocyte populations. During ischaemia, intracellular accumulation of sodium ions is accompanied by chloride and potassium ion influx, triggering water uptake and increase in cell volume (Su *et al.*, 2002; Su, Kintner & Sun, 2002). Under normal, physiological conditions this would be rectified via ion redistribution or regulated volume decrease. Ischaemia induced cell swelling cannot be corrected due to reduced energy availability and the disruption of ion gradients, thus active volume regulation is not an option. The increased astrocyte volume strains the cell membrane, leading to the eventual loss of membrane integrity and cell rupture (Gurer *et al.*, 2009). My data shows that acute injury is not prevented by removing extracellular calcium indicating that this is not a form of the calcium-mediated injury that underlies neuron and oligodendrocyte cell death. Prior work has shown that zero-calcium conditions can exacerbate cytotoxic cell swelling in astrocytes (Thomas *et al.*, 2004), which is consistent with my findings.

6.7.1 DG OGD induced astrocyte cell death is sodium dependent

The data in this chapter show that in the DG, OGD induced astrocyte cell death is sodium dependent, confirming the findings of Thomas *et al.* (2004) in the neonatal optic nerve. In the DG, the replacement of sodium was highly protective and the resulting OGD tolerance of cells was similar to that of WM astrocytes (figure 6.4). Astrocyte cell death in DG was reduced with the non-

specific inhibition of CCCs with furosemide (figure 6.12) but the selective

inhibition of NKCC1 and KCC did not affect DG astrocyte cell death. The data

suggest that cytotoxic sodium influx during OGD occurs via a different route. It is

possible that an alternative pathway for sodium influx is via activated glutamate

receptors, which are known to be permeable to a variety of ions including

sodium (Dzamba, Honsa & Anderova, 2013; Lalo *et al.*, 2011).

The hippocampus is a region of high neuronal activity and so the majority

of hippocampal astrocytes will have processes that interact with synapses.

These perisynaptic processes are rich in ionotropic glutamate receptors, CCCs

and other sodium transporters. The presence of a variety of different channels

on astrocyte perisynaptic processes provides sodium with many routes of entry,

all of which may contribute to ischaemic cell death. The data suggest a

furosemide sensitive but bumetanide and DIOA insensitive transporter, such as

an anion exchanger may be important for DG astrocyte injury. This would

indicate that the sodium and furosemide sensitive injury occur via parallel

pathways.

6.7.2 NKCC1 and KCC are required for CC astrocyte survival

In CC, ischaemia induced cell death was not prevented by the absence

of sodium, indicating a fundamentally different mode of injury to that in DG cells.

The selective and general inhibition of CCCs gave differing results for each

region investigated. Indicating that the roles of particular transporters depend

upon the location of astrocytes and the levels of expression. This work has

determined that in CC, NKCC1 and KCC are important for protecting astrocytes

from ischaemic injury. The inhibition of these transporters caused significantly

higher cell death in WM (figures 6.5 and 6.9). This finding is contrary to previous

work where bumetanide provided protection to neonatal (P10) optic nerve

astrocytes during OGD (Salter & Fern, 2008; Thomas *et al.*, 2004). This suggests that in the adult brain there may be different cell death mechanisms that are both region and development specific. The inhibition of KCC with DIOA increased CC astrocyte cell death but not to the extent seen with bumetanide treatment. It has been found that the inhibition of KCC increased cell swelling under physiological conditions (Ringel & Plesnila, 2008).

The ischaemia induced sodium influx does not affect CC astrocytes to the same extent as DG astrocytes, showing regional differences in the cell death mechanism. The transporter inhibition did not prevent or reduce OGD induced astrocyte death in CC, whereas DG astrocyte death was reduced with the removal of sodium and in the presence of furosemide. The tolerance to OGD seen in CC astrocytes may result from the partial extrusion of any sodium influx. Alternatively, the OGD induced cell death that is observed may arise from the influx of another ion such as potassium. Potassium is also dysregulated during ischaemia and has been found to trigger cell swelling (Su, Kintner & Sun, 2002).

6.7.3 Sodium, CCCs and OGD induced astrocyte cell death

The ischaemia induced sodium influx has been found to be detrimental to DG astrocytes but not CC astrocytes. Suggesting that different mechanisms of cell death exist for different astrocyte populations. The role of sodium transporters such as CCCs has also been found to differ depending upon region. The specific inhibition of CCCs was harmful to CC astrocytes, whereas CCC inhibition in DG astrocytes was protective. This conflicting effect demonstrates the difference in cell death mechanisms between regions and suggests that cytotoxic sodium influx is a significant cell death mechanism in GM. Here the levels of cell death have been manipulated to behave like those in

alternative locations (WM), through the removal of sodium and CCC inhibition. The difference seen in the involvement of CCCs may be due to differing expression levels of these transporters between regions. There is widespread expression of KCCs and NKCC1. Generally, the astrocyte expression of NKCC1 peaks at approximately P21 and the level is constant throughout adulthood, this is so for regions including cortex, corpus callosum and hippocampus (Yan, Dempsey & Sun, 2001a). However, the authors suggested that there may be lower expression levels in the hippocampus compared to other regions. There is evidence to indicate that during ischaemia CCCs remain active and there is an increased expression of NKCC1 (Yan, Dempsey & Sun, 2001b). Therefore in cells with a higher tolerance to ischaemia the transporters will function to regain ionic balance and so the inhibition of the transporters will result in detrimental injury to cells.

The use of sodium free aCSF does not only prevent the action of CCCs but inhibits other sodium transporters such as NHE, NCX and NKA. These transporters have also been implicated in ischaemic injury. In NHE null mice, astrocytes showed increased tolerance to ischaemic injury (Kintner *et al.*, 2004). The inhibition of NCX reverse activity was found to attenuate ischaemic astrocyte injury (Matsuda *et al.*, 2001). Even though there is astrocyte expression of NKA, during ischaemia it is unable to function (Pimentel *et al.*, 2013). The NHE and NCX are involved in the dysregulation of ion homeostasis during ischaemic insult (Boscia *et al.*, 2016). It is possible that one of these transporters has a greater effect on astrocyte cell death, however further investigation into this is required. Alternatively, cytotoxic influx may occur through different, as yet unknown channels and may occur through the entry of a different ion entirely. Sodium is not the only ion which has been implicated in

cell swelling. Increases in extracellular potassium have been found to trigger cell swelling, most likely via NKCC1 but also other transporters (Su *et al.*, 2002; Su, Kintner & Sun, 2002).

Overall this chapter has determined that in DG, astrocyte ischaemic cell death is caused by cytotoxic influx of sodium. Whereas in CC, CCCs appear to have a beneficial role during ischaemia and cell death is not the result of cytotoxic sodium influx but by another mechanism. Further investigation is required into the role of cytotoxic ion influx in CC astrocyte ischaemic cell death.

CHAPTER 7

7 DISCUSSION

Ischaemic stroke is a leading cause of death and disability worldwide (WHO, 2014). There has been little change in therapeutic strategy since the development of tissue plasminogen activator (tPA) and other thrombolytic treatments (Christophe *et al.*, 2017; National Institute of Neurological & Stroke rt, 1995). The nature of ischaemic injury means that prophylactic treatments would be difficult to administer and so the emphasis is on enabling fast recovery and the repair of damaged tissue.

For many years ischaemia research has focussed on the effect that the injury has on neurons, even though all CNS cell types are affected by ischaemic insult. Recently, the effect of ischaemia on glial cells has been investigated, this has been triggered by the discovery of the important role that glial cells have in the CNS. Oligodendrocytes are required to myelinate neuronal axons, allowing fast signal conduction to occur, and to metabolically support axons (Morrison, Lee & Rothstein, 2013; Saab, Tzvetanova & Nave, 2013). Astrocytes have a large and varied role within the CNS, providing support both directly and indirectly to neurons. One major function of astrocytes is the homeostatic maintenance of the ECS and ionic gradients (Bushong *et al.*, 2002; Deitmer & Rose, 1996; Rothstein *et al.*, 1996; Yao *et al.*, 2008), both of which are severely disrupted during ischaemic insult.

This thesis aimed to determine whether astrocyte tolerance to acute ischaemia varied between astrocyte populations located in different regions in the mature CNS. Once the existence of regional astrocyte sensitivity to OGD was established, the mechanism behind the differences in tolerance was investigated. The mechanisms examined were based upon previous work by the

241

group and included the role of glycogen, the involvement of GluRs and sodium influx, the results of which are discussed below.

Regional sensitivity to ischaemic injury has been previously established in neuronal populations (Pulsinelli, Brierley & Plum, 1982). This shows the existence of CNS regional differences to injury and so would suggest that astrocyte populations may also display regional differences to injury. This thesis has shown that astrocyte populations also have different sensitivities to ischaemia depending on their physical location (figure 3.16). It was determined that WM astrocytes were generally more tolerant to OGD than GM astrocytes, which confirms and agrees with findings in the literature (Lukaszevicz *et al.*, 2002; Xu, Sapolsky & Giffard, 2001). Variation in sensitivity to ischaemia was observed between WM astrocyte populations. The DG was found to contain the most sensitive astrocytes whereas the most tolerant were in the CC (figures 3.16 and 3.17). Investigation into the sensitivity of neonatal (P10) astrocytes found that they expressed a similar pattern of tolerance to the adult cells. This indicates that neonatal astrocytes also show regional sensitivity to OGD and this phenomenon is not restricted to adult cells.

Previous studies have found that immature oligodendroglia are very sensitive to ischaemic injury (Salter & Fern, 2005; Salter & Fern, 2008). However, in this work it has been determined that mature oligodendrocytes cell bodies in the adult CNS are very tolerant to acute ischaemic injury (figure 3.22), which is contrary to the view taken in the literature. Studies that have reported oligodendrocyte sensitivity examine cell death after OGD and long periods of reperfusion. Cell death occurs after the re-introduction of physiological conditions, widespread oligodendrocyte cell death has been reported nine hours after ischaemic insult (Mifsud *et al.*, 2014). The evidence in the literature

suggests that the majority of ischaemic oligodendrocyte cell death may be due to sensitivity to reperfusion injury and the production of ROS and subsequent oxidative stress (Juurlink & Sweeney, 1997). These findings also illustrate that astrocytes are much more sensitive to insult than oligodendrocytes (figure 3.23). During this work the criteria used to determine oligodendrocyte cell death was the same as for astrocytes. Using this method cell death was not seen, however this did not account for any damage that may have occurred to oligodendrocyte processes. The effect of ischaemia and other diseases on oligodendrocyte processes and myelin is currently being investigated by the group and others such as the Stys group.

The mechanisms behind the observed regional differences in astrocyte sensitivity to ischaemia were then investigated, beginning with the role of glycogen. Astrocytes contain the major glycogen stores in the brain and these stores can be utilized during times of decreased energy supply or high neuronal activity. Glycogen has been found to be involved in many processes including memory consolidation (Gibbs, Anderson & Hertz, 2006). The breakdown of glycogen results in the production of lactate which may be exported as a possible metabolite source for neurons (Pellerin *et al.*, 1998). Previous work has found that intact glycogen stores conferred tolerance to astrocytes during ischaemic insult in neonatal (P0-2) optic nerves (Fern, 2015), suggesting that these stores may have a prominent role in protecting astrocytes during insult.

This work has confirmed that the presence of large molecule glycogen stores provides astrocyte resistance to OGD (chapter 4). The inhibition of glycogen stores increased astrocyte cell death in CC. The lack of access to glycogen stores caused CC astrocytes to become more sensitive to ischaemic injury as cell death was increased during the OGD period. This suggests that

during ischaemia CC astrocytes are able to metabolise glycogen for a limited time before the cells are affected by OGD.

Investigation into glycogen content found that DG astrocytes contained higher levels of glycogen than CC astrocytes (figure 4.18).This finding agrees with the literature, where higher levels of glycogen in the DG have been found by Oe *et al* (2016) and suggests that glycogen stores are important and necessary to this region. Although the DG contained higher levels of glycogen this did not confer resistance or protection from ischaemic injury. This may be due to an inability to utilize the glycogen stores before cell death occurs as astrocytes in this regions are very sensitive to insult. The hippocampus is a region of high neuronal activity that requires vast amounts of energy, a proportion of this demand is met by the utilization of glycogen stores. It has also been discovered that there are times when glycogen is the preferred substrate, such as the synthesis of glutamate precursors (Gibbs *et al.*, 2007).

The inhibition of glycogen stores had no effect on oligodendrocyte cell death, which suggests that astrocyte glycogen does not have a role in oligodendrocyte tolerance to ischaemia. The death of astrocytes does not appear to affect oligodendrocytes, showing that astrocyte sensitivity to ischaemia does not affect oligodendrocytes. This also indicates that there are different mechanisms of cell death for astrocytes and oligodendrocytes.

Next the role of glutamate receptors as a potential mechanism of astrocyte cell death was investigated. Glutamate and glutamate receptors (GluRs) are responsible for ischaemia induced neuronal cell death via the process of excitotoxicity (Coyle *et al.*, 1981; Lucas & Newhouse, 1957; Pulsinelli, Sarokin & Buchan, 1993). It is widely accepted that astrocytes are resistant to excitotoxicity and so ischaemic astrocyte cell death must be caused via a

separate mechanism. However, oligodendrocytes are susceptible to excitotoxicity, which triggers cytotoxic calcium influx. It has been determined that different glutamate receptors may mediate injury for processes and cell soma (Salter & Fern, 2005). NMDA receptors were found to contribute to oligodendrocyte process damage, whereas AMPA receptors were found to be expressed on cell somas and have been implicated in cell body injury (Salter & Fern, 2005). This work partly informed the investigation into the role of glutamate receptors in OGD induced astrocyte cell death.

Here it has been established that ischaemia induced cell death in adult astrocytes occurs in a calcium independent manner. When external calcium was removed, the amount OGD induced cell death was increased in CC and the rate of cell death was increased in both regions (figures 5.1 and 5.2). Thus, suggesting that calcium influx, as a result of excitotoxicity, does not cause ischaemic astrocyte cell death. Although we have shown that external calcium is not required for OGD induced astrocyte death, it cannot be dismissed that calcium release from internal stores may have a role in ischaemic astrocyte death. The increase in astrocyte death caused by calcium removal may also have been due to the fact that reduced calcium conditions are detrimental to cells. This has been previously reported by Thomas *et al* (2004) and Salter and Fern (2008).

Investigation into the role of GluRs revealed that inhibition of NMDA receptors caused increased cell death, suggesting a role for activated AMPA receptors in astrocyte cell death (figure 5.8).It has been suggested that NMDA receptors are involved in cell survival signalling (Ikonomidou, Stefovska & Turski, 2000; Papadia *et al.*, 2005; Soriano & Hardingham, 2007; Tashiro *et al.*, 2006) and so inhibition of these receptors may prevent these signals, thereby

increasing astrocyte death. The inhibition of GluRs in conjunction with cobalt staining illustrated that cations are able to enter cells via activated GluRs and that this provides a route for cytotoxic ion influx (figure 5.11). Ischaemia induced cell death may occur via cytotoxic influx of ions, just not by the influx of external calcium. GluR pores are permeable to different ions and those expressed by glia have been found to have low permeability to calcium and have been found to be permeable to other ions such as sodium (Palygin *et al.*, 2010).

The final mechanism of ischaemia induced astrocyte cell death to be investigated was the role of sodium. Under physiological conditions increases in intracellular sodium cause astrocyte swelling. These normal increases in cell volume can be corrected via regulated volume decrease (Brookes, 2005). During ischaemia, cytotoxic cell swelling is a prominent event, leading to extensive astrocyte cell death. Previous work had suggested that during ischaemia, astrocyte injury was mediated by sodium influx in P10 ON (Thomas *et al.*, 2004). Here we have shown that sodium free conditions were protective for DG astrocytes but were not beneficial for the CC population (figures 6.3 and 6.4). These results indicate that for GM astrocyte sodium mediated cell death is an important mechanism.

Investigation into the role of the CCCs, specifically NKCC1 and KCC found that the roles for these transporters varied between the CC and DG. Individually, it would appear that these transporters have a somewhat protective role for CC astrocytes, as their inhibition increased cell death. However, this finding is contrary to what has previously been shown, although in other work the focus was reducing the size of infarct and not cell death such as Su *et al* (2002a). Thomas *et al* (2004) did investigate astrocyte death, however this was only in neonatal optic nerve. The only protective effect on DG astrocytes was seen

when all CCCs were inhibited, which decreased cell death (figure 6.13). These results suggest that whilst there is a role for CCCs in DG astrocyte cell death, that NKCC1 and KCC may not be the only transporters involved. Their inhibition did not prevent cell death to the same extent as sodium free conditions, indicating that other sodium channels and transporters could contribute to sodium influx. The difference seen between the regions may be due to variation in expression levels across regions. Yan *et al* (2001 a and b) suggested there is lower NKCC1 expression in the hippocampus. Cytotoxic sodium influx may also occur via over-activated GluRs which show permeability to a variety of ions.

Injury in the CC may be due to increases in a different ion such as potassium or that other transporters are involved in cytotoxic ion influx such as NHE and NCX both of which can also function in a reverse mode. It is possible that ischaemia induced astrocyte cell death occurs as the result of a different mechanism such as acidification. Astrocyte acidosis is thought to arise from accumulation of lactate production from the anaerobic glycolysis of glycogen (Verkhratsky & Parpura, 2015).

7.1 Final Conclusions

Overall this work has shown that different mature astrocyte populations display different sensitivities to ischaemic insult depending on their physical location. It was determined that GM astrocytes are more sensitive to injury than WM astrocytes. Significant variation was also observed within the WM astrocyte populations. The evidence gathered regarding astrocyte sensitivity to ischaemia agrees with what has been shown in the literature. Here it has also been established that mature oligodendrocytes are tolerant to acute ischaemic insult, although their processes may show more sensitivity to injury. Ischaemic infarcts

involve all cell types and often affect multiple regions and so by understanding how these cells react to injury may allow the development of new therapeutic strategies.

Investigation into three possible cell death mechanisms has found significant differences between regions. The presence of glycogen had a greater protective effect in CC astrocytes compared to DG cells. In both regions OGD induced astrocyte cell death occurs independently of calcium. Astrocytes in both regions displayed sensitivity to cytotoxic ion influx via AMPA receptors. Astrocyte cell death in the DG is mediated by sodium influx, however it is unknown through which transporters sodium influx occurs. Although it has been confirmed that cation entry can occur through activated glutamate receptors. Sodium does not mediate ischaemic astrocyte death in CC and cell death in this region may be the result of cytotoxic influx of a different ion, however CCCs were found to have a beneficial role during ischaemia.

The investigation into the role of glycogen stores has found that glycogen has an important role in the protection of CC astrocytes from ischaemic insult, however the increased levels of glycogen seen in DG did not confer protection to DG astrocytes. The regional variations in glycogen levels seen here agree with findings from Oe *et al* (2016). It is possible that CC astrocytes are able to metabolise glycogen for a limited time before the consequences of OGD fully take effect. The potential use of glycogen by astrocytes during insult requires further investigation to understand how glycogen attenuates injury and ultimately protects cells.

Currently the field is analysing transcriptomes and proteomes to determine differences in expression between physiological and ischaemic states. Changes in protein expression may provide clues for the mechanism of cell death or

highlight targets for developing treatments against ischaemic cell death. A recent study by Rakers *et al* (2019) has found an increase in STAT3 during ischaemia, which is involved in triggering apoptosis. The absence of STAT3 caused a reduction in stroke volume and prevented apoptosis (Rakers *et al.*, 2019). This study is also part of the work being carried out into the prevention of astrocyte programmed cell death, with a focus on death signalling pathways during ischaemia. Other pathways that are being investigated are the NF-κB signalling pathway (Zhang *et al.*, 2018), p38-MAPK signalling (Zhang *et al.*, 2019) and phospholipase C pathway (Roque, Mendes-Oliveira & Baltazar, 2019), by preventing these pathways cell death was reduced The inhibition of AQP4 and connexin hemi-channels has been shown to attenuate cell death (Zheng *et al.*, 2019) and protect against reperfusion injury (Chen *et al.*, 2018), the research focus being ion and water movement. Similar to the work in this thesis on CCCs, recently a role for transient receptor potential (TRP) channels in stroke has emerged. These channels are non-specific cation channels which have permeability to calcium and sodium (Gees, Colsoul & Nilius, 2010). TRP channels have been found to be involved in apoptosis (Chen *et al.*, 2017) and can determine the size of ischaemic infarct (Miyanohara *et al.*, 2015).

This work has indicated that CC astrocytes benefit from having access to glycogen stores, functioning NMDA receptors and CCCs. These conditions enable CC astrocytes to show tolerance to ischaemia. Whereas, DG astrocytes show tolerance to insult in the absence of sodium and access to large glycogen stores did not enable cells to survive ischaemia. Investigation into the role of glutamate receptors in astrocyte injury has found that ischaemia induced astrocyte death may be in part mediated by AMPA receptors, providing insight into ischaemic cell death. This mechanism of cell death may be similar to the

oligodendrocyte soma injury mechanism suggested by Salter and Fern (2005). These findings contribute to our knowledge of potential necrotic astrocyte death mechanisms induced by ischaemia. The discovery of how ischaemic cell death occurs may help to develop treatments which can then prevent cell death, which is also being investigated via cell death signalling pathways.

7.2 FUTURE WORK

In regards to the work into astrocyte sensitivity it would be interesting to expand this into other adult brain regions and build a map of astrocyte sensitivity to acute ischaemic insult. Further investigation into neonate regional astrocyte sensitivity would reveal whether the pattern of sensitivity is the same as for the adult astrocytes. Differences in sensitivity may show the presence of alternative cell death mechanisms and age-related changes to astrocytes. To ensure astrocyte cell death is occurring immunofluorescence staining for the presence of cell death factors such as caspases could also be carried out.

To confirm findings of adult astrocyte sensitivity, the experiment could be transferred to an *in vivo* model. The use of a focal model of ischaemia would also allow investigation into the effect of ischaemia on penumbral astrocytes. This could be used to observe any potential regional differences between this population of astrocytes. The effect of astrocyte cell death on neuronal function and survival

The role of glycogen during acute ischaemia could also be expanded by investigating more regions. It would also be interesting to establish whether glycogen store block effects neonatal astrocytes to the same extent as in adult astrocytes. During this work IA (sodium iodoacetate) was only used to prevent access to glycogen stores in astrocytes, it would be useful to repeat this but see

if there is an effect on oligodendrocytes. The ability to access glycogen stores effects astrocyte survival, it would be useful to determine whether these stores also have an effect on neuronal survival.

Further work is required to fully establish the role of cytotoxic ion influx in acute ischaemic injury. This could be achieved by developing a co-staining method to determine the role and location of AMPA receptors. The potential role of other sodium transporters needs to be determined such as NHE and NBC; as well as the possible role of other ions in cytotoxic influx such as potassium. Recently TRP channels have been implicated in ischaemia and have been found to be expressed by glial cells. Using our model of ischaemia it would be interesting to inhibit these channels and observe the effect on ischaemic astrocyte cell death.

8 REFERENCES

Aboul-Enein, F., Rauschka, H., Kornek, B., Stadelmann, C., Stefferl, A., Bruck, W., Lucchinetti, C., Schmidbauer, M., Jellinger, K. & Lassmann, H. (2003) 'Preferential loss of myelin-associated glycoprotein reflects hypoxia-like white matter damage in stroke and inflammatory brain diseases'. *J Neuropathol Exp Neurol*, 62 (1), pp. 25-33.

Albuquerque, C., Engelman, H. S., Lww, J. C. & MacDermott, A. B. (2001) 'Detection of Neurons Expressing Calcium-Permeable AMPA Receptors Using Kainate- Induced Cobalt Uptake', in Lopatin, A. and Nichols, C.G. (eds.) *Methods in Pharmacology and Toxicology. Ion Channel Localization.* Totowa, NJ: Humana Press Inc, pp. 297-309.

Allaman, I., Belanger, M. & Magistretti, P. J. (2011) 'Astrocyte-neuron metabolic relationships: for better and for worse'. *Trends Neurosci*, 34 (2), pp. 76-87.

Allen, N. J., Bennett, M. L., Foo, L. C., Wang, G. X., Chakraborty, C., Smith, S. J. & Barres, B. A. (2012) 'Astrocyte glypicans 4 and 6 promote formation of excitatory synapses via GluA1 AMPA receptors'. *Nature*, 486 (7403), pp. 410-414.

Alvarez-Maubecin, V., Garcia-Hernandez, F., Williams, J. T. & Van Bockstaele, E. J. (2000) 'Functional coupling between neurons and glia'. *J Neurosci*, 20 (11), pp. 4091-4098.

Aoyama, K., Burns, D. M., Suh, S. W., Garnier, P., Matsumori, Y., Shiina, H. & Swanson, R. A. (2005) 'Acidosis causes endoplasmic reticulum stress and caspase-12-mediated astrocyte death'. *J Cereb Blood Flow Metab*, 25 (3), pp. 358-370.

Araque, A., Carmignoto, G. & Haydon, P. G. (2001) 'Dynamic signaling between astrocytes and neurons'. *Annu Rev Physiol*, 63 pp. 795-813.

Araque, A., Parpura, V., Sanzgiri, R. P. & Haydon, P. G. (1999) 'Tripartite synapses: glia, the unacknowledged partner'. *Trends Neurosci*, 22 (5), pp. 208-215.

Astrup, J., Siesjö, B. K. & Symon, L. (1981) 'Thresholds in cerebral ischemia - the ischemic penumbra'. *Stroke*, 12 (6), pp. 723-725.

Astrup, J., Sørensen, P. M. & Sørensen, H. R. (1981) 'Oxygen and glucose consumption related to Na+-K+ transport in canine brain'. *Stroke*, 12 (6), pp. 726-730.

Aurousseau, M. R., Osswald, I. K. & Bowie, D. (2012) 'Thinking of Co(2)(+)-staining explant tissue or cultured cells? How to make it reliable and specific'. *Eur J Neurosci*, 35 (8), pp. 1201-1207.

Azarias, G., Perreten, H., Lengacher, S., Poburko, D., Demaurex, N., Magistretti, P. J. & Chatton, J. Y. (2011) 'Glutamate transport decreases mitochondrial pH and modulates oxidative metabolism in astrocytes'. *J Neurosci*, 31 (10), pp. 3550-3559.

Bachoo, R. M., Kim, R. S., Ligon, K. L., Maher, E. A., Brennan, C., Billings, N., Chan, S., Li, C., Rowitch, D. H., Wong, W. H. & DePinho, R. A. (2004) 'Molecular diversity of

astrocytes with implications for neurological disorders'. *Proc Natl Acad Sci U S A*, 101 (22), pp. 8384-8389.

Bandeira, F., Lent, R. & Herculano-Houzel, S. (2009) 'Changing numbers of neuronal and non-neuronal cells underlie postnatal brain growth in the rat'. *Proc Natl Acad Sci U S A*, 106 (33), pp. 14108-14113.

Barres, B. A. (2008) 'The mystery and magic of glia: a perspective on their roles in health and disease'. *Neuron*, 60 (3), pp. 430-440.

Barreto, G. E., Sun, X., Xu, L. & Giffard, R. G. (2011) 'Astrocyte proliferation following stroke in the mouse depends on distance from the infarct'. *PLoS One*, 6 (11), pp. e27881.

Benjamin, A. M. (1987) 'Influence of Na+, K+, and Ca2+ on glutamine synthesis and distribution in rat brain cortex slices: a possible linkage of glutamine synthetase with cerebral transport processes and energetics in the astrocytes'. *J Neurochem*, 48 (4), pp. 1157-1164.

Bergersen, L., Rafiki, A. & Ottersen, O. P. (2002) 'Immunogold cytochemistry identifies specialized membrane domains for monocarboxylate transport in the central nervous system'. *Neurochem Res*, 27 (1-2), pp. 89-96.

Bergersen, L., Waerhaug, O., Helm, J., Thomas, M., Laake, P., Davies, A. J., Wilson, M. C., Halestrap, A. P. & Ottersen, O. P. (2001) 'A novel postsynaptic density protein: the monocarboxylate transporter MCT2 is co-localized with delta-glutamate receptors in postsynaptic densities of parallel fiber-Purkinje cell synapses'. *Exp Brain Res*, 136 (4), pp. 523-534.

Berkhemer, O. A., Fransen, P. S., Beumer, D., van den Berg, L. A., Lingsma, H. F., Yoo, A. J., Schonewille, W. J., Vos, J. A., Nederkoorn, P. J., Wermer, M. J., van Walderveen, M. A., Staals, J., Hofmeijer, J., van Oostayen, J. A., Lycklama a Nijeholt, G. J., Boiten, J., Brouwer, P. A., Emmer, B. J., de Bruijn, S. F., van Dijk, L. C., Kappelle, L. J., Lo, R. H., van Dijk, E. J., de Vries, J., de Kort, P. L., van Rooij, W. J., van den Berg, J. S., van Hasselt, B. A., Aerden, L. A., Dallinga, R. J., Visser, M. C., Bot, J. C., Vroomen, P. C., Eshghi, O., Schreuder, T. H., Heijboer, R. J., Keizer, K., Tielbeek, A. V., den Hertog, H. M., Gerrits, D. G., van den Berg-Vos, R. M., Karas, G. B., Steyerberg, E. W., Flach, H. Z., Marquering, H. A., Sprengers, M. E., Jenniskens, S. F., Beenen, L. F., van den Berg, R., Koudstaal, P. J., van Zwam, W. H., Roos, Y. B., van der Lugt, A., van Oostenbrugge, R. J., Majoie, C. B., Dippel, D. W. & Investigators, M. C. (2015) 'A randomized trial of intraarterial treatment for acute ischemic stroke'. *N Engl J Med*, 372 (1), pp. 11-20.

Bernardinelli, Y., Azarias, G. & Chatton, J. Y. (2006) 'In situ fluorescence imaging of glutamate-evoked mitochondrial Na+ responses in astrocytes'. *Glia*, 54 (5), pp. 460-470.

Bernardinelli, Y., Magistretti, P. J. & Chatton, J. Y. (2004) 'Astrocytes generate Na+-mediated metabolic waves'. *Proc Natl Acad Sci U S A*, 101 (41), pp. 14937-14942.

Berthet, C., Lei, H., Thevenet, J., Gruetter, R., Magistretti, P. J. & Hirt, L. (2009) 'Neuroprotective role of lactate after cerebral ischemia'. *J Cereb Blood Flow Metab*, 29 (11), pp. 1780-1789.

Bhattacharjee, A. & Kaczmarek, L. K. (2005) 'For K+ channels, Na+ is the new Ca2+'. *Trends Neurosci*, 28 (8), pp. 422-428.

Black, J. A., Waxman, S. G., Friedman, B., Elmer, L. W. & Angelides, K. J. (1989) 'Sodium channels in astrocytes of rat optic nerve in situ: immuno-electron microscopic studies'. *Glia*, 2 (5), pp. 353-369.

Blumenstein, Y., Maximyuk, O. P., Lozovaya, N., Yatsenko, N. M., Kanevsky, N., Krishtal, O. & Dascal, N. (2004) 'Intracellular Na+ inhibits voltage-dependent N-type Ca2+ channels by a G protein betagamma subunit-dependent mechanism'. *J Physiol*, 556 (Pt 1), pp. 121-134.

Boscia, F., Begum, G., Pignataro, G., Sirabella, R., Cuomo, O., Casamassa, A., Sun, D. & Annunziato, L. (2016) 'Glial Na(+) -dependent ion transporters in pathophysiological conditions'. *Glia*, 64 (10), pp. 1677-1697.

Bowman, C. L. & Kimelberg, H. K. (1984) 'Excitatory amino acids directly depolarize rat brain astrocytes in primary culture'. *Nature*, 311 (5987), pp. 656-659.

Bozzo, L., Puyal, J. & Chatton, J. Y. (2013) 'Lactate modulates the activity of primary cortical neurons through a receptor-mediated pathway'. *PLoS One*, 8 (8), pp. e71721.

Bradl, M. & Lassmann, H. (2010) 'Oligodendrocytes: biology and pathology'. *Acta Neuropathol*, 119 (1), pp. 37-53.

Brinkmann, B. G., Agarwal, A., Sereda, M. W., Garratt, A. N., Muller, T., Wende, H., Stassart, R. M., Nawaz, S., Humml, C., Velanac, V., Radyushkin, K., Goebbels, S., Fischer, T. M., Franklin, R. J., Lai, C., Ehrenreich, H., Birchmeier, C., Schwab, M. H. & Nave, K. A. (2008) 'Neuregulin-1/ErbB signaling serves distinct functions in myelination of the peripheral and central nervous system'. *Neuron*, 59 (4), pp. 581-595.

Brookes, N. (2005) 'Mechanisms of Solute Transport in Glia.', in Kettenmann, H. and Ransom, B. (eds.) *Neuroglia.* 2nd edn.: Oxford University Press, pp. 163-176.

Brown, A. M. & Ransom, B. R. (2007) 'Astrocyte glycogen and brain energy metabolism'. *Glia*, 55 (12), pp. 1263-1271.

Brown, A. M., Sickmann, H. M., Fosgerau, K., Lund, T. M., Schousboe, A., Waagepetersen, H. S. & Ransom, B. R. (2005) 'Astrocyte glycogen metabolism is required for neural activity during aglycemia or intense stimulation in mouse white matter'. *J Neurosci Res*, 79 (1-2), pp. 74-80.

Brown, A. M., Tekkok, S. B. & Ransom, B. R. (2003) 'Glycogen regulation and functional role in mouse white matter'. *J Physiol*, 549 (Pt 2), pp. 501-512.

Bunge, R. P. (1968) 'Glial cells and the central myelin sheath'. *Physiol Rev*, 48 (1), pp. 197-251.

Burnashev, N. (1996) 'Calcium permeability of glutamate-gated channels in the central nervous system'. *Curr Opin Neurobiol*, 6 (3), pp. 311-317.

Burnashev, N., Khodorova, A., Jonas, P., Helm, P. J., Wisden, W., Monyer, H., Seeburg, P. H. & Sakmann, B. (1992) 'Calcium-permeable AMPA-kainate receptors in fusiform cerebellar glial cells'. *Science*, 256 (5063), pp. 1566-1570.

Bush, T. G., Puvanachandra, N., Horner, C. H., Polito, A., Ostenfeld, T., Svendsen, C. N., Mucke, L., Johnson, M. H. & Sofroniew, M. V. (1999) 'Leukocyte infiltration, neuronal degeneration, and neurite outgrowth after ablation of scar-forming, reactive astrocytes in adult transgenic mice'. *Neuron*, 23 (2), pp. 297-308.

Bushong, E. A., Martone, M. E., Jones, Y. Z. & Ellisman, M. H. (2002) 'Protoplasmic astrocytes in CA1 stratum radiatum occupy separate anatomical domains'. *J Neurosci*, 22 (1), pp. 183-192.

Busto, R., Globus, M. Y., Dietrich, W. D., Martinez, E., Valdes, I. & Ginsberg, M. D. (1989) 'Effect of mild hypothermia on ischemia-induced release of neurotransmitters and free fatty acids in rat brain'. *Stroke*, 20 (7), pp. 904-910.

Butt, A. M. (2011) 'ATP: a ubiquitous gliotransmitter integrating neuron-glial networks'. *Semin Cell Dev Biol*, 22 (2), pp. 205-213.

Butt, A. M., Colquhoun, K., Tutton, M. & Berry, M. (1994) 'Three-dimensional morphology of astrocytes and oligodendrocytes in the intact mouse optic nerve'. *J Neurocytol*, 23 (8), pp. 469-485.

Butt, A. M., Duncan, A. & Berry, M. (1994) 'Astrocyte associations with nodes of Ranvier: ultrastructural analysis of HRP-filled astrocytes in the mouse optic nerve'. *J Neurocytol*, 23 (8), pp. 486-499.

Butt, A. M., Duncan, A., Hornby, M. F., Kirvell, S. L., Hunter, A., Levine, J. M. & Berry, M. (1999) 'Cells expressing the NG2 antigen contact nodes of Ranvier in adult CNS white matter'. *Glia*, 26 (1), pp. 84-91.

Cao, X., Zhang, Y., Zou, L., Xiao, H., Chu, Y. & Chu, X. (2010) 'Persistent oxygen-glucose deprivation induces astrocytic death through two different pathways and calpain-mediated proteolysis of cytoskeletal proteins during astrocytic oncosis'. *Neurosci Lett*, 479 (2), pp. 118-122.

Charles, A. C., Merrill, J. E., Dirksen, E. R. & Sanderson, M. J. (1991) 'Intercellular signaling in glial cells: calcium waves and oscillations in response to mechanical stimulation and glutamate'. *Neuron*, 6 (6), pp. 983-992.

Chatton, J. Y., Marquet, P. & Magistretti, P. J. (2000) 'A quantitative analysis of L-glutamate-regulated Na+ dynamics in mouse cortical astrocytes: implications for cellular bioenergetics'. *Eur J Neurosci*, 12 (11), pp. 3843-3853.

Chen, C. J., Liao, S. L. & Kuo, J. S. (2000) 'Gliotoxic action of glutamate on cultured astrocytes'. *J Neurochem*, 75 (4), pp. 1557-1565.

Chen, H. & Sun, D. (2005) 'The role of Na-K-Cl co-transporter in cerebral ischemia'. *Neurol Res*, 27 (3), pp. 280-286.

Chen, X., Lu, M., He, X., Ma, L., Birnbaumer, L. & Liao, Y. (2017) 'TRPC3/6/7 Knockdown Protects the Brain from Cerebral Ischemia Injury via Astrocyte Apoptosis Inhibition and Effects on NF-κB Translocation'. *Mol Neurobiol*, 54 (10), pp. 7555-7566.

Chen, Y., Vartiainen, N. E., Ying, W., Chan, P. H., Koistinaho, J. & Swanson, R. A. (2001) 'Astrocytes protect neurons from nitric oxide toxicity by a glutathione-dependent mechanism'. *J Neurochem*, 77 (6), pp. 1601-1610.

Chen, Y., Wang, L., Zhang, L., Chen, B., Yang, L., Li, X., Li, Y. & Yu, H. (2018) 'Inhibition of Connexin 43 Hemichannels Alleviates Cerebral Ischemia/Reperfusion Injury via the TLR4 Signaling Pathway'. *Front Cell Neurosci*, 12 pp. 372.

Chiesa, R., Angeretti, N., Del Bo, R., Lucca, E., Munna, E. & Forloni, G. (1998) 'Extracellular calcium deprivation in astrocytes: regulation of mRNA expression and apoptosis'. *J Neurochem*, 70 (4), pp. 1474-1483.

Choi, D. W. (1987) 'Ionic dependence of glutamate neurotoxicity'. *J Neurosci*, 7 (2), pp. 369-379.

Chong, S. Y., Rosenberg, S. S., Fancy, S. P., Zhao, C., Shen, Y. A., Hahn, A. T., McGee, A. W., Xu, X., Zheng, B., Zhang, L. I., Rowitch, D. H., Franklin, R. J., Lu, Q. R. & Chan, J. R. (2012) 'Neurite outgrowth inhibitor Nogo-A establishes spatial segregation and extent of oligodendrocyte myelination'. *Proc Natl Acad Sci U S A*, 109 (4), pp. 1299-1304.

Choudhury, G. R. & Ding, S. (2015) 'Reactive astrocytes and therapeutic potential in focal ischemic stroke'. *Neurobiol Dis*,

Christophe, B. R., Mehta, S. H., Garton, A. L., Sisti, J. & Connolly, E. S., Jr. (2017) 'Current and future perspectives on the treatment of cerebral ischemia'. *Expert Opin Pharmacother*, 18 (6), pp. 573-580.

Christopherson, K. S., Ullian, E. M., Stokes, C. C., Mullowney, C. E., Hell, J. W., Agah, A., Lawler, J., Mosher, D. F., Bornstein, P. & Barres, B. A. (2005) 'Thrombospondins are astrocyte-secreted proteins that promote CNS synaptogenesis'. *Cell*, 120 (3), pp. 421-433.

Chung, C. S., Caplan, L. R., Yamamoto, Y., Chang, H. M., Lee, S. J., Song, H. J., Lee, H. S., Shin, H. K. & Yoo, K. M. (2000) 'Striatocapsular haemorrhage'. *Brain*, 123 (Pt 9) pp. 1850-1862.

Citri, A. & Malenka, R. C. (2008) 'Synaptic plasticity: multiple forms, functions, and mechanisms'. *Neuropsychopharmacology*, 33 (1), pp. 18-41.

Clark, B. A. & Barbour, B. (1997) 'Currents evoked in Bergmann glial cells by parallel fibre stimulation in rat cerebellar slices'. *J Physiol*, 502 (Pt 2) pp. 335-350.

Coles, J. A. & Tsacopoulos, M. (1981) 'Ionic and possible metabolic interactions between sensory neurones and glial cells in the retina of the honeybee drone'. *J Exp Biol*, 95 pp. 75-92.

Conti, F., DeBiasi, S., Minelli, A. & Melone, M. (1996) 'Expression of NR1 and NR2A/B subunits of the NMDA receptor in cortical astrocytes'. *Glia*, 17 (3), pp. 254-258.

Cornell-Bell, A. H., Finkbeiner, S. M., Cooper, M. S. & Smith, S. J. (1990) 'Glutamate induces calcium waves in cultured astrocytes: long-range glial signaling'. *Science*, 247 (4941), pp. 470-473.

Cotrina, M. L., Kang, J., Lin, J. H., Bueno, E., Hansen, T. W., He, L., Liu, Y. & Nedergaard, M. (1998) 'Astrocytic gap junctions remain open during ischemic conditions'. *J Neurosci*, 18 (7), pp. 2520-2537.

Coyle, J. T., Bird, S. J., Evans, R. H., Gulley, R. L., Nadler, J. V., Nicklas, W. J. & Olney, J. W. (1981) 'Excitatory amino acid neurotoxins: selectivity, specificity, and mechanisms of action. Based on an NRP one-day conference held June 30, 1980'. *Neurosci Res Program Bull*, 19 (4), pp. 1-427.

Dani, J. W., Chernjavsky, A. & Smith, S. J. (1992) 'Neuronal activity triggers calcium waves in hippocampal astrocyte networks'. *Neuron*, 8 (3), pp. 429-440.

David, J. C., Yamada, K. A., Bagwe, M. R. & Goldberg, M. P. (1996) 'AMPA receptor activation is rapidly toxic to cortical astrocytes when desensitization is blocked'. *J Neurosci*, 16 (1), pp. 200-209.

Deitmer, J. W., Bröer, A. & Bröer, S. (2003) 'Glutamine efflux from astrocytes is mediated by multiple pathways'. *J Neurochem*, 87 (1), pp. 127-135.

Deitmer, J. W. & Rose, C. R. (1996) 'pH regulation and proton signalling by glial cells'. *Prog Neurobiol*, 48 (2), pp. 73-103.

Deitmer, J. W. & Rose, C. R. (2010) 'Ion changes and signalling in perisynaptic glia'. *Brain Res Rev*, 63 (1-2), pp. 113-129.

Deneen, B., Ho, R., Lukaszewicz, A., Hochstim, C. J., Gronostajski, R. M. & Anderson, D. J. (2006) 'The transcription factor NFIA controls the onset of gliogenesis in the developing spinal cord'. *Neuron*, 52 (6), pp. 953-968.

Dermietzel, R., Hertberg, E. L., Kessler, J. A. & Spray, D. C. (1991) 'Gap junctions between cultured astrocytes: immunocytochemical, molecular, and electrophysiological analysis'. *J Neurosci*, 11 (5), pp. 1421-1432.

Dewar, D., Underhill, S. M. & Goldberg, M. P. (2003) 'Oligodendrocytes and ischemic brain injury'. *J Cereb Blood Flow Metab*, 23 (3), pp. 263-274.

Dienel, G. A. & Cruz, N. F. (2003) 'Neighborly interactions of metabolically-activated astrocytes in vivo'. *Neurochem Int*, 43 (4-5), pp. 339-354.

Dinuzzo, M., Mangia, S., Maraviglia, B. & Giove, F. (2012) 'The role of astrocytic glycogen in supporting the energetics of neuronal activity'. *Neurochem Res*, 37 (11), pp. 2432-2438.

Djukic, B., Casper, K. B., Philpot, B. D., Chin, L. S. & McCarthy, K. D. (2007) 'Conditional knock-out of Kir4.1 leads to glial membrane depolarization, inhibition of potassium and glutamate uptake, and enhanced short-term synaptic potentiation'. *J Neurosci*, 27 (42), pp. 11354-11365.

Domercq, M., Perez-Samartin, A., Aparicio, D., Alberdi, E., Pampliega, O. & Matute, C. (2010) 'P2X7 receptors mediate ischemic damage to oligodendrocytes'. *Glia*, 58 (6), pp. 730-740.

Doyle, S., Hansen, D. B., Vella, J., Bond, P., Harper, G., Zammit, C., Valentino, M. & Fern, R. (2018) 'Vesicular glutamate release from central axons contributes to myelin damage'. *Nat Commun*, 9 (1), pp. 1032.

Dunham, P. B. & Ellory, J. C. (1981) 'Passive potassium transport in low potassium sheep red cells: dependence upon cell volume and chloride'. *J Physiol*, 318 pp. 511-530.

Dzamba, D., Honsa, P. & Anderova, M. (2013) 'NMDA Receptors in Glial Cells: Pending Questions'. *Curr Neuropharmacol*, 11 (3), pp. 250-262.

Dzamba, D., Honsa, P., Valny, M., Kriska, J., Valihrach, L., Novosadova, V., Kubista, M. & Anderova, M. (2015) 'Quantitative Analysis of Glutamate Receptors in Glial Cells from the Cortex of GFAP/EGFP Mice Following Ischemic Injury: Focus on NMDA Receptors'. *Cell Mol Neurobiol*, 35 (8), pp. 1187-1202.

Eddleston, M. & Mucke, L. (1993) 'Molecular profile of reactive astrocytes--implications for their role in neurologic disease'. *Neuroscience*, 54 (1), pp. 15-36.

Edinger, A. L. & Thompson, C. B. (2004) 'Death by design: apoptosis, necrosis and autophagy'. *Curr Opin Cell Biol*, 16 (6), pp. 663-669.

Emsley, J. G. & Macklis, J. D. (2006) 'Astroglial heterogeneity closely reflects the neuronal-defined anatomy of the adult murine CNS'. *Neuron Glia Biol*, 2 (3), pp. 175-186.

Engelhardt, S., Patkar, S. & Ogunshola, O. O. (2014) 'Cell-specific blood-brain barrier regulation in health and disease: a focus on hypoxia'. *Br J Pharmacol*, 171 (5), pp. 1210-1230.

Erecińska, M. & Silver, I. A. (1994) 'Ions and energy in mammalian brain'. *Prog Neurobiol*, 43 (1), pp. 37-71.

Faulkner, J. R., Herrmann, J. E., Woo, M. J., Tansey, K. E., Doan, N. B. & Sofroniew, M. V. (2004) 'Reactive astrocytes protect tissue and preserve function after spinal cord injury'. *J Neurosci*, 24 (9), pp. 2143-2155.

Fern, R. (1998) 'Intracellular calcium and cell death during ischemia in neonatal rat white matter astrocytes in situ'. *J Neurosci*, 18 (18), pp. 7232-7243.

Fern, R. (2015) 'Ischemic tolerance in pre-myelinated white matter: the role of astrocyte glycogen in brain pathology'. *Journal of Cerebral Blood Flow and Metabolism*, 35 (6), pp. 951-958.

Fern, R. & Moller, T. (2000) 'Rapid ischemic cell death in immature oligodendrocytes: a fatal glutamate release feedback loop'. *J Neurosci*, 20 (1), pp. 34-42.

Fern, R. F., Matute, C. & Stys, P. K. (2014) 'White Matter Injury: Ischemic and Nonischemic'. *Glia*, 62 (11), pp. 1780-1789.

Fernandez-Lopez, D., Natarajan, N., Ashwal, S. & Vexler, Z. S. (2014) 'Mechanisms of perinatal arterial ischemic stroke'. *J Cereb Blood Flow Metab*, 34 (6), pp. 921-932.

Flemmer, A. W., Gimenez, I., Dowd, B. F., Darman, R. B. & Forbush, B. (2002) 'Activation of the Na-K-Cl cotransporter NKCC1 detected with a phospho-specific antibody'. *J Biol Chem*, 277 (40), pp. 37551-37558.

Florence, C. M., Baillie, L. D. & Mulligan, S. J. (2012) 'Dynamic volume changes in astrocytes are an intrinsic phenomenon mediated by bicarbonate ion flux'. *PLoS One*, 7 (11), pp. e51124.

Funfschilling, U., Supplie, L. M., Mahad, D., Boretius, S., Saab, A. S., Edgar, J., Brinkmann, B. G., Kassmann, C. M., Tzvetanova, I. D., Mobius, W., Diaz, F., Meijer, D., Suter, U., Hamprecht, B., Sereda, M. W., Moraes, C. T., Frahm, J., Goebbels, S. & Nave, K. A. (2012) 'Glycolytic oligodendrocytes maintain myelin and long-term axonal integrity'. *Nature*, 485 (7399), pp. 517-521.

Gallo, V., Patneau, D. K., Mayer, M. L. & Vaccarino, F. M. (1994) 'Excitatory amino acid receptors in glial progenitor cells: molecular and functional properties'. *Glia*, 11 (2), pp. 94-101.

Ge, W. P., Miyawaki, A., Gage, F. H., Jan, Y. N. & Jan, L. Y. (2012) 'Local generation of glia is a major astrocyte source in postnatal cortex'. *Nature*, 484 (7394), pp. 376-380.

Gees, M., Colsoul, B. & Nilius, B. (2010) 'The role of transient receptor potential cation channels in Ca2+ signaling'. *Cold Spring Harb Perspect Biol*, 2 (10), pp. a003962.

Gibbs, M. E., Anderson, D. G. & Hertz, L. (2006) 'Inhibition of glycogenolysis in astrocytes interrupts memory consolidation in young chickens'. *Glia*, 54 (3), pp. 214-222.

Gibbs, M. E., Lloyd, H. G., Santa, T. & Hertz, L. (2007) 'Glycogen is a preferred glutamate precursor during learning in 1-day-old chick: biochemical and behavioral evidence'. *J Neurosci Res*, 85 (15), pp. 3326-3333.

Goldberg, M. P. & Choi, D. W. (1993) 'Combined oxygen and glucose deprivation in cortical cell culture: calcium-dependent and calcium-independent mechanisms of neuronal injury'. *J Neurosci*, 13 (8), pp. 3510-3524.

Gordon, G. R., Choi, H. B., Rungta, R. L., Ellis-Davies, G. C. & MacVicar, B. A. (2008) 'Brain metabolism dictates the polarity of astrocyte control over arterioles'. *Nature*, 456 (7223), pp. 745-749.

Gordon, G. R., Mulligan, S. J. & MacVicar, B. A. (2007) 'Astrocyte control of the cerebrovasculature'. *Glia*, 55 (12), pp. 1214-1221.

Goss, J. R., O'Malley, M. E., Zou, L., Styren, S. D., Kochanek, P. M. & DeKosky, S. T. (1998) 'Astrocytes are the major source of nerve growth factor upregulation following traumatic brain injury in the rat'. *Exp Neurol*, 149 (2), pp. 301-309.

Griffiths, I., Klugmann, M., Anderson, T., Yool, D., Thomson, C., Schwab, M. H., Schneider, A., Zimmermann, F., McCulloch, M., Nadon, N. & Nave, K. A. (1998) 'Axonal swellings and degeneration in mice lacking the major proteolipid of myelin'. *Science*, 280 (5369), pp. 1610-1613.

Gurer, G., Gursoy-Ozdemir, Y., Erdemli, E., Can, A. & Dalkara, T. (2009) 'Astrocytes are more resistant to focal cerebral ischemia than neurons and die by a delayed necrosis'. *Brain Pathol*, 19 (4), pp. 630-641.

Halassa, M. M., Fellin, T., Takano, H., Dong, J. H. & Haydon, P. G. (2007) 'Synaptic islands defined by the territory of a single astrocyte'. *J Neurosci*, 27 (24), pp. 6473-6477.

Hama, H., Hara, C., Yamaguchi, K. & Miyawaki, A. (2004) 'PKC signaling mediates global enhancement of excitatory synaptogenesis in neurons triggered by local contact with astrocytes'. *Neuron*, 41 (3), pp. 405-415.

Hayakawa, K., Nakano, T., Irie, K., Higuchi, S., Fujioka, M., Orito, K., Iwasaki, K., Jin, G., Lo, E. H., Mishima, K. & Fujiwara, M. (2010) 'Inhibition of reactive astrocytes with

fluorocitrate retards neurovascular remodeling and recovery after focal cerebral ischemia in mice'. *J Cereb Blood Flow Metab*, 30 (4), pp. 871-882.

Hertz, L., O'Dowd, B. S., Ng, K. T. & Gibbs, M. E. (2003) 'Reciprocal changes in forebrain contents of glycogen and of glutamate/glutamine during early memory consolidation in the day-old chick'. *Brain Res*, 994 (2), pp. 226-233.

Hertz, L. & Rothman, D. L. (2017) 'Glutamine-Glutamate Cycle Flux Is Similar in Cultured Astrocytes and Brain and Both Glutamate Production and Oxidation Are Mainly Catalyzed by Aspartate Aminotransferase'. *Biology (Basel)*, 6 (1),

Hertz, L., Xu, J., Song, D., Du, T., Li, B., Yan, E. & Peng, L. (2015) 'Astrocytic glycogenolysis: mechanisms and functions'. *Metab Brain Dis*, 30 (1), pp. 317-333.

Hirabayashi, Y. & Gotoh, Y. (2005) 'Stage-dependent fate determination of neural precursor cells in mouse forebrain'. *Neurosci Res*, 51 (4), pp. 331-336.

Hof, P. R., Pascale, E. & Magistretti, P. J. (1988) 'K+ at concentrations reached in the extracellular space during neuronal activity promotes a Ca2+-dependent glycogen hydrolysis in mouse cerebral cortex'. *J Neurosci*, 8 (6), pp. 1922-1928.

Hollmann, M., Hartley, M. & Heinemann, S. (1991) 'Ca2+ permeability of KA-AMPA--gated glutamate receptor channels depends on subunit composition'. *Science*, 252 (5007), pp. 851-853.

Hossain, M. I., Roulston, C. L. & Stapleton, D. I. (2014) 'Molecular basis of impaired glycogen metabolism during ischemic stroke and hypoxia'. *PLoS One*, 9 (5), pp. e97570.

Hulse, R. E., Winterfield, J., Kunkler, P. E. & Kraig, R. P. (2001) 'Astrocytic clasmatodendrosis in hippocampal organ culture'. *Glia*, 33 (2), pp. 169-179.

Hypothermia after Cardiac Arrest Study, G. (2002) 'Mild therapeutic hypothermia to improve the neurologic outcome after cardiac arrest'. *N Engl J Med*, 346 (8), pp. 549-556.

Ikonomidou, C., Stefovska, V. & Turski, L. (2000) 'Neuronal death enhanced by N-methyl-D-aspartate antagonists'. *Proc Natl Acad Sci U S A*, 97 (23), pp. 12885-12890.

Iliff, J. J., Wang, M., Liao, Y., Plogg, B. A., Peng, W., Gundersen, G. A., Benveniste, H., Vates, G. E., Deane, R., Goldman, S. A., Nagelhus, E. A. & Nedergaard, M. (2012) 'A paravascular pathway facilitates CSF flow through the brain parenchyma and the clearance of interstitial solutes, including amyloid β'. *Sci Transl Med*, 4 (147), pp. 147ra111.

Illarionova, N. B., Gunnarson, E., Li, Y., Brismar, H., Bondar, A., Zelenin, S. & Aperia, A. (2010) 'Functional and molecular interactions between aquaporins and Na,K-ATPase'. *Neuroscience*, 168 (4), pp. 915-925.

Innocenti, B., Parpura, V. & Haydon, P. G. (2000) 'Imaging extracellular waves of glutamate during calcium signaling in cultured astrocytes'. *J Neurosci*, 20 (5), pp. 1800-1808.

Jacobsen, C. T. & Miller, R. H. (2003) 'Control of astrocyte migration in the developing cerebral cortex'. *Dev Neurosci*, 25 (2-4), pp. 207-216.

James, G. & Butt, A. M. (2002) 'P2Y and P2X purinoceptor mediated Ca2+ signalling in glial cell pathology in the central nervous system'. *Eur J Pharmacol*, 447 (2-3), pp. 247-260.

Janzer, R. C. & Raff, M. C. (1987) 'Astrocytes induce blood-brain barrier properties in endothelial cells'. *Nature*, 325 (6101), pp. 253-257.

Jayakumar, A. R. & Norenberg, M. D. (2010) 'The Na-K-Cl Co-transporter in astrocyte swelling'. *Metab Brain Dis*, 25 (1), pp. 31-38.

Jonas, P. & Burnashev, N. (1995) 'Molecular mechanisms controlling calcium entry through AMPA-type glutamate receptor channels'. *Neuron*, 15 (5), pp. 987-990.

Jones, E. V., Bernardinelli, Y., Tse, Y. C., Chierzi, S., Wong, T. P. & Murai, K. K. (2011) 'Astrocytes control glutamate receptor levels at developing synapses through SPARC-beta-integrin interactions'. *J Neurosci*, 31 (11), pp. 4154-4165.

Juurlink, B. H. & Sweeney, M. I. (1997) 'Mechanisms that result in damage during and following cerebral ischemia'. *Neurosci Biobehav Rev*, 21 (2), pp. 121-128.

Kacem, K., Lacombe, P., Seylaz, J. & Bonvento, G. (1998) 'Structural organization of the perivascular astrocyte endfeet and their relationship with the endothelial glucose transporter: a confocal microscopy study'. *Glia*, 23 (1), pp. 1-10.

Kahle, K. T., Simard, J. M., Staley, K. J., Nahed, B. V., Jones, P. S. & Sun, D. (2009) 'Molecular mechanisms of ischemic cerebral edema: role of electroneutral ion transport'. *Physiology (Bethesda)*, 24 pp. 257-265.

Kang, P., Lee, H. K., Glasgow, S. M., Finley, M., Donti, T., Gaber, Z. B., Graham, B. H., Foster, A. E., Novitch, B. G., Gronostajski, R. M. & Deneen, B. (2012) 'Sox9 and NFIA coordinate a transcriptional regulatory cascade during the initiation of gliogenesis'. *Neuron*, 74 (1), pp. 79-94.

Karadottir, R., Cavelier, P., Bergersen, L. H. & Attwell, D. (2005) 'NMDA receptors are expressed in oligodendrocytes and activated in ischaemia'. *Nature*, 438 (7071), pp. 1162-1166.

Kessaris, N., Fogarty, M., Iannarelli, P., Grist, M., Wegner, M. & Richardson, W. D. (2006) 'Competing waves of oligodendrocytes in the forebrain and postnatal elimination of an embryonic lineage'. *Nat Neurosci*, 9 (2), pp. 173-179.

Kim, W. T., Rioult, M. G. & Cornell-Bell, A. H. (1994) 'Glutamate-induced calcium signaling in astrocytes'. *Glia*, 11 (2), pp. 173-184.

Kintner, D. B., Luo, J., Gerdts, J., Ballard, A. J., Shull, G. E. & Sun, D. (2007) 'Role of Na+-K+-Cl- cotransport and Na+/Ca2+ exchange in mitochondrial dysfunction in astrocytes following in vitro ischemia'. *Am J Physiol Cell Physiol*, 292 (3), pp. C1113-1122.

Kintner, D. B., Su, G., Lenart, B., Ballard, A. J., Meyer, J. W., Ng, L. L., Shull, G. E. & Sun, D. (2004) 'Increased tolerance to oxygen and glucose deprivation in astrocytes from Na(+)/H(+) exchanger isoform 1 null mice'. *Am J Physiol Cell Physiol*, 287 (1), pp. C12-21.

Kirino, T. (1982) 'Delayed neuronal death in the gerbil hippocampus following ischemia'. *Brain Res*, 239 (1), pp. 57-69.

Kirischuk, S., Kettenmann, H. & Verkhratsky, A. (1997) 'Na+/Ca2+ exchanger modulates kainate-triggered Ca2+ signaling in Bergmann glial cells in situ'. *FASEB J*, 11 (7), pp. 566-572.

Kirischuk, S., Kettenmann, H. & Verkhratsky, A. (2007) 'Membrane currents and cytoplasmic sodium transients generated by glutamate transport in Bergmann glial cells'. *Pflugers Arch*, 454 (2), pp. 245-252.

Kirischuk, S., Parpura, V. & Verkhratsky, A. (2012) 'Sodium dynamics: another key to astroglial excitability?'. *Trends Neurosci*, 35 (8), pp. 497-506.

Kirmse, K. & Kirischuk, S. (2006) 'Ambient GABA constrains the strength of GABAergic synapses at Cajal-Retzius cells in the developing visual cortex'. *J Neurosci*, 26 (16), pp. 4216-4227.

Krasnow, A. M. & Attwell, D. (2016) 'NMDA Receptors: Power Switches for Oligodendrocytes'. *Neuron*, 91 (1), pp. 3-5.

Kucukdereli, H., Allen, N. J., Lee, A. T., Feng, A., Ozlu, M. I., Conatser, L. M., Chakraborty, C., Workman, G., Weaver, M., Sage, E. H., Barres, B. A. & Eroglu, C. (2011) 'Control of excitatory CNS synaptogenesis by astrocyte-secreted proteins Hevin and SPARC'. *Proc Natl Acad Sci U S A*, 108 (32), pp. E440-449.

Kukley, M., Capetillo-Zarate, E. & Dietrich, D. (2007) 'Vesicular glutamate release from axons in white matter'. *Nat Neurosci*, 10 (3), pp. 311-320.

Kwon, I., Kim, E. H., del Zoppo, G. J. & Heo, J. H. (2009) 'Ultrastructural and temporal changes of the microvascular basement membrane and astrocyte interface following focal cerebral ischemia'. *J Neurosci Res*, 87 (3), pp. 668-676.

Káradóttir, R., Hamilton, N. B., Bakiri, Y. & Attwell, D. (2008) 'Spiking and nonspiking classes of oligodendrocyte precursor glia in CNS white matter'. *Nat Neurosci*, 11 (4), pp. 450-456.

Lalo, U., Pankratov, Y., Kirchhoff, F., North, R. A. & Verkhratsky, A. (2006) 'NMDA receptors mediate neuron-to-glia signaling in mouse cortical astrocytes'. *J Neurosci*, 26 (10), pp. 2673-2683.

Lalo, U., Pankratov, Y., Parpura, V. & Verkhratsky, A. (2011) 'Ionotropic receptors in neuronal-astroglial signalling: what is the role of "excitable" molecules in non-excitable cells'. *Biochim Biophys Acta*, 1813 (5), pp. 992-1002.

Langer, J., Stephan, J., Theis, M. & Rose, C. R. (2012) 'Gap junctions mediate intercellular spread of sodium between hippocampal astrocytes in situ'. *Glia*, 60 (2), pp. 239-252.

Lauritzen, K. H., Morland, C., Puchades, M., Holm-Hansen, S., Hagelin, E. M., Lauritzen, F., Attramadal, H., Storm-Mathisen, J., Gjedde, A. & Bergersen, L. H. (2014) 'Lactate receptor sites link neurotransmission, neurovascular coupling, and brain energy metabolism'. *Cereb Cortex*, 24 (10), pp. 2784-2795.

Laywell, E. D. & Steindler, D. A. (1991) 'Boundaries and wounds, glia and glycoconjugates. Cellular and molecular analyses of developmental partitions and adult brain lesions'. *Ann N Y Acad Sci*, 633 pp. 122-141.

Lee, J. M., Grabb, M. C., Zipfel, G. J. & Choi, D. W. (2000) 'Brain tissue responses to ischemia'. *J Clin Invest*, 106 (6), pp. 723-731.

Lee, S., Leach, M. K., Redmond, S. A., Chong, S. Y., Mellon, S. H., Tuck, S. J., Feng, Z. Q., Corey, J. M. & Chan, J. R. (2012a) 'A culture system to study oligodendrocyte myelination processes using engineered nanofibers'. *Nat Methods*, 9 (9), pp. 917-922.

Lee, S. H., Kim, W. T., Cornell-Bell, A. H. & Sontheimer, H. (1994) 'Astrocytes exhibit regional specificity in gap-junction coupling'. *Glia*, 11 (4), pp. 315-325.

Lee, Y., Morrison, B. M., Li, Y., Lengacher, S., Farah, M. H., Hoffman, P. N., Liu, Y., Tsingalia, A., Jin, L., Zhang, P. W., Pellerin, L., Magistretti, P. J. & Rothstein, J. D. (2012b) 'Oligodendroglia metabolically support axons and contribute to neurodegeneration'. *Nature*, 487 (7408), pp. 443-448.

Lenart, B., Kintner, D. B., Shull, G. E. & Sun, D. (2004) 'Na-K-Cl cotransporter-mediated intracellular Na+ accumulation affects Ca2+ signaling in astrocytes in an in vitro ischemic model'. *J Neurosci*, 24 (43), pp. 9585-9597.

Leuchtmann, E. A., Ratner, A. E., Vijitruth, R., Qu, Y. & McDonald, J. W. (2003) 'AMPA receptors are the major mediators of excitotoxic death in mature oligodendrocytes'. *Neurobiol Dis*, 14 (3), pp. 336-348.

Levison, S. W., de Vellis, J. & Goldman, J. E. (2005) 'Astrocyte Development', in Rao, M.S. and Jacobson, M. (eds.) *Developmental Neuobiology* 4th edn. New York: Kluwer Academic / Plenum Publishers, pp. 197-222.

Levison, S. W. & Goldman, J. E. (1993) 'Both oligodendrocytes and astrocytes develop from progenitors in the subventricular zone of postnatal rat forebrain'. *Neuron*, 10 (2), pp. 201-212.

Li, L., Lundkvist, A., Andersson, D., Wilhelmsson, U., Nagai, N., Pardo, A. C., Nodin, C., Ståhlberg, A., Aprico, K., Larsson, K., Yabe, T., Moons, L., Fotheringham, A., Davies, I., Carmeliet, P., Schwartz, J. P., Pekna, M., Kubista, M., Blomstrand, F., Maragakis, N., Nilsson, M. & Pekny, M. (2008) 'Protective role of reactive astrocytes in brain ischemia'. *J Cereb Blood Flow Metab*, 28 (3), pp. 468-481.

Liesi, P. & Silver, J. (1988) 'Is astrocyte laminin involved in axon guidance in the mammalian CNS?'. *Dev Biol*, 130 (2), pp. 774-785.

Liu, D., Smith, C. L., Barone, F. C., Ellison, J. A., Lysko, P. G., Li, K. & Simpson, I. A. (1999) 'Astrocytic demise precedes delayed neuronal death in focal ischemic rat brain'. *Brain Res Mol Brain Res*, 68 (1-2), pp. 29-41.

Liu, X., Van Vleet, T. & Schnellmann, R. G. (2004) 'The role of calpain in oncotic cell death'. *Annu Rev Pharmacol Toxicol*, 44 pp. 349-370.

Liu, Z. & Chopp, M. (2015) 'Astrocytes, therapeutic targets for neuroprotection and neurorestoration in ischemic stroke'. *Prog Neurobiol*,

Lucas, D. R. & Newhouse, J. P. (1957) 'The toxic effect of sodium L-glutamate on the inner layers of the retina'. *AMA Arch Ophthalmol*, 58 (2), pp. 193-201.

Ludwin, S. K. (1997) 'The pathobiology of the oligodendrocyte'. *J Neuropathol Exp Neurol*, 56 (2), pp. 111-124.

Lukaszevicz, A. C., Sampaïo, N., Guégan, C., Benchoua, A., Couriaud, C., Chevalier, E., Sola, B., Lacombe, P. & Onténiente, B. (2002) 'High sensitivity of protoplasmic cortical astroglia to focal ischemia'. *J Cereb Blood Flow Metab*, 22 (3), pp. 289-298.

Lundgaard, I., Luzhynskaya, A., Stockley, J. H., Wang, Z., Evans, K. A., Swire, M., Volbracht, K., Gautier, H. O., Franklin, R. J., Charles, F.-C., Attwell, D. & Karadottir, R. T. (2013) 'Neuregulin and BDNF induce a switch to NMDA receptor-dependent myelination by oligodendrocytes'. *PLoS Biol*, 11 (12), pp. e1001743.

Lynch, J. K. & Nelson, K. B. (2001) 'Epidemiology of perinatal stroke'. *Curr Opin Pediatr*, 13 (6), pp. 499-505.

Mabuchi, T., Kitagawa, K., Kuwabara, K., Takasawa, K., Ohtsuki, T., Xia, Z., Storm, D., Yanagihara, T., Hori, M. & Matsumoto, M. (2001) 'Phosphorylation of cAMP response element-binding protein in hippocampal neurons as a protective response after

exposure to glutamate in vitro and ischemia in vivo'. *J Neurosci*, 21 (23), pp. 9204-9213.

Machler, P., Wyss, M. T., Elsayed, M., Stobart, J., Gutierrez, R., von Faber-Castell, A., Kaelin, V., Zuend, M., San Martin, A., Romero-Gomez, I., Baeza-Lehnert, F., Lengacher, S., Schneider, B. L., Aebischer, P., Magistretti, P. J., Barros, L. F. & Weber, B. (2016) 'In Vivo Evidence for a Lactate Gradient from Astrocytes to Neurons'. *Cell Metab*, 23 (1), pp. 94-102.

MacVicar, B. A., Feighan, D., Brown, A. & Ransom, B. (2002) 'Intrinsic optical signals in the rat optic nerve: role for K(+) uptake via NKCC1 and swelling of astrocytes'. *Glia*, 37 (2), pp. 114-123.

Magistretti, P. J. & Allaman, I. (2018) 'Lactate in the brain: from metabolic end-product to signalling molecule'. *Nat Rev Neurosci*, 19 (4), pp. 235-249.

Mallon, B. S., Shick, H. E., Kidd, G. J. & Macklin, W. B. (2002) 'Proteolipid promoter activity distinguishes two populations of NG2-positive cells throughout neonatal cortical development'. *J Neurosci*, 22 (3), pp. 876-885.

Manley, G. T., Fujimura, M., Ma, T., Noshita, N., Filiz, F., Bollen, A. W., Chan, P. & Verkman, A. S. (2000) 'Aquaporin-4 deletion in mice reduces brain edema after acute water intoxication and ischemic stroke'. *Nat Med*, 6 (2), pp. 159-163.

Marcoux, F. W., Morawetz, R. B., Crowell, R. M., DeGirolami, U. & Halsey, J. H., Jr. (1982) 'Differential regional vulnerability in transient focal cerebral ischemia'. *Stroke*, 13 (3), pp. 339-346.

Marques, S., Zeisel, A., Codeluppi, S., van Bruggen, D., Mendanha Falcao, A., Xiao, L., Li, H., Haring, M., Hochgerner, H., Romanov, R. A., Gyllborg, D., Munoz Manchado, A., La Manno, G., Lonnerberg, P., Floriddia, E. M., Rezayee, F., Ernfors, P., Arenas, E., Hjerling-Leffler, J., Harkany, T., Richardson, W. D., Linnarsson, S. & Castelo-Branco, G. (2016) 'Oligodendrocyte heterogeneity in the mouse juvenile and adult central nervous system'. *Science*, 352 (6291), pp. 1326-1329.

Matsuda, T., Arakawa, N., Takuma, K., Kishida, Y., Kawasaki, Y., Sakaue, M., Takahashi, K., Takahashi, T., Suzuki, T., Ota, T., Hamano-Takahashi, A., Onishi, M., Tanaka, Y., Kameo, K. & Baba, A. (2001) 'SEA0400, a novel and selective inhibitor of the Na+-Ca2+ exchanger, attenuates reperfusion injury in the in vitro and in vivo cerebral ischemic models'. *J Pharmacol Exp Ther*, 298 (1), pp. 249-256.

Matsui, K., Jahr, C. E. & Rubio, M. E. (2005) 'High-concentration rapid transients of glutamate mediate neural-glial communication via ectopic release'. *J Neurosci*, 25 (33), pp. 7538-7547.

Matsui, T., Omuro, H., Liu, Y. F., Soya, M., Shima, T., McEwen, B. S. & Soya, H. (2017) 'Astrocytic glycogen-derived lactate fuels the brain during exhaustive exercise to maintain endurance capacity'. *Proc Natl Acad Sci U S A*, 114 (24), pp. 6358-6363.

Matthias, K., Kirchhoff, F., Seifert, G., Hüttmann, K., Matyash, M., Kettenmann, H. & Steinhäuser, C. (2003) 'Segregated expression of AMPA-type glutamate receptors and glutamate transporters defines distinct astrocyte populations in the mouse hippocampus'. *J Neurosci*, 23 (5), pp. 1750-1758.

Matute, C. (2006) 'Oligodendrocyte NMDA receptors: a novel therapeutic target'. *Trends Mol Med*, 12 (7), pp. 289-292.

Matute, C., Alberdi, E., Ibarretxe, G. & Sanchez-Gomez, M. V. (2002) 'Excitotoxicity in glial cells'. *Eur J Pharmacol*, 447 (2-3), pp. 239-246.

Matute, C., Domercq, M. & Sánchez-Gómez, M. V. (2006) 'Glutamate-mediated glial injury: mechanisms and clinical importance'. *Glia*, 53 (2), pp. 212-224.

Matute, C., Sánchez-Gómez, M. V., Martínez-Millán, L. & Miledi, R. (1997) 'Glutamate receptor-mediated toxicity in optic nerve oligodendrocytes'. *Proc Natl Acad Sci U S A*, 94 (16), pp. 8830-8835.

Mayer, M. L., Westbrook, G. L. & Guthrie, P. B. (1984) 'Voltage-dependent block by Mg2+ of NMDA responses in spinal cord neurones'. *Nature*, 309 (5965), pp. 261-263.

McIver, S. R., Muccigrosso, M., Gonzales, E. R., Lee, J. M., Roberts, M. S., Sands, M. S. & Goldberg, M. P. (2010) 'Oligodendrocyte degeneration and recovery after focal cerebral ischemia'. *Neuroscience*, 169 (3), pp. 1364-1375.

McKenna, M. C. (2007) 'The glutamate-glutamine cycle is not stoichiometric: fates of glutamate in brain'. *J Neurosci Res*, 85 (15), pp. 3347-3358.

McKenna, M. C. (2013) 'Glutamate pays its own way in astrocytes'. *Front Endocrinol (Lausanne)*, 4 pp. 191.

Mellergard, P., Ouyang, Y. B. & Siesjo, B. K. (1994) 'The regulation of intracellular pH is strongly dependent on extracellular pH in cultured rat astrocytes and neurons'. *Acta Neurochir Suppl (Wien)*, 60 pp. 34-37.

Mercado, A., Mount, D. B. & Gamba, G. (2004) 'Electroneutral cation-chloride cotransporters in the central nervous system'. *Neurochem Res*, 29 (1), pp. 17-25.

Meyer, N., Richter, N., Fan, Z., Siemonsmeier, G., Pivneva, T., Jordan, P., Steinhauser, C., Semtner, M., Nolte, C. & Kettenmann, H. (2018) 'Oligodendrocytes in the Mouse Corpus Callosum Maintain Axonal Function by Delivery of Glucose'. *Cell Rep*, 22 (9), pp. 2383-2394.

Michalski, J. P., Anderson, C., Beauvais, A., De Repentigny, Y. & Kothary, R. (2011) 'The proteolipid protein promoter drives expression outside of the oligodendrocyte lineage during embryonic and early postnatal development'. *PLoS One*, 6 (5), pp. e19772.

Micu, I., Jiang, Q., Coderre, E., Ridsdale, A., Zhang, L., Woulfe, J., Yin, X., Trapp, B. D., McRory, J. E., Rehak, R., Zamponi, G. W., Wang, W. & Stys, P. K. (2006) 'NMDA receptors mediate calcium accumulation in myelin during chemical ischaemia'. *Nature*, 439 (7079), pp. 988-992.

Micu, I., Plemel, J. R., Lachance, C., Proft, J., Jansen, A. J., Cummins, K., van Minnen, J. & Stys, P. K. (2016) 'The molecular physiology of the axo-myelinic synapse'. *Exp Neurol*, 276 pp. 41-50.

Middeldorp, J. & Hol, E. M. (2011) 'GFAP in health and disease'. *Prog Neurobiol*, 93 (3), pp. 421-443.

Mifsud, G., Zammit, C., Muscat, R., Di Giovanni, G. & Valentino, M. (2014) 'Oligodendrocyte pathophysiology and treatment strategies in cerebral ischemia'. *CNS Neurosci Ther*, 20 (7), pp. 603-612.

Minelli, A., Castaldo, P., Gobbi, P., Salucci, S., Magi, S. & Amoroso, S. (2007) 'Cellular and subcellular localization of Na+-Ca2+ exchanger protein isoforms, NCX1, NCX2, and NCX3 in cerebral cortex and hippocampus of adult rat'. *Cell Calcium*, 41 (3), pp. 221-234.

Minnerup, J., Sutherland, B. A., Buchan, A. M. & Kleinschnitz, C. (2012) 'Neuroprotection for stroke: current status and future perspectives'. *Int J Mol Sci*, 13 (9), pp. 11753-11772.

Miyanohara, J., Shirakawa, H., Sanpei, K., Nakagawa, T. & Kaneko, S. (2015) 'A pathophysiological role of TRPV1 in ischemic injury after transient focal cerebral ischemia in mice'. *Biochem Biophys Res Commun*, 467 (3), pp. 478-483.

Mobius, W., Patzig, J., Nave, K. A. & Werner, H. B. (2008) 'Phylogeny of proteolipid proteins: divergence, constraints, and the evolution of novel functions in myelination and neuroprotection'. *Neuron Glia Biol*, 4 (2), pp. 111-127.

Molofsky, A. V. & Deneen, B. (2015) 'Astrocyte development: A Guide for the Perplexed'. *Glia*, 63 (8), pp. 1320-1329.

Mongin, A. A., Aksentsev, S. L., Orlov, S. N., Slepko, N. G., Kozlova, M. V., Maximov, G. V. & Konev, S. V. (1994) 'Swelling-induced K+ influx in cultured primary astrocytes'. *Brain Res*, 655 (1-2), pp. 110-114.

Mongin, A. A. & Kimelberg, H. K. (2005) 'ATP regulates anion channel-mediated organic osmolyte release from cultured rat astrocytes via multiple Ca2+-sensitive mechanisms'. *Am J Physiol Cell Physiol*, 288 (1), pp. C204-213.

Morland, C., Henjum, S., Iversen, E. G., Skrede, K. K. & Hassel, B. (2007) 'Evidence for a higher glycolytic than oxidative metabolic activity in white matter of rat brain'. *Neurochem Int*, 50 (5), pp. 703-709.

Morrison, B. M., Lee, Y. & Rothstein, J. D. (2013) 'Oligodendroglia: metabolic supporters of axons'. *Trends Cell Biol*, 23 (12), pp. 644-651.

Moseley, A. E., Williams, M. T., Schaefer, T. L., Bohanan, C. S., Neumann, J. C., Behbehani, M. M., Vorhees, C. V. & Lingrel, J. B. (2007) 'Deficiency in Na,K-ATPase alpha isoform genes alters spatial learning, motor activity, and anxiety in mice'. *J Neurosci*, 27 (3), pp. 616-626.

Motulsky, H. J. (2019) 'GraphPad Statistics Guide'. [Online]. Available at: https://www.graphpad.com/guides/prism/8/statistics/index.htm (Accessed: March).

Müller, T., Grosche, J., Ohlemeyer, C. & Kettenmann, H. (1993) 'NMDA-activated currents in Bergmann glial cells'. *Neuroreport*, 4 (6), pp. 671-674.

Nagy, B., Hovhannisyan, A., Barzan, R., Chen, T. J. & Kukley, M. (2017) 'Different patterns of neuronal activity trigger distinct responses of oligodendrocyte precursor cells in the corpus callosum'. *PLoS Biol*, 15 (8), pp. e2001993.

Nakamura-Tsuruta, S., Yasuda, M., Nakamura, T., Shinoda, E., Furuyashiki, T., Kakutani, R., Takata, H., Kato, Y. & Ashida, H. (2012) 'Comparative analysis of carbohydrate-binding specificities of two anti-glycogen monoclonal antibodies using ELISA and surface plasmon resonance'. *Carbohydr Res*, 350 pp. 49-54.

National Institute of Neurological, D. & Stroke rt, P. A. S. S. G. (1995) 'Tissue plasminogen activator for acute ischemic stroke'. *N Engl J Med*, 333 (24), pp. 1581-1587.

Naylor, E., Aillon, D. V., Barrett, B. S., Wilson, G. S., Johnson, D. A., Harmon, H. P., Gabbert, S. & Petillo, P. A. (2012) 'Lactate as a biomarker for sleep'. *Sleep*, 35 (9), pp. 1209-1222.

Nedergaard, M., Ransom, B. & Goldman, S. A. (2003) 'New roles for astrocytes: redefining the functional architecture of the brain'. *Trends Neurosci*, 26 (10), pp. 523-530.

Newman, E. A., Frambach, D. A. & Odette, L. L. (1984) 'Control of extracellular potassium levels by retinal glial cell K+ siphoning'. *Science*, 225 (4667), pp. 1174-1175.

Newman, L. A., Korol, D. L. & Gold, P. E. (2011) 'Lactate produced by glycogenolysis in astrocytes regulates memory processing'. *PLoS One*, 6 (12), pp. e28427.

Nielsen, S., Nagelhus, E. A., Amiry-Moghaddam, M., Bourque, C., Agre, P. & Ottersen, O. P. (1997) 'Specialized membrane domains for water transport in glial cells: high-resolution immunogold cytochemistry of aquaporin-4 in rat brain'. *J Neurosci*, 17 (1), pp. 171-180.

Nishizawa, Y. (2001) 'Glutamate release and neuronal damage in ischemia'. *Life Sci*, 69 (4), pp. 369-381.

Noda, M. & Hiyama, T. Y. (2005) 'Sodium-level-sensitive sodium channel and salt-intake behavior'. *Chem Senses*, 30 Suppl 1 pp. i44-45.

Nowak, L., Bregestovski, P., Ascher, P., Herbet, A. & Prochiantz, A. (1984) 'Magnesium gates glutamate-activated channels in mouse central neurones'. *Nature*, 307 (5950), pp. 462-465.

O'Collins, V. E., Macleod, M. R., Donnan, G. A., Horky, L. L., van der Worp, B. H. & Howells, D. W. (2006) '1,026 experimental treatments in acute stroke'. *Ann Neurol*, 59 (3), pp. 467-477.

O'Connor, E. R. & Kimelberg, H. K. (1993) 'Role of calcium in astrocyte volume regulation and in the release of ions and amino acids'. *J Neurosci*, 13 (6), pp. 2638-2650.

O'Donnell, M. E., Tran, L., Lam, T. I., Liu, X. B. & Anderson, S. E. (2004) 'Bumetanide inhibition of the blood-brain barrier Na-K-Cl cotransporter reduces edema formation in the rat middle cerebral artery occlusion model of stroke'. *J Cereb Blood Flow Metab*, 24 (9), pp. 1046-1056.

Oe, Y., Baba, O., Ashida, H., Nakamura, K. C. & Hirase, H. (2016) 'Glycogen distribution in the microwave-fixed mouse brain reveals heterogeneous astrocytic patterns'. *Glia*, 64 (9), pp. 1532-1545.

Ogata, K. & Kosaka, T. (2002) 'Structural and quantitative analysis of astrocytes in the mouse hippocampus'. *Neuroscience*, 113 (1), pp. 221-233.

Orkand, R. K., Nicholls, J. G. & Kuffler, S. W. (1966) 'Effect of nerve impulses on the membrane potential of glial cells in the central nervous system of amphibia'. *J Neurophysiol*, 29 (4), pp. 788-806.

Orthmann-Murphy, J. L., Freidin, M., Fischer, E., Scherer, S. S. & Abrams, C. K. (2007) 'Two distinct heterotypic channels mediate gap junction coupling between astrocyte and oligodendrocyte connexins'. *J Neurosci*, 27 (51), pp. 13949-13957.

Palygin, O., Lalo, U., Verkhratsky, A. & Pankratov, Y. (2010) 'Ionotropic NMDA and P2X1/5 receptors mediate synaptically induced Ca2+ signalling in cortical astrocytes'. *Cell Calcium*, 48 (4), pp. 225-231.

Pangrsic, T., Potokar, M., Stenovec, M., Kreft, M., Fabbretti, E., Nistri, A., Pryazhnikov, E., Khiroug, L., Giniatullin, R. & Zorec, R. (2007) 'Exocytotic release of ATP from cultured astrocytes'. *J Biol Chem*, 282 (39), pp. 28749-28758.

Pantoni, L., Garcia, J. H. & Gutierrez, J. A. (1996) 'Cerebral white matter is highly vulnerable to ischemia'. *Stroke*, 27 (9), pp. 1641-1646; discussion 1647.

Papadia, S. & Hardingham, G. E. (2007) 'The dichotomy of NMDA receptor signaling'. *Neuroscientist*, 13 (6), pp. 572-579.

Papadia, S., Stevenson, P., Hardingham, N. R., Bading, H. & Hardingham, G. E. (2005) 'Nuclear Ca2+ and the cAMP response element-binding protein family mediate a late phase of activity-dependent neuroprotection'. *J Neurosci*, 25 (17), pp. 4279-4287.

Parpura, V., Fisher, E. S., Lechleiter, J. D., Schousboe, A., Waagepetersen, H. S., Brunet, S., Baltan, S. & Verkhratsky, A. (2017) 'Glutamate and ATP at the Interface Between Signaling and Metabolism in Astroglia: Examples from Pathology'. *Neurochem Res*, 42 (1), pp. 19-34.

Patneau, D. K., Wright, P. W., Winters, C., Mayer, M. L. & Gallo, V. (1994) 'Glial cells of the oligodendrocyte lineage express both kainate- and AMPA-preferring subtypes of glutamate receptor'. *Neuron*, 12 (2), pp. 357-371.

Payne, J. A., Rivera, C., Voipio, J. & Kaila, K. (2003) 'Cation-chloride co-transporters in neuronal communication, development and trauma'. *Trends Neurosci*, 26 (4), pp. 199-206.

Pellerin, L. & Magistretti, P. J. (1994) 'Glutamate uptake into astrocytes stimulates aerobic glycolysis: a mechanism coupling neuronal activity to glucose utilization'. *Proc Natl Acad Sci U S A*, 91 (22), pp. 10625-10629.

Pellerin, L. & Magistretti, P. J. (1997) 'Glutamate uptake stimulates Na+,K+-ATPase activity in astrocytes via activation of a distinct subunit highly sensitive to ouabain'. *J Neurochem*, 69 (5), pp. 2132-2137.

Pellerin, L., Pellegri, G., Bittar, P. G., Charnay, Y., Bouras, C., Martin, J. L., Stella, N. & Magistretti, P. J. (1998) 'Evidence supporting the existence of an activity-dependent astrocyte-neuron lactate shuttle'. *Dev Neurosci*, 20 (4-5), pp. 291-299.

Perea, G., Sur, M. & Araque, A. (2014) 'Neuron-glia networks: integral gear of brain function'. *Front Cell Neurosci*, 8 pp. 378.

Petito, C. K., Olarte, J. P., Roberts, B., Nowak, T. S. & Pulsinelli, W. A. (1998) 'Selective glial vulnerability following transient global ischemia in rat brain'. *Journal of Neuropathology and Experimental Neurology*, 57 (3), pp. 231-238.

Pfrieger, F. W. & Barres, B. A. (1997) 'Synaptic efficacy enhanced by glial cells in vitro'. *Science*, 277 (5332), pp. 1684-1687.

Pierre, K., Pellerin, L., Debernardi, R., Riederer, B. M. & Magistretti, P. J. (2000) 'Cell-specific localization of monocarboxylate transporters, MCT1 and MCT2, in the adult mouse brain revealed by double immunohistochemical labeling and confocal microscopy'. *Neuroscience*, 100 (3), pp. 617-627.

Pimentel, V. C., Zanini, D., Cardoso, A. M., Schmatz, R., Bagatini, M. D., Gutierres, J. M., Carvalho, F., Gomes, J. L., Rubin, M., Morsch, V. M., Moretto, M. B., Colino-Oliveira, M., Sebastião, A. M. & Schetinger, M. R. (2013) 'Hypoxia-ischemia alters

nucleotide and nucleoside catabolism and Na+,K+-ATPase activity in the cerebral cortex of newborn rats'. *Neurochem Res*, 38 (4), pp. 886-894.

Plotkin, M. D., Snyder, E. Y., Hebert, S. C. & Delpire, E. (1997) 'Expression of the Na-K-2Cl cotransporter is developmentally regulated in postnatal rat brains: a possible mechanism underlying GABA's excitatory role in immature brain'. *J Neurobiol*, 33 (6), pp. 781-795.

Powell, E. M. & Geller, H. M. (1999) 'Dissection of astrocyte-mediated cues in neuronal guidance and process extension'. *Glia*, 26 (1), pp. 73-83.

Pruss, R. M., Akeson, R. L., Racke, M. M. & Wilburn, J. L. (1991) 'Agonist-activated cobalt uptake identifies divalent cation-permeable kainate receptors on neurons and glial cells'. *Neuron*, 7 (3), pp. 509-518.

Pulsinelli, W., Sarokin, A. & Buchan, A. (1993) 'Antagonism of the NMDA and non-NMDA receptors in global versus focal brain ischemia'. *Prog Brain Res*, 96 pp. 125-135.

Pulsinelli, W. A., Brierley, J. B. & Plum, F. (1982) 'Temporal profile of neuronal damage in a model of transient forebrain ischemia'. *Ann Neurol*, 11 (5), pp. 491-498.

Rakers, C., Schleif, M., Blank, N., Matušková, H., Ulas, T., Händler, K., Torres, S. V., Schumacher, T., Tai, K., Schultze, J. L., Jackson, W. S. & Petzold, G. C. (2019) 'Stroke target identification guided by astrocyte transcriptome analysis'. *Glia*, 67 (4), pp. 619-633.

Rakic, P. (1971) 'Neuron-glia relationship during granule cell migration in developing cerebellar cortex. A Golgi and electronmicroscopic study in Macacus Rhesus'. *J Comp Neurol*, 141 (3), pp. 283-312.

Ransom, B. R. & Fern, R. (1997) 'Does astrocytic glycogen benefit axon function and survival in CNS white matter during glucose deprivation?'. *Glia*, 21 (1), pp. 134-141.

Rao, K. V., Panickar, K. S., Jayakumar, A. R. & Norenberg, M. D. (2005) 'Astrocytes protect neurons from ammonia toxicity'. *Neurochem Res*, 30 (10), pp. 1311-1318.

Remahl, S. & Hildebrand, C. (1982) 'Changing relation between onset of myelination and axon diameter range in developing feline white matter'. *J Neurol Sci*, 54 (1), pp. 33-45.

Ringel, F. & Plesnila, N. (2008) 'Expression and functional role of potassium-chloride cotransporters (KCC) in astrocytes and C6 glioma cells'. *Neurosci Lett*, 442 (3), pp. 219-223.

Rinholm, J. E., Hamilton, N. B., Kessaris, N., Richardson, W. D., Bergersen, L. H. & Attwell, D. (2011) 'Regulation of oligodendrocyte development and myelination by glucose and lactate'. *J Neurosci*, 31 (2), pp. 538-548.

Rojas, H., Ramos, M. & Dipolo, R. (2004) 'A genistein-sensitive Na+/Ca2+ exchange is responsible for the resting [Ca2+]i and most of the Ca2+ plasma membrane fluxes in stimulated rat cerebellar type 1 astrocytes'. *Jpn J Physiol*, 54 (3), pp. 249-262.

Roque, C., Mendes-Oliveira, J. & Baltazar, G. (2019) 'G protein-coupled estrogen receptor activates cell type-specific signaling pathways in cortical cultures: relevance to the selective loss of astrocytes'. *J Neurochem*, 149 (1), pp. 27-40.

Rose, C. R. & Ransom, B. R. (1996) 'Intracellular sodium homeostasis in rat hippocampal astrocytes'. *J Physiol*, 491 (Pt 2) pp. 291-305.

Rose, C. R. & Ransom, B. R. (1997) 'Gap junctions equalize intracellular Na+ concentration in astrocytes'. *Glia*, 20 (4), pp. 299-307.

Rose, C. R., Ransom, B. R. & Waxman, S. G. (1997) 'Pharmacological characterization of Na+ influx via voltage-gated Na+ channels in spinal cord astrocytes'. *J Neurophysiol*, 78 (6), pp. 3249-3258.

Rose, C. R. & Verkhratsky, A. (2016) 'Principles of sodium homeostasis and sodium signalling in astroglia'. *Glia*,

Rothstein, J. D., Dykes-Hoberg, M., Pardo, C. A., Bristol, L. A., Jin, L., Kuncl, R. W., Kanai, Y., Hediger, M. A., Wang, Y., Schielke, J. P. & Welty, D. F. (1996) 'Knockout of glutamate transporters reveals a major role for astroglial transport in excitotoxicity and clearance of glutamate'. *Neuron*, 16 (3), pp. 675-686.

Rouach, N., Koulakoff, A., Abudara, V., Willecke, K. & Giaume, C. (2008) 'Astroglial metabolic networks sustain hippocampal synaptic transmission'. *Science*, 322 (5907), pp. 1551-1555.

Ruminot, I., Gutiérrez, R., Peña-Münzenmayer, G., Añazco, C., Sotelo-Hitschfeld, T., Lerchundi, R., Niemeyer, M. I., Shull, G. E. & Barros, L. F. (2011) 'NBCe1 mediates the acute stimulation of astrocytic glycolysis by extracellular K+'. *J Neurosci*, 31 (40), pp. 14264-14271.

Rusnakova, V., Honsa, P., Dzamba, D., Stahlberg, A., Kubista, M. & Anderova, M. (2013) 'Heterogeneity of astrocytes: from development to injury - single cell gene expression'. *PLoS One*, 8 (8), pp. e69734.

Rzigalinski, B. A., Liang, S., McKinney, J. S., Willoughby, K. A. & Ellis, E. F. (1997) 'Effect of Ca2+ on in vitro astrocyte injury'. *J Neurochem*, 68 (1), pp. 289-296.

Saab, A. S., Tzvetanova, I. D. & Nave, K. A. (2013) 'The role of myelin and oligodendrocytes in axonal energy metabolism'. *Curr Opin Neurobiol*, 23 (6), pp. 1065-1072.

Saab, A. S., Tzvetavona, I. D., Trevisiol, A., Baltan, S., Dibaj, P., Kusch, K., Mobius, W., Goetze, B., Jahn, H. M., Huang, W., Steffens, H., Schomburg, E. D., Perez-

Samartin, A., Perez-Cerda, F., Bakhtiari, D., Matute, C., Lowel, S., Griesinger, C., Hirrlinger, J., Kirchhoff, F. & Nave, K. A. (2016) 'Oligodendroglial NMDA Receptors Regulate Glucose Import and Axonal Energy Metabolism'. *Neuron*, 91 (1), pp. 119-132.

Saez, I., Duran, J., Sinadinos, C., Beltran, A., Yanes, O., Tevy, M. F., Martinez-Pons, C., Milan, M. & Guinovart, J. J. (2014) 'Neurons have an active glycogen metabolism that contributes to tolerance to hypoxia'. *J Cereb Blood Flow Metab*, 34 (6), pp. 945-955.

Salter, M. G. & Fern, R. (2005) 'NMDA receptors are expressed in developing oligodendrocyte processes and mediate injury'. *Nature*, 438 (7071), pp. 1167-1171.

Salter, M. G. & Fern, R. (2008) 'The mechanisms of acute ischemic injury in the cell processes of developing white matter astrocytes'. *J Cereb Blood Flow Metab*, 28 (3), pp. 588-601.

Sanchez-Abarca, L. I., Tabernero, A. & Medina, J. M. (2001) 'Oligodendrocytes use lactate as a source of energy and as a precursor of lipids'. *Glia*, 36 (3), pp. 321-329.

Schipke, C. G., Ohlemeyer, C., Matyash, M., Nolte, C., Kettenmann, H. & Kirchhoff, F. (2001) 'Astrocytes of the mouse neocortex express functional N-methyl-D-aspartate receptors'. *FASEB J*, 15 (7), pp. 1270-1272.

Schousboe, A. (2003) 'Role of astrocytes in the maintenance and modulation of glutamatergic and GABAergic neurotransmission'. *Neurochem Res*, 28 (2), pp. 347-352.

Schousboe, A., Scafidi, S., Bak, L. K., Waagepetersen, H. S. & McKenna, M. C. (2014) 'Glutamate metabolism in the brain focusing on astrocytes'. *Adv Neurobiol*, 11 pp. 13-30.

Seifert, G., Rehn, L., Weber, M. & Steinhäuser, C. (1997) 'AMPA receptor subunits expressed by single astrocytes in the juvenile mouse hippocampus'. *Brain Res Mol Brain Res*, 47 (1-2), pp. 286-294.

Seifert, G. & Steinhauser, C. (2001) 'Ionotropic glutamate receptors in astrocytes'. *Prog Brain Res*, 132 pp. 287-299.

Sekerdag, E., Solaroglu, I. & Gursoy-Ozdemir, Y. (2018) 'Cell Death Mechanisms in Stroke and Novel Molecular and Cellular Treatment Options'. *Curr Neuropharmacol*, 16 (9), pp. 1396-1415.

Serwanski, D. R., Jukkola, P. & Nishiyama, A. (2017) 'Heterogeneity of astrocyte and NG2 cell insertion at the node of ranvier'. *J Comp Neurol*, 525 (3), pp. 535-552.

Shannon, C., Salter, M. & Fern, R. (2007) 'GFP imaging of live astrocytes: regional differences in the effects of ischaemia upon astrocytes'. *J Anat*, 210 (6), pp. 684-692.

Shibata, T., Yamada, K., Watanabe, M., Ikenaka, K., Wada, K., Tanaka, K. & Inoue, Y. (1997) 'Glutamate transporter GLAST is expressed in the radial glia-astrocyte lineage of developing mouse spinal cord'. *J Neurosci*, 17 (23), pp. 9212-9219.

Shih, A. Y., Johnson, D. A., Wong, G., Kraft, A. D., Jiang, L., Erb, H., Johnson, J. A. & Murphy, T. H. (2003) 'Coordinate regulation of glutathione biosynthesis and release by Nrf2-expressing glia potently protects neurons from oxidative stress'. *J Neurosci*, 23 (8), pp. 3394-3406.

Sickmann, H. M., Walls, A. B., Schousboe, A., Bouman, S. D. & Waagepetersen, H. S. (2009) 'Functional significance of brain glycogen in sustaining glutamatergic neurotransmission'. *J Neurochem*, 109 Suppl 1 pp. 80-86.

Silver, I. A. & Erecińska, M. (1997) 'Energetic demands of the Na+/K+ ATPase in mammalian astrocytes'. *Glia*, 21 (1), pp. 35-45.

Simard, M., Arcuino, G., Takano, T., Liu, Q. S. & Nedergaard, M. (2003) 'Signaling at the gliovascular interface'. *J Neurosci*, 23 (27), pp. 9254-9262.

Simons, M. & Nave, K. A. (2015) 'Oligodendrocytes: Myelination and Axonal Support'. *Cold Spring Harb Perspect Biol*, 8 (1), pp. a020479.

Slezak, M., Pfrieger, F. W. & Soltys, Z. (2006) 'Synaptic plasticity, astrocytes and morphological homeostasis'. *J Physiol Paris*, 99 (2-3), pp. 84-91.

Sofroniew, M. V. (2009) 'Molecular dissection of reactive astrogliosis and glial scar formation'. *Trends Neurosci*, 32 (12), pp. 638-647.

Soleimani, M. & Burnham, C. E. (2001) 'Na+:HCO(3-) cotransporters (NBC): cloning and characterization'. *J Membr Biol*, 183 (2), pp. 71-84.

SOLS, A. & CRANE, R. K. (1954) 'Substrate specificity of brain hexokinase'. *J Biol Chem*, 210 (2), pp. 581-595.

Song, H., Stevens, C. F. & Gage, F. H. (2002) 'Astroglia induce neurogenesis from adult neural stem cells'. *Nature*, 417 (6884), pp. 39-44.

Soriano, F. X. & Hardingham, G. E. (2007) 'Compartmentalized NMDA receptor signalling to survival and death'. *J Physiol*, 584 (Pt 2), pp. 381-387.

Sotelo-Hitschfeld, T., Niemeyer, M. I., Machler, P., Ruminot, I., Lerchundi, R., Wyss, M. T., Stobart, J., Fernandez-Moncada, I., Valdebenito, R., Garrido-Gerter, P., Contreras-Baeza, Y., Schneider, B. L., Aebischer, P., Lengacher, S., San Martin, A., Le Douce, J., Bonvento, G., Magistretti, P. J., Sepulveda, F. V., Weber, B. & Barros, L. F. (2015) 'Channel-mediated lactate release by K(+)-stimulated astrocytes'. *J Neurosci*, 35 (10), pp. 4168-4178.

Stroke.org.uk (2016) 'State of the Nation - Stroke Statistics'. Stroke Association [Online]. Available at: : http://www.stroke.org.uk/resource-sheet/state-nation-stroke-statistics (Accessed: 11 November).

Su, G., Kintner, D. B., Flagella, M., Shull, G. E. & Sun, D. (2002) 'Astrocytes from Na(+)-K(+)-Cl(-) cotransporter-null mice exhibit absence of swelling and decrease in EAA release'. *Am J Physiol Cell Physiol*, 282 (5), pp. C1147-1160.

Su, G., Kintner, D. B. & Sun, D. (2002) 'Contribution of Na(+)-K(+)-Cl(-) cotransporter to high-[K(+)](o)- induced swelling and EAA release in astrocytes'. *Am J Physiol Cell Physiol*, 282 (5), pp. C1136-1146.

Supplie, L. M., Duking, T., Campbell, G., Diaz, F., Moraes, C. T., Gotz, M., Hamprecht, B., Boretius, S., Mahad, D. & Nave, K. A. (2017) 'Respiration-Deficient Astrocytes Survive As Glycolytic Cells In Vivo'. *J Neurosci*, 37 (16), pp. 4231-4242.

Suzuki, A., Stern, S. A., Bozdagi, O., Huntley, G. W., Walker, R. H., Magistretti, P. J. & Alberini, C. M. (2011) 'Astrocyte-neuron lactate transport is required for long-term memory formation'. *Cell*, 144 (5), pp. 810-823.

Swanson, R. A. (1992) 'Physiologic coupling of glial glycogen metabolism to neuronal activity in brain'. *Can J Physiol Pharmacol*, 70 Suppl pp. S138-144.

Swanson, R. A. & Choi, D. W. (1993) 'Glial glycogen stores affect neuronal survival during glucose deprivation in vitro'. *J Cereb Blood Flow Metab*, 13 (1), pp. 162-169.

Takano, T., Oberheim, N., Cotrina, M. L. & Nedergaard, M. (2009) 'Astrocytes and ischemic injury'. *Stroke*, 40 (3 Suppl), pp. S8-12.

Takata, F., Dohgu, S., Matsumoto, J., Takahashi, H., Machida, T., Wakigawa, T., Harada, E., Miyaji, H., Koga, M., Nishioku, T., Yamauchi, A. & Kataoka, Y. (2011) 'Brain pericytes among cells constituting the blood-brain barrier are highly sensitive to tumor necrosis factor-α, releasing matrix metalloproteinase-9 and migrating in vitro'. *J Neuroinflammation*, 8 pp. 106.

Tanaka, J., Toku, K., Zhang, B., Ishihara, K., Sakanaka, M. & Maeda, N. (1999) 'Astrocytes prevent neuronal death induced by reactive oxygen and nitrogen species'. *Glia*, 28 (2), pp. 85-96.

Tashiro, A., Sandler, V. M., Toni, N., Zhao, C. & Gage, F. H. (2006) 'NMDA-receptor-mediated, cell-specific integration of new neurons in adult dentate gyrus'. *Nature*, 442 (7105), pp. 929-933.

Tekkok, S. B., Brown, A. M., Westenbroek, R., Pellerin, L. & Ransom, B. R. (2005) 'Transfer of glycogen-derived lactate from astrocytes to axons via specific monocarboxylate transporters supports mouse optic nerve activity'. *J Neurosci Res*, 81 (5), pp. 644-652.

Tekkok, S. B. & Goldberg, M. P. (2001) 'Ampa/kainate receptor activation mediates hypoxic oligodendrocyte death and axonal injury in cerebral white matter'. *J Neurosci*, 21 (12), pp. 4237-4248.

Thomas, R., Salter, M. G., Wilke, S. R., Husen, A., Allcock, N., Nivison, M., Nnoli, A. N. & Fern, R. (2004) 'Acute ischemic injury of astrocytes is mediated by Na-K-Cl cotransport and not Ca2+ influx at a key point in white matter development'. *Journal of Neuropathology and Experimental Neurology*, 63 (8), pp. 856-871.

Thoren, A. E., Helps, S. C., Nilsson, M. & Sims, N. R. (2005) 'Astrocytic function assessed from 1-14C-acetate metabolism after temporary focal cerebral ischemia in rats'. *J Cereb Blood Flow Metab*, 25 (4), pp. 440-450.

Ting, J. T., Daigle, T. L., Chen, Q. & Feng, G. (2014) 'Acute brain slice methods for adult and aging animals: application of targeted patch clamp analysis and optogenetics'. *Methods Mol Biol*, 1183 pp. 221-242.

Tress, O., Maglione, M., May, D., Pivneva, T., Richter, N., Seyfarth, J., Binder, S., Zlomuzica, A., Seifert, G., Theis, M., Dere, E., Kettenmann, H. & Willecke, K. (2012) 'Panglial gap junctional communication is essential for maintenance of myelin in the CNS'. *J Neurosci*, 32 (22), pp. 7499-7518.

Truett, G. E., Heeger, P., Mynatt, R. L., Truett, A. A., Walker, J. A. & Warman, M. L. (2000) 'Preparation of PCR-quality mouse genomic DNA with hot sodium hydroxide and tris (HotSHOT)'. *Biotechniques*, 29 (1), pp. 52, 54.

Tsacopoulos, M., Evêquoz-Mercier, V., Perrottet, P. & Buchner, E. (1988) 'Honeybee retinal glial cells transform glucose and supply the neurons with metabolic substrate'. *Proc Natl Acad Sci U S A*, 85 (22), pp. 8727-8731.

Tsacopoulos, M., Veuthey, A. L., Saravelos, S. G., Perrottet, P. & Tsoupras, G. (1994) 'Glial cells transform glucose to alanine, which fuels the neurons in the honeybee retina'. *J Neurosci*, 14 (3 Pt 1), pp. 1339-1351.

Tsai, H. H., Li, H., Fuentealba, L. C., Molofsky, A. V., Taveira-Marques, R., Zhuang, H., Tenney, A., Murnen, A. T., Fancy, S. P., Merkle, F., Kessaris, N., Alvarez-Buylla, A., Richardson, W. D. & Rowitch, D. H. (2012) 'Regional astrocyte allocation regulates CNS synaptogenesis and repair'. *Science*, 337 (6092), pp. 358-362.

Vaity, C., Al-Subaie, N. & Cecconi, M. (2015) 'Cooling techniques for targeted temperature management post-cardiac arrest'. *Crit Care*, 19 pp. 103.

Verkhratsky, A., Noda, M., Parpura, V. & Kirischuk, S. (2013) 'Sodium fluxes and astroglial function'. *Adv Exp Med Biol*, 961 pp. 295-305.

Verkhratsky, A. & Parpura, V. (2015) 'Astrogliopathology in neurological, neurodevelopmental and psychiatric disorders'. *Neurobiol Dis*,

Verkhratsky, A. & Steinhäuser, C. (2000) 'Ion channels in glial cells'. *Brain Res Brain Res Rev*, 32 (2-3), pp. 380-412.

Ververken, D., Van Veldhoven, P., Proost, C., Carton, H. & De Wulf, H. (1982) 'On the role of calcium ions in the regulation of glycogenolysis in mouse brain cortical slices'. *J Neurochem*, 38 (5), pp. 1286-1295.

Voskuhl, R. R., Peterson, R. S., Song, B., Ao, Y., Morales, L. B., Tiwari-Woodruff, S. & Sofroniew, M. V. (2009) 'Reactive astrocytes form scar-like perivascular barriers to leukocytes during adaptive immune inflammation of the CNS'. *J Neurosci*, 29 (37), pp. 11511-11522.

Voutsinos-Porche, B., Bonvento, G., Tanaka, K., Steiner, P., Welker, E., Chatton, J. Y., Magistretti, P. J. & Pellerin, L. (2003) 'Glial glutamate transporters mediate a functional metabolic crosstalk between neurons and astrocytes in the mouse developing cortex'. *Neuron*, 37 (2), pp. 275-286.

Walz, W. & Hertz, L. (1982) 'Ouabain-sensitive and ouabain-resistant net uptake of potassium into astrocytes and neurons in primary cultures'. *J Neurochem*, 39 (1), pp. 70-77.

Walz, W. & Mukerji, S. (1988) 'Lactate production and release in cultured astrocytes'. *Neurosci Lett*, 86 (3), pp. 296-300.

Wang, Z., Haydon, P. G. & Yeung, E. S. (2000) 'Direct observation of calcium-independent intercellular ATP signaling in astrocytes'. *Anal Chem*, 72 (9), pp. 2001-2007.

Watts, A. G., Sanchez-Watts, G., Emanuel, J. R. & Levenson, R. (1991) 'Cell-specific expression of mRNAs encoding Na+,K(+)-ATPase alpha- and beta-subunit isoforms within the rat central nervous system'. *Proc Natl Acad Sci U S A*, 88 (16), pp. 7425-7429.

Wender, R., Brown, A. M., Fern, R., Swanson, R. A., Farrell, K. & Ransom, B. R. (2000) 'Astrocytic glycogen influences axon function and survival during glucose deprivation in central white matter'. *J Neurosci*, 20 (18), pp. 6804-6810.

WHO (2014) 'The top 10 causes of death.'. [Online]. Available at: http://www.who.int/mediacentre/factsheets/fs310/en/ (Accessed: November 2016).

Wilhelmsson, U., Bushong, E. A., Price, D. L., Smarr, B. L., Phung, V., Terada, M., Ellisman, M. H. & Pekny, M. (2006) 'Redefining the concept of reactive astrocytes as cells that remain within their unique domains upon reaction to injury'. *Proc Natl Acad Sci U S A*, 103 (46), pp. 17513-17518.

Willard, S. S. & Koochekpour, S. (2013) 'Glutamate, glutamate receptors, and downstream signaling pathways'. *Int J Biol Sci*, 9 (9), pp. 948-959.

Wu, T. C. & Grotta, J. C. (2013) 'Hypothermia for acute ischaemic stroke'. *Lancet Neurol*, 12 (3), pp. 275-284.

Wyss, M. T., Jolivet, R., Buck, A., Magistretti, P. J. & Weber, B. (2011) 'In vivo evidence for lactate as a neuronal energy source'. *J Neurosci*, 31 (20), pp. 7477-7485.

Xu, J., Song, D., Xue, Z., Gu, L., Hertz, L. & Peng, L. (2013) 'Requirement of glycogenolysis for uptake of increased extracellular K+ in astrocytes: potential implications for K+ homeostasis and glycogen usage in brain'. *Neurochem Res*, 38 (3), pp. 472-485.

Xu, L., Sapolsky, R. M. & Giffard, R. G. (2001) 'Differential sensitivity of murine astrocytes and neurons from different brain regions to injury'. *Exp Neurol*, 169 (2), pp. 416-424.

Yan, Y., Dempsey, R. J. & Sun, D. (2001a) 'Expression of Na(+)-K(+)-Cl(-) cotransporter in rat brain during development and its localization in mature astrocytes'. *Brain Res*, 911 (1), pp. 43-55.

Yan, Y., Dempsey, R. J. & Sun, D. (2001b) 'Na+-K+-Cl- cotransporter in rat focal cerebral ischemia'. *J Cereb Blood Flow Metab*, 21 (6), pp. 711-721.

Yao, X., Hrabetová, S., Nicholson, C. & Manley, G. T. (2008) 'Aquaporin-4-deficient mice have increased extracellular space without tortuosity change'. *J Neurosci*, 28 (21), pp. 5460-5464.

Ye, Z. C., Wyeth, M. S., Baltan-Tekkok, S. & Ransom, B. R. (2003) 'Functional hemichannels in astrocytes: a novel mechanism of glutamate release'. *J Neurosci*, 23 (9), pp. 3588-3596.

Yu, X. M. & Salter, M. W. (1998) 'Gain control of NMDA-receptor currents by intracellular sodium'. *Nature*, 396 (6710), pp. 469-474.

Zerlin, M., Levison, S. W. & Goldman, J. E. (1995) 'Early patterns of migration, morphogenesis, and intermediate filament expression of subventricular zone cells in the postnatal rat forebrain'. *J Neurosci*, 15 (11), pp. 7238-7249.

Zhang, L. Y., Hu, Y. Y., Zhao, C. C., Qi, J., Su, A. C., Lou, N., Zhang, M. Y., Li, L., Xian, X. H., Gong, J. X., Zhao, H., Zhang, J. G., Li, W. B. & Zhang, M. (2019) 'The mechanism of GLT-1 mediating cerebral ischemic injury depends on the activation of p38 MAPK'. *Brain Res Bull*, 147 pp. 1-13.

Zhang, M., Ma, Y., Chai, L., Mao, H., Zhang, J. & Fan, X. (2018) 'Storax Protected Oxygen-Glucose Deprivation/Reoxygenation Induced Primary Astrocyte Injury by Inhibiting NF-κB Activation'. *Front Pharmacol*, 9 pp. 1527.

Zhang, Y. & Barres, B. A. (2010) 'Astrocyte heterogeneity: an underappreciated topic in neurobiology'. *Curr Opin Neurobiol*, 20 (5), pp. 588-594.

Zhao, G. & Flavin, M. P. (2000) 'Differential sensitivity of rat hippocampal and cortical astrocytes to oxygen-glucose deprivation injury'. *Neurosci Lett*, 285 (3), pp. 177-180.

Zheng, Y., Pan, C., Chen, M., Pei, A., Xie, L. & Zhu, S. (2019) 'miR-29a ameliorates ischemic injury of astrocytes in vitro by targeting the water channel protein aquaporin 4'. *Oncol Rep*, 41 (3), pp. 1707-1717.

Zhuo, L., Sun, B., Zhang, C. L., Fine, A., Chiu, S. Y. & Messing, A. (1997) 'Live astrocytes visualized by green fluorescent protein in transgenic mice'. *Dev Biol*, 187 (1), pp. 36-42.